

SOME DYNAMIC ASPECTS OF STRUCTURAL MANIPULATION

ANTHONY DOUGLAS HUGHES

Thesis Submitted for th Degree of
Doctor of Philosophy

University of Edinburgh

July 1975



CONTENTS

	<u>Page Number</u>
ACKNOWLEDGEMENTS	V
SYNOPSIS	VI
<u>CHAPTER 1</u>	
<u>INTRODUCTION</u>	
1.1. Research Motivation.	1
1.2. Existing Techniques Related to the Problem of Minimising Structural Response.	8
1.21. Structural Optimisation.	8
1.22. Small Perturbation Analysis as a Method of Determining the Sensitivities of Eigenvalues to Parameter Changes in Dynamical Systems.	10
1.3. Vibration Control Using Structural Manipulation.	15
<u>CHAPTER 2</u>	
<u>THE EFFECT OF PARAMETER CHANGES ON THE RESPONSE OF A SINGLE DEGREE OF FREEDOM SYSTEM</u>	
2.1. Equations of Motion.	18
2.2. The Variation of Frequency.	20
2.3. The Variation of Mass and Stiffness.	20
2.4. The Variation of Damping.	22
2.5. Conclusions.	22

CHAPTER 3

PARAMETER CHANGES IN MULTI-DEGREE OF FREEDOM SYSTEMS

3.1.	Introduction.	24
3.2.	Response as a Function of a Single Variable Stiffness Parameter.	24
3.3.	Response as a Function of Two Parameters.	36
3.4.	Response as a General Function of M Variable Parameters.	43
3.5.	Variable Mass.	44

CHAPTER 4

THE ASSESSMENT AND EFFECT OF PARAMETER CHANGES

4.1.	Introduction.	48
4.2.	The Feasibility of Achieving A Desired Response Using One or Two Parameters.	48
4.21.	A Single Variable Parameter.	48
4.22.	Two Variable Parameters.	51
4.3.	The Criteria Governing the Effectiveness of Parameter Changes.	53
4.4.	The Practical Application of Effectiveness Criteria to a Helicopter Fuselage.	56
4.41.	Discussion of Results.	70
4.5.	Parameter Changes in Real Structures.	72
4.6.	Other Techniques for Assimilating the Effectiveness of Parameter Changes.	79
4.61.	Response as a Function of Frequency and Stiffness.	79
4.62.	Multiple Responses as a Function of Structural Parameters.	82

CHAPTER 5

COMPUTATIONAL ANALYSIS

5.1.	Introduction.	88
5.2.	The Structural Manipulation Programme.	89
5.21.	General Description.	89
5.22.	Programming Techniques.	98
5.3.	Conclusions.	106

CHAPTER 6

EXPERIMENTAL ANALYSIS

6.1.	Introduction.	108
6.2.	The Design and Development of a Variable Stiffness Element.	109
6.21.	General Specification.	109
6.22.	The Electro-Mechanical Spring.	109
6.23.	Interchangeable Spring Elements.	111
6.24.	The Air Spring.	111
6.25.	The Variable Length Cantilever Spring.	119
6.3.	The Test Structure.	121
6.4.	Experimental Equipment.	130
6.5.	Experimental Procedure.	134
6.51.	The Measurement of Structural Response as a Function of Variable Stiffness.	137
6.52.	The Measurement of Natural Frequencies, Normal Mode Shapes and Associated Damping.	139
6.6.	The Mathematical Model of the Test Structure.	145
6.7.	Results.	149

Contents (Continued)

	<u>Page Number</u>
6.71. Natural Frequencies, Normal Mode Shapes and Associated Damping.	149
6.72. Response as a Function of Variable Stiffness.	164
6.8. Conclusions.	168
6.81. The Mathematical Model of the Test Structure.	168
6.82. Response as a Function of Variable Stiffness.	169
 <u>CHAPTER 7</u>	
 <u>CONCLUSIONS</u>	 170
 <u>APPENDICES</u>	 175
 <u>REFERENCES</u>	 200
 <u>PUBLISHED WORK</u>	 204

ACKNOWLEDGMENTS

The Author wishes to thank the following: Several people at Westland Helicopters Ltd. for their help and encouragement, Dr. G.T.S Done for his valuable assistance and supervision, Mr.G.Smith for his help in the construction of the experimental apparatus and to Mrs.S.M.Boyes and DR.W.Hughes for their superb work in the typing and preparation of the thesis respectively. Thanks also go to Miss S.Mack for her help in the typing of the thesis.

SYNOPSIS

The response of both single and multi-degree of freedom systems is examined as a function of structural parameters. These parameters are either the variation of mass at a structural node or the variation of stiffness between two points in the structure (as represented by a linear spring). In both single and multi-degree of freedom systems the variation of either a mass or a stiffness parameter is seen to produce a circular response locus in the complex plane at some other point in the structure. The form of the circular response locus is verified experimentally by varying a single stiffness parameter in a simple test structure. Where two or more parameters are varied simultaneously then an area of feasible response is formed in the complex plane, for any given values of the parameters the response must lie within the bounds of this region.

The properties of the response circle and feasible response regions are investigated and are used to develop criteria which enable the relative effectiveness of parameters in achieving a desired response to be determined. These effectiveness criteria are used in the analysis of a simplified model of a helicopter fuselage and are shown to be successful in highlighting sensitive areas of the fuselage for the purpose of structural modification. An interactive computer programme which is used to perform the above mentioned analyses on structural models is also described.

CHAPTER 1

INTRODUCTION

1.1. Research Motivation.

The motivation for the research presented in this thesis came from the helicopter industry. The problem, which is a common one, concerns the undesirable rotor induced vibration levels that often exist in a helicopter fuselage. The design specifications for modern helicopters include the maximum permissible vibratory acceleration levels that are allowed to exist in certain parts of the fuselage structure; of particular importance are the passenger and crew areas where considerable discomfort can be experienced as a result of high levels of vibration. If this particular specification is not achieved then modifications must be made to the structure in order to reduce the vibratory response to an acceptable level.

The vibratory forces and moments that are inherent in the operation of a helicopter rotor are produced at the rotor head. These are the resultant of loads generated on an individual rotor blade at frequencies which are multiples of the rotor speed. Depending on the number of rotor blades used certain frequency components reinforce each other and others cancel out. The most important of these non-cancelling components is the fundamental one which occurs at a frequency which is equal to the product of the number of blades and the rotor speed. The loads that are generated at the rotor head are vertical, longitudinal and lateral shear forces and rolling and pitching moments. It is the response of the airframe to these loadings that constitutes the vibratory problem of the helicopter.

During the design process there are several aspects of the helicopter

1.1. (Continued)

design that are considered in order to ensure that vibration levels are kept to a minimum. There are three main methods by which this may be achieved, namely,

- a) By reducing the vibratory force input to the fuselage.
- b) By the use of force cancellation devices such as dynamic vibration absorbers.
- c) By means of structural modifications.

In the case of the Westland Lynx helicopter method (a) was used indirectly in an attempt to dynamically isolate the engine and main rotor gearbox from the fuselage using flexible mountings [21]. The geometry and dynamic characteristics of the engine and gearbox couplings and supports were varied in order to find the configuration that gave the smallest response at the gearbox mounting points. In method (b) the use of vibration absorbers is avoided wherever possible at the design stage since these often impose a considerable weight penalty on the structure. Another method that is commonly used, which involves structural modification, is to estimate the natural frequencies of the structure and to determine whether any of these are close to the major excitation frequency. Where this is the case then structural modification is employed to move the offending frequency away from that of the excitation forces. There are however, difficulties in this type of approach for it is not always obvious which areas of the airframe are most suitable for structural modification. Thus there is the real need to be able to predict accurately the effect of structural modifications on the response at points in the airframe.

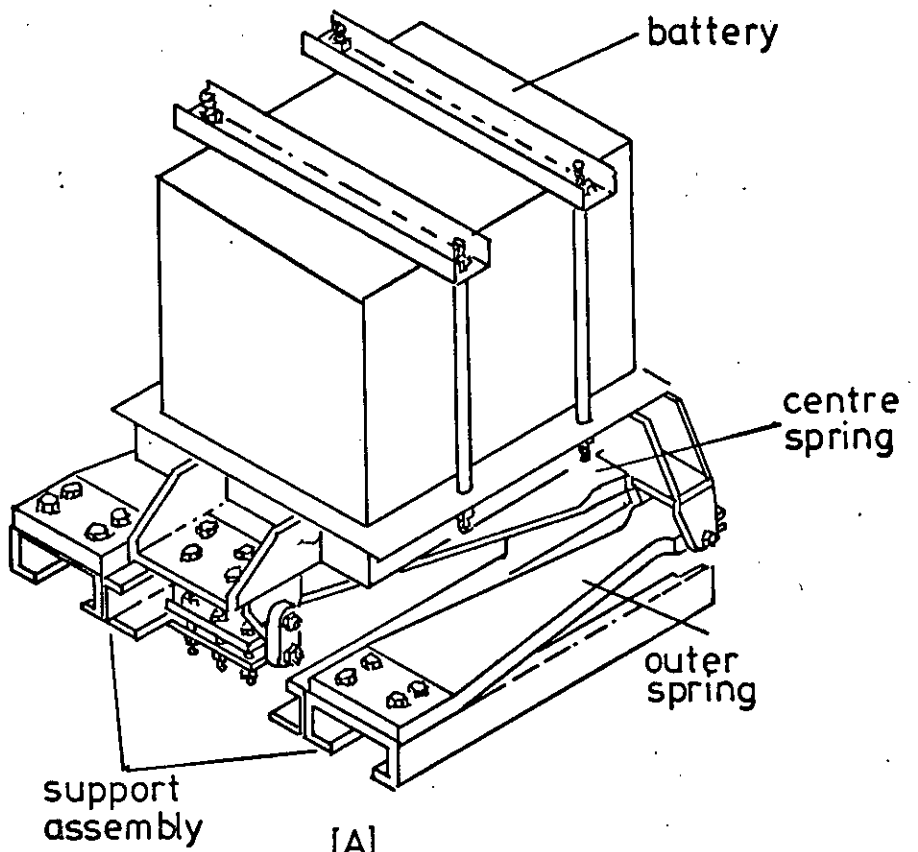
Even though efforts are made during the design stage of the helicopter to reduce vibration levels it is often found when the helicopter is first flight tested that these are still unacceptable and there is usually

1.1. (Continued)

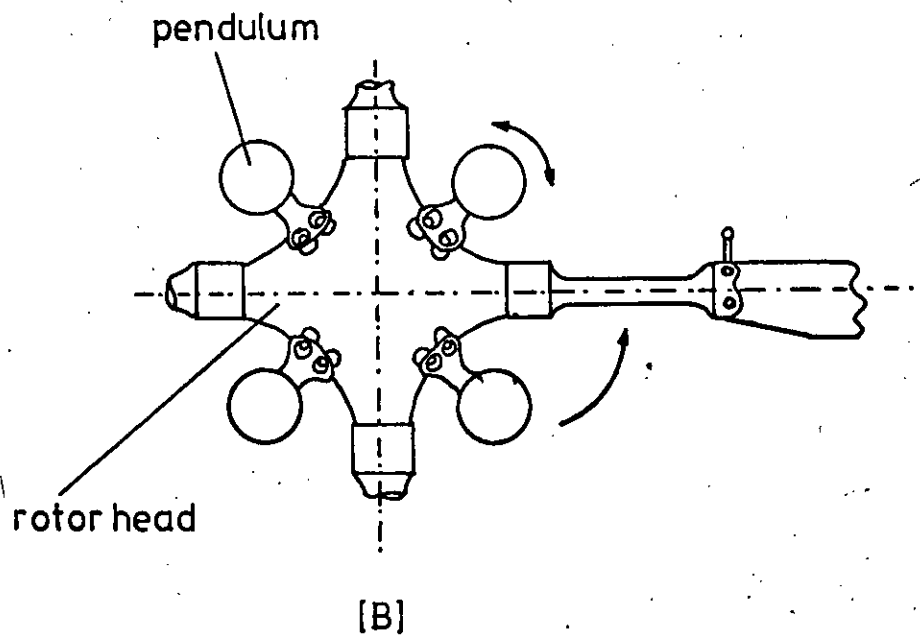
considerable pressure on the dynamicists involved to come up with a satisfactory solution to the problem. At this stage there are two main methods of reducing undesirable vibration levels, namely, by using vibration absorbers and by structural modification.

In the first instance structural modification is often used to help solve the problem. A series of potentially useful modifications is drawn up and each modification is tried in turn, under flight conditions, in order to determine how effective it is in reducing the required vibration levels. Where a particular modification is found to be successful then it is incorporated into the existing structure. Most modifications involve stiffening up the structure in some way and are chosen largely on the basis of experience and intuition. The choices are sometimes influenced by results from an analysis of a simplified model of the helicopter; the model used in the case of the Lynx helicopter is described in Chapter 4.

Having modified the structure to the best effect by incorporating certain modifications the vibratory response may be further reduced by means of dynamic vibration absorbers. These may be used to suppress vibration globally with respect to the fuselage itself or locally at specified points in the structure. The simplest vibration absorber consists of a mass, spring, dashpot system which is tuned to resonate at the excitation frequency of the structure. This type of absorber is usually mounted close to the point at which the vibration level is to be reduced and is intended to suppress vibration only on a local basis. In practice the mass in such a device is usually an existing piece of heavy equipment such as a battery; an example of a battery absorber is shown in figure 1.1. (a). Other types of absorber, which suppress vibration globally,



[A]
Battery vibration absorber



[B]
Bifilar Pendulum Absorbers

Dynamic Vibration Absorbers

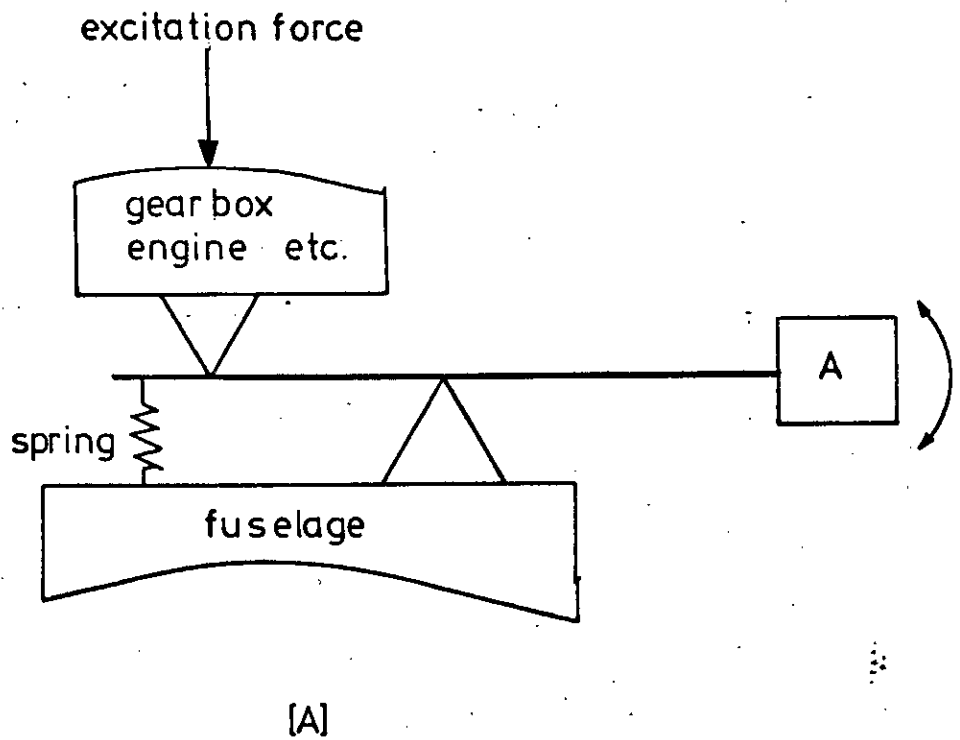
1.1. (continued)

are normally situated close to the source of excitation. Typical examples of these include the bifilar pendulum absorber, DAVI absorbers and the Bell "Nodamagic" system.

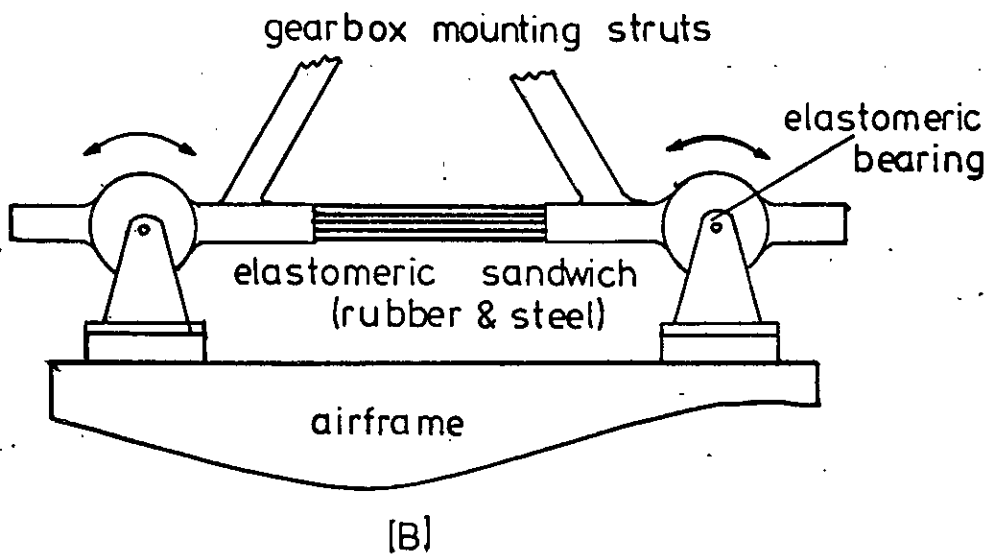
The bifilar pendulum absorber was first used to reduce torsional vibration in an engine crankshaft. [22] Where the helicopter is concerned, a set of bifilar absorbers is fitted in the plane of the rotor head as shown in figure 1.1. (b) and is effective in reducing forces in that plane. The absorber consists of a large mass which acts as the pendulum bob and is mounted at the end of a very small radius arm. Unlike some types of absorber, once the pendula have been tuned to a given frequency then they remain in tune even if the frequency changes. This is due to the fact that the dynamic stiffness of the pendulum, as provided by the centrifugal force, increases or decreases with a similar change in the rotor frequency. The bifilar absorber has been successfully applied in practice to production helicopters by the Sikorsky Aircraft Company [23].

The Dynamic Anti-Resonant Vibration Isolation System (DAVI) was patented by the Karman Aircraft Corporation [24] and consists of the mass, spring arrangement shown schematically in figure 1.2. (a). The system is tuned to the excitation frequency such that the mass A resonates on the end of the rigid bar. In any practical application the engine and main rotor gearbox would most likely be mounted on a set of absorbers in an attempt to isolate this substructure from the rest of the fuselage. DAVI absorbers are at present still in an experimental form and have not been applied in a practical situation.

A similar arrangement to the DAVI absorber is the Bell "Nodamagic" system shown in figure 1.2. (b). The main rotor gearbox is mounted



DAVI Vibration Absorber



Bell "Nodamagic" Gearbox Mounting System

1.1. (Continued)

on a beam supported by elastomeric bearings. The beam and carried mass are tuned to resonate in the first "free-free" normal mode of the beam at the external excitation frequency. The beam supports are positioned to coincide with the nodes of the normal mode in an attempt to minimise any forces transmitted to the airframe.

Dynamic absorbers are essentially force cancellation devices and are often very effective in reducing vibratory responses. Their main disadvantage, however, is that they often impose a considerable weight penalty on the structure, e.g. the bifilar can add as much as 4% to the total weight of the helicopter. Battery absorbers and other similar devices, with the exception of the bifilar, also have to be tuned to a given frequency in order to operate in an optimum manner. The rotor speed, which is governed, can vary in certain circumstances by a small amount and if this does happen then the excitation frequency changes and the absorber becomes detuned and is consequently not so effective.

It is evident that whenever a structural modification has to be made, whether it is at the design stage of the helicopter or during the flight test trials, then there is always the problem of identifying those areas of the structure that have the greatest potential in either affecting or reducing the desired vibratory responses. Thus although the primary aim of any investigation using structural modification would be to reduce to a minimum the vibration levels in selected areas of the helicopter fuselage, there are two secondary aims of a more general nature. Firstly, there is the need to develop techniques which will give a better understanding of the way in which the dynamic response of a complex structure varies as a function of its structural parameters, and secondly, criteria must be

1.1. (Continued)

developed which will highlight areas within the structure which are potentially effective in reducing the desired vibration levels.

1.2. Existing Techniques Related to the Problem of Minimising Structural Response.

1.21. Structural Optimisation.

Computer bases formal optimisation routines are commonly used in the Aerospace industry in a wide variety of applications. A general optimisation procedure contains an objective function, variables and a set of constraints which may be applied to the parameters themselves or which may be of an independent nature such as stiffness or frequency requirements. Typically, an optimisation procedure can be applied to a finite element model of a complex structure in order to achieve a minimum weight configuration. The structure would normally be subjected to a set of excitation forces and the variables in the problem would be the sizes of the elements. The constraints could include any of the following: stress constraints, constraints on the displacements and also on the sizes of the elements. An example of a procedure such as this is given by Venkayya [25].

Dynamic constraints can be considered in the optimisation process, e.g. it might be required that one or more of the natural frequencies of the structure should assume given values or alternatively that there should be a given interval between two natural frequencies..Turner [26] develops a procedure which proportions the members of an elastic structure so that one or more of its natural frequencies assumes a given value and the total mass of the structure is a minimum. Constraints of this form are normally considered in order to satisfy the flutter requirements of fixed wing aircraft.

1.21. (Continued)

A particularly practical method has been developed by Taig and Kerr [29] at the British Aircraft Corporation where automated optimisation methods are routinely used in the design of all new aircraft. The method is capable of producing a minimum weight structure whilst considering strength, stiffness and frequency requirements simultaneously. The approach is based on the strain energy density of individual structural elements and all the above mentioned requirements are developed in terms of these. The variables considered in the process are real structural parameters and there is consequently no need to perform a subsequent design operation in order to convert idealised structure dimensions to feasible detail sizes.

The problem of minimising structural response can be tackled using formal optimisation techniques. The method requires a mathematical model of the structure in order to calculate the dynamic response of the system due to a given set of excitation forces. The response at one or more points in the structure is minimised as a function of a given set of structural parameters. Constraints can be imposed on the sizes of the parameters as in the previous problems. Ellis [27] of Westland Helicopters Ltd., describes a process by which a very much simplified model of the upper decking structure, main gear box and engine of a helicopter was optimised in order that the force inputs to the fuselage were a minimum. The problem contained only a few variable parameters representing the geometry and stiffness of the substructure. A Simplex procedure was used in the optimisation routine and the results obtained were used in order to obtain a feel for the vibration problem of the helicopter. An attempt was subsequently made to optimise a simple model of the whole helicopter containing 20 nodes and 25 linearly tapered beam elements.

1.21. (Continued)

In this particular case it was required to minimise the response in the area of the pilot's seat subject to variations in the flexibility of elements in the engine-gearbox area. It was found that the procedure required approximately $1\frac{1}{2}$ hours of C.P.U. time for one computer run and the idea was consequently abandoned.

The results of the latter application demonstrate quite clearly one of the main disadvantages of formal optimisation procedures. It is apparent that in large structures there are often many thousands of parameters and to consider each of these as variables in an optimisation process would be beyond the scope of even the largest and most efficient of modern day computers. A reduced selection of the most likely parameters would therefore have to be chosen as the variables in the problem. However, this approach is not entirely satisfactory for there is no way of knowing whether the minimum solution achieved is a global minimum or just a local one, i.e. could a better solution have been achieved using a different set of parameters? The results from an optimisation process also give no indication as to the relative effectiveness of given parameters for the purpose of achieving a minimum solution, and by virtue of the predetermined way in which the search for this minimum is carried out the process effectively lacks the freedom which enables any sort of feel or insight into the problem to be obtained.

1.22. Small Perturbation Analysis as a Method of Determining the Sensitivity of Eigenvalues to Parameter Changes in Dynamical Systems.

The three methods outlined in this section can be used in an indirect manner to assess the effect of structural modifications on the dynamic response of a system. The methods attempt in one way or another to determine the sensitivity of eigenvalues to changes in certain

1.22. (Continued)

parameters of the system. It is assumed that if any close natural frequencies of the system can be moved away from the excitation frequency then this will result in a reduction of the total dynamic response of the system due to the contributions of the associated normal modes. Of the three methods examined only those of Sciarra are aimed directly at the reduction of structural response. The methods of Newman and Simpson are of a more academic nature and are aimed more specifically at the problem of flutter in aircraft lifting surfaces. The Methods of Sciarra. [16,17,18]

Sciarra considers the problem of reducing the dynamic response of a helicopter fuselage directly. Two distinct approaches are used, namely, dynamic vibration absorption and structural modification.

Vibration Absorbers.

A technique is developed that will predict the effect on structural response of introducing dynamic vibration absorbers into the system. The amount by which the vibration levels can be reduced at specified points in the structure is calculated and is used as a measure of the effectiveness of the absorber. Where more than one absorber is used then Sciarra shows that it is sometimes necessary to detune one or more of them in order to achieve the optimum reduction in vibratory response. Because of the weight penalty incurred by using vibration absorbers this approach is usually only used after an attempt has been made at structural modification.

Structural Modification.

In the second approach it is assumed that if the natural frequencies of the structure are moved away from the excitation frequency then this will result in a general lowering of the dynamic

1.22. (Continued)

response of the system. The problem thus reduces to one of assessing the effect of changes in structural parameters on particular natural frequencies of the system. The effectiveness of parameters is based on the strain energy of individual structural elements. In the first instance a finite element analysis is performed to yield the eigenvalues and eigenvectors of the system, then the modal strain energy distribution throughout the structure is found for the mode shape whose natural frequency is to be modified. The strain energies of each structural element are calculated and listed in descending order, those elements with the highest values are considered the best candidates for modification of the natural frequency. An alternative method of calculating the strain energies using the damped forced response in place of the mode shape is also mentioned. Sciarra points out that the procedure can be made more optimal from the point of view of minimising weight by considering strain energy densities rather than strain energy alone.

This technique is useful in that it indicates the potentially effective elements for the purpose of structural modification. The use of strain energy as an effectiveness criterion is seen to be relevant in as much that vibration levels were reduced using the suggested modifications; the method, however, does not give any direct indication as to the magnitude of the parameter changes that would be required.

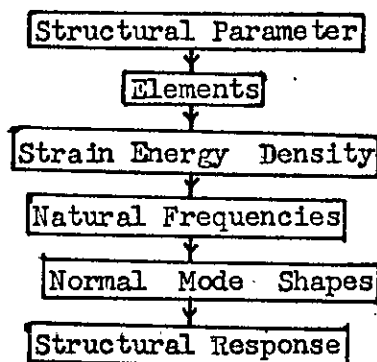
One way of resizing structural elements [30] is given as

$$\Delta t = \frac{\alpha (\text{strain energy density of the element})}{(\text{max strain energy density of any element})}.$$

where Δt is the change in the parameter (area, thickness, moment of inertia) and α is an arbitrary constant which represents the maximum allowable weight

1.22. (Continued)

penalty. It is not however, obvious whether the magnitude of the parameter change chosen in this way will produce the optimum reduction in vibration levels. The process by which real structural parameters are used to reduce the dynamic response is involved and contains several assumptions; the flow diagram shown in figure 1.3. represents this process.



The Route by which Structural Response is Affected by Changes in a Structural Parameter.

Figure 1.3.

The Method of Newman [1]

This method is aimed specifically at the problem of flutter of aircraft lifting surfaces, although the analysis could be applied to the equations of motion of any linear dynamical system. The technique involves the reduction of the general equations of motion of an N degree of freedom system to a set of first order differential equations of the form

$$\dot{\underline{q}}^* = \underline{M} \underline{q}^* \quad (1.1.)$$

Where $\dot{q}_1^* = q_{n+1}^* \quad i = 1, 2, \dots, n$

and $q_1^* = q_1^* \quad i = 1, 2, \dots, n$

1.22. (Continued)

q_i being the generalised coordinates of the system and \underline{M} is a $(2n \times 2n)$ matrix whose elements are functions of the system matrices such as mass, stiffness and damping. If λ_i are the eigenvalues of \underline{M} then the method sets out to determine the rate of change of λ_i with the individual elements of \underline{M} , i.e. to find $\frac{d\lambda_i}{dm_{jk}}$. This derivative is referred to as the condition number for the jk^{th} element of \underline{M} with respect to the i^{th} eigenvalue. Those elements with the largest condition numbers are considered to be the ones to which the eigenvalue is most sensitive.

The method can thus be used to identify the potentially effective elements for the purpose of altering a given eigenvalue. However, any change in a real structural parameter usually affects more than one element of matrix \underline{M} which may result in an undesirable effect on the eigenvalue under consideration. For the same reasons the reverse process of relating an element m_{ij} to any given parameter is complex, and consequently it is most likely that considerable difficulties would be experienced should this method be applied to a practical problem.

A method similar to that of Newman is given by Woodcock [19]. The method is used to calculate the eigenvalue sensitivities, only this time they are obtained without having to reduce the equations of motion of the system to a set of first order differentials.

The Method of Simpson [2]

In this method the sensitivities of eigenvalues to changes in structural parameters are determined using techniques suggested by Kron [20] for the solution of large scale eigenvalue problems. Kron's method can be applied to the solution of eigenvalue problems which are too large for a given computer to handle. The technique requires

1.22. (Continued)

that the composite system be split into N subsystems, for each of which the eigenvalues may be extracted easily. The equations of motion of the composite system are derived by recourse to the concept of a constrained primitive Lagrangian followed by an application of Hamilton's principle. An "Intersection Lambda" matrix is derived whose order is small compared with that of the composite system. The eigenvalues of this matrix are identical to those of the composite system and can be extracted quite easily.

Simpson considers a change in a structural parameter δ in one of the subsystems and develops an expression for the eigenvalue sensitivity $\frac{d\lambda}{d\delta}$; an expression for the eigenvector sensitivities is also developed. The method provides useful information concerning the sensitivities of eigenvalues directly in terms of real structural parameters, and unlike the methods of Newman and Woodcock the procedure is not further complicated if a structural parameter affects more than one element of the mass or stiffness matrices.

The methods of Newman, Simpson and Woodcock are very much of an academic nature and would probably contain serious limitations when applied to a truly practical problem. The method of Sciarra, on the other hand, has been developed from a practical view point and has been proved successful in its application.

1.3. Vibration Control Using Structural Manipulation.

The theory developed in this thesis is based on a little known property of linear structures that was first noticed by Vincent [3] of Westland Helicopters Ltd. If a structure is excited by a single sinusoidal force whilst either mass at a point or the stiffness between two points (as represented by a linear spring) is

1.3. (Continued)

continuously varied then the response in the complex plane at some other point is seen to trace out a circular locus. This simple yet elegant result forms the basis for all the subsequent analysis that is developed.

By way of an introduction to this approach the response of a single degree of freedom system is determined as a function of mass, stiffness and damping. The variation of all three of these parameters is seen to produce a circular locus. Throughout the analysis structural response is given in terms of receptances, i.e. response per unit force. The theory is extended to cover the case of parameter variations in multi-degree of freedom systems. For the variation of a single mass or stiffness parameter the simple circular locus is shown to exist. However, where two parameters are varied simultaneously an area of "feasible response" is found in the complex plane and for any given values of the two chosen parameters the resultant response must lie within the bounds of the feasible region. It will be shown that it is possible to determine whether a desired response is feasible or not for any given combination of parameters. A general matrix equation for the response as a function of M variable parameters is also developed.

With reference to the practical application of this theory, criteria are developed for the purpose of assessing the effectiveness or sensitivity of parameters; several of the properties of response circles and feasible response regions are incorporated in these. The criteria can be used to determine areas of a structure which are potentially effective in reducing vibration levels. The practical application of the theory is demonstrated using a simplified model of a helicopter fuselage. The analysis is undertaken in order to

1.3. (Continued)

highlight sensitive areas of the fuselage for structural modification in order to reduce vibration levels in the passenger and crew areas. The results are compared with those obtained from a practical analysis.

An experimental analysis is undertaken to verify the form of the circular response locus as a function of variable stiffness. The analysis is performed on a simple test structure in which the stiffness of a linear spring element is varied. The results obtained are compared with those predicted theoretically.

An interactive computer program is developed for the purpose of testing the theory. The program is used as an aid to the research process and also as a means of performing practical analyses on structures containing up to 60 degrees of freedom.

The methods outlined in the following chapters form the basis for a completely new approach to the problem of vibration reduction by means of structural modification. The method is intended to give a better understanding and also a "feel" for the problem, both of which are lacking in existing techniques.

CHAPTER 2

THE EFFECT OF PARAMETER CHANGES ON THE RESPONSE OF

A SINGLE DEGREE OF FREEDOM SYSTEM

2.1. Equations of Motion.

Although possibly of little practical importance, a brief study of the various parameter changes in a simple one degree of freedom system is helpful in understanding similar changes in more complicated cases. It is intended to show how the response of the system varies with frequency, mass, stiffness and damping.

The equations of motion of a single degree of freedom system subject to harmonic excitation at circular frequency ω may be written

$$m\ddot{x} + \frac{h\dot{x}}{\omega} + kx = Fe^{i\omega t} \quad (2.1)$$

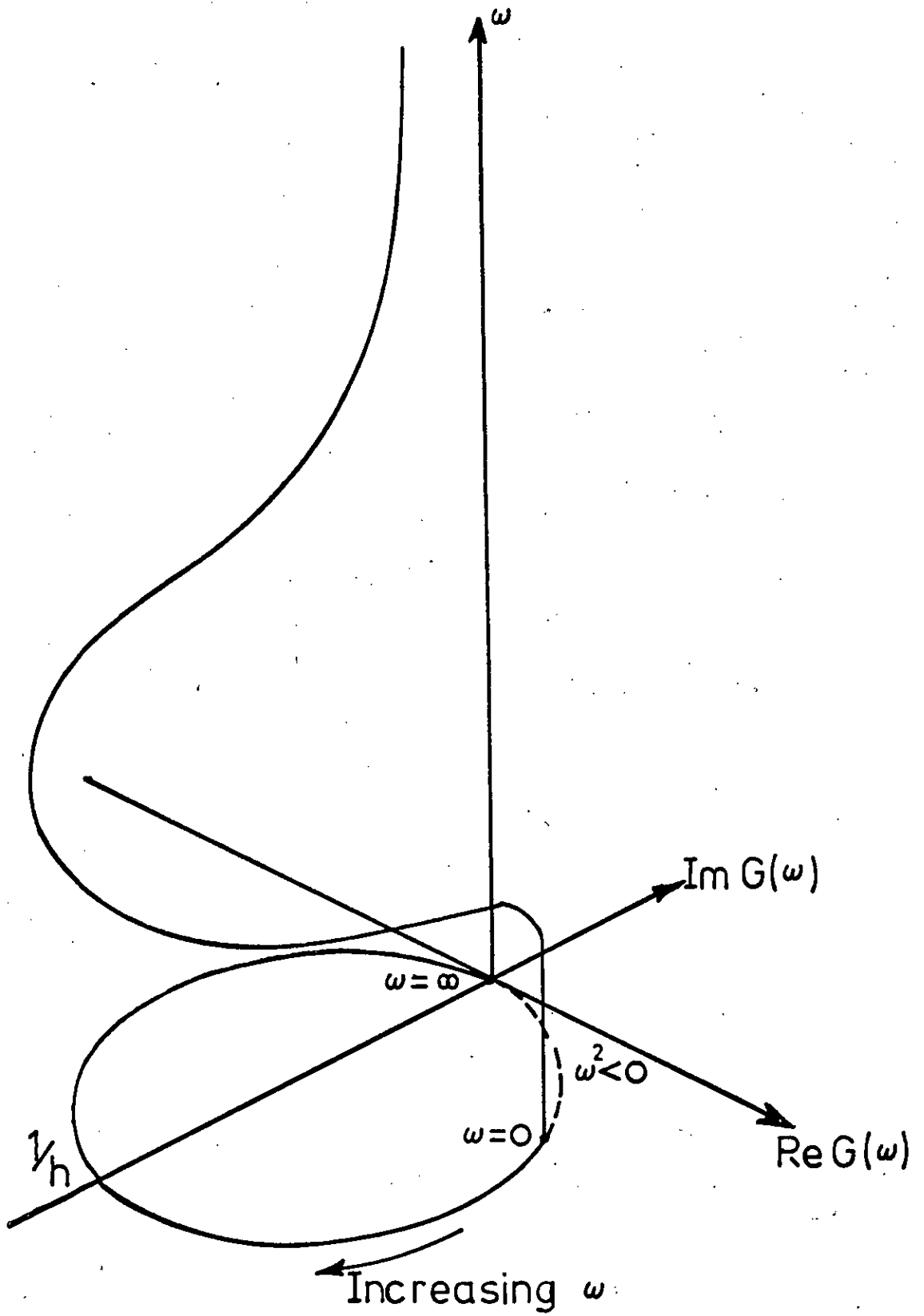
where m is the mass, k the stiffness and F the magnitude of the excitation. The damping, represented by constant h , is considered to be hysteretic in the analysis that follows. The steady state solution for the response is given by

$$x = G(\omega)Fe^{i\omega t} \quad (2.2)$$

where

$$G(\omega) = \frac{1}{(k - m\omega^2) + ih} \quad (2.3)$$

and is the complex receptance of the system. Since the receptance is the response per unit magnitude of excitation, it is this quantity that is considered in the ensuing analysis rather than the response itself.



The Response of a Single Degree of Freedom System
as a Function of Frequency

2.2. The Variation of Frequency.

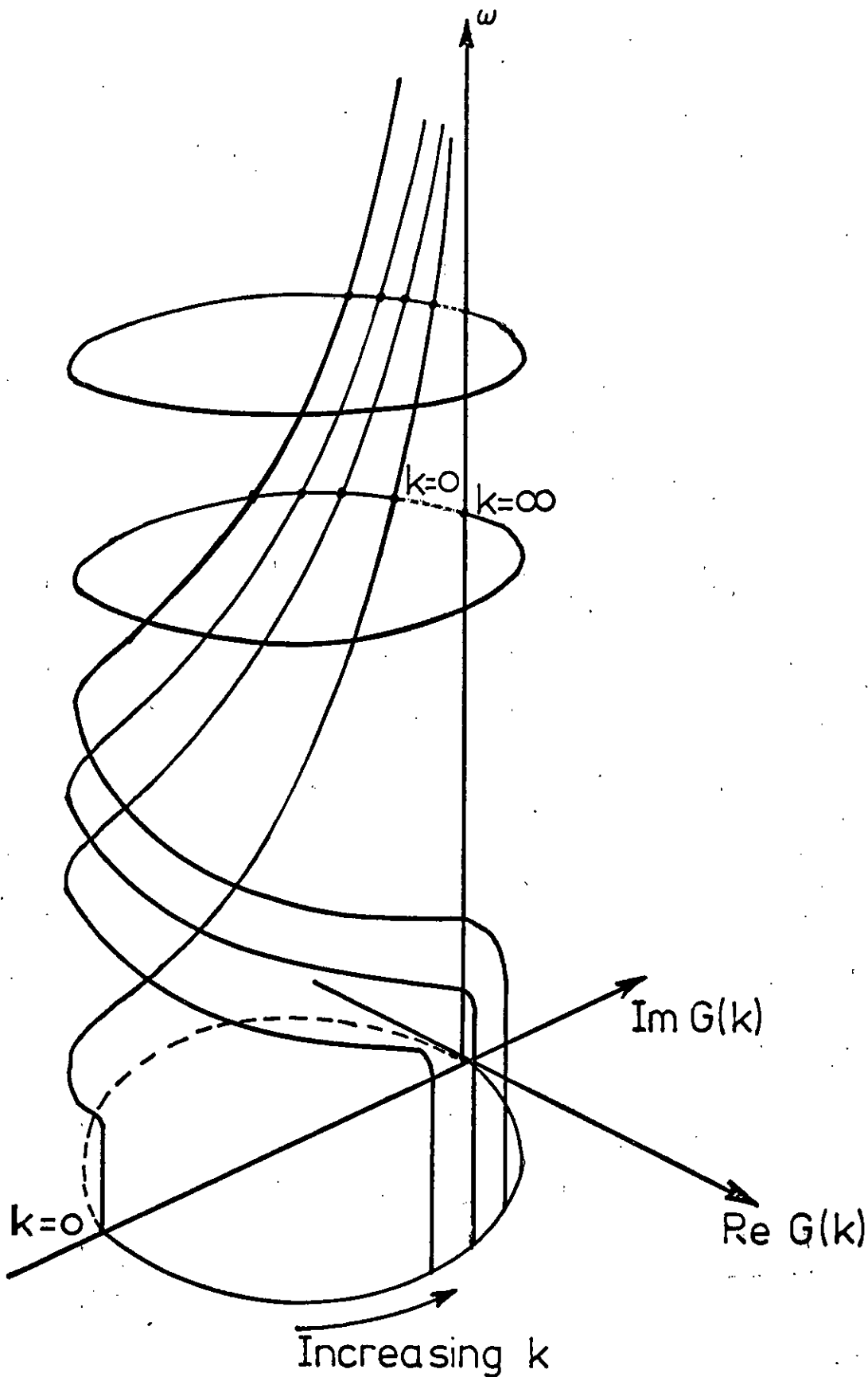
The results of varying frequency are well known and so need only be considered briefly. It can be shown that the locus of the tip of the receptance vector $G(\omega)$ in the complex plane, as ω varies, is a circle diameter $1/h$ passing through the origin and centre on the negative imaginary axis [4]. Figure 2.1. shows the circle as a projection of the three dimensional locus produced by including ω as the vertical coordinate. The complete circle can only be realised by considering imaginary values of ω i.e. $\omega^2 < 0$ (shown dotted in the figure). Various points of interest, including the direction in which the circle is traced out for increasing values of ω , are also shown.

2.3. The Variation of Mass and Stiffness.

The circular locus described in section 2.2. arises by virtue of the variation in the real part of the denominator $(k - m\omega^2)$ in equation 2.3. Thus, it may be seen that a variation in m or k produces the same locus. For increasing values of k the direction in which the locus is traced out (anti-clockwise) is opposite to that for increasing values of m and ω^2 . Arcs corresponding to negative values of m and k exist in a manner similar to that for $\omega^2 < 0$. Listed below are the coordinates in the complex plane corresponding to some of the more important values of m , k and ω .

$$\begin{array}{ll} \omega = m = k = \infty & [0, 0] \\ \omega = m = 0 & [k/(k^2 + h^2), -h/(k^2 + h^2)] \\ k = 0 & [-m\omega^2/(m^2\omega^4 + h^2), -h/(m^2\omega^4 + h^2)] \end{array}$$

If the circles for $G(k)$ are plotted in three dimensions for all values of ω , a circular cylindrical envelope is developed. Figure 2.2. shows a pictorial representation of this.



Response as a Function of Stiffness and Frequency
(One Degree of Freedom)

Figure 2.2.

2.3. (Continued)

Those parts of the loci corresponding to negative values of k are shown as dotted lines. In addition it is possible to plot, on the envelope, curves of constant k ; these are of the same type as those shown in Figure 2.1.

2.4. The Variation of Damping.

Varying the damping coefficient h in equation 2.3. produces a circular locus diameter $k/(k - m\omega^2)$ with its centre on the real axis and passing through the origin. Where $\omega > \sqrt{\frac{k}{m}}$ the circle lies on the positive real axis (for $\omega < \sqrt{\frac{k}{m}}$ on the negative real axis) and the locus is traced out in an anti-clockwise direction for increasing values of h (for $\omega < \sqrt{\frac{k}{m}}$ the direction is clockwise).

In practice inherent damping in a structure is a difficult quantity to model precisely and it is not envisaged that parameter changes of this form would be used to alter the structural characteristics. Consequently, the effects of changes in structural damping are not considered further in this analysis.

2.5. Conclusions.

It has been demonstrated that the independent variation of any of the parameters in a single degree of freedom system produces a simple circular locus in the complex plane. When an increase or decrease in stiffness is accompanied by a similar change in the mass, as is often the case in practice, a variation in one parameter tends to cancel out the effect of a change in the other; but clearly combinations of parameter changes do not further complicate the analysis.

It will be shown in Chapter 3 that the simple form of the circular locus carries over to systems with many degrees of freedom,

for varying mass and stiffness, but not for varying frequency.

CHAPTER 3

PARAMETER CHANGES IN MULTI-DEGREE OF FREEDOM SYSTEMS

3.1. Introduction.

The general case of an N degree of freedom system subjected to a single point excitation is considered. The response at any point in the structure is examined and the main properties are developed for the case of varying stiffness. At the end of the section varying mass is considered, and is seen to produce a response locus of the same type as that obtained for varying stiffness. The complete development of the theory for variable mass is shown to be unnecessary since, by implication, the properties and observations for this are similar to those appertaining to variable stiffness. A simple analogy is made between variable mass as a parameter and a special case of variable stiffness. In this way it is possible to use just one set of equations to describe the response at a point in a structure as a function of mass, stiffness or mixed parameters.

The effect on the response is examined for the variation of one, two and M stiffness parameters. Having developed the theory, certain facts and observations are made within the analysis; some information is given only on the grounds that it is interesting, whilst a fuller treatment and discussion of the application of the theory is given in Chapter 4.

3.2. Response as a Function of a Single Variable Stiffness

Parameter.

As in the single degree of freedom case, the response of the system is expressed in terms of receptances. The latter follow from

3.2. (Continued)

consideration of the equations of motion of an N degree of freedom system which may be written

$$\underline{M}\ddot{\underline{x}} + \underline{C}\dot{\underline{x}} + \underline{K}\underline{x} = \underline{F}e^{i\omega t} \quad (3.1)$$

where \underline{M} , \underline{C} and \underline{K} are the mass, damping and stiffness matrices respectively. The system is considered to be subject to harmonic excitation at circular frequency ω and, since no further advantage may be gained from using hysteretic damping, the damping is considered to be viscous. The steady state solution for the response is given by

$$\underline{\bar{x}} = \underline{x}e^{i\omega t} \quad (3.2)$$

where

$$\underline{x} = \underline{G}\underline{F} \quad (3.3)$$

$$\text{and } \underline{G} = [\underline{K} - \underline{M}\omega^2 + i\underline{C}\omega]^{-1} \quad (3.4)$$

which is the receptance matrix for the system. Figure 3.1. shows schematically the system to which the equations apply. It represents a structure having many degrees of freedom, for which it is required to examine the response at a material point q due to a single forced excitation at point p. The structure is modified by inserting a linear spring of stiffness k between points r and s having mutually compatible degrees of freedom. The spring is adjusted so as to exert zero force when the system is in equilibrium.

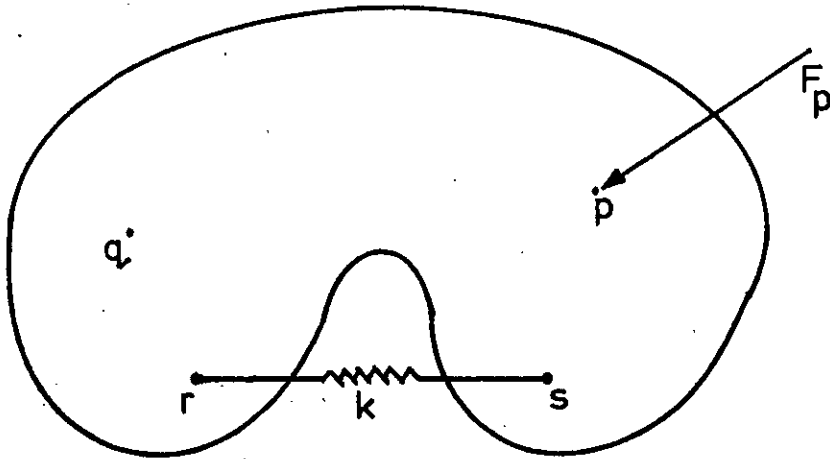


Figure 3.1.

Schematic Representation of the Structure and Variable Stiffness Element

Considering the original structure as a free body, the introduced spring exerts forces F_r and F_s at points r and s respectively, where

$$F_r = k(x_s - x_r) = -F_s \quad (3.5)$$

This gives a relationship between the parameter k and the structural variables of force and displacement. Equation 3.5 thus provides a rigorous definition of the form of the parameter change where stiffness is concerned. The forcing vector \underline{F} in equation 3.3 now contains three non-zero elements F_p , F_r and F_s , the latter two being dependent on the structural displacements x_r and x_s , whilst the elements of immediate

3.2. (Continued)

interest in the displacement vector \underline{x} are x_q , x_r and x_s . By partitioning and expanding the relevant parts of equation 3.3. we can write

$$\begin{aligned} x_q &= G_{qp} F_p + G_{qr} F_r + G_{qs} F_s \\ x_r &= G_{rp} F_p + G_{rr} F_r + G_{rs} F_s \\ x_s &= G_{sp} F_p + G_{sr} F_r + G_{ss} F_s \end{aligned} \quad (3.6)$$

Where G_{ij} is the complex receptance giving the displacement at point i due to a ^{unit} force at point j . The forcing terms F_r and F_s may be substituted from equation 3.5. and subsequent elimination of x_r and x_s in equation 3.6. gives

$$\frac{x_q}{F_p} = G_{qp} + \frac{k(G_{sp} - G_{rp})(G_{qr} - G_{qs})}{1 + k(G_{rr} + G_{ss} - G_{rs} - G_{sr})} \quad (3.7.)$$

This is now the modified complex receptance between points p and q in terms of the variable parameter k and the original receptances G_{ij} .

Equation 3.7. may be written in the more general form

$$\begin{aligned} \alpha &= u + iv \\ &= (e + if) + \frac{k(a + ib)}{1 + k(c + id)} \end{aligned} \quad (3.8)$$

where $\alpha = \frac{x_q}{F_p}$ and a, b, c, d, e and f are all real constants.

Now from equation 3.8.

$$(u - e) + i(v - f) = \frac{a + ib}{1/k + c + id}$$

and rearranging this gives

$$\frac{[1/k] + c + id}{(u - e)^2 + (v - f)^2} = \frac{(a + ib) [(u - e) - i(v - f)]}{(u - e)^2 + (v - f)^2}$$

3.2. (Continued)

then equating the imaginary parts and thus eliminating k leads to the equation

$$d [(u - e)^2 + (v - f)^2] = b(u - e) - a(v - f)$$

which on simplifying gives

$$\begin{aligned} [u - (e + b/2d)]^2 + [v - (f - a/2d)]^2 \dots \\ = \frac{a^2 + b^2}{4d^2} \end{aligned}$$

which is the equation of a circle radius $\sqrt{\frac{a^2 + b^2}{4d^2}}$

and centre $[e + b/2d, f - a/2d]$

Thus, as k varies between $-\infty$ and $+\infty$ the locus of the tip of the receptance vector α traces out a circle in the complex plane. It is interesting to note that equation 3.8. may be regarded as providing a mapping from the k plane, which is in general complex, to the α plane. This may be seen to be an example of the bilinear class of mappings represented by the general equation

$$w = \frac{ak + b}{ck + d}$$

where a, b, c and d are complex constants and for which it is known [7] that circles and straight lines (a circle with infinite radius) in the k plane map into circles or straight lines in the w plane. In this case we consider only real values of k , providing a straight line in the k plane, which maps into a circle in the α plane. If damping were incorporated into the stiffness by introducing an imaginary component into the parameter k , then, provided that both real and imaginary parts can be plotted on a straight line, the mapping on to the α plane is still a circle.

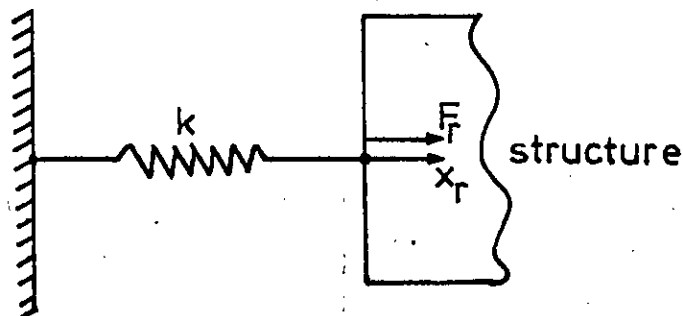
The geometric properties of the response circle in the α plane

3.2. (Continued)

depend on the constants a , b , c , d , e and f which in turn depend indirectly on the examination and forcing points and on the position of the introduced spring. Appendix A contains a table relating these constants to the complex receptances G_{ij} .

Equation 3.7. has been derived for the case where $p \neq q \neq r \neq s$. However, it is possible to consider conditions other than these, and listed below are the results for the combinations of p , q , r and s encountered in practice.

- (1) p or $q = r$ or s . It can be shown that equation 3.7 still applies with the relevant subscripts interchanged.
- (2) $p = q = r$ or s . The subscripts may be interchanged as in case (1).
- (3) r or $s = 0$. This can be interpreted as indicating that the introduced spring has one of its ends anchored to a ground reference point as shown below.



3.2. (Continued)

In this case

$$F_r = -kx_r$$

and expanding equation 3.3. as before we obtain

$$\frac{x_q}{F_p} = \frac{G_{qp} + k \frac{(-G_{rp} G_{qr})}{1 + kG_{rr}}}{1 + kG_{rr}} \quad (3,9)$$

This result may be obtained directly from equation 3.7. by considering the subscript s to be zero, with the condition that $G_{ij} = 0$ where i or j = 0. Thus, a zero subscript may be taken as referring to a rigid point for which the cross receptance between this and any other point is zero. It can now be seen that one equation, namely equation 3.7. can be used for all possible values and combinations of p, q, r and s.

In the latter half of this section some of the more important properties of response circles are examined with a view to obtaining a better understanding of how a particular parameter change affects the response of the system.

In equation 3.8. the complex receptance $\alpha = \frac{x_q}{F_p}$ may be

split into its real and imaginary components which are

$$u = e + \frac{k [a + k(ac + bd)]}{1 + 2ck + k^2(c^2 + d^2)} \quad (3.10)$$

$$v = f + \frac{k [(b + k(bc - ad)]}{1 + 2ck + k^2(c^2 + d^2)} \quad (3.11)$$

These equations lead to the coordinates of two important points on the response circle, namely those at which $k = 0$ and $k = \infty$; substituting these values in equations 3.10. and 3.11. gives

$$k = 0 \dots\dots [e, f]$$

3.2. (Continued)

$$k = \infty \dots \dots \left[\begin{array}{cc} e + \frac{ac + bd}{c^2 + d^2}, & f + \frac{bc - ad}{c^2 + d^2} \end{array} \right]$$

It is these two points which bound the arc of the circle corresponding to negative values of k . There are, however, two arcs to choose from, and it is necessary to determine the direction in which the locus is traced out for increasing values of k before any decision can be made.

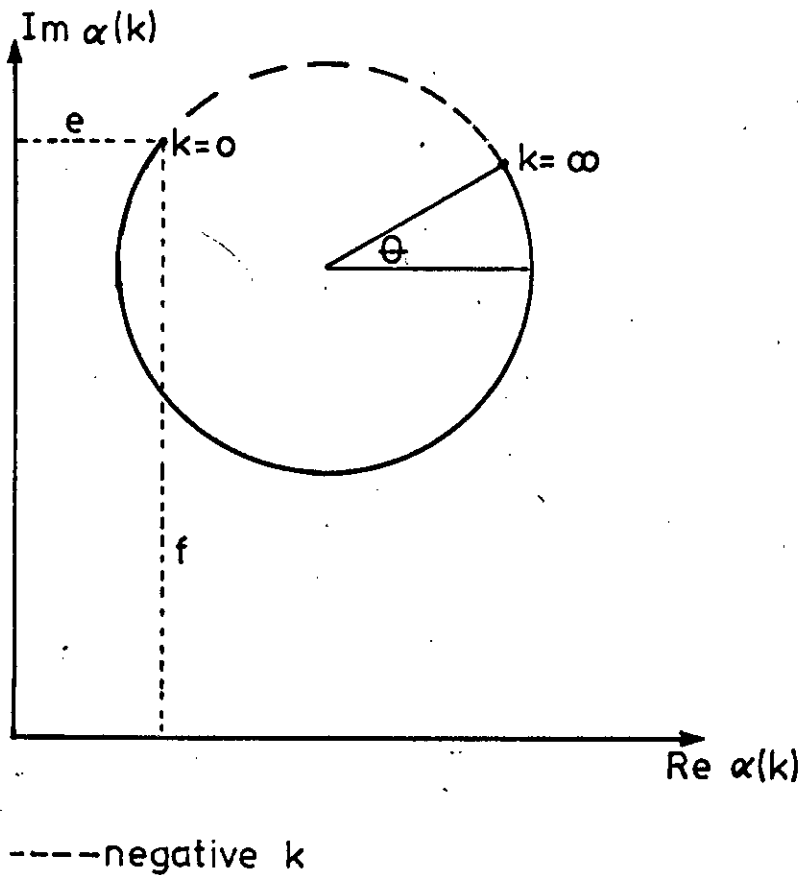


Figure 3.2.

Response Circle for Varying Stiffness

3.2. (Continued)

Figure 3.2. represents a typical response circle and Θ defines the angle between its horizontal diameter and any other point corresponding to a given value of k . From equation 3.10. and equation 3.11.

Θ can be obtained as a function of k and may be written

$$\Theta = \pi/2 + \tan^{-1} \left[\frac{b/d}{a/d} \right] - 2 \tan^{-1} \left[\frac{dk}{1 + ck} \right] \quad (3.12)$$

The constant d in the second term in the above equation is not cancelled since its sign plays a significant part in determining the quadrant in which the angle Θ lies. In order to determine whether Θ is an increasing or decreasing function of k , it is necessary to calculate $\frac{d\Theta}{dk}$ from equation 3.12. Thus, by differentiating with respect to k , we obtain

$$\frac{d\Theta}{dk} = \frac{-2d}{(1 + ck)^2 + d^2 k^2} \quad (3.13)$$

from which it can be seen that the locus travels in an anti-clockwise direction for the negative values of the constant d that invariably occur in practice. In addition to this, it is interesting to note that the point at which $\frac{d\Theta}{dk}$ is a maximum, i.e.

$$k = \frac{-c}{c^2 + d^2}$$

is displaced by 90° round the circle from the point at which $\frac{d\Theta}{dk}$ is a minimum (in fact zero, occurring at $k = \infty$). The rate of change of Θ with k is a useful quantity in that it bears a direct relationship to the ability of any given parameter to change the response of the system. This property can be seen from equation 3.13. to depend only on the position of the introduced spring and not on the examination and forcing points q and p . Equation 3.12. can be rearranged to

3.2. (Continued)

give k as a function of Θ i.e.

$$k = \frac{\tan p}{d - c \tan p}$$

where

$$p = \frac{\pi/4 + \tan^{-1} \left[\frac{b/d}{a/d} \right]}{2} - \frac{\Theta}{2}$$

This is an extremely useful equation, particularly in the computational side of the analysis where it is often necessary to calculate the stiffness value corresponding to a given response.

At the beginning of this section, it was assumed that the stiffness parameter k was real. However, the implication of this on the bounded nature of the response is not immediately obvious. In order to clarify this point, consider equation 3.10. with the constant e omitted for convenience

$$u = \frac{k [a + k (ac + bd)]}{1 + 2ck + k^2 (c^2 + d^2)} \quad (3.14)$$

This gives the real coordinate of the response as a function of k .

Equation 3.14. may now be rearranged to give a quadratic in k which is

$$k^2 [u(c^2 + d^2) - (ac + bd)] + k (2cu - a) + u \quad (3.15)$$

$$= 0$$

Solving this equation for k yields two roots for any given value of

u , and if these roots are to be real, as is the requirement in practice, then the following condition must be satisfied

$$4u^2 d^2 - 4ubd - a^2 < 0 \quad (3.16)$$

By considering the limiting case where equation 3.16. is zero and solving for u , then

3.2. (Continued)

$$u = \frac{b \mp \sqrt{a^2 + b^2}}{2d}$$

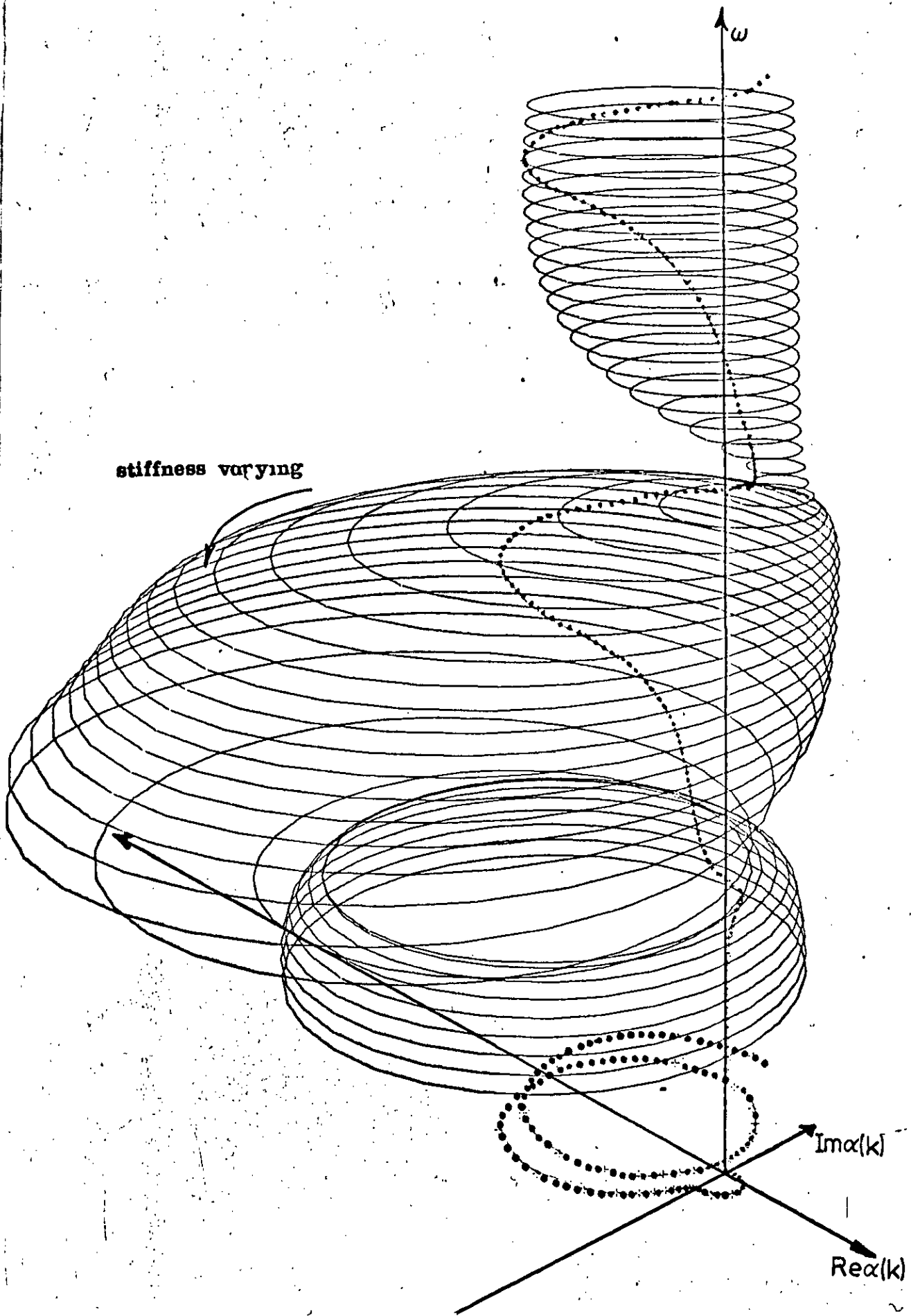
which corresponds to the real coordinate for the centre of the response circle plus or minus its radius. The imaginary component for the response given by equation 3.11. may be analysed in exactly the same manner, and is found to yield the result that

$$v = \frac{-a \mp \sqrt{a^2 + b^2}}{2d}$$

for the condition that k is real. When these two observations are taken together, the implication is that there are finite limits imposed on the maximum and minimum size of the receptance vector owing to the real nature of the parameter k .

As with the single degree of freedom case (see Figure 2.2.) it is possible, by introducing the forcing frequency ω as a coordinate, to construct a surface corresponding to a given stiffness parameter upon which three dimensional response curves can be drawn for various values of that parameter. Figure 3.3. shows a pictorial representation of a typical surface, the response curve corresponding to $k = 0$ (shown dotted) is projected below on to the complex plane. The latter is often referred to as the Kennedy-Pancu plot for the system.

In the last half of this section, consideration has been given to some of the properties of response circles in the complex plane. In Chapter 4 these will be expanded and discussed in more detail, and a description will be given of how these principles can be applied to practical examples



Response as a Function of Stiffness and Frequency

Figure 3.3.

3.3. Response as a Function of Two Parameters.

As in Section 3.2., the response at point q, on the structure, due to a force at point p, is sought. This time the variable stiffness elements k_1 and k_2 are connected between points r, s and t, v respectively. The forces F_r , F_s , F_t and F_v are given by

$$\begin{aligned} F_r &= k_1 (x_s - x_r) = -F_s & (3.17) \\ F_t &= k_2 (x_v - x_t) = -F_v \end{aligned}$$

Equations 3.3. can again be used to give the relevant equations

$$\begin{aligned} x_i &= \sum_j G_{ij} F_j & i = q, r, s, t, v & (3.18) \\ & & j = p, q, r, s, t, v \end{aligned}$$

substituting for F_r , F_s , F_t and F_v in equations 3.18. and eliminating x_r , x_s , x_t and x_v gives

$$\frac{x_q}{F_p} = G_{qp} + \frac{k_1 \phi_1(k_2) + \phi_2(k_2)}{k_1 \phi_3(k_2) + \phi_4(k_2)} \quad (3.19)$$

where $\phi_i(k_2)$ are complex linear functions of k_2 and are given in full in Appendix B. In order to understand how the locus of $\frac{x_q}{F_p}$ in equation 3.19. appears on the complex plane as k_1 and k_2 vary simultaneously it is necessary to examine how the function behaves when one parameter varies and the other is held constant. If, for instance, k_1 is held constant whilst k_2 is allowed to vary then it can be seen that equation 3.19 provides a mapping of the same type as that given in equation 3.7., i.e. it results in a circular locus. If k_1 assumes a different value then another circular locus is produced as k_2 varies. If all possible values of k_1 are considered then the corresponding k_2 loci lie on the circular locus for the system when k_1

3.3. (Continued)

alone is varying. This is illustrated in Figure 3.4.

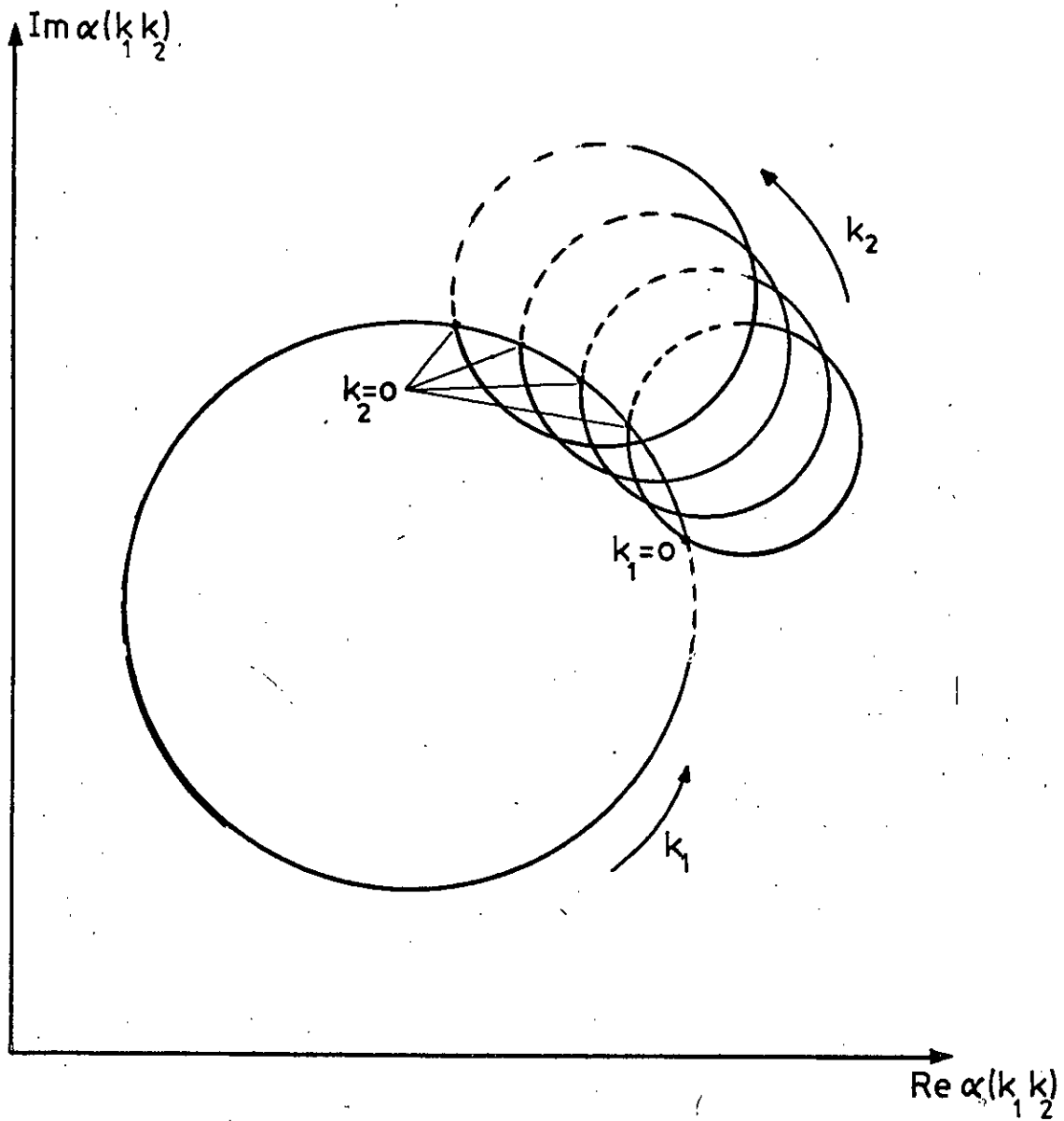
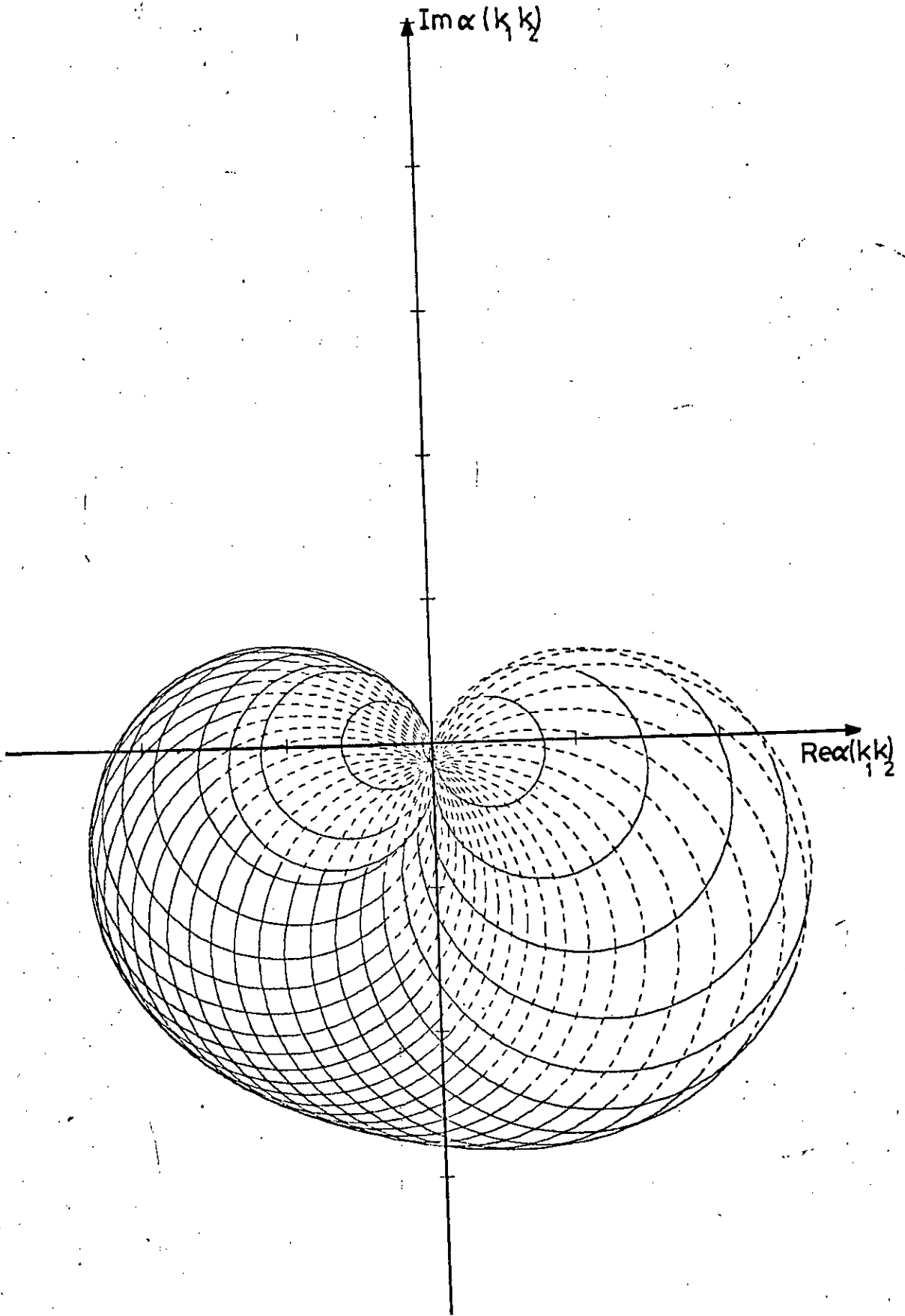


Figure 3.4.

Response Circles for Two Structural Parameters

3.3. (Continued)

By considering all possible combinations of k_1 and k_2 , a region in the complex plane is formed, inside which the response at point q due to an oscillatory force at point p must lie. This is referred to as a "Feasible Response Region". Figure 3.5. shows an example produced in the same manner as indicated in Figure 3.4.



Feasible Response Region made up of Response Circles.

Figure 3.5.

3.3. (Continued)

On examination the region appears to have two boundaries and is doubly covered, i.e. a given response may be achieved using either of two pairs of values of k_1 and k_2 . The boundaries, however, do not exhibit this property, for it may be deduced from the graphical construction that on any boundary the circles for k_1 and k_2 intersect at a tangent. Thus, there can only exist one pair of values of k_1 , k_2 for each point on the boundary. These facts may now be obtained in a more rigorous fashion. Mathematically the boundaries are given when the Jacobian

$\partial(u,v) / \partial(k_1,k_2)$
is zero [6] i.e.

$$\begin{vmatrix} \frac{\partial u}{\partial k_1} & \frac{\partial u}{\partial k_2} \\ \frac{\partial v}{\partial k_1} & \frac{\partial v}{\partial k_2} \end{vmatrix} = 0$$

or, alternatively

$$\text{Im} \left[\frac{\partial \alpha}{\partial k_1} \cdot \overline{\frac{\partial \alpha}{\partial k_2}} \right] = 0 \quad (3.20)$$

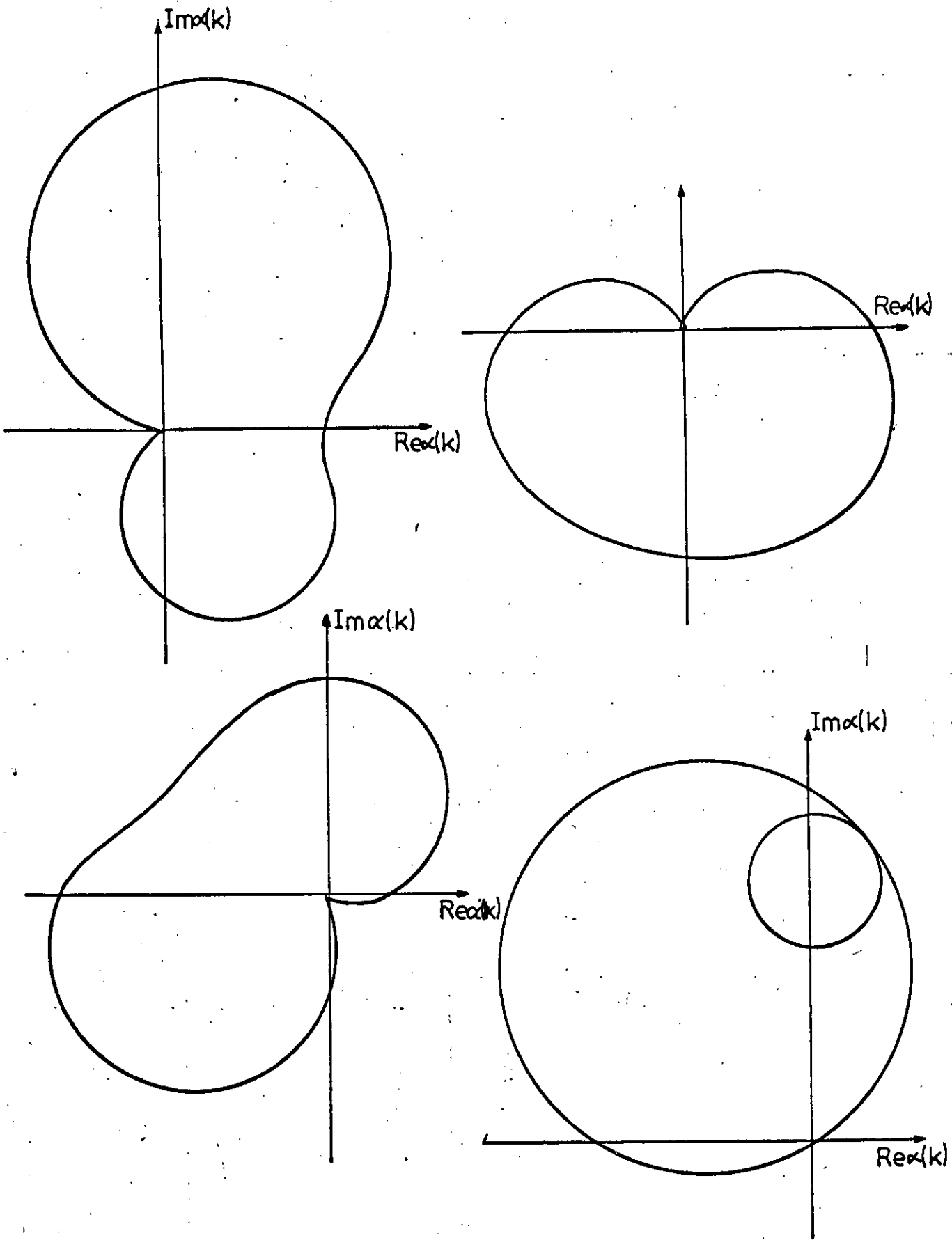
where $\overline{\frac{\partial \alpha}{\partial k_2}}$ is the complex conjugate of $\frac{\partial \alpha}{\partial k_2}$ and

$$\alpha = u + iv = \frac{x_q}{F_p}$$

Equation 3.20 is of second order in k_1 and k_2 , thus confirming the possible existence of two boundaries. By virtue of the fact that the values of k_1 and k_2 on these boundaries are uniquely defined it is possible to calculate their coordinates directly. Substituting a

3.3. (Continued)

range of values for k_1 into equation 3.20. (see Appendix C for expanded version of this equation) the two corresponding values of k_2 (one for each boundary) and hence the coordinates of that point may be calculated. By choosing enough values of k_1 the boundaries may be plotted directly. Figure 3.6. shows some examples of typical Feasible Regions. The system for which these were calculated is described in Appendix D.



The Boundaries of Some Typical Feasible Response Regions.

Figure 3.6.

3.4. Response as a General Function of M Variable Parameters.

In Section 3.3. the setting up and reduction of equations 3.6. to give a single expression for the complex receptance in equation 3.7. becomes rapidly more complex as the number of variables considered increases. As a consequence of this a general matrix expression for the complex receptance, in terms of M variable parameters, is developed.

The response at the examination point q may be written in terms of the external force, internal spring force and the corresponding receptances G_{ij}

$$x_q = G_{qp} F_p + k_1 \delta_1 (G_{q1} - G_{q2}) + k_2 \delta_2 (G_{q3} - G_{q4}) \dots$$

$$\dots + k_m \delta_m (G_{q, 2m-1} - G_{q, 2m}) \quad (3.21)$$

where k_i is the i^{th} variable stiffness parameter and

$$\delta_i = x_{2i} - x_{2i-1}$$

is the extension of the i^{th} spring (x_{2i} and x_{2i-1} being the actual displacement at each end). Equation 3.21. may be alternatively expressed

$$x_q = G_{qp} F_p + \underline{AK} \underline{\delta} \quad (3.22)$$

Where \underline{A} is a $(1 \times m)$ row vector of terms

$$\left\{ (G_{q1} - G_{q2}), (G_{q3} - G_{q4}) \dots (G_{q,2m-1} - G_{q, 2m}) \right\}$$

\underline{K} is the $m \times m$ diagonal matrix of stiffness parameters k_i , and $\underline{\delta}$ is a $(m \times 1)$ column vector of extensions.

The values of δ_i may themselves be expressed in the same way as x_q in equation 3.22.

$$\delta_1 = F_p (G_{2p} - G_{1p}) - \delta_1 k_1 [(G_{22} - G_{21}) - (G_{12} - G_{11})] -$$

$$k_2 \delta_2 [(G_{24} - G_{23}) - (G_{14} - G_{13})] \dots$$

3.4. (Continued)

$$\begin{aligned} \delta_2 &= F_p (G_{4p} - G_{3p}) - \delta_1 k_1 [(G_{42} - G_{41}) - (G_{32} - G_{31})] \dots\dots \\ &\vdots \\ \delta_m &= F_p (G_{2m,p} - G_{2m-1,p}) \dots\dots - k_m \delta_m [(G_{2m,2m} - G_{2m,2m-1}) \\ &\quad - (G_{2m-1,2m} - G_{2m-1,2m-1})] \end{aligned} \quad (3.23)$$

This may also be written in matrix form $\underline{\delta} = \underline{F}_p \underline{B} - \underline{CK} \underline{\delta}$ which gives $\underline{\delta} = [\underline{I} + \underline{CK}]^{-1} \underline{F}_p \underline{B}$ (3.24)

Where \underline{B} is the $(m \times 1)$ column vector of terms.

$$\left\{ (G_{2p} - G_{1p}), (G_{4p} - G_{3p}) \dots\dots (G_{2m,p} - G_{2m-1,p}) \right\}$$

and \underline{C} is the $(m \times m)$ matrix of complex constants whose elements are given by

$$C_{ij} = (G_{2i,2j} - G_{2i,2j-1}) - (G_{2i-1,2j} - G_{2i-1,2j-1})$$

The expression for $\underline{\delta}$ in equation 3.24. may be substituted into equation 3.22. to give

$$\frac{x_q}{F_p} = G_{qp} + \underline{A} [\underline{K}^{-1} + \underline{C}]^{-1} \underline{B} \quad (3.25)$$

which provides the complex receptance $\frac{x_q}{F_p}$ as a general function of m

variable stiffness parameters. Although any number of parameters may be considered, the reduction of equation 3.25. to give a single expression is still complicated by the inversion of the terms in the brackets.

3.5. Variable Mass.

In order to understand what effect a variation of mass has on the response of a system, it is necessary to consider what forces an additional mass exerts on a point in an accelerating structure.

3.5. (Continued)

Consider a point x_r with acceleration \ddot{x}_r at which an additional mass m is attached. The inertia force exerted on that point is given by

$$F_r = -m\ddot{x}_r \quad (3.26)$$

using the solution for \bar{x} given in equation 3.2. F_r may be obtained directly in terms of the displacement x_r i.e.

$$F_r = m\omega^2 x_r \quad (3.27)$$

As in Sections 3.2. and 3.3. equation 3.3. may be expanded to give

$$x_q = G_{qp} F_p + G_{qr} F_r \quad (3.28)$$

$$x_r = G_{rp} F_p + G_{rr} F_r$$

Substituting for F_r from equation 3.27. and eliminating x_r between equations 3.28 gives the following expression for the receptance as a function of the variable parameter m .

$$\frac{x_q}{F_p} = G_{qp} + \frac{m\omega^2 G_{qr} G_{rp}}{1 - m\omega^2 G_{rr}} \quad (3.29)$$

This is of the same form as equation 3.7. and thus results in a circular locus on the complex plane as m varies between $-\infty$ and $+\infty$. The direction in which the locus travels can again be shown to depend on the sign of the constant d as defined in Section 3.2. The negative values of d found in practice combined with the negative sign in the denominator of equation 3.29 cause the locus to travel in a clockwise direction for increasing values of m ; this agrees with the results obtained for the single degree of freedom case.

Having shown that varying mass produces circular locus in the complex plane, it can be further demonstrated that the equations and properties of response circles derived for varying stiffness also

3.5. (Continued)

apply for varying mass. To do this an analogy must be drawn between mass and stiffness as variable parameters. Consider a grounded stiffness parameter attached at a point x_r in the structure. The force the spring exerts on that point is given by

$$F_r = -kx_r \quad (3.30)$$

Now the force exerted by an additional mass, m , at the same point x_r is given by

$$F_r = m^* x_r \quad (3.31)$$

where $m^* = m\omega^2$. Equation 3.31. is identical to equation 3.30 apart from the change in sign of the parameter. Thus, the general equation for the response which is given by

$$\frac{x_q}{F_p} = G_{qp} + \frac{k(G_{sp} - G_{rp})(G_{qr} - G_{qs})}{1 + k(G_{rr} + G_{ss} - G_{rs} - G_{sr})} \quad (3.32)$$

may be used for varying mass if those constants multiplied by the parameter k are modified by changing their signs. Now, for the mass parameter defined in equation 3.31. the response equation 3.32.

becomes

$$\frac{x_q}{F_p} = G_{qp} + \frac{k(G_{rp}G_{qr})}{1 - kG_{rr}} \quad (3.33.)$$

where all the G_{ij} with a subscript s are set to zero and the signs of those remaining constants which are multiplied by k are changed.

Since equation 3.33. refers to variable mass, then

$$k \equiv m^* \equiv m\omega^2$$

and

$$\frac{x_q}{F_p} = G_{qp} + \frac{m\omega^2(G_{rp}G_{qr})}{1 - m\omega^2 G_{rr}}$$

3.5. (Continued)

which is identical to equation 3.29. The simplicity of this approach can also be used in the equation describing the response as a function of two variable parameters. Thus, it is possible to use just one set of universal equations which apply for mass, stiffness and mixed combinations of parameters. It should be remembered that in using this method the mass parameter refers to m^* and should be divided by ω^2 to obtain the true value of the parameter m .

CHAPTER 4

THE ASSESSMENT AND EFFECT OF PARAMETER CHANGES

4.1. Introduction.

The theory governing parameter changes in both single and multi-degree of freedom systems has been developed in the two previous chapters. In Chapter 4 the techniques involved in the practical application of this theory are discussed. Particular emphasis is placed on the ability of any given parameter or parameters to change the response at a specified point in a structure; this ability is interpreted as being representative of the effectiveness of those parameters. Several criteria are developed which enable the effectiveness of the parameters to be measured.

Other aspects considered here include the feasibility of achieving a desired response, minimum responses and the relationship between idealised parameters and those encountered in real structures. In the last section, some interesting, but less well developed, techniques are discussed, including the case where multiple responses are examined as functions of structural parameters.

4.2. The Feasibility of Achieving a Desired Response Using One or Two Parameters.

4.2.1. A Single Variable Parameter.

In the most general case it is required to know whether or not a specified response is feasible using just one variable parameter. The desired response is given in terms of its real and imaginary components in the complex plane. These components may be obtained as functions of the chosen stiffness parameter k and are given by

4.21. (Continued)

$$u = e + \frac{k(a + k(ac+bd))}{1 + 2ck + k^2(c^2+d^2)} \quad (4.1)$$

and

$$v = f + \frac{k(b + k(bc-ad))}{1 + 2ck + k^2(c^2 + d^2)} \quad (4.2)$$

If the required response is feasible, then it should be possible to choose a value of k which when substituted into equations 4.1. and 4.2. yields the desired coordinates. The condition for feasibility may be determined mathematically by re-arranging equations 4.1. and 4.2. into quadratics in k . These are respectively

$$k^2((u-e)(c^2+d^2) - (ac+bd)) + k(2c(u-e)-a) + (u-e) = 0 \quad (4.3)$$

and

$$k^2((v-f)(c^2+d^2) - (bc-ad)) + k(2b(v-f)-b) + (v-f) = 0 \quad (4.4)$$

By substituting the desired coordinates (u,v) into the above equations, and then solving for k in each, it is possible to determine whether or not the response is feasible. The condition is simple; if any of the four roots of the equations are imaginary, then the response is not feasible. Where all four roots are real, then the one coincident root in each pair is the value of k that will provide the desired response.

Although this general approach does cover all possible response requirements, it is found that in most practical cases of manipulating a structure to produce a desired vibratory response, the aim would be to minimise the response over all or part of the structure. (An exception to this would be in order to change a normal mode shape). Thus, in the case where zero or a minimum response is sought, then a slightly different approach to the solution of the problem is needed.

4.21. (Continued)

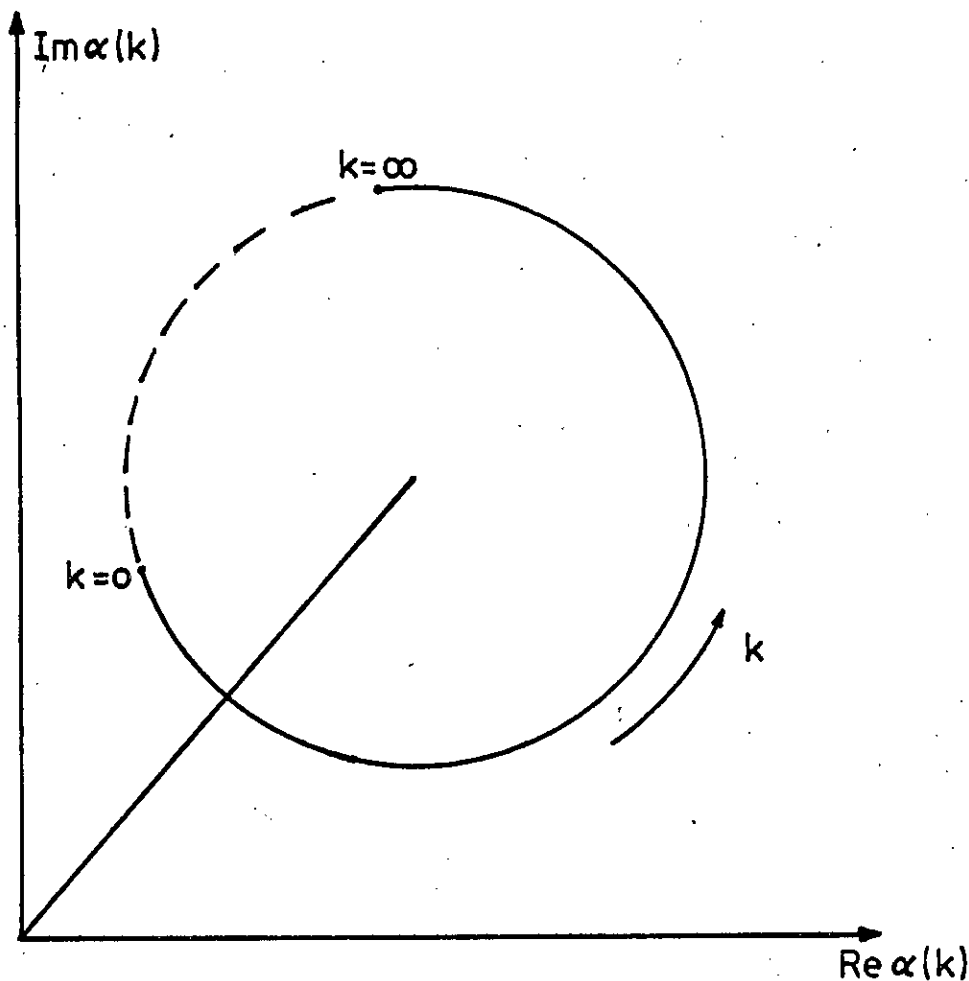


Figure 4.1.

Calculating the Minimum Response for a Given Parameter

Figure 4.1. shows a typical response circle. The value of k corresponding to the minimum response vector is given by the intersection of the circle and the straight line joining the centre of the circle to the origin. The minimum response may alternatively be calculated by considering the square of the magnitude of the response vector $|\alpha|^2 = (u^2 + v^2)$. The value of k corresponding to the minimum of $|\alpha|^2$ is the same as that for $|\alpha|$. Substituting for u and v from equations 4.1. and 4.2. gives $|\alpha|^2$ as a function of k

$$|\alpha|^2 = \frac{(Ak^2 + Bk + C)}{(Pk^2 + Qk + R)} \quad (4.5)$$

4.21. (Continued)

where A, B, C, P, Q and R are real constants and are defined in Appendix I. The minimum value of $|\alpha|^2$ is obtained by differentiating equation 4.5. with respect to k and equating the result to zero.

This leads to the following quadratic in k

$$k^2(AQ-BP) + 2k(AR-CQ) + (BR-PC) = 0 \quad (4.6)$$

The roots of this equation are the values of k corresponding to the maximum and minimum values of $|\alpha|^2$. Which of the two values of k corresponds to the minimum value of $|\alpha|^2$ may be determined in the usual way by substituting each value in turn into the second derivative of $|\alpha|^2$ with respect to k and examining the sign of the resultant. The first and second derivatives of $|\alpha|^2$ with respect to k are given in Appendix I.

4.22. Two Variable Parameters.

Determining the feasibility or minimum of a response using only one variable parameter poses few problems mathematically. However, the solution to the same problems becomes somewhat more complicated when considering two or more parameters. The advantages of using two parameters as opposed to one are considerable, for if a desired response is to be attainable, then it must lie within the corresponding feasible response region as defined in Chapter 3, Section 3.3. The chances of achieving a desired response are thus greatly increased using two parameters, and so indeed is the possibility of achieving zero response.

The direct calculation of the minimum of a response as a function of two parameters is complex mathematically and is not considered here. Far more important is the possibility of achieving zero response, i.e. does the relevant feasible region encompass the origin? Consider first the general case of the feasibility of any response $\alpha = u + iv$. The response



4.22. (Continued)

vector may be written as a function of the two stiffness parameters k_1 and k_2

$$\alpha = A + iB + \frac{\theta_1 + i\theta_2}{\theta_3 + i\theta_4} \quad (4.7)$$

where A and B are real constants and θ_1 are linear functions of k_1 and k_2 as defined in Appendix C. The desired response coordinates (u,v) may be substituted into equation 4.7. and, re-arranged, this gives

$$(B-v)\theta_4 - (A-u)\theta_3 - i((A-u)\theta_4 + (B-v)\theta_3) = \theta_1 + i\theta_2 \quad (4.8)$$

Equating the real and imaginary parts of equation 4.8. in turn gives

$$\theta_1 = (B-v)\theta_4 - (A-u)\theta_3 \quad (4.9)$$

$$\theta_2 = (A-u)\theta_4 - (B-v)\theta_3 \quad (4.10)$$

Equation 4.9. may be re-arranged to give k_1 as a function of k_2 which is then substituted into equation 4.10. to give a quadratic in k_2 . If the roots of this quadratic are real, then the desired response is feasible and the corresponding values of k_1 can be determined by substituting the calculated values of k_2 into equation 4.9. and solving for k_1 . Either of the two pairs of values of k_1 and k_2 may be used to achieve the desired response. The feasibility of zero response is just a special case of this analysis and needs no further explanation.

Although the ability to determine the feasibility of a response is useful in itself, it does not give any indication as to the effectiveness of the parameter or parameters being used to achieve that response. However, it could be argued that if a given response is feasible then the parameter that produces that response must be totally effective for the purpose for which it was intended. Thus, it is

4.22. (Continued)

possible to use feasibility as an effective criterion. The exact definition of this will be given in Section 4.4.

4.3. The Criteria Governing the Effectiveness of Parameter Changes.

Prior to the development of any criteria for the purpose of judging the effectiveness of parameters, it is necessary to define just what it is that the parameters are required to be effective in doing. The objectives of any given parameter change may be categorised into one of three groups, namely,

- i) to achieve any general response;
- ii) to achieve a minimum response;
- iii) to achieve zero response.

Having defined and chosen a suitable objective, attention may now be focused on the parameters themselves in an attempt to determine which of the available selections is most effective in achieving the desired goal. In the cases of (i) and (iii), if the objective is achieved, then it is not possible to judge one parameter as being more effective than another. Where a minimum response is required, the effectiveness criterion is the size of the minimum response obtained for each parameter; the smaller the value the more effective the parameter is. Minimum response is not so much a measure of sensitivity, but a simple statement of the ability of a parameter to achieve zero response. In this instance and those that follow, effectiveness is not considered to be an absolute quantity but is intended to refer to the relative merits of parameters.

In practical applications of structural manipulation, it is advantageous to be able to recognise regions in a structure which are more effective than others in producing changes in a specified response.

4.3. (Continued)

The existence of such regions can be identified by the presence of an abundance of effective parameters within them. These parameters, however, are not required to be effective in producing a specific response, but should possess the ability to affect changes in the response over as wide a range as possible. In this instance, the diameter of the response circle is chosen as the effectiveness criterion, and is considered to be representative of the ability of that parameter to change the response under consideration. By calculating the circle diameters for all the available parameters, their relative effectiveness may be determined.

Where the aim of the process of manipulation is to reduce the response at a point in the structure to a minimum, then the latter criterion may be modified slightly to take this into account. Consider the two response circles shown in Figure 4.2. corresponding to parameter k_1 and parameter k_2 . On the basis of circle diameter parameter k_1 would be considered to be more effective in changing the response than parameter k_2 .

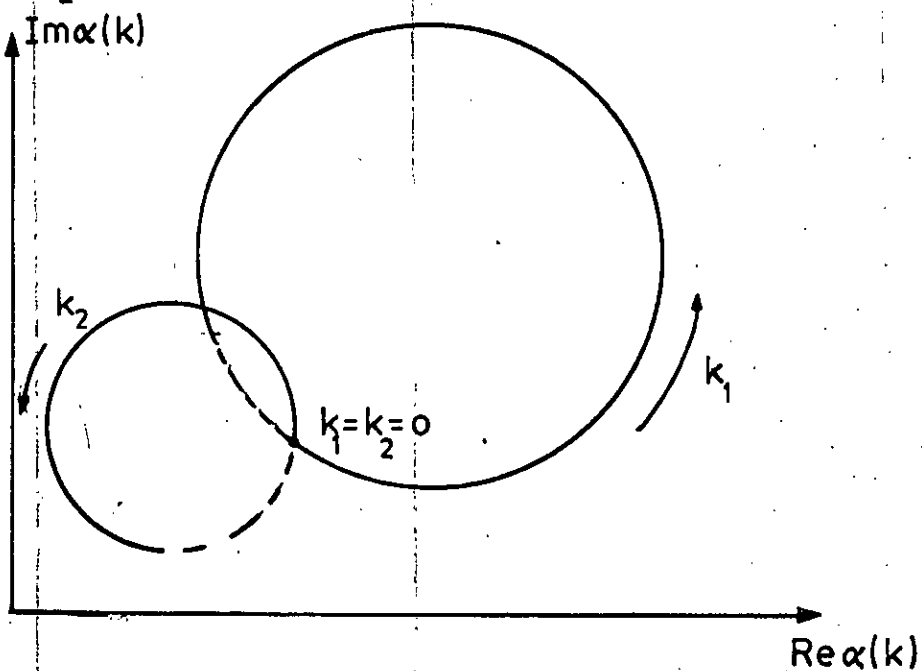


Figure 4.2.

Response Circles

4.3. (Continued)

However, where it is required to minimise the response parameter k_1 is ineffective, while k_2 is by comparison far more effective. Thus, with the bias towards minimisation, a new effectiveness criterion may be defined as the portion of the response circle for which the response may be reduced over its present value. The amount by which the response may be reduced can be represented by the line AB shown in Figure 4.3. This, however, does not take into account the size of the circle, and hence a more representative measure would be the length of the arc CD. This is referred to as the bias diameter of the circle.

The criteria that have been developed in this section have been formulated in order to highlight certain qualities of structural parameters. The best criteria for achieving desired response characteristics can only emerge as a result of the experience gained in using them.

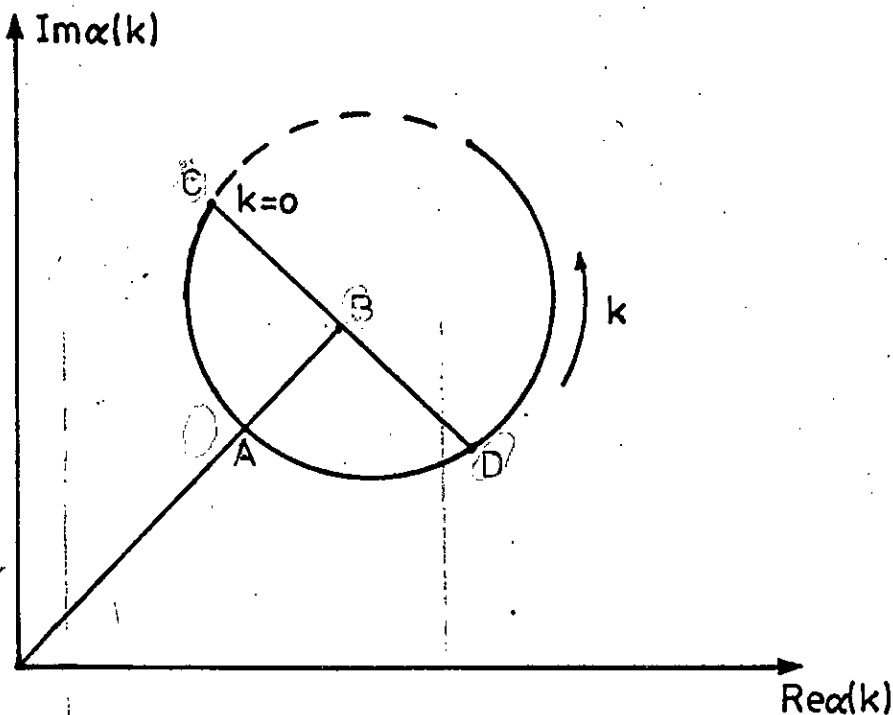


Figure 4.3.

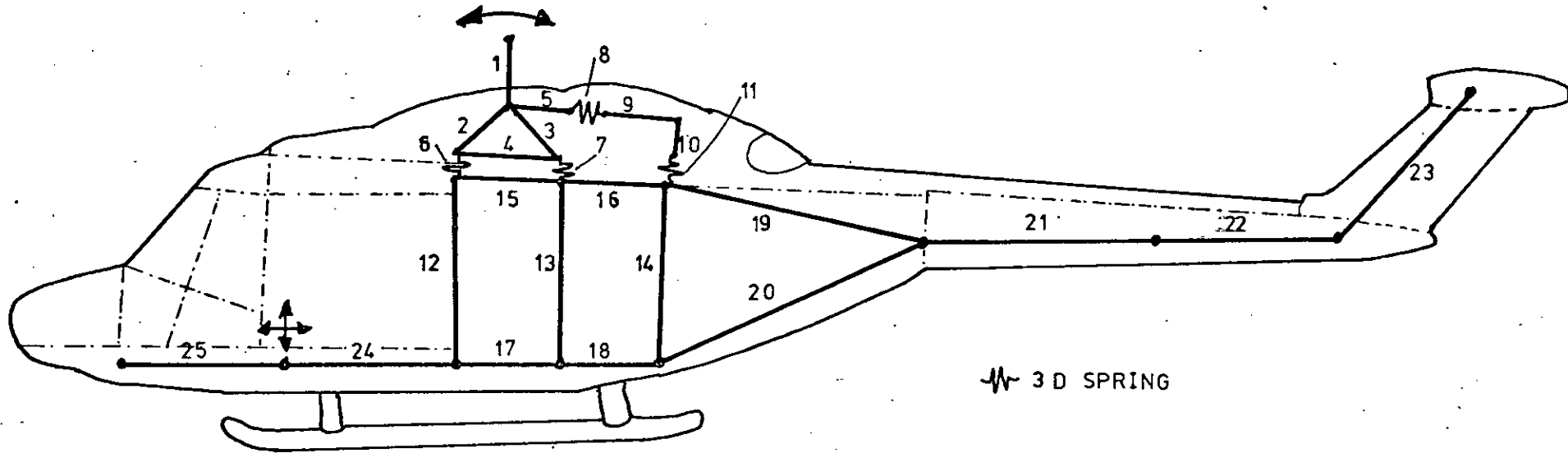
The Portion of the Circle Effective in Decreasing the Magnitude of the Response

4.4. The Practical Application of Effectiveness Criteria to a Helicopter Fuselage.

This chapter deals with the practical application of structural manipulation and would not be complete without an example to illustrate the use of the techniques developed. In addition, the example helps to define and explain more clearly the bases upon which the effectiveness criteria lie.

The example chosen is representative of the practical problem which provided the incentive for this research. Under consideration is the very much simplified two-dimensional model of a helicopter fuselage. The structure contains 20 nodes interconnected by 25 linearly tapering beam elements. Each node possesses three degrees of freedom, two translation and one rotation, making a total of 60 degrees of freedom. The layout of the model along with the element and node numbering is shown in Figures 4.4. and 4.5. respectively. Mass and stiffness data for the model was obtained from Westland Helicopters Limited, whilst damping was included in the form of a percentage of critical damping in each normal mode. The analysis was performed using the structural manipulation programme described in Chapter 5, the aim being to determine which parts of the fuselage structure were most sensitive in reducing the rotor induced vibration levels in the region of the pilot's seat (Node 18 in Figure 4.5.) The structure was excited by a sinusoidal torque, of frequency 21.7 Hz at node 8. Both the vertical and horizontal responses at node 18 were examined, although only the results for the latter have been included here. Only stiffness parameters connected between adjacent nodes were considered. In this way parameter changes could be directly related to existing structural elements. By imposing this restriction the

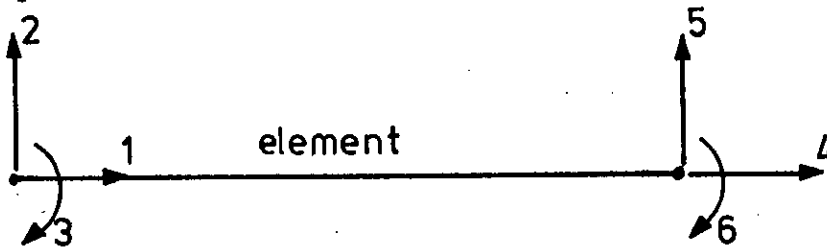
Figure 4.4.
-57-



Helicopter 'Stick Model' Element Numbering.

4.4. (Continued)

total number of parameters being associated with each element was three. These are defined in Figure 4.6. The total number of stiffness parameters associated with the structure was 75.



Parameter coordinates [1,4]
[2,5]
[3,6]

Figure 4.6.

Stiffness Parameters Associated with an Element

Four criteria were used in order to determine those parts of the structure which were most effective in reducing the vibration levels.

Firstly, by considering just one parameter at a time, the following were calculated for each of the 75 parameters:-

- i) Circle diameter.
- ii) Bias Diameter.
- iii) Minimum Response.

The values corresponding to (i) and (ii) have been sorted in descending order and are normalised such that they lie in the range 0-1. The value one is assigned to the most effective parameter, and zero to the least effective parameter. It should be remembered that these criteria are used to determine relative quantities and are not indicative of absolute effectiveness. Where minimum response is

4.4. (Continued)

concerned the values encountered are usually spread over a wide range making them unsuitable for normalisation in the manner just described. Consequently, the logarithms of the inverse of the minimum responses have been calculated, sorted and normalised in the range 0-1.

Each parameter has associated with it three sensitivity values; these are used in two ways to produce an equivalent figure for the elements of the structure. Every element has associated with it three parameters, the first value assigned to the element is that of the most sensitive parameter. This is intended to show that if an element has an effective parameter associated with it, then that element is effective regardless of the effectiveness of the other two related parameters. The second measure is the average sensitivity for the three parameters.

The results are presented in the form of line graphs where the ordinates refer to the various effectiveness criteria and the horizontal axis represents the various elements of the structure. For each element, the shaded ordinate refers to the best parameter value, whilst the unshaded ordinate shows the average of the three parameter values.

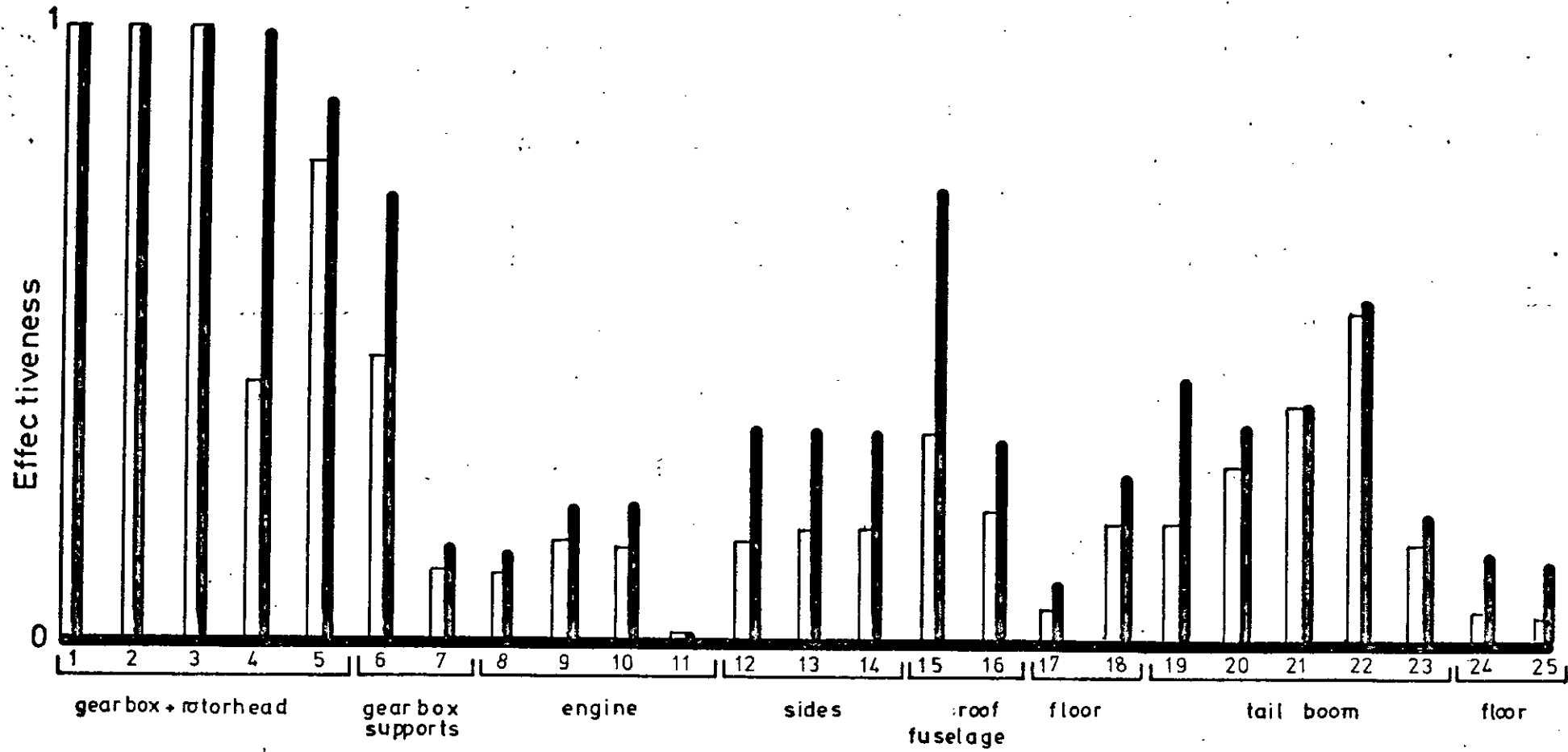
The fourth criterion involves parameters combined in pairs. Each pair was assessed to see if it could produce zero response at the pilot's seat. In the case of stiffness, there were 75 parameters and 2,775 possible paired combinations, many of which satisfied the required criterion. The number of times an element occurred in a successful pair was noted and the results were tabulated in descending order, having been normalised in the range 0-1 as before. This measure can be interpreted as providing the relative effectiveness of a

4.4. (Continued)

given element to actually produce zero response in conjunction with another undefined element. The results for element occurrence are also presented as line graphs.

The four criteria outlined above were recalculated, only this time the variable parameters were changes in point mass at each of the nodes. The total number of parameters in this case was 60. The results for variable mass are plotted as line graphs in exactly the same way as for the stiffness parameters. This time the numbers on the x axis refer to the structure nodes and have been arranged in groups representing well defined areas of the structure. The results for both variable mass and stiffness are given in Figures 4.7. - 4.14. It will be noted that in Figure 4.14. the ordinate referring to the best parameter value has been omitted. The values that should have been presented here were all unity or very close to unity, and their presence tended to obscure the remaining ordinates.


 — average value
 — best parameter per element



Variable stiffness: Circle diameter.

Figure 4.7.
-62-

Figure 4.8.
-65-

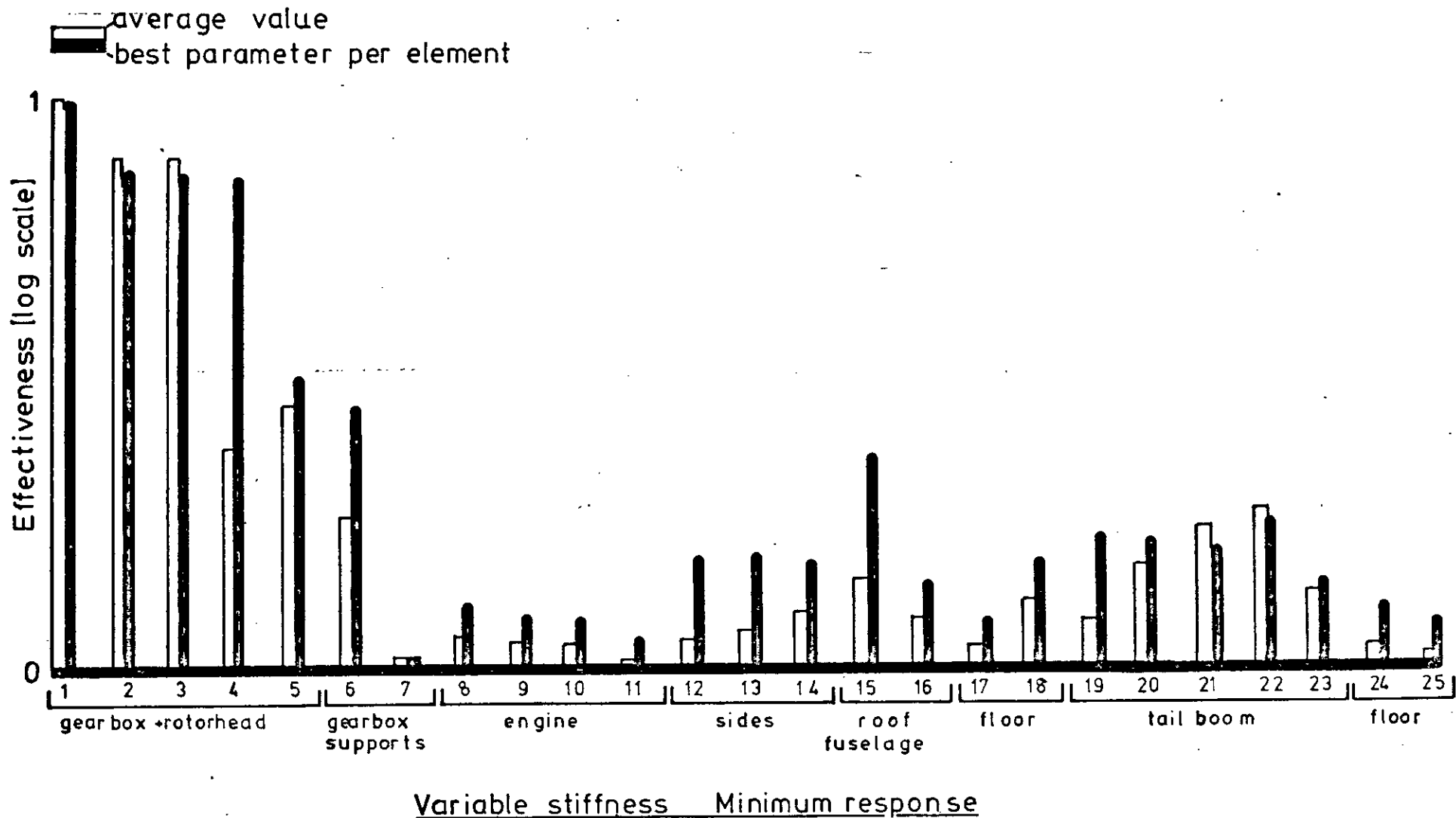
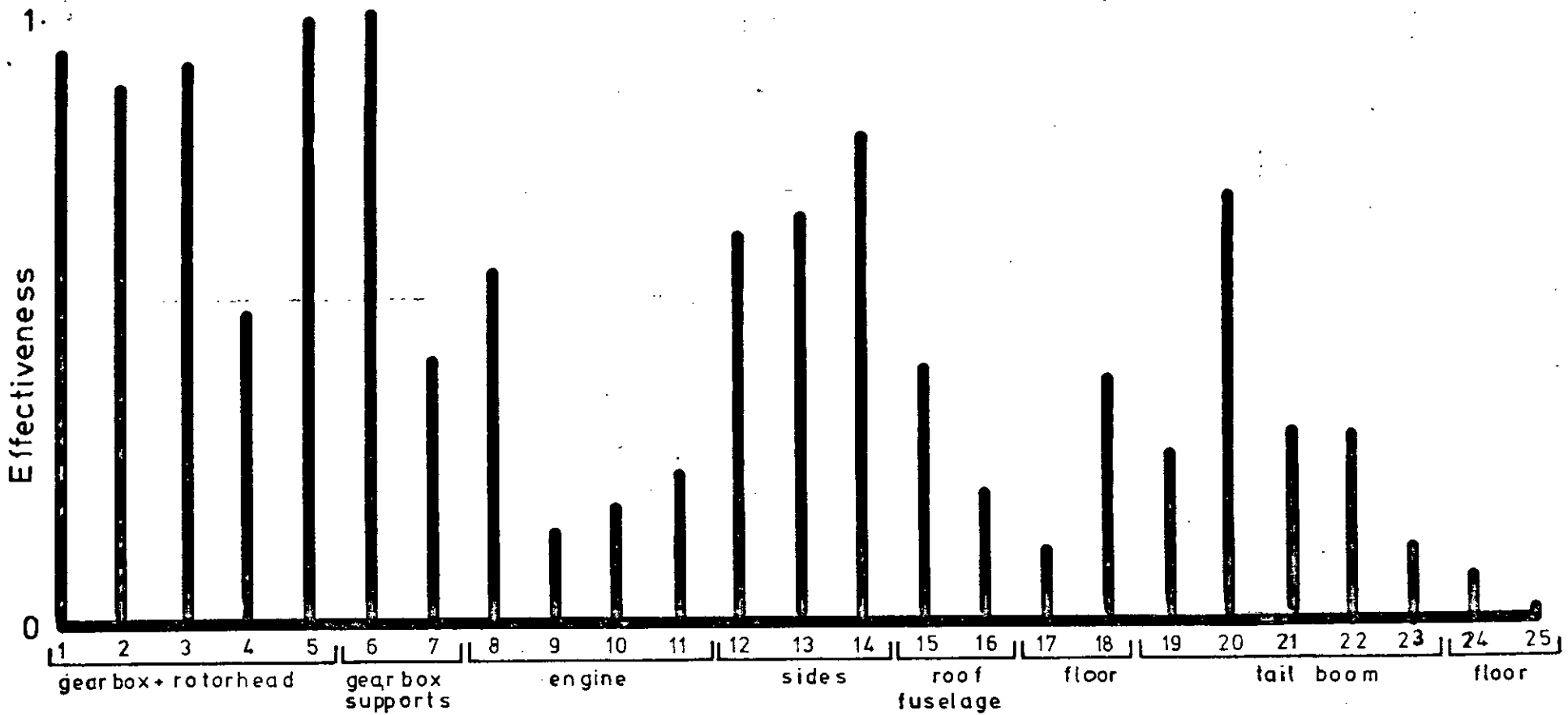


Figure 4.9.
-64-



Variable stiffness Element Occurrence [Zero response]

average value
 best parameter per element

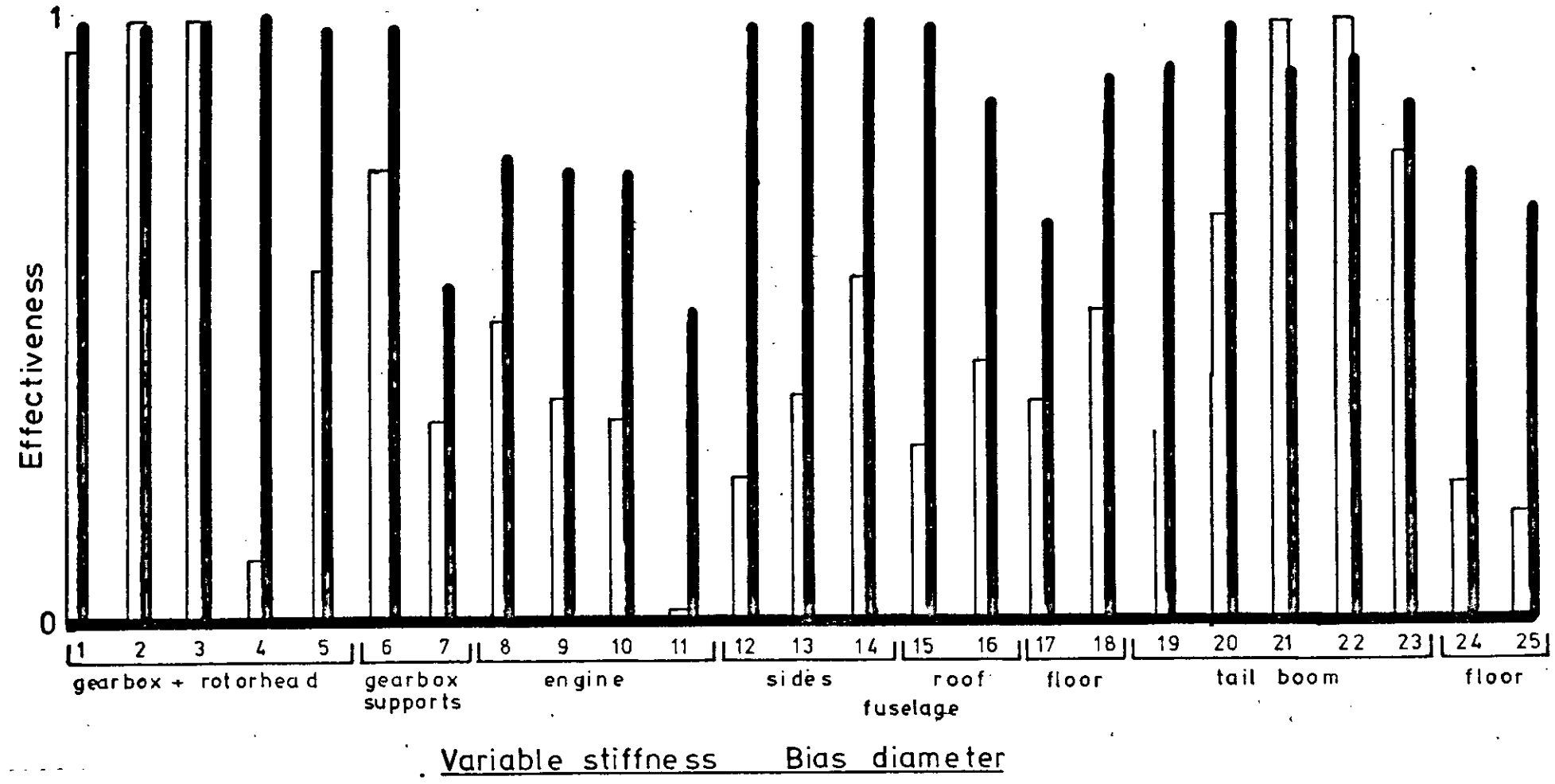


Figure 4.10.
 -65-

average value
 best parameter per element

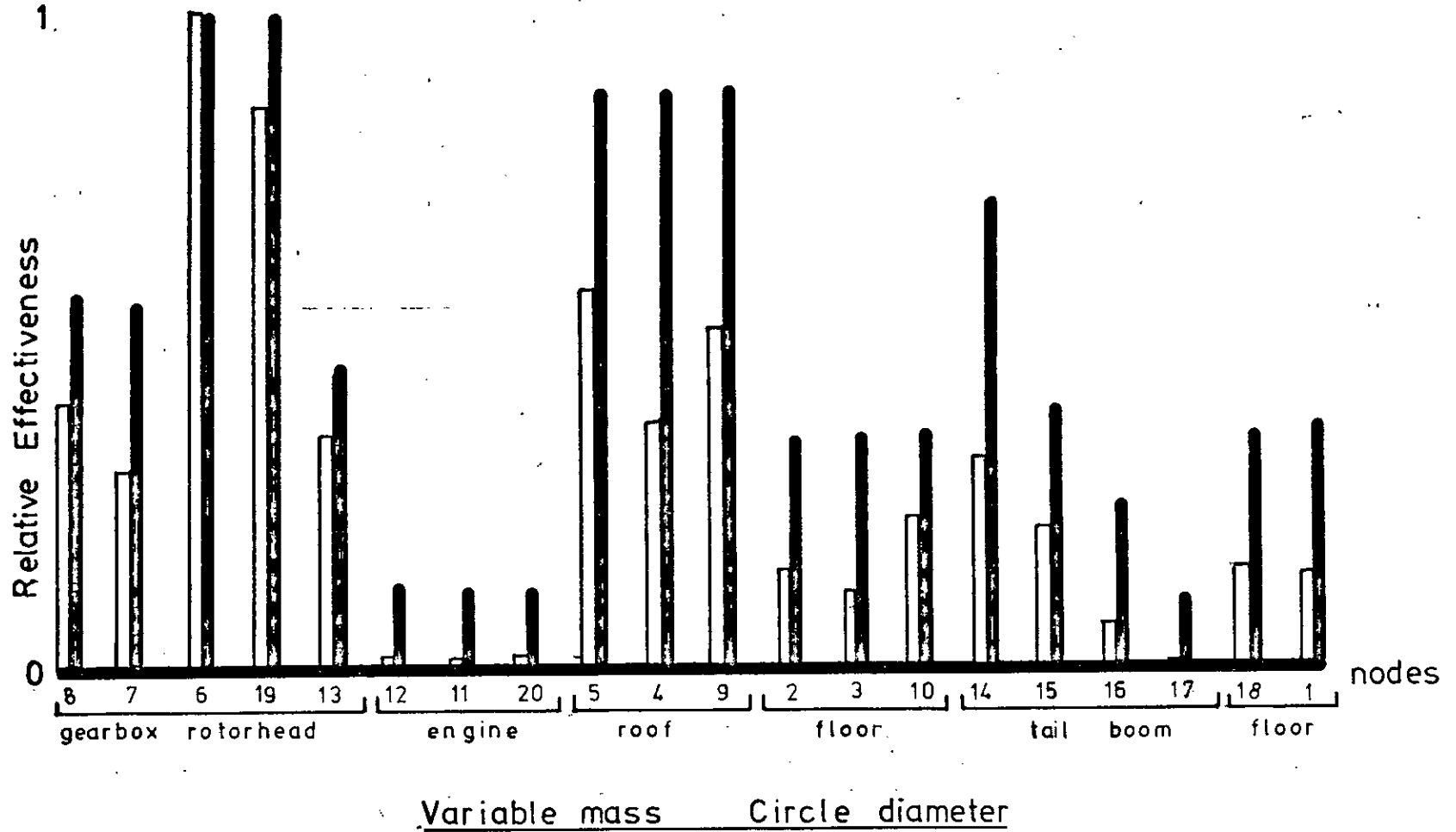
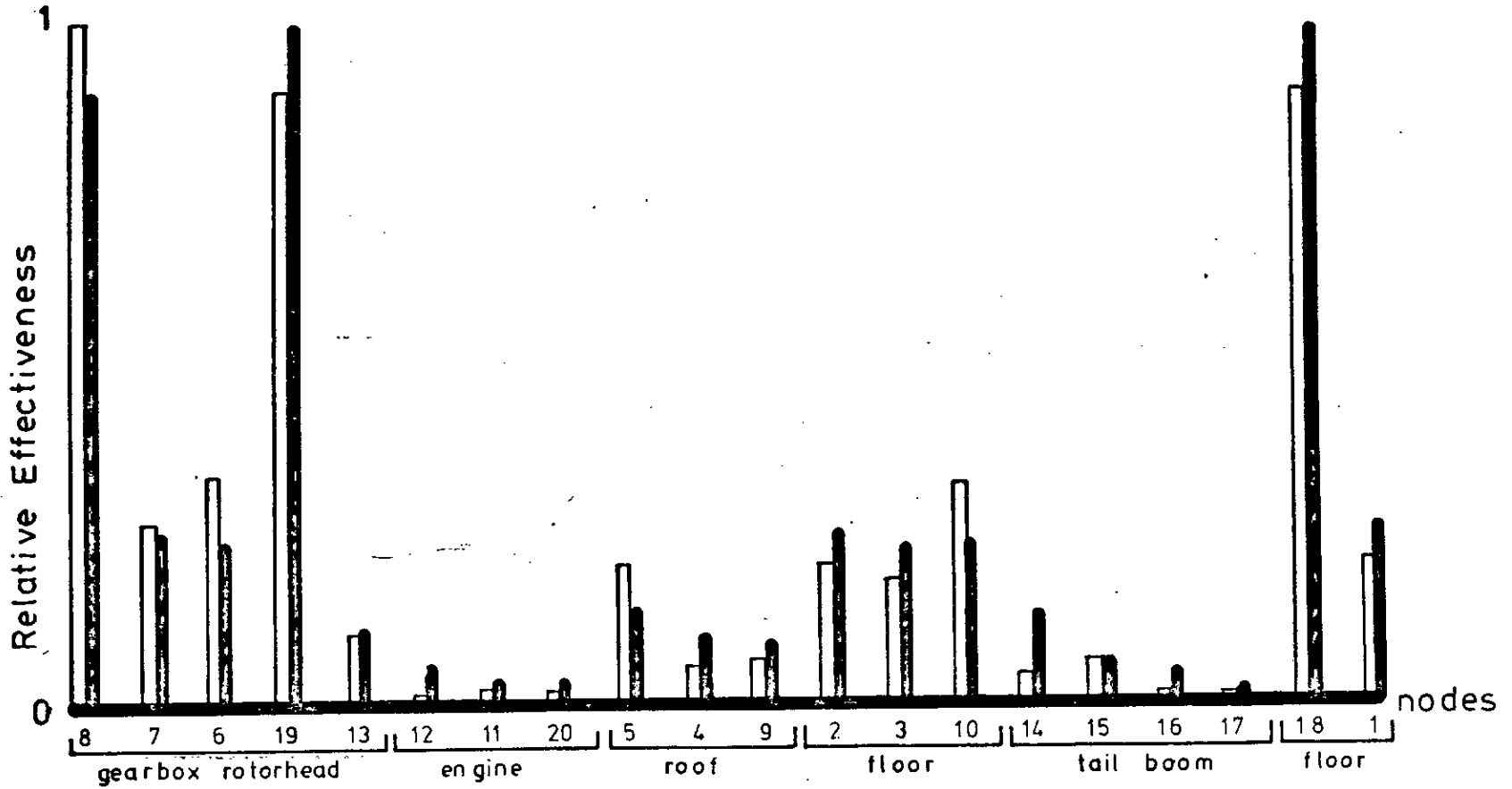


Figure 4.11.

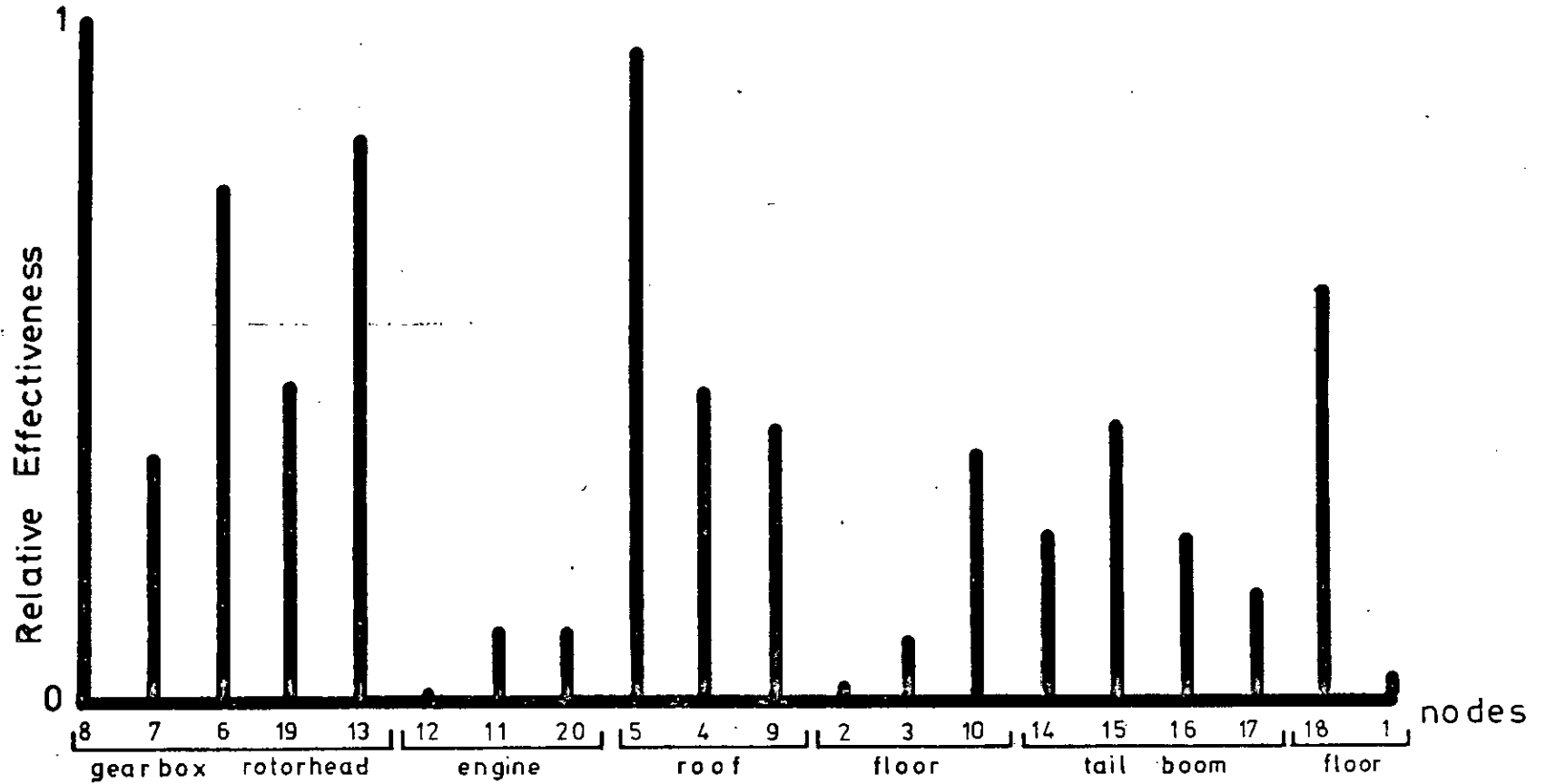
average value
 best parameter per element



Variable mass Minimum response

Figure 4.12.
 -67-

Figure 4.13.



Variable mass No de Occurrence [Zero response]

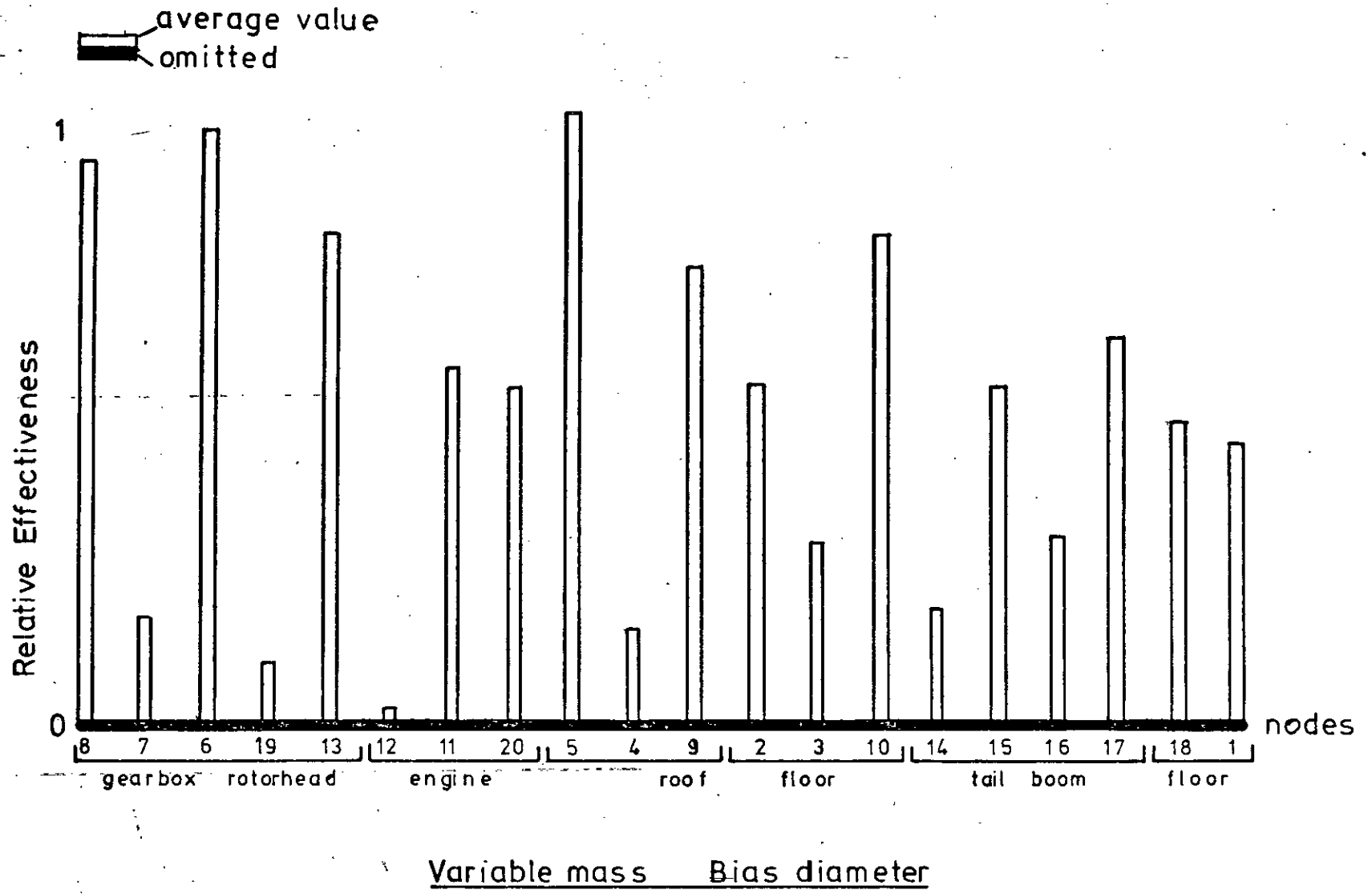


Figure 4.14.

4.41. Discussion of Results.

It is already known that, for this particular helicopter, the gear box and tail boom are suitable areas for modification in order to alleviate vibration in the area of the Pilot's seat. This knowledge was gained over a period of time through a process of trial and error, helped by a limited amount of theoretical analysis. As a result of this, the gear box mountings were considerably stiffened and so was the tail boom between nodes 22 and 23.

The results for variable stiffness shown in Figures 4.7. - 4.10. are mutually consistent in that they show the same three sensitive areas in the fuselage, namely, the gear box, tail boom and fuselage sides. This agrees broadly with what is known about the helicopter. What is interesting is that the same message comes across regardless of the criterion chosen, which tends to indicate the relevancy of the chosen criteria. In considering these three main areas, the importance of the gear box and fuselage sides is intuitively obvious. The former since it is close to the source of excitation, and the latter because of its ability to transmit forces, mainly in shear, to the front sub-structure. The importance of the tail boom is not so intuitively obvious and it is encouraging that the analysis has highlighted this area.

The results for variable mass shown in Figures 4.11. - 4.14. are reasonably consistent for all but the bias diameter criterion. The gear box and fuselage sides are again highlighted as sensitive areas, with nodes 6 and 19 being shown to be particularly effective by the circle diameter criterion. The minimum response criterion shows nodes 8 and 18 to be sensitive in the reduction of vibration levels; this is intuitively obvious since these nodes represent the forcing and examination

4.21. (Continued)

points respectively. An infinite increase in mass at either of these points would effectively reduce the response to zero. It is interesting to note how the sensitivity to changes in mass varies along the tail boom. The circle diameter, minimum response and node occurrence criteria all indicate that relative effectiveness decreases towards the end of the tail boom. Where stiffness parameters are concerned, with the possible exception of element 23, the circle diameter and minimum response criteria indicate the reverse trend, i.e. effectiveness increases along the tail boom. For both mass and stiffness parameters the engine is indicated as a relatively insensitive area.

Of the four criteria used in the analysis of the helicopter fuselage, only the bias diameter results have proved in any way inconclusive. For stiffness parameters the results are less well defined but still indicate the same sensitive areas as the other criteria. For mass parameters, however, the results seem to show no trends whatsoever; this seems strange when it is considered that the bias diameter criterion contains elements of the circle diameter and minimum response criteria, which both indicate clearly the sensitive areas in the structure.

The conclusions drawn here are tentative ones based on a limited amount of experience in this particular field of interpretation. The exercise was primarily intended to demonstrate the use of the various criteria developed in this section. However, although there is still a great deal of work to be done on the development of this practical form of analysis, there is strong evidence to indicate its power and potential.

4.5. Parameter Changes in Real Structures.

This section is complementary to the previous one in that it deals with some aspects of the practical implementation of structural manipulation. The emphasis here is placed on the relationship between the simple parameters used throughout this analysis and those encountered in real structures. The simplicity of the aforementioned analysis comes as a direct result of the form of the parameter changes chosen. It would, however, be unrealistic to expect similar changes to be either encountered or useful in any practical sense. What is required is a direct relationship between the practical structural parameters such as beam dimension, web depth and skin thickness and the idealised linear spring parameters. Progress can be made in this direction by constructing an equivalent spring model of a simple finite element.

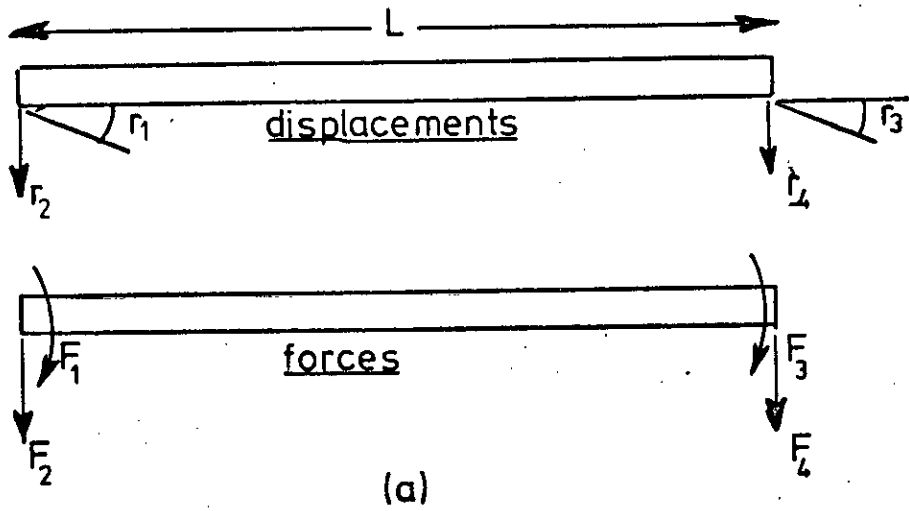
Consider the simple beam element shown in Figure 4.15(a). The uniform beam, which is inextensible, possesses four degrees of freedom r_1 , r_2 , r_3 and r_4 as shown, second moment of area I and Young's Modulus E . The stiffness matrix for the beam is well known and is given in Figure 4.15(b).

By considering the equilibrium of the beam, the following relationships may be obtained

$$F_2 = -F_4 \quad (4.11)$$

$$F_3 = -F_1 - F_4 \frac{l}{2} = -F_1 + F_2 \frac{l}{2} \quad (4.12)$$

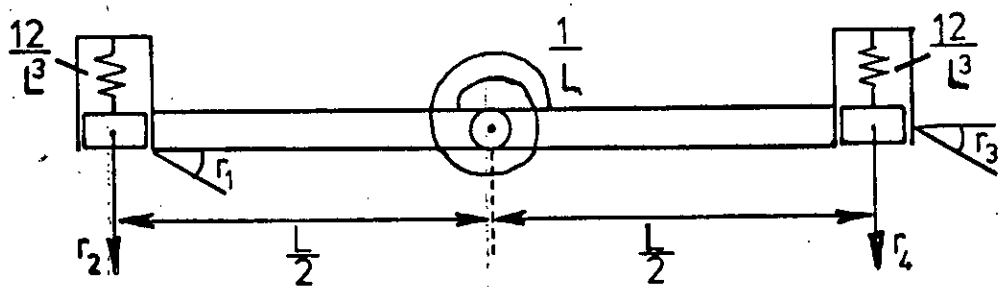
These two relationships imply an interdependency between some of the elements of the stiffness matrix \underline{K} . In fact, if elements k_{11} , k_{12} and k_{22} are known, then the values of all the other elements can be determined using equation 4.11., 4.12. and symmetry. These three terms form the elements of the stiffness matrix of the cantilever beam shown



$$K = EI \begin{bmatrix} \frac{4}{L} & \frac{6}{L^2} & \frac{2}{L} & -\frac{6}{L^2} \\ & \frac{12}{L^3} & \frac{6}{L^2} & -\frac{12}{L^3} \\ & & \frac{4}{L} & -\frac{6}{L^2} \\ & & & \frac{12}{L^3} \end{bmatrix}$$

SYMM

(b)
stiffness matrix



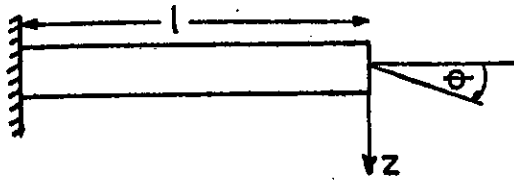
equivalent spring system

Beam Element and Equivalent Spring System

Figure 4.15.

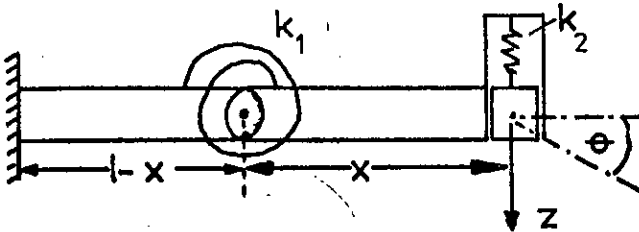
4.5. (Continued)

in Figure 4.16(a).



$$\underline{K} = \begin{bmatrix} \frac{4}{l} & -\frac{6}{l^2} \\ -\frac{6}{l^2} & \frac{12}{l^3} \end{bmatrix} EI$$

[A]



$$\underline{K} = \begin{bmatrix} k + k \frac{x^2}{2} & -kx \\ -kx & k_2 \end{bmatrix} EI$$

[B]

Figure 4.16.

Cantilever Beam and Equivalent Spring System

The equivalent spring system shown in Figure 4.16(b) consists of two rigid beams, total length l , hinged at a distance x from the free end. A rotational spring of stiffness k_1 connects the beams at the hinge, whilst a linear spring of stiffness k_2 is situated in the constraint arrangement at the free end of the beam. For the two systems to be equivalent, the elements of their respective stiffness matrices must be the same. Hence, equating the relevant terms leads to the following

4.5. (Continued)

values of k_1 , k_2 and x

$$\begin{aligned} k_1 &= 1/L \\ k_2 &= 12/L^3 \\ x &= L/2 \end{aligned} \tag{4.13}$$

Using these values, the beam in Figure 4.15(a) may be represented by the equivalent spring system shown in Figure 4.15(c).

The theory can be extended to cover the general case of a linearly tapering beam with second moment of area I_0 at one end and a taper ratio r . The analysis proceeds along the same lines as for the uniform beam, but requires that the stiffness matrix for a Tapered beam be determined. This is given in Appendix K and refers to a beam of I cross section. The stiffness matrix could, however, have been calculated for a beam of any cross section. Equating the elements of the two stiffness matrices as before gives the following values of k_1 , k_2 and x

$$\begin{aligned} k_1 &= \frac{12}{5L^3} (2r^2 + r + 2) \\ k_2 &= \frac{1}{4L} \frac{(r^4 + 4r^3 + 10r^2 + 4r + 1)}{(2r^2 + r + 2)} \\ x &= \frac{L}{12} \frac{(17r^2 + 6r + 7)}{(2r^2 + r + 2)} \end{aligned} \tag{4.14}$$

It will be noted that these values degenerate to those given in equation 4.13. when the taper ratio is unity.

It has been shown that a finite element beam can be modelled in terms of the simple parameters used in the structural manipulation theory. These parameters are directly related to the real structural variables r , E and I_0 . However, the parameters k_1 and k_2 cannot be

4.5. (Continued)

varied independently since they are directly related. This situation leads to the consideration of a special case of parameter variation, namely, two stiffness parameters varying simultaneously but in a related manner.

Consider the simplest case where the two parameters k_1 and k_2 have the following linear relationship

$$k_1 = \beta k_2 \quad (4.15)$$

where β is a real constant. The response at a point in the structure may be given as a function of k_1 and k_2 and is

$$\alpha = \frac{ak_1 + bk_2 + ck_1k_2}{1 + dk_1 + ek_2 + fk_1k_2} \quad (4.16)$$

where the constants a, b, c, d, e and f are complex and are defined in Appendix C. The constant G_{qp} has been omitted from equation 4.16. for the sake of simplicity. Substituting for k_2 from equation 4.15. gives

$$\alpha = \frac{k_1^2 c\beta + k_1(a + b\beta)}{k_1^2 f\beta + k_1(d + e\beta) + 1} \quad (4.17)$$

Equation 4.17. may be considered as providing a mapping from the k_1 plane to the α plane. Any complex mapping such as this may be made up of a series of simpler mappings. In this case, there are two mappings which take the form

$$Z = \frac{Ak_1 + B}{Ck_1 + D} \quad (4.18)$$

and
$$\alpha = Z^2 + E \quad (4.19)$$

where the constants A, B, C, D and E are all complex. Equation 4.18. is an example of a Bilinear Class of mapping and maps straight lines in the

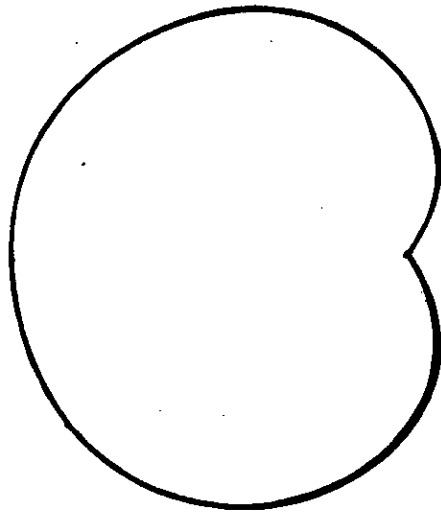
4.5. (Continued)

k_1 plane into circles in the Z plane. Equation 4.19. maps the circles in the Z plane into Cassini Ovals in the α plane [7]. A Cassini Oval or Cassinian is a higher plane curve of the same type as Cartesian Ovals, limaçons and cardioids (see Figure 4.17.). A Cassinian is defined as the locus of a point which moves so that the product of its distance from two fixed points $(0, \pm a)$ is a constant k^2 . The equation of this curve in cartesian coordinates is

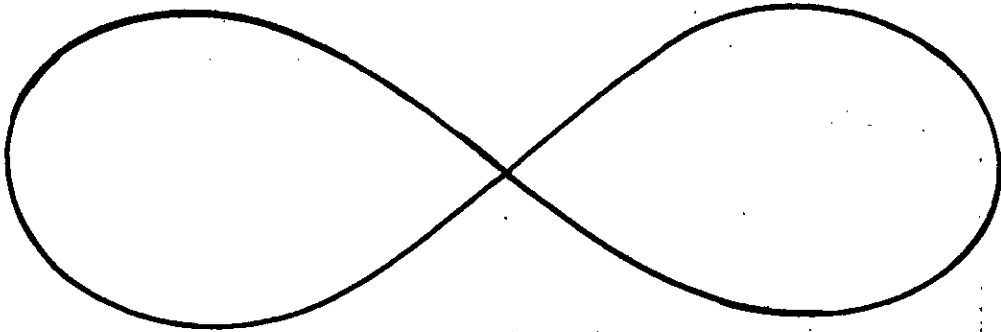
$$(x^2 + y^2 + c^2)^2 - 4a^2x^2 = k^2$$

where $c^2 = k + a^2$. If $k < a$, there are two separate ovals each enclosing a focus and the curve is said to be bipartite. If $k > a$ the two ovals merge into one. When $k = a$, the curve is a lemniscate. The boundaries of the feasible response regions are examples of this type of curve. Thus, when two stiffness parameters are varied in a related manner, the response no longer lies within a feasible region but on a closed curve whose form is determined by the nature of the relationship between the two parameters. The analysis of these curves is known to be complex, but there is sufficient justification for a closer investigation into their mathematical properties.

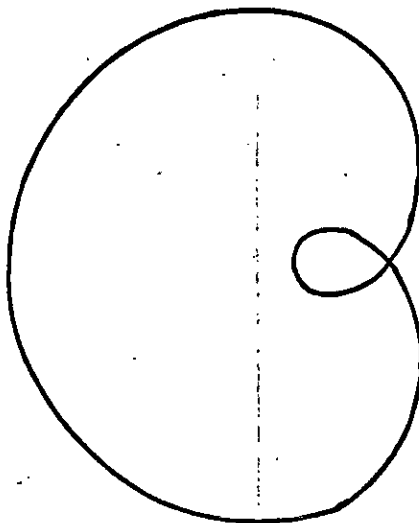
A direct relationship between real structural parameters and linear spring elements has been shown to exist. The practical application of the theory developed around this work has not been attempted, but it is clear that real parameter changes can only be represented by combinations of idealised parameters. The variation of these parameters in a related manner imposes tighter restrictions on the response at a point in the structure than if they had been allowed to vary independently.



Cardioid



Lemniscate



Limaçon

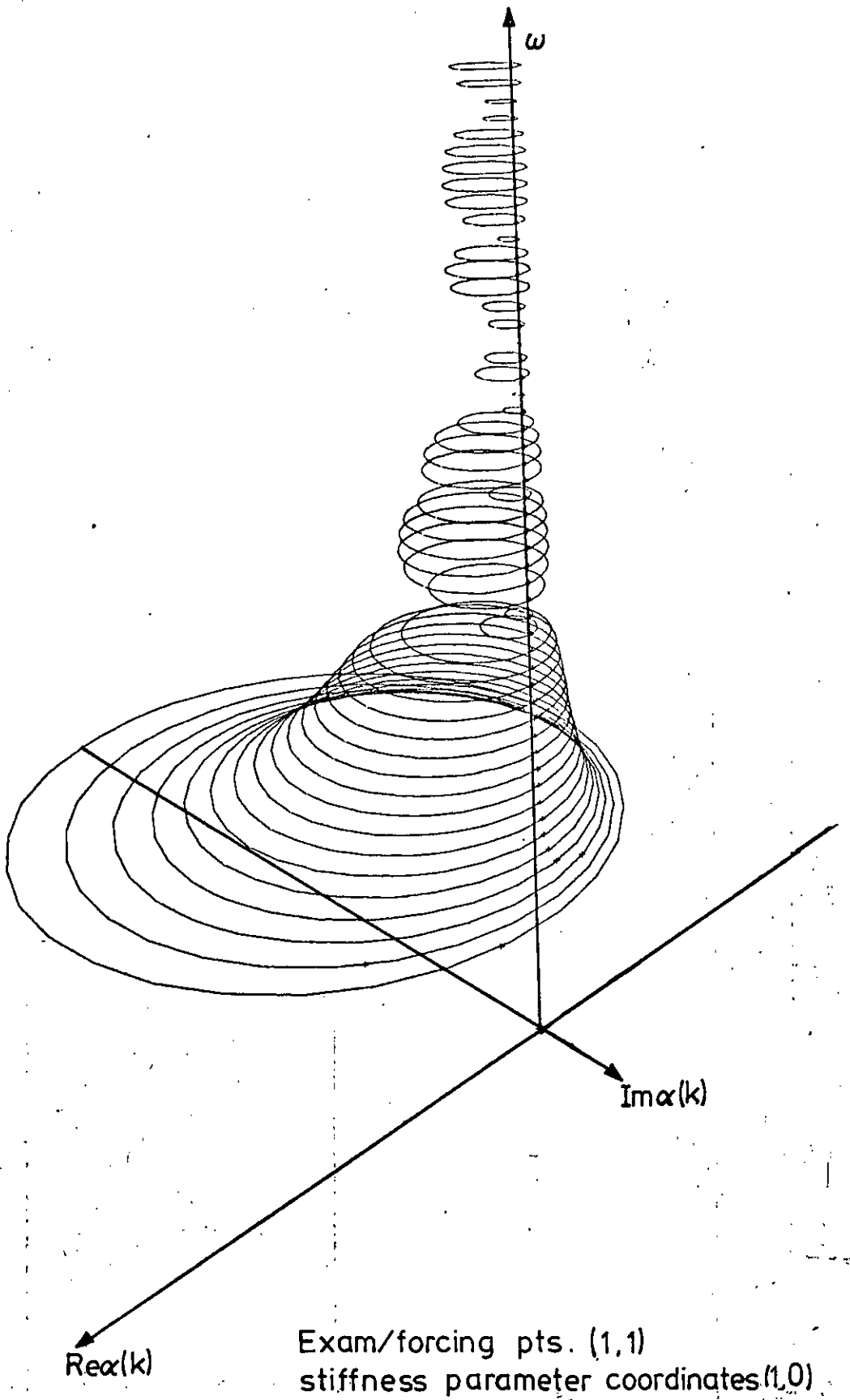
Examples of Special Cases of Cartesian Ovals

4.6. Other Techniques for Assimilating the Effectiveness of Parameter Changes.

This last section contains some of the more interesting aspects of the main analysis which have not been fully developed, but which may have potential usefulness. A single response is examined as a function of frequency and stiffness and the case of multiple responses as functions of structural parameters is also considered.

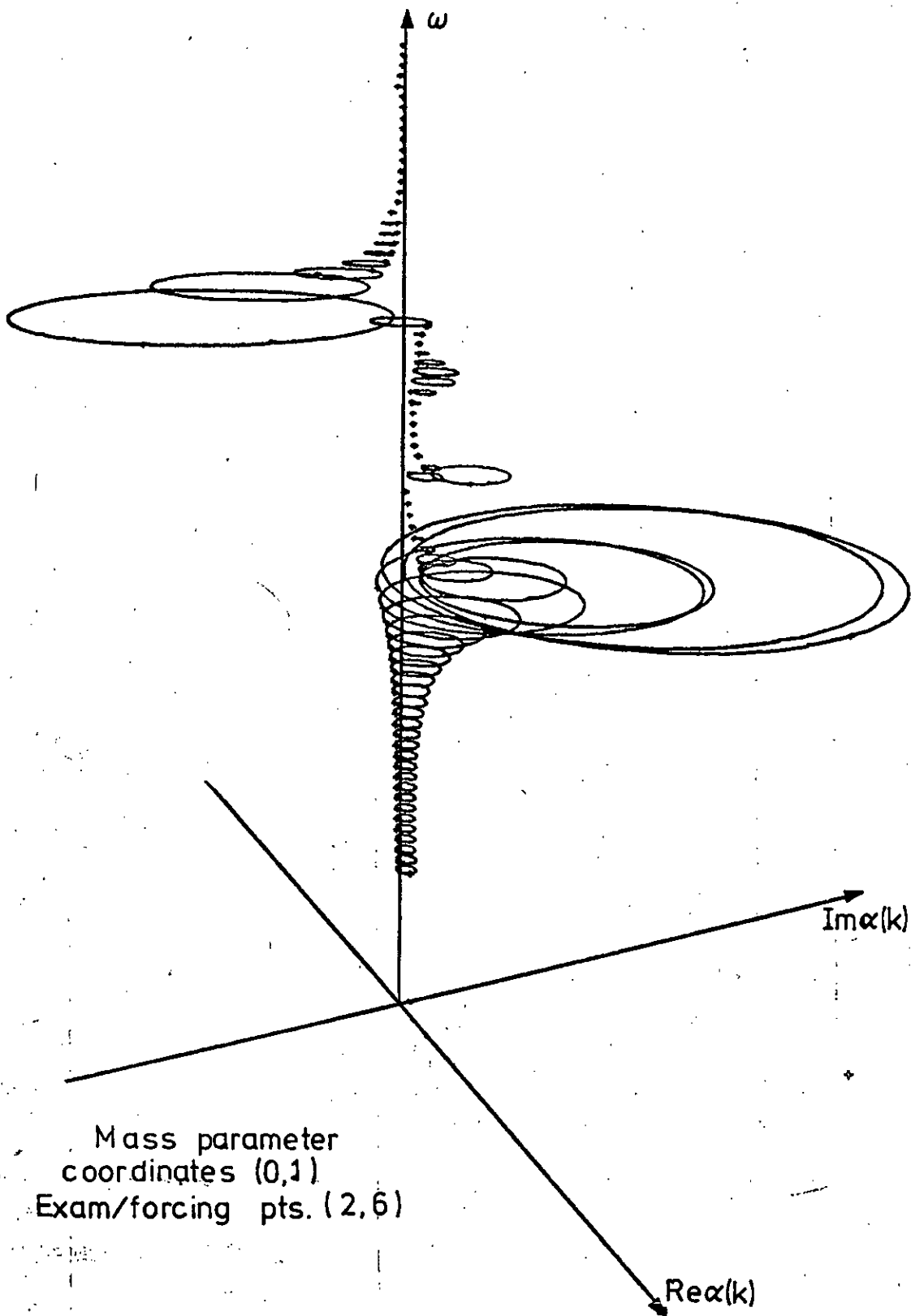
4.61. Response as a Function of Frequency and Stiffness.

In Chapter 3, an example was given of a three dimensional response plot, for which the response was considered as a function of frequency and stiffness. The plot consists of a set of response circles representing a single variable parameter and calculated over a range of frequency. If an infinite number of circles were plotted in the given range, then a cylindrical envelope would be developed upon which the response must lie for a given value of stiffness and frequency. Figures 4.18. and 4.19. show two examples of these plots, both were calculated using the mathematical model of the experimental structure described in Chapter 6. These plots can be used to give some indication of the effectiveness of single parameters as a function of frequency. The size of the response circle, which has already been used as an effectiveness criteria, can be plotted against frequency and the resulting graph represents the relative effectiveness of that parameter in a given frequency range. In order to produce this graph, the frequency range of interest is chosen and the circle diameter for the given parameter is calculated at a specified number of points within that range. A curve is then fitted through



Response as a Function of Stiffness and Frequency.

Figure 4.18.



Response as a Function of Frequency and Stiffness

4.61. (Continued)

these points and the resulting graph is shown in Figures 4.20. and

4.21. These are the circle diameter against frequency plots referring to the same systems that were used to produce Figures 4.18. and 4.19. They do, however, include the graphs for several other parameters as well. The peaks in these plots may be interpreted as being representative of frequency ranges in which the associated parameters are potentially effective. The curves were produced using the structural manipulation programme. The process by which they are obtained can be time-consuming, for it involves calculating new receptance matrices for each value of frequency.

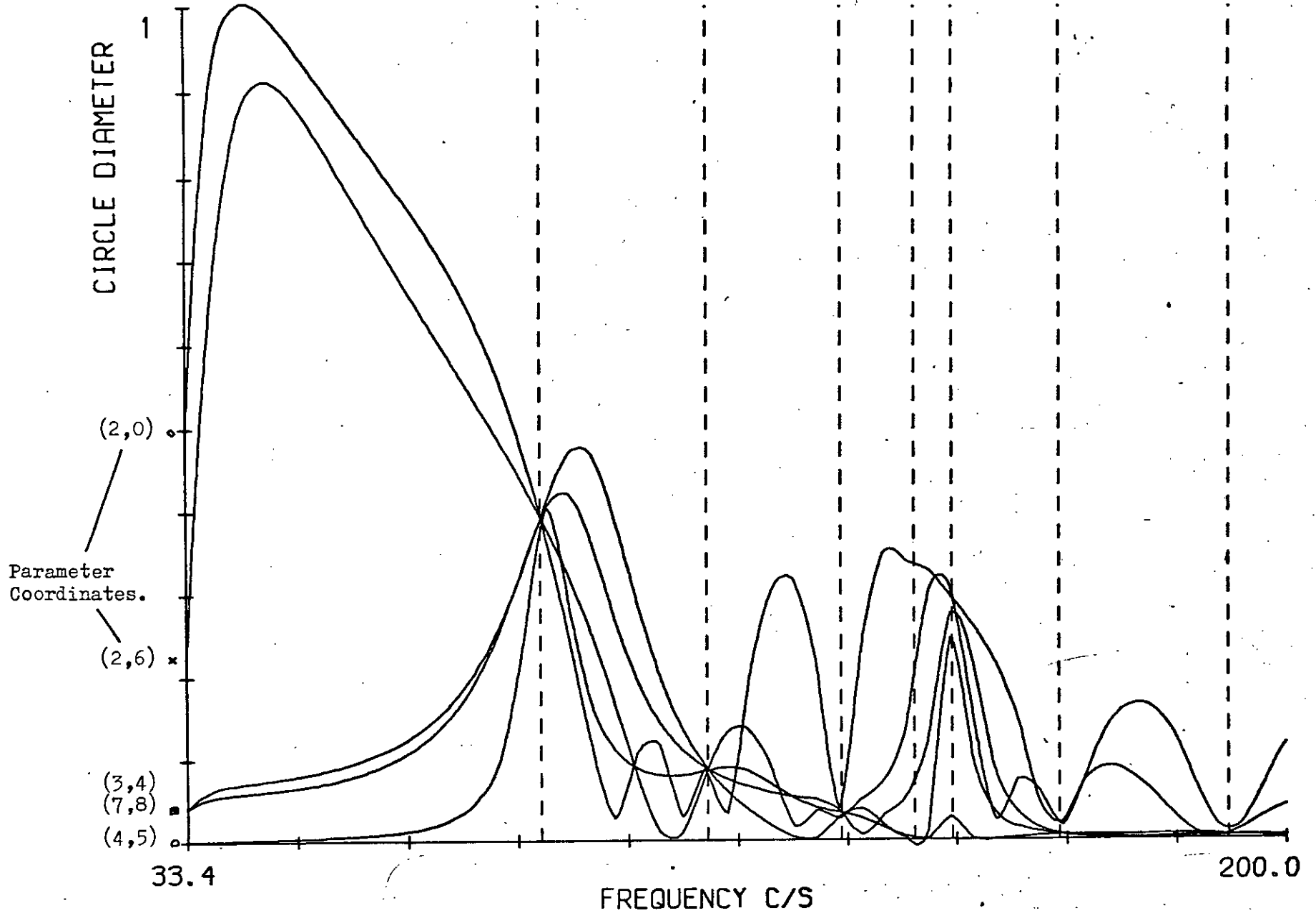
4.62. Multiple Responses as a Function of Structural Parameters.

Consideration so far in this analysis has been given exclusively to examining the behaviour of a single response as a function of one or more structural parameters. However, it is often desirable to be able to consider a set of responses collectively. In this section a set of n responses are considered as a function of a single stiffness parameter k . The aim being to calculate the value of k for which the sum of the response vectors is a minimum. It will be shown that, once formulated, the problem cannot be tackled analytically but must be solved using an iterative procedure. The case in which the responses are considered as a function of more than one parameter is not considered.

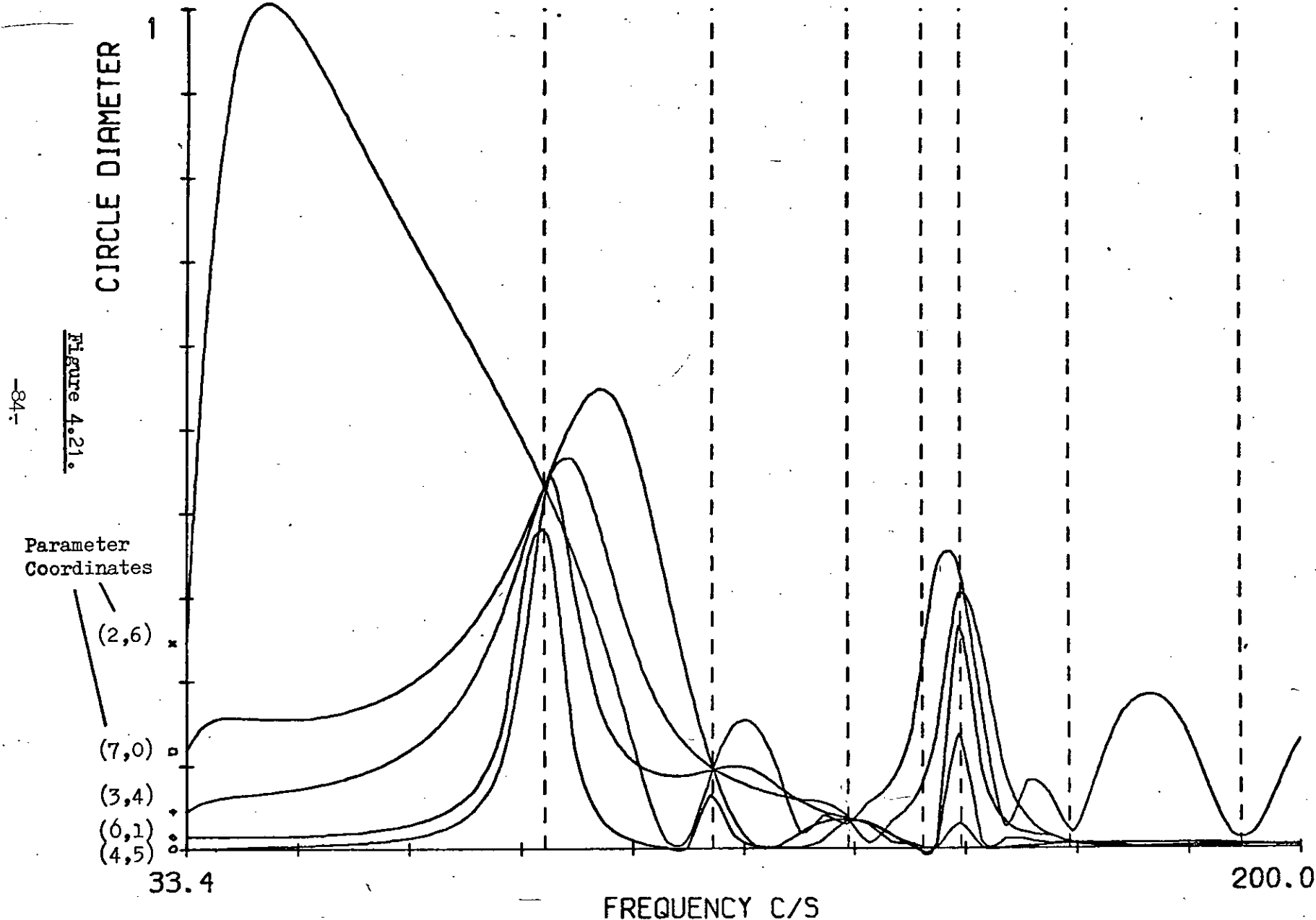
In its simplest form the problem involves calculating the minimum of a single response as a function of one stiffness parameter. This case was dealt with in Section 4.21., and was found to have an analytical solution.

Consider a set of n responses α_i and a single variable stiffness

Figure 4.20.



Circle Diameter Against Frequency For Five Parameters.



Circle Diameter Against Frequency for Five Parameters.

4.62. (Continued)

parameter k ; it is required to find the value of k for which $\sum_{i=1}^n |\alpha|_i$ is a minimum. If p is the point of excitation and the parameter k is attached to the structure at points r and s , the response α_i is given by

$$\alpha_i = \frac{G_{ip} + k((G_{sp} - G_{rp})(G_{ir} - G_{is}))}{1 + k(G_{rr} + G_{ss} - G_{rs} - G_{sr})} \quad (4.20)$$

which may be written more generally

$$\alpha_i = \frac{u_i + iv_i = e_i + if_i + k(a_i + ib_i)}{1 + k(c_i + id_i)} \quad (4.21)$$

The real and imaginary components of α_i are

$$u_i = \frac{e_i + k(a_i + k(a_i c_i + b_i d_i))}{1 + 2c_i k + k^2(c_i^2 + d_i^2)} \quad (4.22)$$

and

$$v_i = \frac{f_i + k(b_i + k(b_i c_i - a_i d_i))}{1 + 2c_i k + k^2(c_i^2 + d_i^2)} \quad (4.23)$$

Now

$$\begin{aligned} |\alpha|_i &= (u_i + v_i)^{\frac{1}{2}} \\ &= \frac{(A_i k^2 + B_i k + C_i)^{\frac{1}{2}}}{(P_i k^2 + Q_i k + R_i)^{\frac{1}{2}}} \end{aligned} \quad (4.24)$$

where A_i, B_i, C_i, P_i, Q_i and R_i are defined in Appendix I.

The minimum of the function $\sum_{i=1}^n |\alpha|_i$ is given when

$$\frac{d}{dk} \sum_{i=1}^n |\alpha|_i \equiv \sum_{i=1}^n \frac{d}{dk} |\alpha|_i = 0$$

4.62. (Continued)

The first derivation of $|\alpha_i|$ with respect to k is

$$\frac{d|\alpha_i|}{dk} = \frac{(A_1 k^2 + B_1 k + C_1)^{-\frac{1}{2}} (2A_1 k + B_1) - (2P_1 k + Q_1)(A_1 k^2 + B_1 k + C_1)^{\frac{1}{2}}}{2(P_1 k^2 + Q_1 k + R_1)^{\frac{3}{2}}}$$

(4.25)

It will be noted from equation 4.20. that P_1 , Q_1 and R_1 are functions of the position of the parameter k only and therefore are the same for all i . Thus

$$\sum_{i=1}^n \frac{d|\alpha_i|}{dk} = \frac{(P_1 k^2 + Q_1 k + R_1)^{-\frac{1}{2}} \sum_{i=1}^n ((A_1 k^2 + B_1 k + C_1)^{-\frac{1}{2}} (2A_1 k + B_1)) - (2P_1 k + Q_1)(P_1 k^2 + Q_1 k + R_1)^{-3/2} \sum_{i=1}^n (A_1 k^2 + B_1 k + C_1)^{\frac{1}{2}}}{2}$$

(4.26)

Equating equation 4.26. to zero gives

$$\frac{(P_1 k^2 + Q_1 k + R_1)}{(2P_1 k + Q_1)} = \frac{\sum_{i=1}^n (A_1 k^2 + B_1 k + C_1)^{\frac{1}{2}}}{\sum_{i=1}^n (2A_1 k + B_1)(A_1 k^2 + B_1 k + C_1)^{-\frac{1}{2}}}$$

(4.27)

which cannot be readily solved analytically. Consequently, the root of equation 4.26. corresponding to the minimum value of $\sum_{i=1}^n |\alpha_i|$ is obtained using an iterative search procedure. (Nottingham Algorithms Group Library Subroutine EOGBAF [13]). The routine requires the gradient of the function and a good initial estimate of the required root. The latter is obtained by calculating the minimum of the function $\sum_{i=1}^n |\alpha_i|^2$ which is assumed to be a good approximation of the required minimum and can be determined analytically. The

sum of the squares of the moduli of the response vectors is given by

$$\sum_{i=1}^n |\alpha_i|^2 = (P_1 k^2 + Q_1 k + R_1)^{-1} \sum_{i=1}^n (A_1 k^2 + B_1 k + C_1) \quad (4.28)$$

4.62. (Continued)

If the first derivative, with respect to k , of equation 4.28. is calculated and equated to zero then the following quadratic in k is obtained

$$k^2 (\bar{A}Q_1 - \bar{B}P_1) + 2k(\bar{A}R_1 - \bar{C}Q_1) + (\bar{B}R_1 - \bar{C}Q_1) = 0 \quad (4.29)$$

where

$$\bar{A} = \sum_{i=1}^n A_i$$

$$\bar{B} = \sum_{i=1}^n B_i$$

$$\bar{C} = \sum_{i=1}^n C_i$$

Equation 4.29. can be solved and the root corresponding to the minimum value of $\sum |\alpha_i|^2$ is found in the usual way from the second derivative of the function. In practice the iterative procedure converges rapidly using this initial estimate.

Using the structural manipulation programme, the minimum of the sum of a set of response vectors is calculated for all the available stiffness parameters in a given system. The results are sorted in ascending order of minimum response and tabulated to give the sum of the response vectors and the corresponding value of the stiffness parameter.

CHAPTER 5

COMPUTATIONAL ANALYSIS

5.1. Introduction.

The mathematical analysis outlined in the previous chapters includes a certain amount of matrix algebra, in particular the solution of eigenvalue problems and the inversion of matrices. Where the order of the matrices involved is greater than three, then the solution of these problems becomes too complex to be performed by hand and it is necessary to resort to the computer to perform these tasks. Initially, programmes were written to perform specific operations in order to test the theory being developed; however, it became increasingly obvious that the computer was going to become an indispensable tool playing a major role in the development of the analysis. The programmes that had already been developed were being expanded to provide ever more detailed and diversified forms of information, and it soon became apparent that the process as a whole was becoming too slow and complicated to be able to produce the required results in an efficient manner. What was needed was a more general interactive programme capable of fast data handling and with the facilities to perform any or all of the calculations previously handled by separate programmes. A Structural Manipulation Programme was consequently written to run on-line on the ICL 475 computer operated by the Edinburgh Regional Computing Centre. The programme was intended as a research tool which could be expanded without impairing its performance and which could be run as a truly interactive process by either speeding up or eliminating the time-consuming procedures normally associated with matrix operations.

5.1. (Continued)

In the sections that follow, it is not intended to give a detailed description of the internal operation of the programme, instead the underlying concepts behind the programming techniques and the general capabilities of the programme are discussed.

5.2. The Structural Manipulation Programme.

5.2.1. General Description.

The Structural Manipulation Programme, which contains approximately 5,000 statements, is designed to run on-line using the Edinburgh Multi-Access System. The input and output of data to and from the process is achieved using a teletype, although there is the capability of using other devices. The programme consists of a main driver section and a set of 27 external routines. The driver section contains procedures which allow the external routines to be selected in order to perform specific mathematical operations. The external routines are designed as self-contained units which are independent of the rest of the process in a manner which allows them to be added to or deleted from the system without affecting the existing procedures. Although the programme is large, the sections of it that are used in any one given operation are by comparison relatively small and can be executed with the maximum of speed and efficiency. Thus, by virtue of the way in which the programme is put together, it is integrated yet capable of continuous development and expansion without impairing the efficiency of the existing sections.

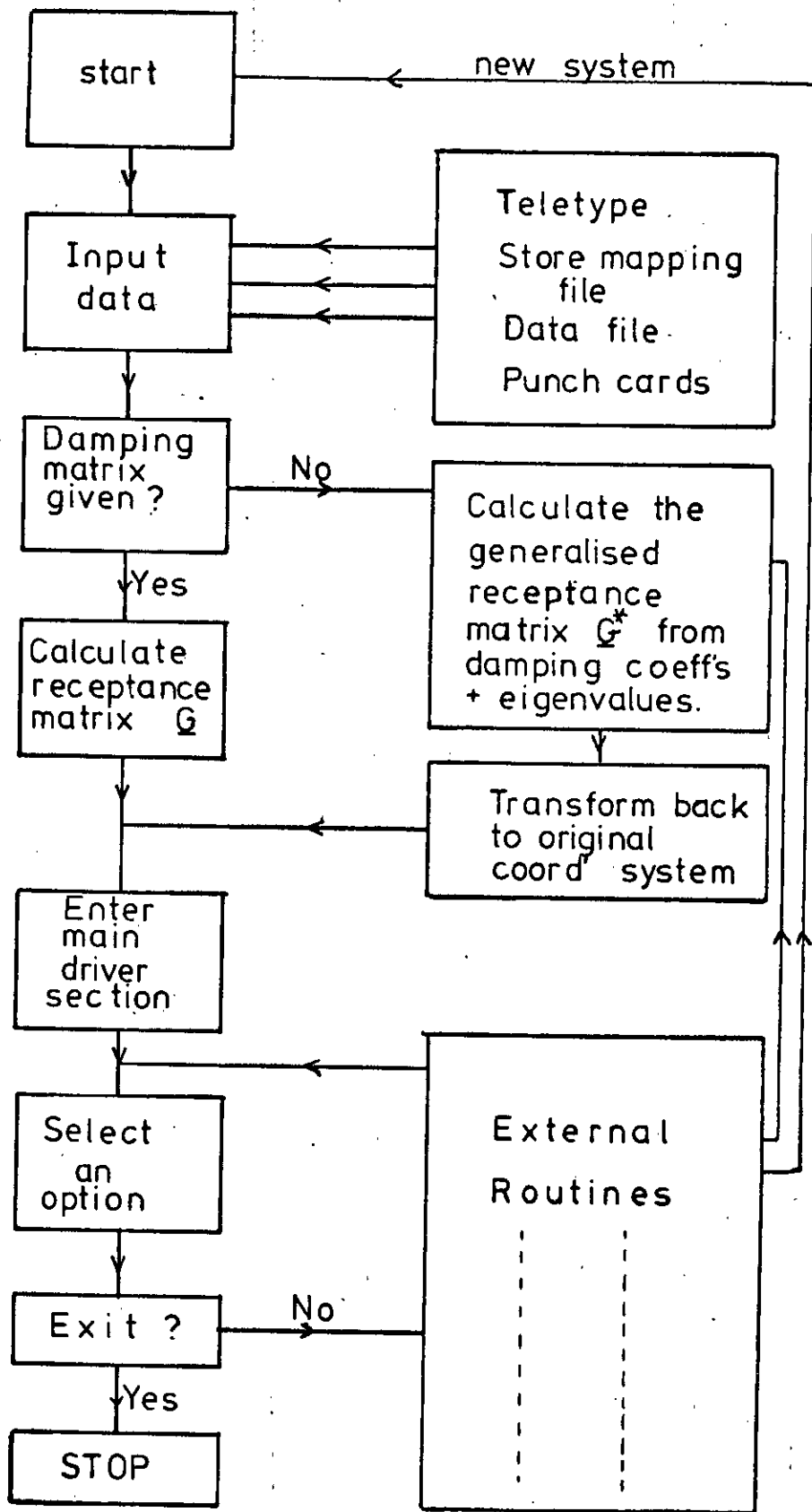
The Structural Manipulation Programme is designed to perform analyses on the mathematical models of real structures. This usually takes the form of mathematical operations which use data from the receptance matrices of the relevant systems. The calculation of these

5.21. (Continued)

matrices is time consuming, but they need only be calculated once for a given value of frequency. In very broad terms the programme performs operations in three main areas, namely, reading in system data, calculating the receptance matrices for the system and performing mathematical analyses using the receptance data. The system data takes the form of mass stiffness and damping matrices, M , K and C respectively. Where damping is not given explicitly in the form of a matrix, then it may be included as a percentage of critical damping in each normal mode. This involves the calculation of eigenvalues of the system and also the generalised transformation matrix formed from the associated eigenvectors. The damping matrix in the generalised coordinate system can be calculated from these values and then transformed back into the original coordinate system, (details of this along with the calculation of the real and imaginary parts of the receptance matrix are given in Section 5.22). A simplified flow diagram of the programme is given in Figure 5.1.

Once the system data has been read in and the receptance matrices calculated, then the main driver section of the programme is entered and the user is then asked to select any one of the 44 options available in the programme. Some of the more important options are described below.

- (I) The real and imaginary parts of the receptance matrix are calculated for a constant value of frequency, option (1) allows this value to be changed and the new receptance matrices calculated.
- (II) The natural frequencies and normal mode shapes of the system can be listed.



PROGRAM FLOW DIAGRAM

Figure 5.1.

5.21. (Continued)

(III) Both mass and stiffness parameters can be considered in the programme; a stiffness parameter is defined as the change in stiffness between two mutually compatible points in the structure which are referred to as the spring coordinates. A mass parameter is defined as the change in mass at one of the structural nodes, this point being referred to as the mass coordinate. There are no restrictions imposed on the points at which mass may be varied in the structure. Where stiffness is concerned, then any of the following restrictions may be applied to the parameters:-

No restrictions, i.e. stiffness may be varied between any two spring coordinates.

Parameters may be restricted to being associated with existing structural elements.

Grounded parameters, i.e. a spring connected between any point in the structure and ground, may not be allowed.

Option (III) may be used to impose any of these restrictions on the selected parameters.

(IV) Structural Manipulation theory may be used to determine what the response at a point in the structure will be for a given value of a parameter. This parameter change may be incorporated into the system by inserting the parameter value into

5.21. (Continued)

(IV) (Continued)

the structure stiffness matrix. If the parameter value is k and the spring coordinates are r and s , then the following elements of the stiffness matrix are modified:

$$k(r,r) \rightarrow k(r,r) + k$$

$$k(s,s) \rightarrow k(s,s) + k$$

$$k(r,s) \rightarrow k(r,s) - k$$

$$k(s,r) \rightarrow k(s,r) - k$$

Option (IV) is used to insert both mass and stiffness parameter values into their respective matrices.

Checks are made to ensure that the matrices remain positive definite.

(V) It will be noted in option (IV) that the predicted response should be achieved where that particular parameter value is inserted into the stiffness matrix, and the new receptance matrices for the system are calculated. Where the damping in the system was originally specified in matrix form, then the response is achieved. However, where the damping is specified as a percentage of critical damping in each normal mode, then a change in the mass or stiffness data results in a change of damping since the latter depends on the eigenvalues of the system. Option (V) may be used to ensure that the generalised damping matrix remains constant when the modified receptance matrices are calculated. See

5.21. (Continued)

(V) (Continued)

Section 5.22. (Damping)

- (VI) For a given parameter, forcing point and response examination point, the data concerning the response circle produced by that parameter change can be listed. The following data is given:

The diameter and position of the centre of the circle, the response coordinates of the points at which the parameter is zero and infinity and the value of the minimum response.

- (VII) Given the restrictions imposed by option (III) there are procedures within the programme which will select automatically all the possible parameter changes within the structure. Option (VII) is used to calculate the circle diameter, bias diameter and minimum response for all the chosen parameters. These three values are taken as being representative of the relative effectiveness of the parameters. The exact definition of these criteria is given in Chapter 4, Section 4.3. The effectiveness criteria are sorted, normalised in the range 0-1 and listed in descending order. Where all the parameters are associated with elements, then a further analysis is performed giving the relative effectiveness of structural elements based on the effectiveness of the parameters associated with them.

5.21. (Continued)

(VIII) Option (VIII) uses the same list of parameters as is given in option (VII), only this time the parameters are combined in pairs and each pair is assessed to see if it can produce zero response. The total number of parameters, the number of possible paired combinations and the number of pairs achieving zero response are listed. An element analysis similar to that in option (VII) is performed where the number of times a given element occurs in a successful pair of parameters is tabulated in descending order, the values having been normalised in the range 0-1 (See Chapter 4, Section 4.3.). When a given pair is successful in achieving zero response, then the values of those parameters can also be listed.

(IX) The Structural Manipulation programme may be used to plot out the following graphical information:-

- (a) Three-dimensional response plots as functions of frequency and stiffness. See Figure 4.18. and 4.19.
- (b) Graphs of circle diameter against frequency. See Figure 4.20. and 4.21.
- (c) The boundaries of the feasible response regions. See Figure 3.6.
- (d) The construction of feasible response regions from response circles. See Figure 3.4.

5.21. (Continued)

- (X) Option (X) is used to consider a set of responses as a function of a single variable stiffness parameter. The sum of the magnitudes of the response vectors is minimised as a function of the stiffness parameter. The procedure may be used to select all the possible stiffness parameters as in option (VII) and to calculate the minimum vector sum for each parameter. The vector sums are listed in ascending order, with the values of the parameters used to produce them.
- (XI) The programme contains its own finite element capabilities which can be used to generate structure stiffness matrices. Option (XI) allows any system data associated with the elements and nodes of the structure to be altered on an individual basis without having to resubmit all the other associated data. This may take the form of changes to mass or inertia data, Young's Modulus, second moment of area of beam elements, the position of structure nodes and the connectivity of elements.
- (XII) There are procedures for listing the following system data:- Receptance matrices; the constants involved in both single and double parameter response equations (see Appendices A and B), all the system data such as mass, stiffness and damping matrices, node coordinates and element connectivity.

5.21. (Continued)

(XIII) The programme possesses the ability to retain various forms of useful system data from one run to the next. This eliminates the need to recalculate data each time the programme is run, thus saving time; in addition, the maximum amount of information on the system is always available. The following list gives an indication of the type of data retained:-

Mass, stiffness and damping matrices.

Eigenvalues, eigenvectors and transformation matrices.

The receptance matrices (calculated for the last specified value of frequency).

All element and node data.

A complete record of all the systems ever used and a description of the graphical output from the programme.

A record of any alterations that have been made to individual systems.

Most of the options not mentioned here perform only trivial tasks which are not directly associated with structural manipulation. An example of the output from the programme for some of the aforementioned options is given in Appendix G.

5.22. Programming Techniques.

File Mapping.

The fast data handling capabilities of the Structural Manipulation Programme are achieved using the file mapping facilities available on the ICL 475 computer. Normally, a programme allocates storage space for the arrays and variables that are declared within it and before any analysis can take place data must be read in and assigned to the relevant variables. This procedure must take place every time the programme is run even if the input data is the same on each occasion. When the arrays are large, then the time taken to read in the data can be quite considerable, and this is not desirable in an essentially interactive process. However, if file mapping techniques are used, then once the input data has been read in there is no need to repeat this operation on subsequent occasions.

File mapping involves the mapping of programme variables on to a file. (A file is an area of computer storage space which is assigned to a specified user process). The allocation of storage space for programme variables is arranged to coincide exactly with the space assigned to a store mapping file. Thus, once values have been assigned to these variables, then the data is stored from run to run on the store map file, and when the programme is re-run the same storage space is allocated for the variables and they automatically have the same values assigned to them as on the previous run. If the values of the variables are changed whilst running the programme, then these changes are automatically echoed in the store map file. The maximum size of array the programme is capable of handling in this manner is about 60 x 60. For a system of this size the amount of storage space the programme

5.22. (Continued)

needs is approximately 294 K bytes, which is far in excess of what would normally be allowed using conventional techniques. The maximum use of the store map file is made by storing useful programme generated data such as natural frequencies and normal mode shapes in the same manner. Thus, file mapping techniques not only save valuable running time, but also allow for larger amounts of computer storage space to be used than would normally be possible.

Coordinate Systems.

One of the more important features of any mathematical model is the coordinate system in which it is defined. All the information concerning the model is given at points whose positions are defined in this coordinate system. The information that is of interest here concerns the node and element numbering and the numbering of the degrees of freedom of the model. Two systems are used in the programme, the user system and the redundant system. The node and element numbering of the structure is the same in both systems, and is arbitrarily defined by the user. The two systems differ in the numbering of the degrees of freedom of the structure. If the structure possesses n active degrees of freedom, m nodes and the maximum number of degrees of freedom for any node is l , then the number of redundant degrees of freedom is given by

$$(l \times m) - n$$

Only the active degrees of freedom are numbered in the user system whereas the redundant system includes the inactive ones as well. In both systems the numbers are assigned such that they increase sequentially with the node numbers. This is best illustrated by an example.

Consider the simple structure shown in Figure 5.2. It consists of

5.22. (Continued)

Coordinate Systems (Continued).

three inextensible beams rigidly connected at nodes 2 and 3. The maximum number of degrees of freedom at any node is two and the number of redundant degrees of freedom is five.

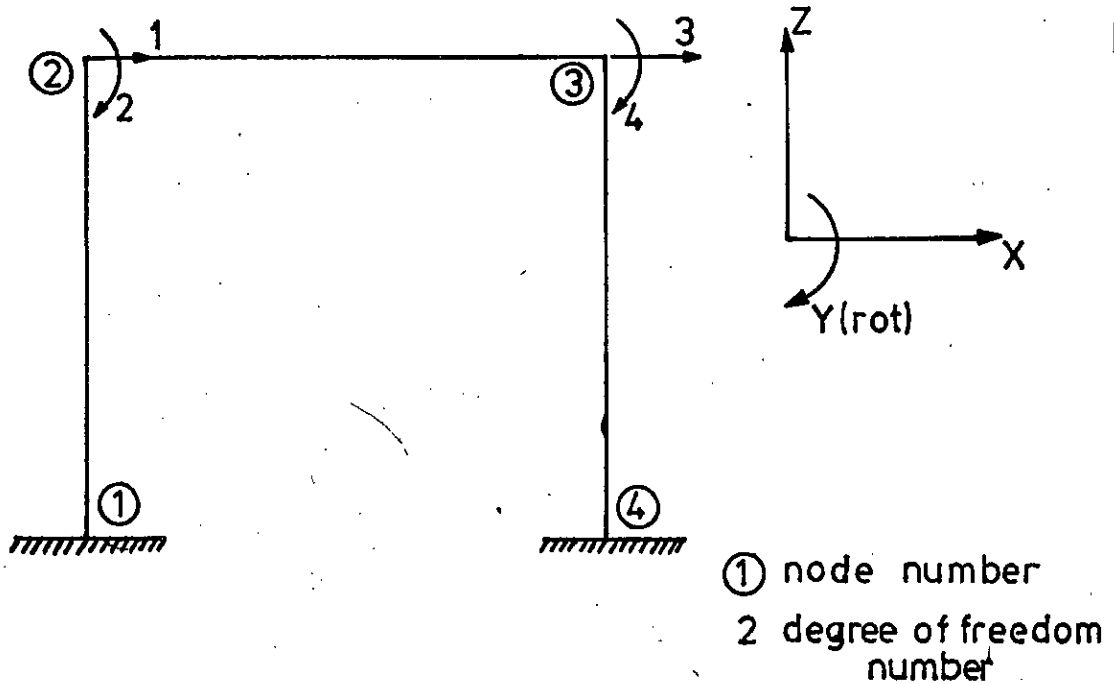


Figure 5.2.

Degree of Freedom Numbering in a Simple Structure

The numbering of the degrees of freedom in the two systems is given in Tables 5.1. and 5.2.

5.22. (Continued)

Node	x	y (rot)
1	0	0
2	1	2
3	1	3
4	0	0

Table 5.1.

User System

Node	x	y (rot)
1	1	2
2	3	4
3	5	6
4	7	8

Table 5.2.

Redundant System

In the user system the rigid nodes are identified by zero's. Degrees of freedom 1, 2, 7 and 8 in the redundant system are identified as being rigidly constrained by including them in a redundant list, degree of freedom 5 is also included in this list since it is equivalent to degree of freedom 3. The redundant system has two main advantages. Firstly, it is not necessary to store the degree of freedom numbers in arrays since they can be calculated directly for any given node and coordinate direction using the formula

$$\text{DOF number} = a + (b-1) * c$$

where a is the coordinate direction (in the example x = 1, and y (rot) = 2), b is the node number and c is the maximum number of degrees of freedom per node. The second advantage concerns the automatic selection of parameter coordinates. The simple piece of programme code shown overleaf selects the coordinates in pairs

% CYCLE I = 1,1,C

% CYCLE J = 1,1, NODE

% CYCLE K = J,1, NODE

R = I + (J-1)* C

S = 1 + (K-1)* C

% REPEAT

% REPEAT

% REPEAT

where R and S are the selected coordinates, NODE is the number of nodes in the structure and C is defined above. The coordinate pairs are checked against the list of redundant coordinates, and any pair containing a redundant degree of freedom is rejected. The successful pairs are transformed to the user system where they are checked for element association and also for mechanical coupling with the examination point. This physical coupling is an obvious necessity otherwise the variation of that particular parameter would be meaningless. The test for coupling between two points, i and j, is if the element G_{ij} of the receptance matrix is non-zero.

Damping and the Calculation of the Receptance Matrices.

In simple mass, spring, dashpot systems, damping is specified directly in the form of a matrix; in reality, however, damping is seldom encountered in this form. Where complex structures are modelled using finite element techniques, then damping may be included in the model in the form of a percentage of critical damping in each normal mode. The magnitude of the damping factors can either

* is the computer symbol for multiplication.

5.22. (Continued)

be estimated or measured experimentally. In order to introduce damping into the system, the equations of motion are transformed into generalised coordinates using the generalised transformation matrix \underline{R} which is obtained directly from the eigenvectors of the system. It is known [14] that the transformation matrix \underline{R} will uncouple the undamped equations of motion of an N degree of freedom system in the following way. If the equations of motion of the undamped system are given by

$$\underline{M} \ddot{\underline{x}} + \underline{K} \underline{x} = 0 \quad (5.1)$$

Then, substituting for \underline{x} in equation 5.1. using the generalised transformation

$$\underline{x} = \underline{R} \underline{q} \quad (5.2)$$

where \underline{q} are the generalised coordinates of the system; and pre-multiplying by \underline{R}^T (the transpose of matrix \underline{R}) gives

$$\underline{R}^T \underline{M} \underline{R} \ddot{\underline{q}} + \underline{R}^T \underline{K} \underline{R} \underline{q} = 0 \quad (5.3)$$

in which

$$\underline{R}^T \underline{M} \underline{R} = \underline{M}^* = \underline{I}$$

and

$$\underline{R}^T \underline{K} \underline{R} = \underline{K}^* = \underline{\lambda}$$

where \underline{M}^* and \underline{K}^* are the generalised mass and stiffness matrices respectively and $\underline{\lambda}$ is the ($N \times N$) diagonal matrix of eigenvalues λ_i .

Now, if the damped equations of motion of the system are to be uncoupled by transforming to generalised coordinates, then the generalised damping matrix \underline{E}^* will be of the form

$$\underline{E}^* = \text{diag} [2 \zeta_i \omega_i] \quad (5.4)$$

where ζ_i is the damping factor in the i^{th} normal mode and ω_i is the i^{th} natural frequency of the system. The forced generalised equations

5.22. (Continued)

of motion of the system may be written

$$\underline{M}^* \ddot{\underline{q}} + \underline{E}^* \dot{\underline{q}} + \underline{K}^* \underline{q} = \underline{F}^* e^{i\omega t} \quad (5.5)$$

where $\underline{F}^* = \underline{R}^T \underline{F}$

The steady state solution for the response \underline{q} is given by

$$\underline{q} = \underline{q} e^{i\omega t}$$

where

$$\underline{q} = \underline{G}^* \underline{F}^* \quad (5.6)$$

and

$$\underline{G}^* = \text{diag} [(\lambda_1 - \omega^2) + 2i\zeta_1 \omega_1 \omega]^{-1} \quad (5.7)$$

which is the generalised complex receptance matrix for the system.

Equation 5.7. may be written in the more general form

$$\underline{G}^* = [\underline{A} + i\underline{B}]^{-1} \quad (5.8)$$

where \underline{A} is the (N x N) diagonal matrix of terms $(\lambda_1 - \omega^2)$ and \underline{B} is the (N x N) diagonal matrix of terms $(2\zeta_1 \omega_1 \omega)$. If the real and imaginary components of \underline{G}^* are \underline{C}^* and \underline{D}^* respectively, then from equation 5.8.

$$[\underline{C}^* + i\underline{D}^*] [\underline{A} + i\underline{B}] = \underline{I} \quad (5.9)$$

Equating the real and imaginary parts of equation 5.9. gives

$$\underline{C}^* \underline{A} - \underline{D}^* \underline{B} = \underline{I} \quad (5.10)$$

and

$$\underline{D}^* \underline{A} + \underline{C}^* \underline{B} = \underline{0} \quad (5.11)$$

Equations 5.10. and 5.11. may be solved simultaneously to give \underline{C}^* and \underline{D}^* as functions of \underline{A} and \underline{B} as follows

$$\underline{C}^* = [\underline{A} + \underline{B} \underline{A}^{-1} \underline{B}]^{-1}$$

and

$$\underline{D}^* = - \underline{C}^* \underline{B} \underline{A}^{-1}$$

5.22. (Continued)

Matrix A is chosen for inversion since the inversion of matrix B which contains small terms associated with the damping of the system might lead to numerical errors. The real and imaginary parts of the generalised complex receptance matrix G* may thus be calculated from the eigenvalues of the system and the damping factors in each normal mode. Equation 5.6. may now be transformed back to the original coordinate system to give the response vector x as follows

$$\underline{x} = \underline{G} \underline{F} = \underline{R} \underline{G}^* \underline{R}^T \underline{F}$$

If the real and imaginary parts of G are C and D respectively, then they may be given in terms of the real and imaginary parts of G* as follows

$$\underline{C} = \underline{R} \underline{C}^* \underline{R}^T$$

and

$$\underline{D} = \underline{R} \underline{D}^* \underline{R}^T$$

It is the elements of matrices C and D that are used in Appendix A to calculate the constants involved in the equation for the receptance as a function of variable stiffness.

If the damping matrix E had been specified explicitly then the matrices A and B would have been calculated as follows

$$\underline{A} = [\underline{K} - \underline{M}\omega^2]$$

and

$$\underline{B} = \underline{E}\omega$$

The real and imaginary components of the receptance matrix G are now given by

$$\underline{C} = [\underline{A} + \underline{B} \underline{A}^{-1} \underline{B}]^{-1}$$

and

$$\underline{D} = -\underline{C} \underline{B} \underline{A}^{-1}$$

5.22. (Continued)

It will be noted that the inversion of matrices when working in generalised coordinates is simple, since the matrices involved are all diagonal. Also with reference to Section 5.21. Option (V), it is matrix $\underline{B} = \underline{E}^{-1}\underline{C}$ which is held constant in order that the damping of the system remains unchanged when the eigenvalues of the same system are altered.

5.3. Conclusions.

A brief description of some of the capabilities of the Structural Manipulation Programme has been given. The programme which has been developed and improved over a two and a half year period is at present in a well tried and tested state. It has been shown to be a useful tool in the practical application of structural manipulation and its development is not limited just to consideration of ways of achieving minimum response at specified points in a structure. Research is at present being carried out into the possibility of adapting the Structural Manipulation theory developed here to tackle the problem of flutter in aircraft lifting surfaces. The aim would be to manipulate the relevant substructure variables in order to achieve a specified normal mode configuration. There should be relatively little difficulty in adapting the programme to produce results relating to the effectiveness of parameters in changing a normal mode shape.

Under normal operating conditions when the programme is being run on-line, a restriction of two minutes CPU* time is imposed, and

[* Central Processor Unit.]

5.3. (Continued)

this tends to limit the size of systems that can be considered, and also the scale of mathematical operations that can be performed. In order to save time, wherever possible iterative procedures are avoided and matrix analyses are performed using diagonal matrices. A great deal of emphasis has also been placed on the production of concise results which present information in a qualitative rather than quantitative form. The programme is intended to give a rapid analysis of a simple structural model with the broad aim of producing results which will indicate, in the most general sense, those areas of that structure which are most suitable for modification for the purpose of reducing vibration levels.

CHAPTER 6

EXPERIMENTAL ANALYSIS

6.1. Introduction.

The aim of the experimental analysis was to examine the dynamic response at a point in a structure and to verify that the locus of that response vector traces out a circle when the stiffness of a simple spring element in the structure is varied. It was not considered necessary to examine the more complicated situations involving two or more parameters, for it was evident that the results pertaining to these cases could be arrived at equally well by allowing each parameter to vary individually in turn. Thus, if the form of the response can be verified for a single variable parameter, then those results involving more than one parameter may also be assumed to be true. This is by virtue of the fact that the response circle forms the constituent part in higher order cases.

As well as verifying the form of the response, the accuracy of the values is compared with those obtained theoretically. The latter must obviously depend very much on the degree of accuracy to which the experimental structure can be modelled mathematically. In order to determine the accuracy, the natural frequencies of the experimental structure were measured and used as the basis for comparison between experiment and theory.

To achieve the objectives outlined above, a test structure was built and a continuously variable stiffness element was designed to operate in conjunction with this. The structure was to be realistic, yet not unduly complicated by too many unnecessary degrees of freedom,

6.1. (Continued)

and consideration was to be given in its design to the ease with which it could be modelled mathematically. A programme controlled transfer function analyser was used to measure the response of the structure. The experiment was divided into two stages; the measurement of structural response as a function of variable stiffness, and the determination of the natural frequencies, mode shapes and damping of the structure. The remaining sections in this chapter describe the construction of the experimental equipment, the techniques involved in the analysis and the measurement of the results.

6.2. The Design and Development of a Variable Stiffness Element.

6.21. General Specification.

Ideally, the variable stiffness element should have linear characteristics and be continuously variable in a manner causing the least possible disturbance to the experimental system. In the preliminary design stages, four ideas were considered; an electro-mechanical spring, interchangeable spring elements, an air spring and a variable length cantilever spring. The first two ideas were rejected on the grounds that they were unsuitable. Two prototypes of the air spring were built, but the idea was abandoned owing to technical difficulties. Finally, a variable length cantilever spring was designed and incorporated in the structure. This had the desired characteristics and was used successfully to vary stiffness within the structure. A brief description of each of the four ideas is given below.

6.22. The Electro-mechanical Spring.

Figure 6.1. shows the schematic representation of an electro-mechanical spring, consisting of a solenoid mounted between two points in a structure. A linear potentiometer is attached between the same

6.22. (Continued)

two points and produces a signal which is directly proportional to their relative displacements. This signal is used as the input to a variable gain amplifier whose output is then fed directly to the solenoid. The system is adjusted so that the solenoid applies zero force when the structure is in equilibrium.

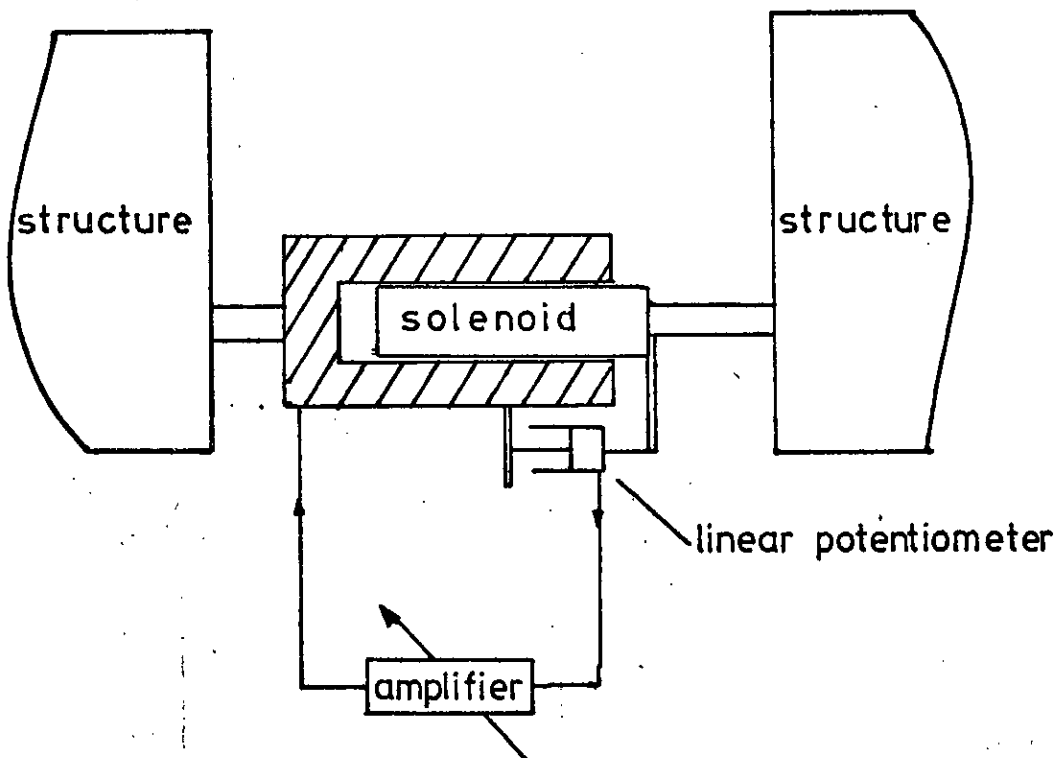


Figure 6.1.

Schematic Representation of an Electro-mechanical Spring

6.22. (Continued)

The stiffness of the solenoid can be varied, without disturbing the structure, by altering the gain of the amplifier. The inadequacies of this system are concerned with the solenoid. Firstly, it is difficult to arrange for the solenoid to operate efficiently in both the push and pull modes; and secondly, the maximum force output and hence the maximum stiffness of solenoids of a suitable size is not large enough to be compatible with the envisaged stiffness of the experimental structure.

6.23. Interchangeable Spring Elements.

An adequate, though not altogether satisfactory method of achieving variable stiffness in a structure is to use a set of linear spring elements each with a different stiffness constant. However, the disadvantages of this arrangement include the limited range of stiffness for a given spring size and the considerable disturbance that would be caused in the structure when changing the elements. This idea was only to be considered as a last resort.

6.24. The Air Spring.

The single acting air spring consisting of a column of air trapped between a cylinder and a movable piston is used in a wide variety of applications mainly connected with suspension systems. In most cases the highly non-linear nature of the air spring is either used to some specific advantage or is considered to be of no great importance. If the air spring is considered to be double acting as shown in Figure 6.2., then for small displacements the stiffness of the spring may be considered to be approximately constant.

6.24. (Continued)

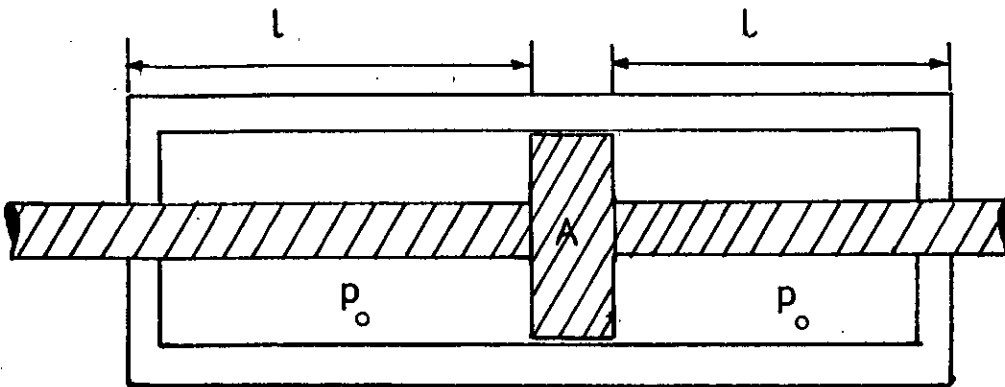


Figure 6.2.

Double Acting Air Spring

By varying the initial pressure P_0 in the cylinder, the stiffness of the spring may be altered and a wide range of values may be achieved without any undesirable increase in weight.

Theoretically, the air spring offers reasonable scope for development, and in the initial stages of the experimental investigation a considerable amount of time and effort was spent on its design and construction. The project, however, never reached a satisfactory conclusion and was abandoned. The design of the air spring is unfortunately marred by the technical difficulties associated with its construction. These are severe enough to make the time scale for the project quite unreasonable. The theory of the air spring and the state of progress achieved during its development are discussed briefly here.

The system depicted in Figure 6.2. consists of a cylinder of length $2l$ and cross sectional area A . A double shafted piston is positioned centrally within the cylinder and held there in equilibrium

6.24. (Continued)

by equal pressures P_0 on either side. The gas within the cylinder may be considered to obey the adiabatic law.

$$PV^\gamma = \text{constant} \quad (6.1)$$

where P is the pressure, V the volume and γ is the ratio of specific heat for that particular gas. For the sake of simplicity, the latter is considered to be unity in the remaining analysis. If the piston is displaced from the equilibrium position by a distance x , then the new pressures to the right and left of the piston are P_1 and P_2 respectively. From equation 6.1. these are related by

$$P_0 V_0 = P_1 V_1 = P_1 (l - x)A \quad (6.2)$$

$$P_0 V_0 = P_2 V_2 = P_2 (l + x)A$$

The resultant force on the piston is then

$$(P_1 - P_2)A = \frac{2P_0 A l x}{l^2 - x^2} \quad (6.3)$$

If $l^2 \gg x^2$, then this may be approximated by

$$(P_1 - P_2)A = \frac{2P_0 A x}{l} \quad (6.4)$$

which provides a linear relationship between force and displacement.

The discrepancy in using this approximation may be estimated from the graphs given in Appendix E which show the relationship between

$$\frac{(P_1 - P_2)A}{2AP_0} \quad \text{and} \quad \frac{x}{l} \quad \text{for both equations 6.3. and 6.4.}$$

The error in the approximation can be seen to be small for values of $\frac{x}{l}$ up to 0.3 where it is 11%.

Having obtained a configuration with linear characteristics, it is now required to examine the parameters affecting the stiffness of the

6.24. (Continued)

spring. The latter may be obtained from equation 6.4. and is given by

$$k = \frac{2P_0 A}{\ell} \quad (6.5)$$

Once the physical dimensions of the spring have been decided upon, varying the initial pressure P_0 is the only means whereby the stiffness of the spring can be altered. The length and area of the cylinder have a definite effect on the spring's sensitivity to small displacements. High sensitivities can be achieved using either large values of A or small values of ℓ . But as ℓ becomes small, it will tend to violate the necessary condition that $\ell^2 \gg x^2$ for linearity in equation 6.3. Considering a spring with a maximum working displacement of 0.25" and a 2.0" cylinder ($\ell = 1"$), then the error in using the approximation in equation 6.2. is less than 2%. Thus, although not critical, decreasing the size of ℓ still further is not a desirable way of increasing the sensitivity of the spring. However, increasing the piston area A , which depends on the square of its diameter, is an effective way of increasing sensitivity without introducing any undesirable characteristics.

The theory shows the air spring to be a viable concept; the practical implementation of this however involves a considerable amount of technical difficulty. The problems fall into two main categories. The first of these involves the provision of dynamic, yet gas-tight seals, whilst the second involves the minimisation of the friction forces between moving parts. Two air springs were built in an effort to provide satisfactory solutions to these problems. The experience gained in each case provided useful information, but neither version succeeded in possessing the desired characteristics. Both versions of

6.24. (Continued)

the air spring are described here, and a discussion of the merits and undesirable qualities of each is given.

Version I.

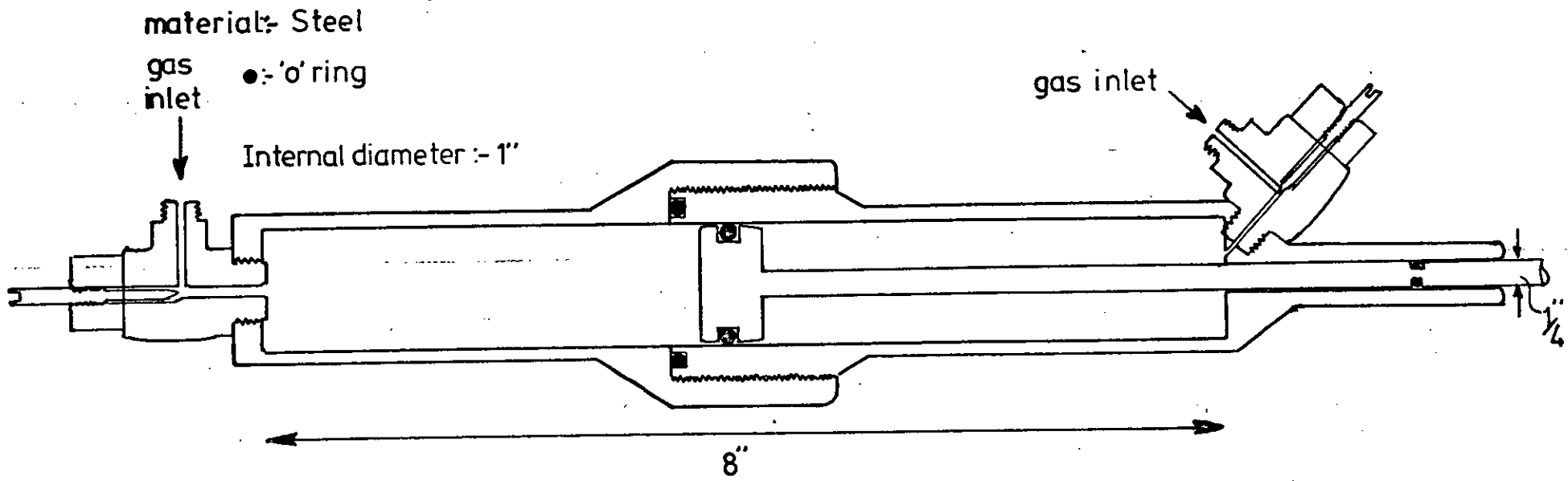
The first version of the air spring is shown in Figure 6.3. and consists of a closed cylinder containing a single shafted piston. O rings inset on the shaft and the piston serve both as bearings and as gas-tight seals. Both sides of the piston were pressurised through the needle valves at either end of the cylinder. The gas used throughout the initial stages of the investigation was compressed air being generated from a portable compressor. The maximum available pressure was 110 p.s.i.

The air spring was tested in the horizontal position using an initial pressure of 50 p.s.i. and with a 2 lb. mass attached to the piston. With the cylinder clamped, the piston was excited by an electromagnetic vibrator over a range of frequencies. The system exhibited no form of magnified response. Large friction forces were found to exist between the O rings and cylinder, although these were considerably reduced once the piston had been set in motion. The unbalanced effect caused by having only one shaft on the piston was sufficient enough to cause it to creep down the cylinder. It was found that even when subjected to the maximum available pressure of 110 p.s.i., the small displacement encountered ($\approx .050''$) was insufficient to cause any significant resultant force on the piston, i.e. there was no effective spring action.

Version II.

In the light of the observations made from the first air spring, Version II was designed incorporating the following modifications:

Figure 6.3.
-116-



Air Spring Version I

Version II (Continued)

- (i) A double shafted piston mounted in linear bearings to eliminate any radial loads on the O rings.
- (ii) The use of maximum tolerances to reduce friction.
- (iii) Increased piston area and reduced cylinder length to increase sensitivity to small displacements.
- (iv) A flexible diaphragm between the piston and cylinder instead of an O ring.
- (v) Greater accuracy in the manufacture of all parts.
- (vi) The use of CO₂ instead of air (maximum pressure 750 p.s.i.).

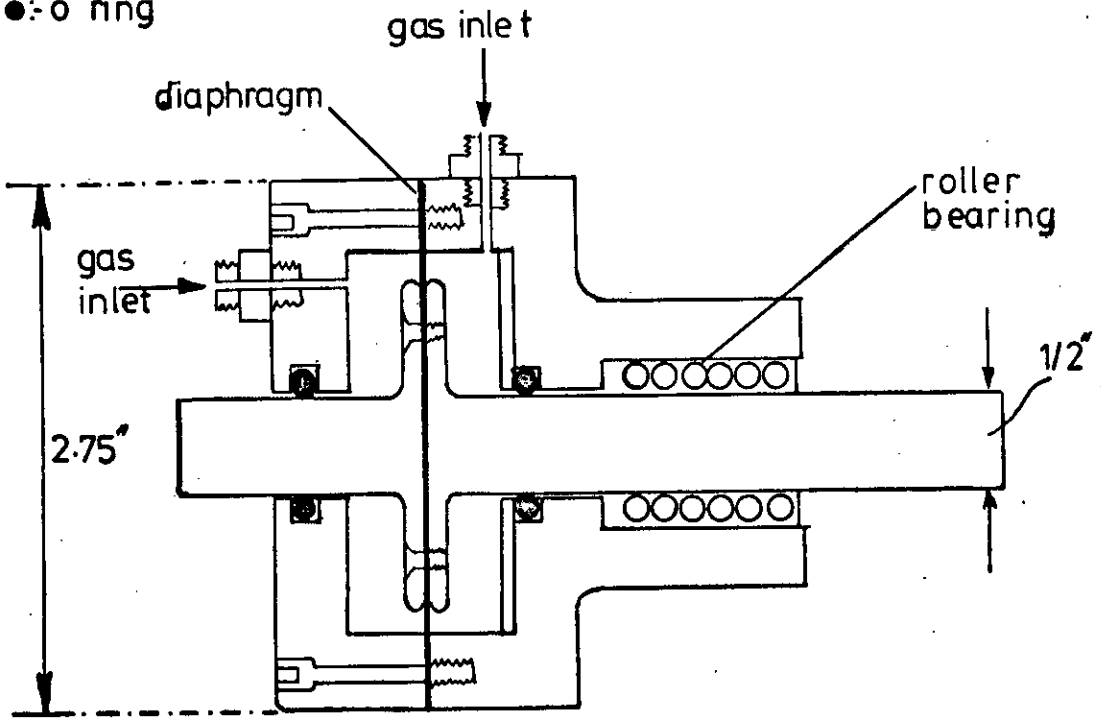
Apart from incorporating several improvements to reduce friction, Version II of the air spring was designed in order to achieve increased sensitivity and also to assess the effectiveness of using a diaphragm as a flexible seal between the piston and cylinder rather than an O ring. It was hoped that whilst still retaining an effective gas-tight seal, this arrangement would allow sufficient freedom of movement yet not possess any of the undesirable frictional qualities of its predecessor. Figure 6.4.(a) shows the layout of the spring. The length of the cylinder has been reduced to one inch ($l = 0.5''$), which with the maximum expected displacement of 0.1" causes the departure from the linear law to be only 4%.

Tests were carried out initially to determine the ideal material

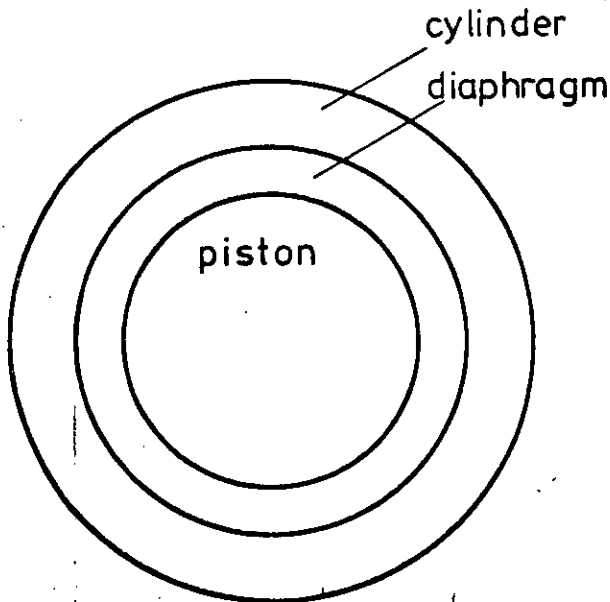
1" Internal diameter, stroke $\pm .5$ "

material:- Aluminium

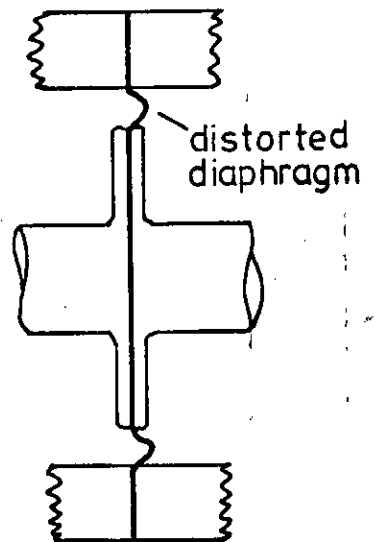
●: 'o' ring



(a)



(b)



(c)

Air Spring Version II

Figure 6.4.

6.24. Version II (Continued)

and optimum size for the diaphragm. Firstly, several thicknesses of rubber sheet were tried, ranging from 0.015" (surgeons gloves) to 0.1" thick. In each case these proved to be too flexible and were easily deformed by the substantial pressure differences within the cylinder (see Figure 6.4.(c)). Next, steel shim varying in thickness from 0.002" to 0.01" was used in an attempt to obtain flexibility yet eliminate any stretching of the diaphragm. Besides changing the thickness of the steel, the ratio of the area of the diaphragm to that of the piston was also varied (see Figure 6.4.(b)). However, when sufficient latitude of movement had been achieved the diaphragm soon cracked due to fatigue. Considerable difficulty was also experienced in obtaining a gas-tight seal between the two halves of the cylinder. This was most probably the cumulative effect of using a gasket rather than an O ring to provide a seal, and the increased forces accompanying the higher gas pressures. No frequency response characteristics were obtained for Version II.

6.25. The Variable Length Cantilever Spring.

Originally, it was intended that the variable stiffness element should be capable of being attached between any two compatible points in the structure. By restricting the generality of this statement and considering only the simplest form of parameter variation, namely a linear spring with one end attached to the structure and the other end to ground, it is possible to construct the equivalent system shown in Figure 6.5(1). This consists of a cantilever beam clamped at the lower end and attached to the structure at the other via a rigid connecting rod. Rotational releases at either end of the connecting rod ensure that only horizontal forces are transmitted to the structure. The

6.25. (Continued)

cantilever applies an external force to the structure which is proportional to displacement and is given by

$$F = \frac{3EI}{L^3} x \quad (6.6)$$

where E is Young's modulus for the material and I and L are the second moment of area and length respectively. The stiffness at the end of the cantilever can be varied by altering its length; this is achieved using an adjustable clamp, details of which are given in Appendix F. The arrangement is simple to operate and is capable of producing a wide range of stiffnesses.

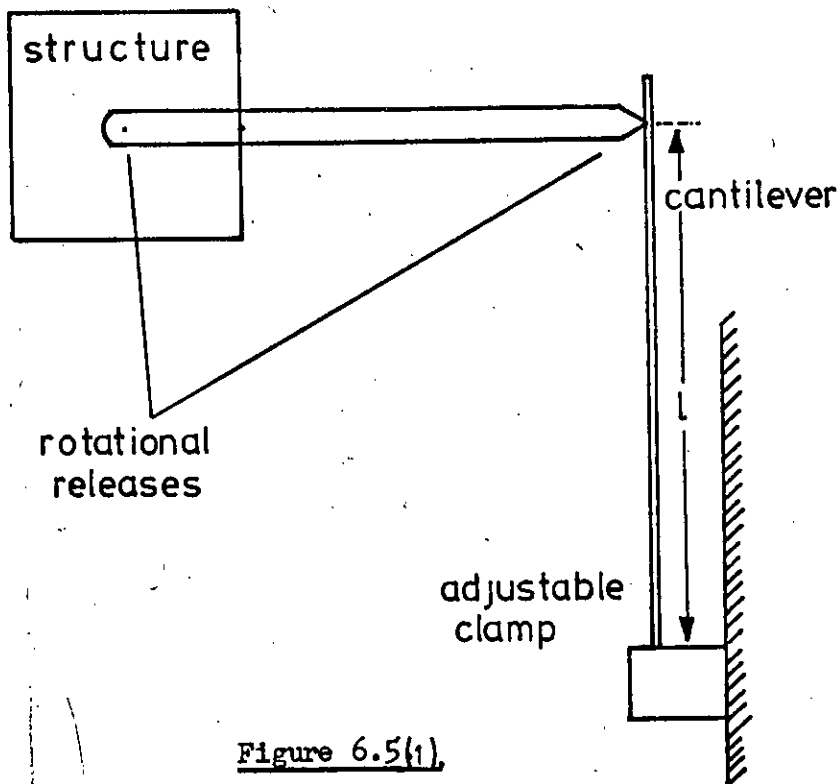


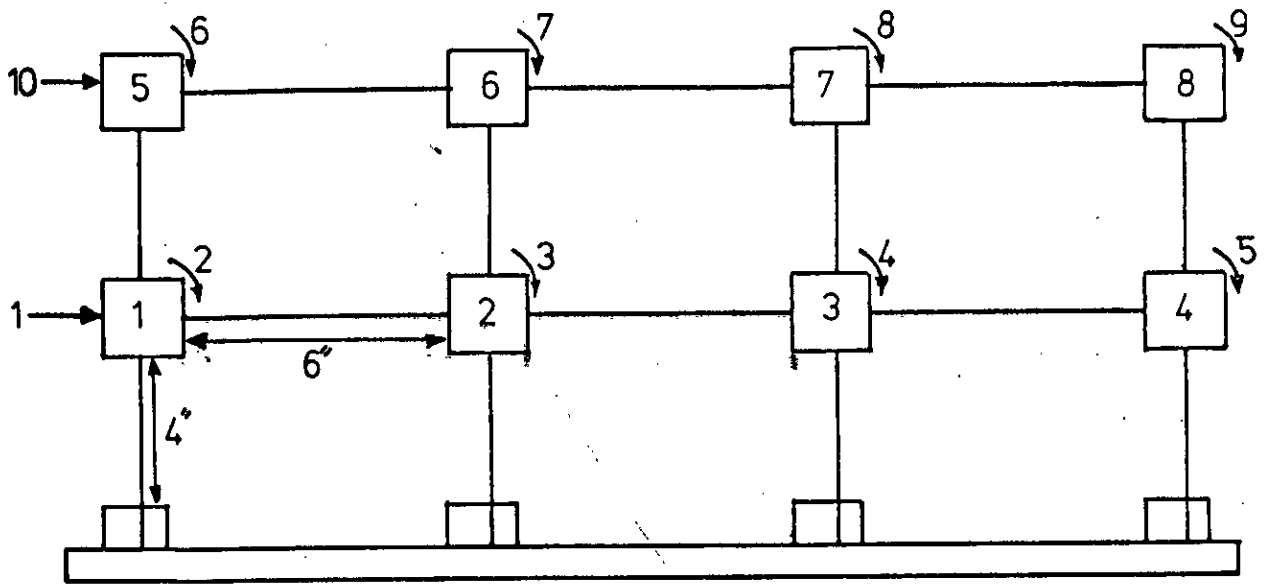
Figure 6.5(i),
Variable Length Cantilever

6.3. The Test Structure.

The test structure which is made up of steel blocks interconnected by spring steel strips is shown in Figure 6.5.(a). The dimensions of the structure were initially determined in order that the highest natural frequency of the system should not exceed 159 Hz. This restriction comes as a result of the limited resolution of frequency in the oscillator that is used to drive the exciters. For frequencies up to 159 Hz, the resolution is 0.1 Hz, after which it increases to 1.0 Hz. The disadvantages of the latter are obvious. Through a process of trial and error the 6" x 4" rectangular arrangement shown in the figure was found to have natural frequencies in the range 0-159 Hz.

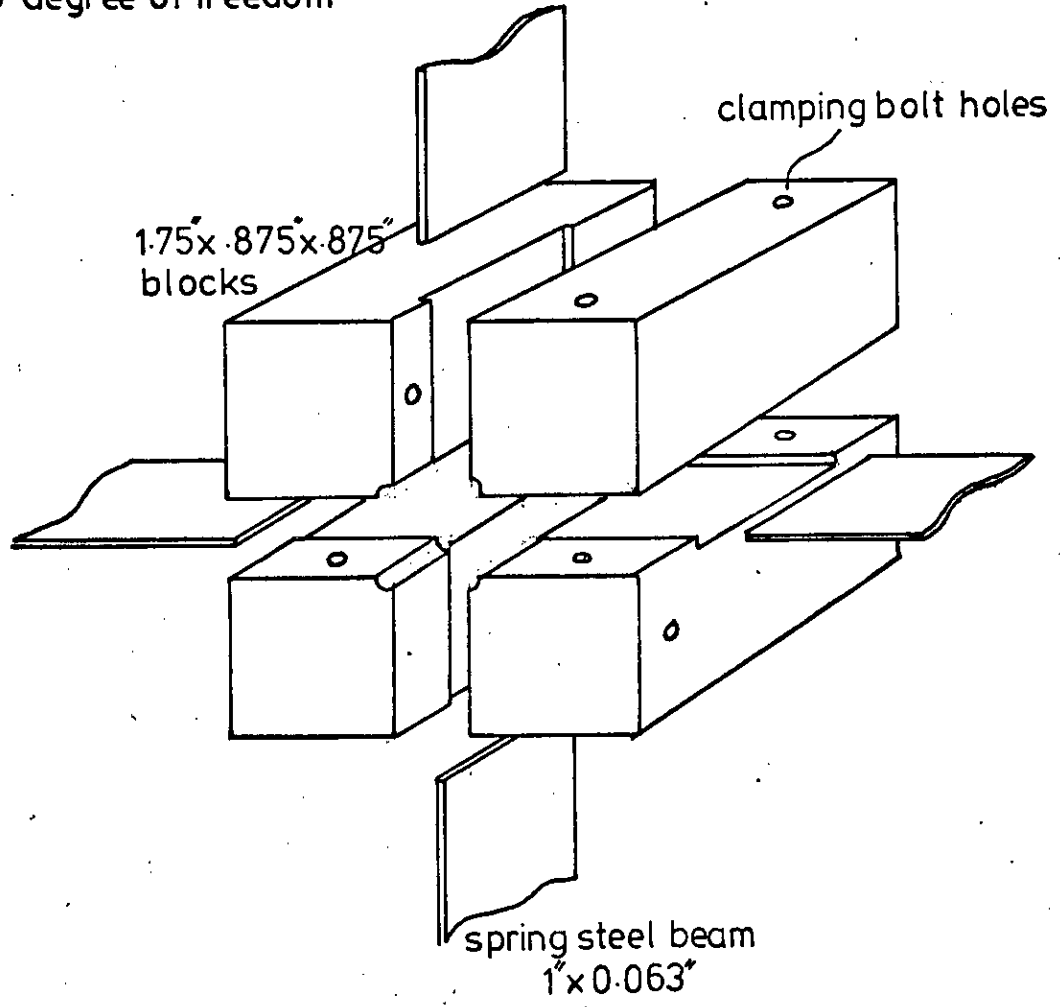
The test structure consists of eight 1.75" square steel blocks inter-connected by 1.0" x 0.063" spring steel strips to form a 6" x 4" rectangular grid. The structure is considered to possess ten degrees of freedom, two translations and eight rotations. For reasons that will become apparent later, this was reduced to eight by constraining degrees of freedom 9 and 10 (Block 8 rigid). This arrangement increases the stiffness of the structure and causes the two highest natural frequencies to exceed the desired limit of 159 Hz. This undesirable characteristic was considered unavoidable at the time the modification was made. The modified structure is the one referred to throughout the rest of this section.

The blocks, each representing a structural node, consist of four 0.875" x 0.875" x 1.75" slotted sections and are joined together as shown in the exploded diagram in Figure 6.5.(b). The blocks are deliberately made large in order that their mass should be very much greater than that of any attached instrumentation. A hole drilled



3 node number [a]

5 degree of freedom



[b]

Test Structure and Node Block

6.3. (Continued)

centrally through the block allows for the attachment of accelerometers to measure the horizontal and rotational acceleration at that point. A representation of the latter is achieved by mounting an accelerometer off the centre line of the block with its least sensitive axis in the horizontal direction.

The structure is excited externally in either of two ways, horizontally at block 1 or in the form of a torque at block 2. Both these forms of excitation are necessary in order to properly excite the normal modes of the structure. The horizontal excitation force is transmitted to the structure via the coupling arrangement shown in Figure 6.6.

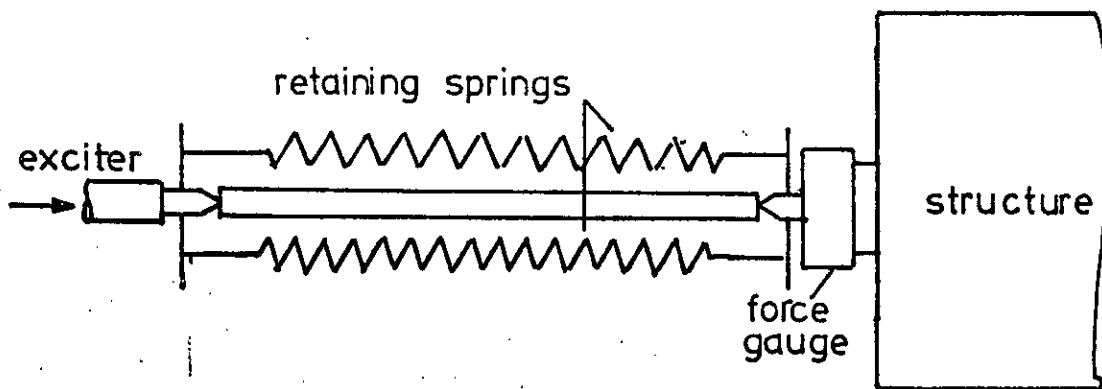


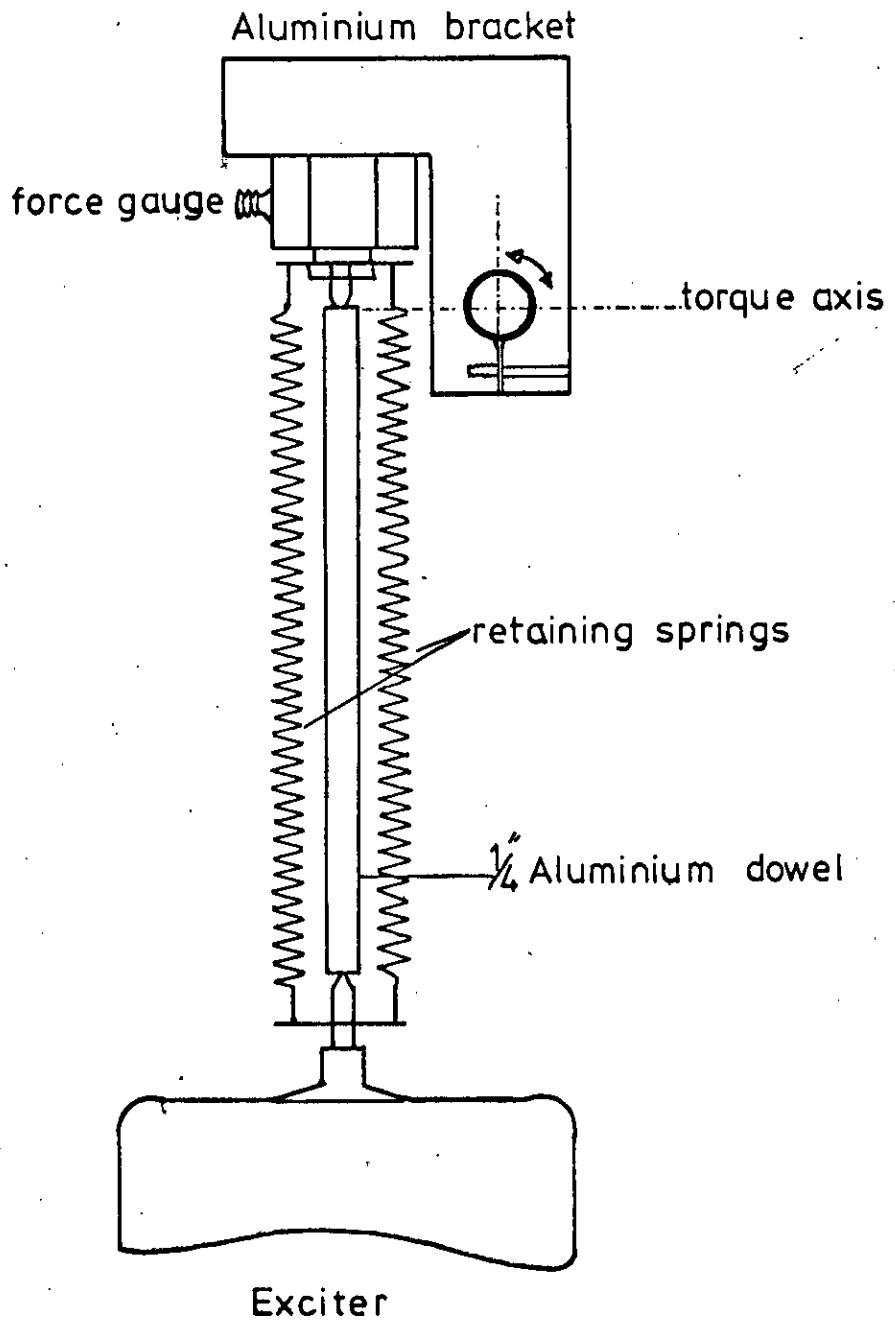
Figure 6.6.

Coupling Mechanism from the Exciter to the Structure

6.3. (Continued)

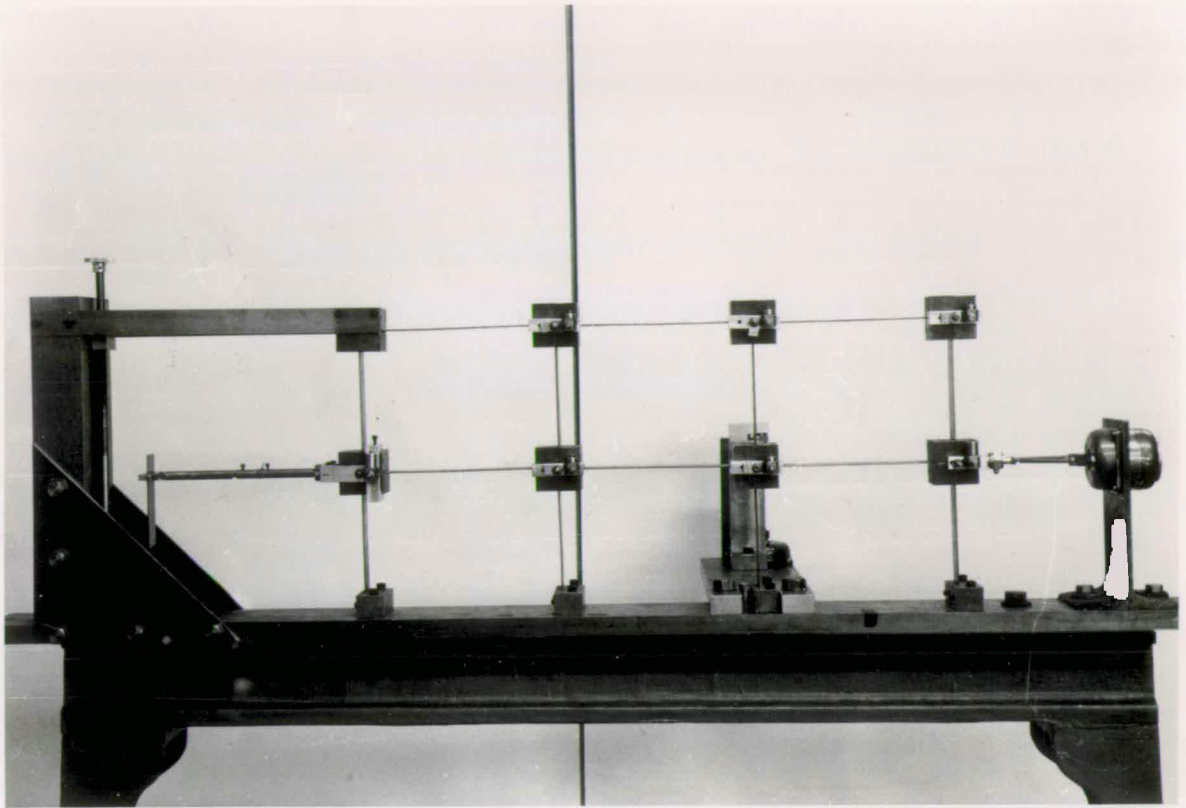
The coupling consists of two pointed spigots attached to the vibrator and structure; a piece of 0.25" aluminium dowel completes the connection and is located in position by dimples at either end. The retaining springs are tensioned sufficiently to prevent the connecting bar from falling out when the coupling is in tension. The system only transmits horizontal forces to the structure and allows for a certain degree of misalignment between the two spigots, thus minimising any lateral forces on the exciter.

The application of a pure torque to the structure was originally achieved using the arrangement shown in Figure 6.7. (see also photograph (B) in Figure 6.8.). The torque was generated at the fixed end of the coupling by means of an offset vibrator as shown in the figure. This was then transmitted to the structure via a torque tube and a set of two expandable bellows. The bellows were included to allow any horizontal motion of the structure relative to the exciter. This system resulted in some undesirable non-linear effects and was later replaced by the rigid bar shown in photograph (C) in figure 6.8. In practice the structure exhibits very little horizontal motion when excited in the rotational mode and consequently the increased flexibility introduced by the more rigid connection does not significantly affect the measurement of the higher modes of the system. The cantilever spring described in Section 6.25. is attached to the structure at block 4, thereby allowing the stiffness to be varied in the horizontal direction at that point. A general impression of the test structure may be obtained from the photographs in Figure 6.8.



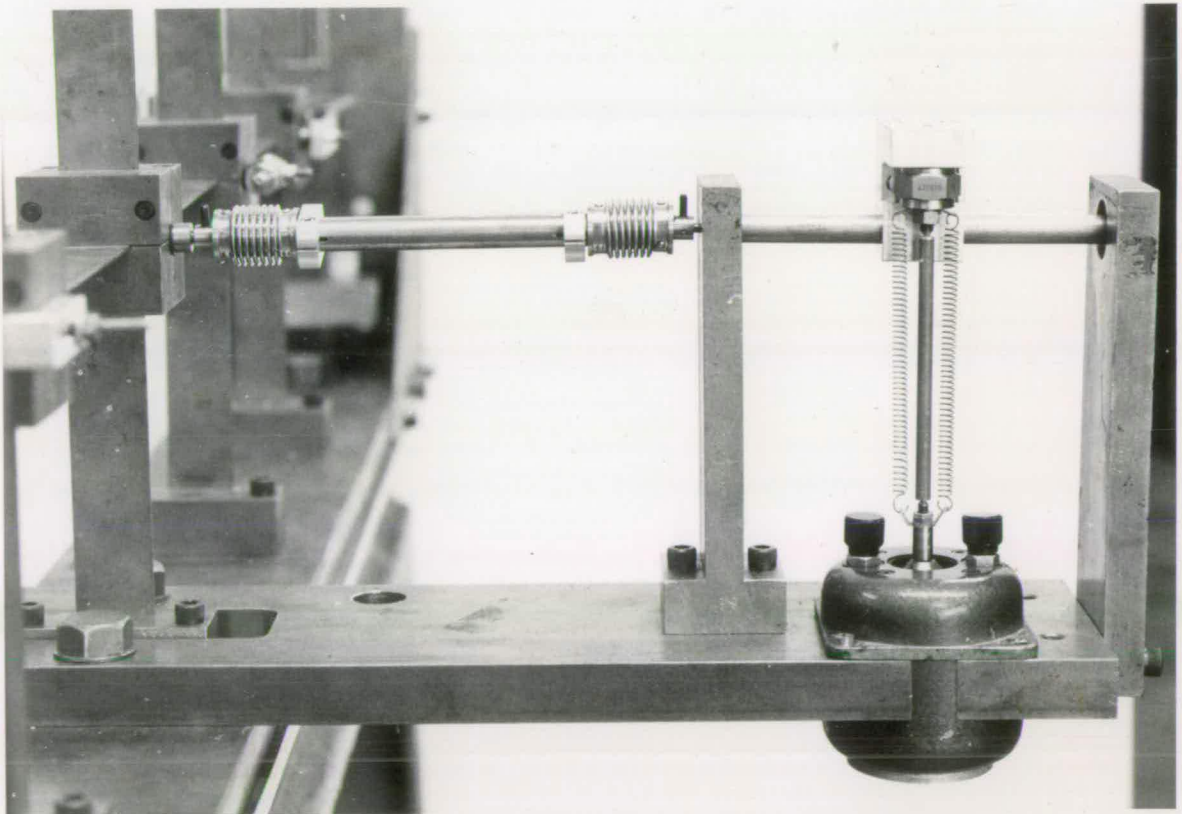
Generation of a Torque

Figure 6.7.



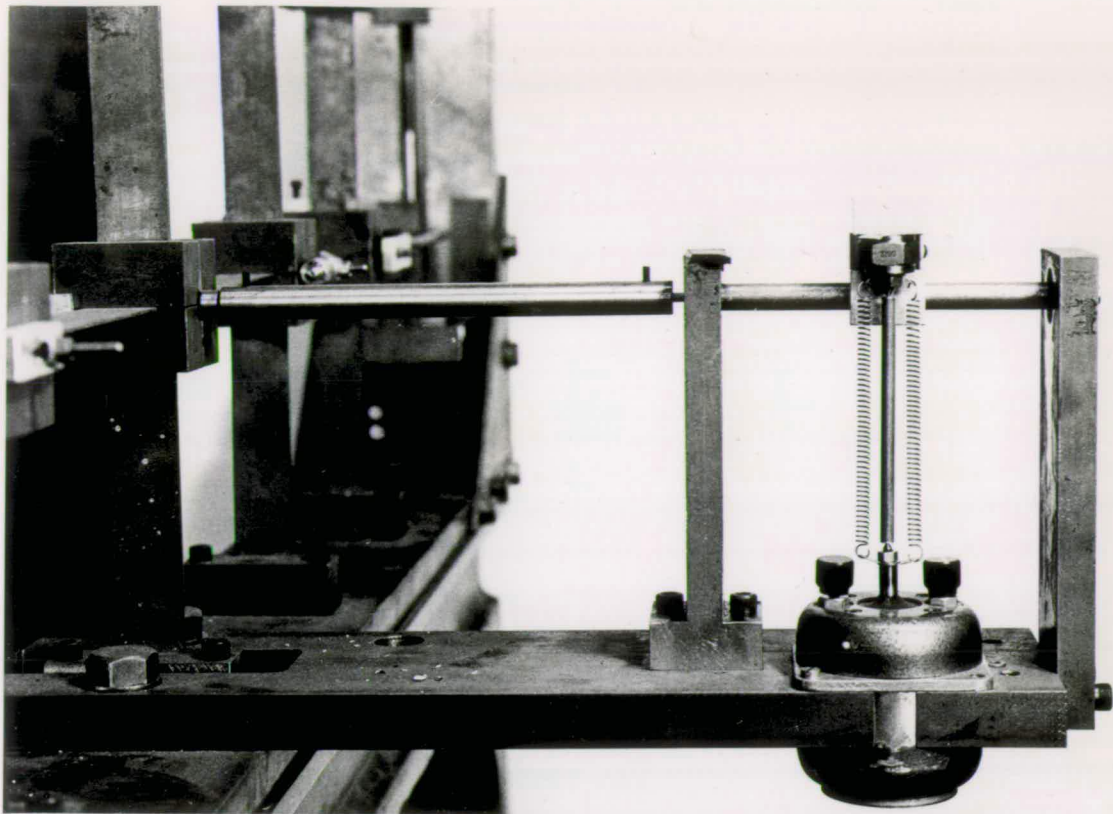
(A)

The Test Structure.



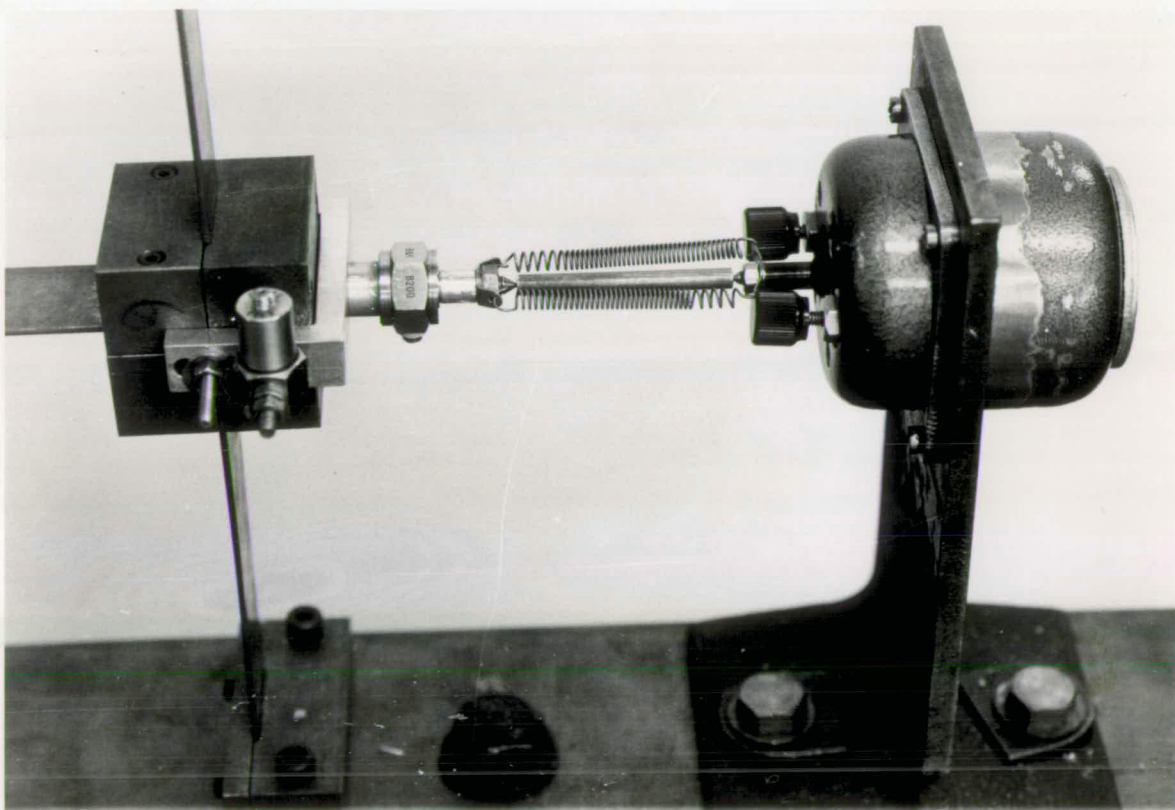
(B)

Applied Torque Using Bellows Couplings. Figure 6.8.



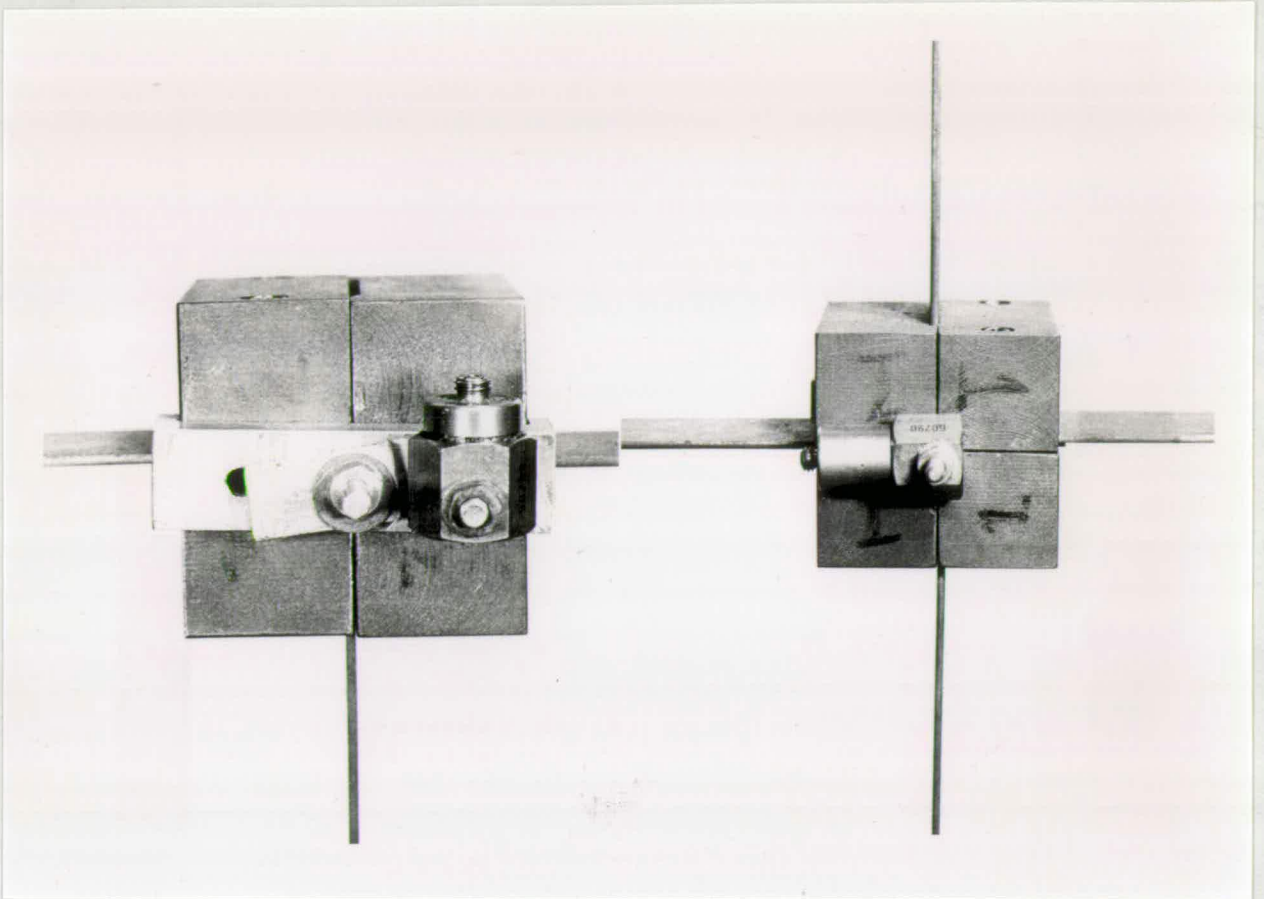
(C)

Applied Torque Using a Rigid Coupling.



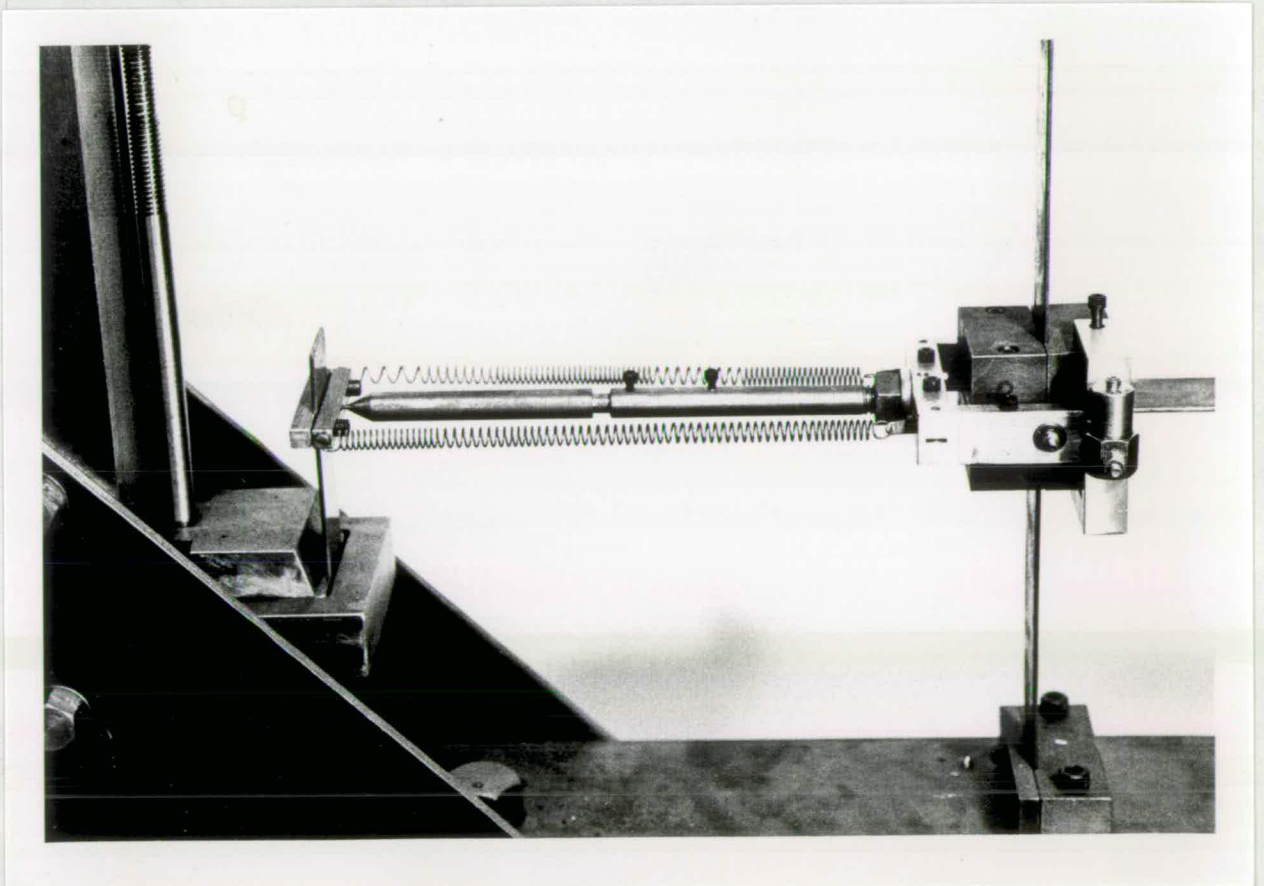
(D)

Horizontal Exciter. Figure 6.8.



(E)

Accelerometer Stations.



(F)

Variable Stiffness Cantilever Spring. Figure 6.8.

6.3. (Continued)

At the beginning of this section, it was mentioned that the original test structure was modified in order to rigidly constrain degrees of freedom 9 and 10 at block 8. This modification was made after considering the results of an initial investigation into the way in which structural response varies as a function of stiffness. It became apparent that the response locus was not circular as had been predicted, but appeared in the form shown in Figure 6.9.

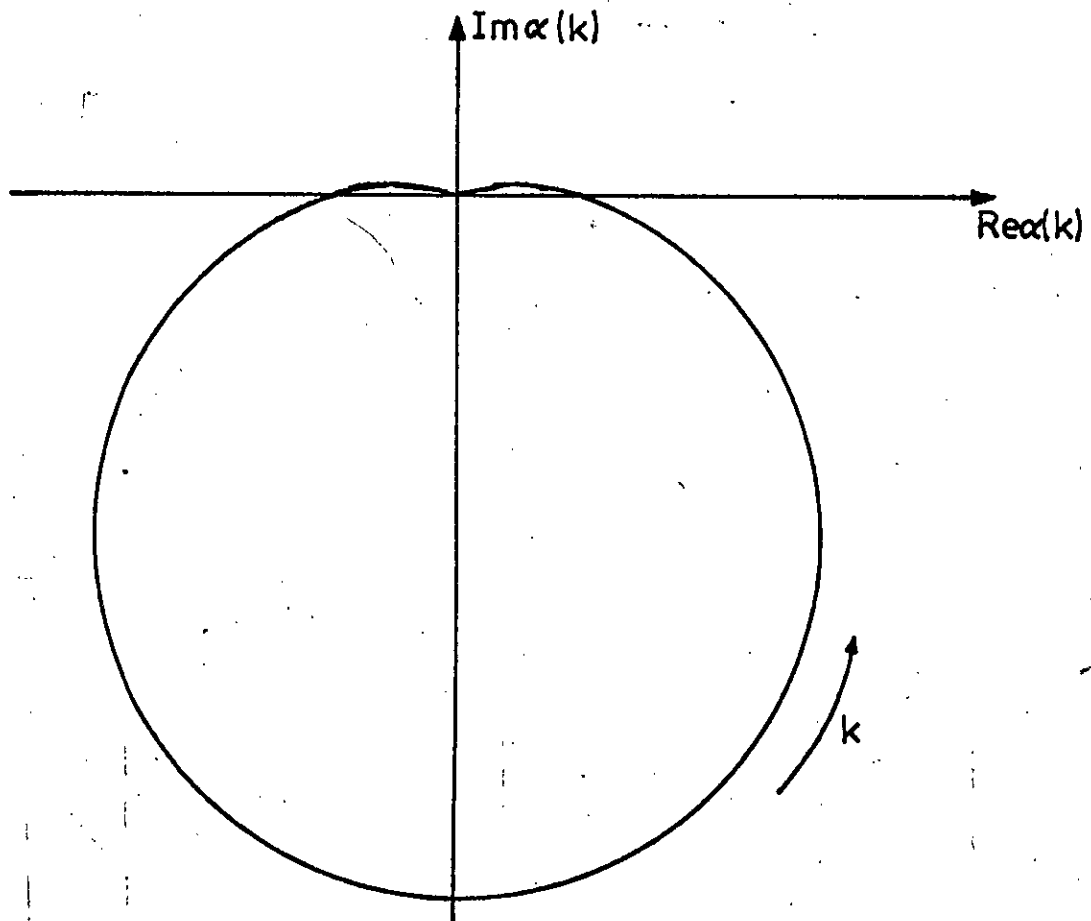


Figure 6.9.

Response as a Function of Stiffness in the Original Test Structure

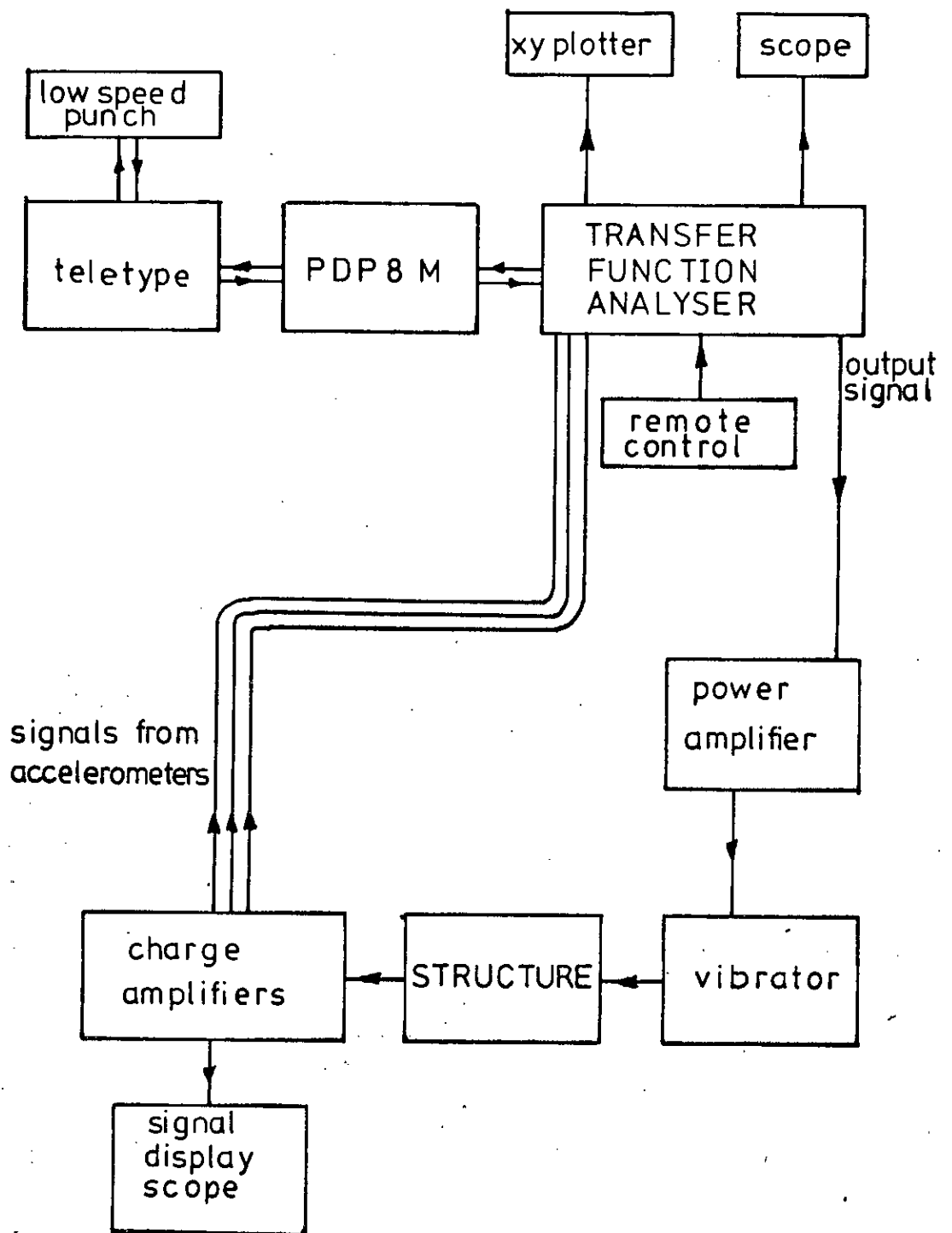
6.3. (Continued)

The locus shown here is characteristic of the one produced when two stiffness parameters, one very much more effective than the other, are varied simultaneously and in a related manner (see Chapter 4, Section 4.4.). Thus, it would appear that the stiffness element connected at block 4 was somehow affecting the stiffness at that point in more than one direction. The most likely cause of this would seem to be the non-symmetric nature of the structure at the point of attachment of the variable stiffness element. By making node 8 rigid, the symmetry of the structure was restored; that is with respect to block 4. A more comprehensive explanation of this phenomena cannot be given, but the fact that an almost perfect circular locus was obtained when the aforementioned modifications had been included would tend to indicate that the previous assumptions were correct. The results presented in the latter part of this chapter refer to the modified structure.

6.4. Experimental Equipment.

The experimental equipment was intended for the purpose of measuring the response at a point in a structure. Figure 6.10. shows a block diagram of the system which consists of a Program Controlled Transfer Function Analyser (PCTFA) with associated peripheral equipment, and the test structure itself. The PCTFA was used to control the experimental variables and to take response readings. The system comprises a solartron JML600A Transfer Function Analyser (TFA), with a high frequency extension unit, these being controlled through an interface by a PDP8 mini-computer. The PCTFA provides the following capabilities:

- i) Automatic frequency response measurement.
- ii) Multi-point analysis (up to 30 channels).
- iii) Display of response readings on an XY plotter or



Schematic Representation of Experimental Equipment

Figure 6.10.

6.4. (Continued)

- iii) Cathode ray tube.
- iv) On line programme development and processing of measured data.

The parameters under software control are:

- i) The magnitude and frequency of the driving signal.
- ii) Input sensitivity.
- iii) The number of cycles of integration in the correlation process.
- iv) Input channel selection.
- v) An analogue output to plotter or scope.
- vi) Provision for the additional input or output of information in the form of a Binary Coded Decimal Number (BCD), providing an alternative control channel to the tele-type.

The software package incorporated in the system is a modified version of DEC FOCAL 8 called Dynamic FOCAL. This includes the necessary commands for controlling the transfer function analyser.

Details of the operation may best be obtained by describing a typical sequence of operations leading up to the taking of a response reading. The frequency and magnitude (0-10v) of the driver signal are set up using the oscillator contained within the TFA. This signal is then fed through a power amplifier to a vibrator which excites the system under test. Signals from the accelerometers attached to the structure are then fed back to the PCTFA via suitable charge amplifiers. On the present system only ten of the thirty channels are operative. For

6.4. (Continued)

any chosen channel the input signal is connected to the digital correlator whose input sensitivity is set to "auto range" to find the right input level automatically. At this stage the correlator picks out only the fundamental sine wave component in the signal and rejects the noise content and all other harmonics. This is achieved by multiplying the waveform by sine and cosine reference signals derived from the function generator. Digital integrators in both the sine and cosine channels average their respective multiplier outputs for a period equal to a finite number of cycles of the excitation frequency. The correlation process has the effect of rejecting all harmonics other than the fundamental. Noise rejection, however, increases with the number of cycles of integration, which may be set to 10, 100 or 1,000 cycles of the fundamental frequency. The outputs from the sine and cosine integrators are directly proportional to the "In phase" and "Quadrature" components respectively of the waveform being measured. These may be displayed as cartesian, polar or log polar coordinates.

The major proportion of the available 8K of storage space in the PDP8 computer is taken up by Dynamic Focal, which leaves only enough space to store 75 pairs of response coordinates. Although somewhat restrictive, this is normally adequate for most purposes and allows sufficient scope to perform simple mathematical operations, such as sorting and scaling, on the stored data. The facility for displaying the data on an oscilloscope allows instantaneous viewing of experimental results, of which particular importance is attached to frequency response plots.

The apparatus thus constitutes a fully integrated system capable of the automatic control and measurement of the dynamic response

6.4. (Continued)

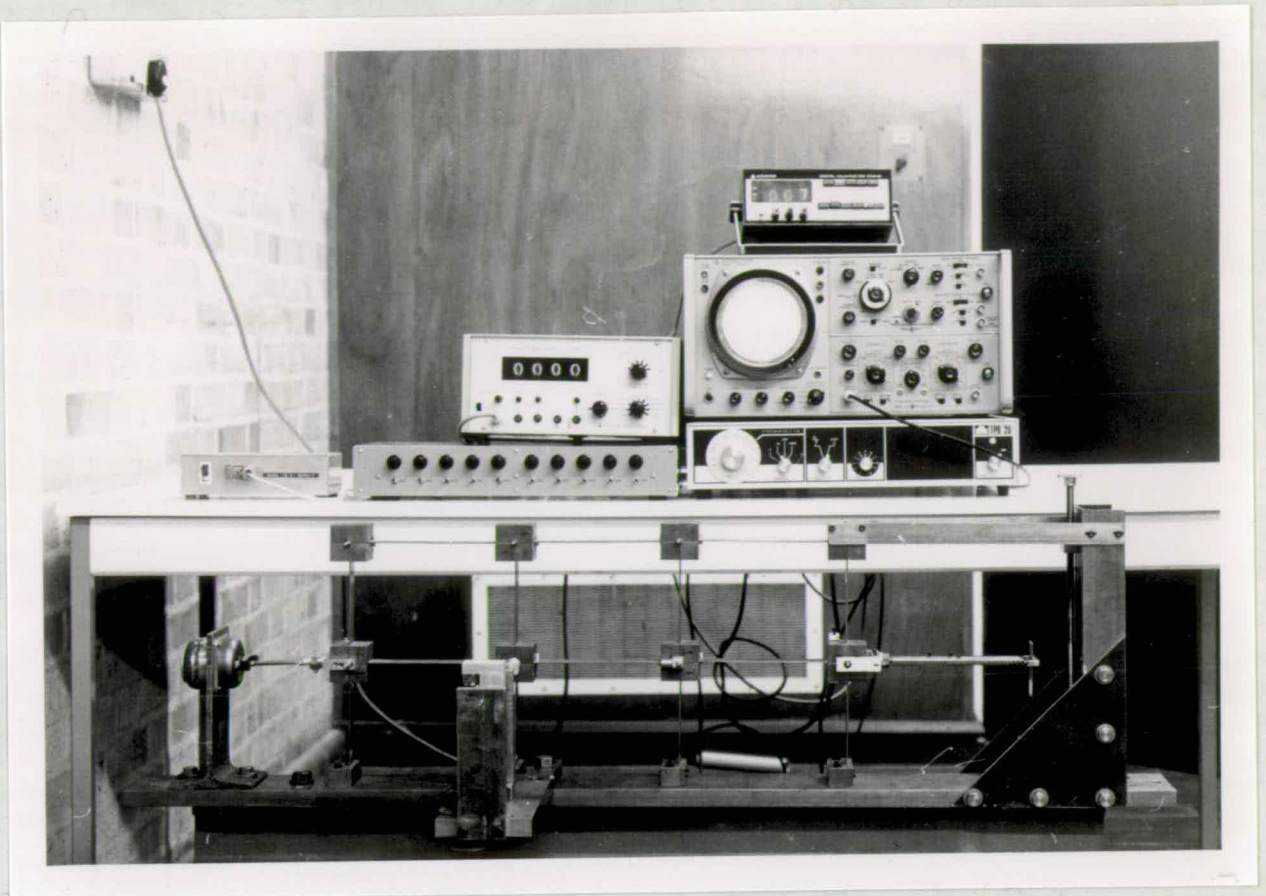
of a structure. The photographs given in Figures 6.11. and 6.12. give a general impression of the equipment.

6.5. Experimental Procedure.

The experimental procedure may be divided into two sections. The first of these is concerned with the measurement of structural response as a function of variable stiffness; the second refers to the measurement of the natural frequencies and normal mode shapes of the structure. Both of these involve the measurement of response, the former being at constant frequency, whilst the latter requires that a set of response readings be taken over a specified range of frequencies.

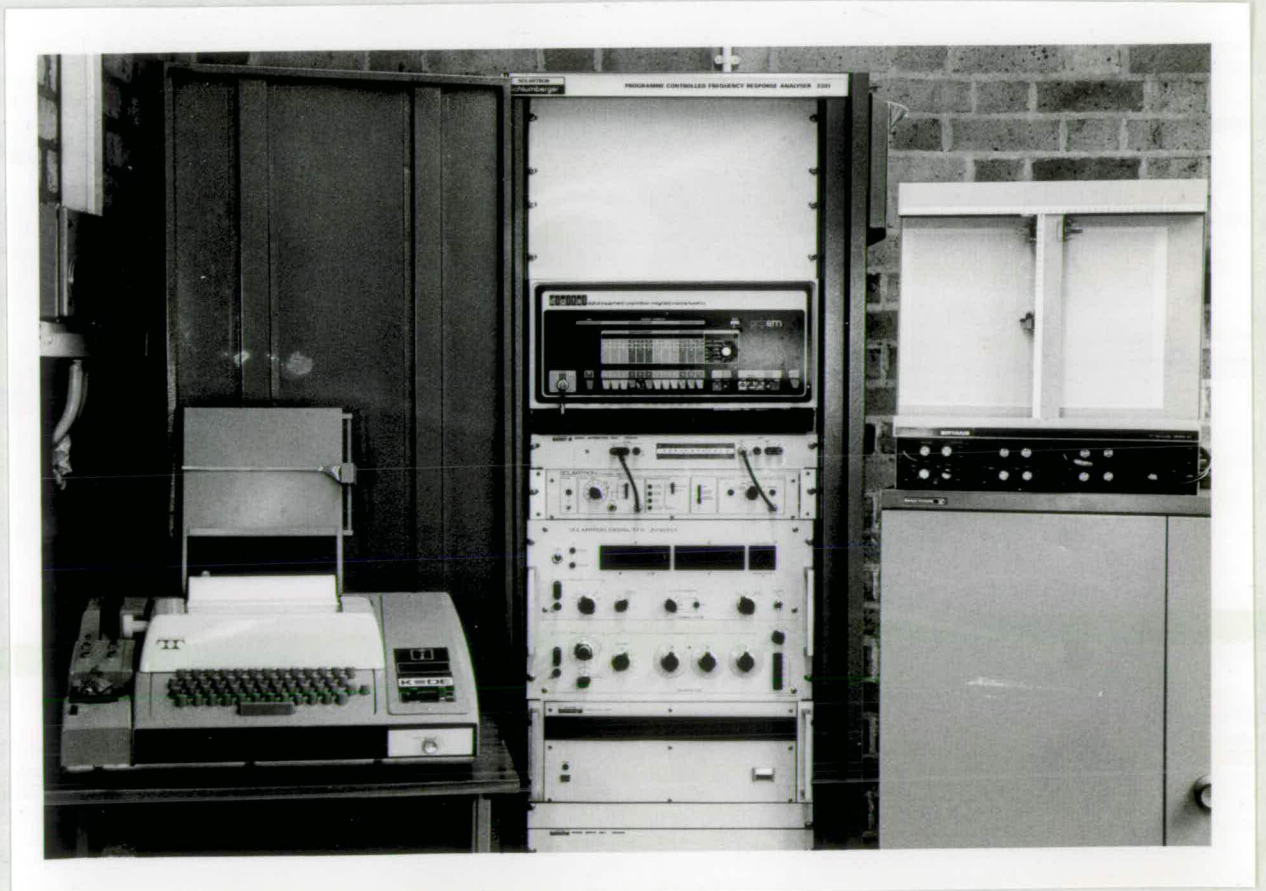
Each response reading has associated with it a phase angle which is defined with respect to the reference signal generated by the TFA's internal oscillator. It is common practice to take this same signal as being representative of the sinusoidal force input to the structure from the exciter, in reality, however, this signal is not a strictly true representation. The force applied by the exciter is proportional to the current passing through the coil (when stationary) and is also dependent on the impedance of the structure to which it is attached. In both cases considered above, the impedance of the structure does change and thus the input voltage to the exciter cannot be taken as being truly representative of either the magnitude or the phase of the force output.

The magnitude and phase of the force input to the structure can be determined by means of a force gauge inserted between the exciter and structure. The phase relationship between the response and the true force input can be calculated from the separate phase angles between each of these and the original reference signal. If the magnitude of



(a)
The Test Structure and Associated Equipment.

Figure 6.11.



(b)
The PCTFA, Teletype and XY Plotter. Figure 6.12.

6.5. (Continued)

the true force input changes then the size of the response vector can be compensated for accordingly. Figure 6.13. shows the response vector in both the true force coordinate system and in the coordinate system referring to the reference signal.

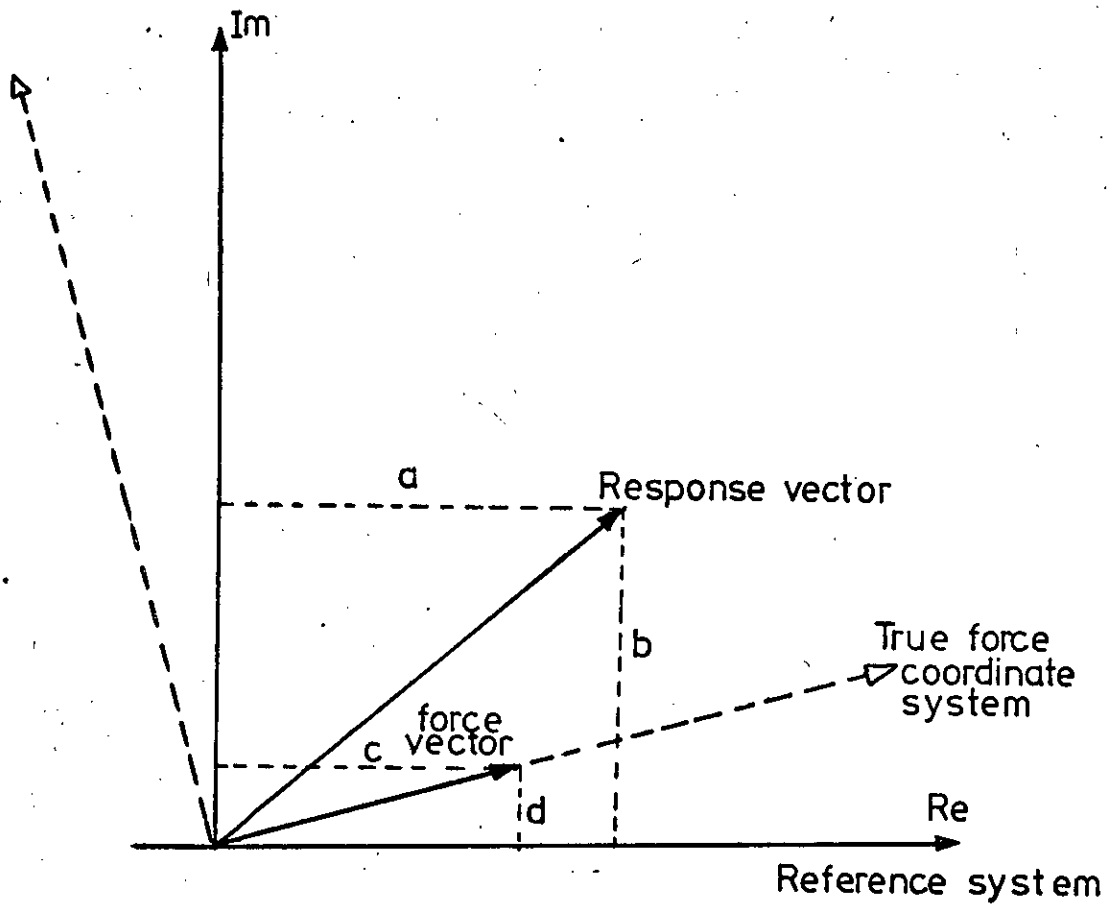


Figure 6.13.

Force Reference Coordinate Systems

6.5. (Continued)

If the magnitude of the forcing vector obtained on the first reading in any given set is taken as a reference and all subsequent values are adjusted accordingly, then the coordinates of the response vector in the true force reference system may be calculated as follows. Let the cartesian coordinates (in the reference system) of the force and response vectors be (a,b) and (c,d) respectively, and the magnitude of the forcing vector on the first reading be e . Then the coordinates of the response vector in the true force reference system are (x,y) where

$$x = \frac{e(ac + bd)}{a^2 + b^2}$$

and
$$y = \frac{e(ad - bc)}{a^2 + b^2}$$

All subsequent readings can be adjusted in this manner, thus effectively compensating for any changes in the magnitude and phase of the true force input to the structure.

6.51. The Measurement of Structural Response as a Function of Variable Stiffness.

The aim of the first part of the experimental analysis was to be able to reproduce the circular locus for varying stiffness predicted in the theory. Ideally, the point at which the response is examined was chosen to be particularly sensitive to any variation in the stiffness parameter. This sensitivity was maximised by choosing an excitation frequency close to, but greater than, one of the natural frequencies of the system, and by attaching the stiffness element at a point in the structure which possessed a large amplitude of vibration in the normal mode associated with this frequency. Also the stiffness

6.5. (Continued)

element was varied over a sufficiently wide range of values so as to produce as large an arc of the response circle as possible. The exact frequency at which the experiment was carried out was determined by a process of trial and error based on the quality of the results obtained. Having chosen the values of the various experimental parameters, control was passed to the PCTFA. Here, a small programme was written to control the experiment and required as initial input data, the magnitude and frequency of the excitation signal and the number of cycles of integration to be used in the correlation process. The computer was now set up to take response readings and store them. The measuring cycle was started by remote control using the external input facility of the PCTFA. This eliminated the need to use the teletype as an input device and also meant that the entire experimental analysis could be performed in the proximity of the test structure, the latter being situated some distance away from the PCTFA.

A typical measuring cycle involved the following steps:

- i) The variable stiffness element was set to maximum stiffness.
- ii) The programme was started and the necessary parameters read in.
- iii) The structure was excited at the required magnitude and frequency and allowed to settle.
- iv) The measuring cycle was initiated by remote control and a response reading taken.
- v) The stiffness of the variable element was reduced by a small amount and another reading taken.

6.51. (Continued)

Altering the stiffness of the cantilever entailed loosening a retaining bolt and lowering the clamp by means of the screw thread arrangement shown in Appendix F. The clamp was uniformly tightened after each change using a torque wrench. The measuring process was repeated until sufficient data had been collected, at which time the sequence was terminated. The response readings were sorted, scaled and displayed on the screen of a storage oscilloscope. The information was presented as a series of points in the complex plane. If the data was satisfactory, then a hard copy was obtained on an XY plotter and in addition the coordinates of each point were punched out on paper tape.

The following information was also noted:

The magnitude (lb f) and frequency (Hz) of the excitation force.

The calibrated output of the accelerometer (V/g).

Any scaling factors involved in the measured data.

The examination and forcing points and the position of the stiffness element.

6.52. The Measurement of Natural Frequencies, Normal Mode Shapes and Associated Damping.

Although not the most important part of the experimental programme, the measurement of natural frequencies and normal mode shapes is necessary since they form the basis for comparison between the experimental and theoretical models. The results are obtained using simple techniques rather than some of the more comprehensive methods developed in the recent past [10, 11, 12]. The time taken to develop working versions of these techniques is disproportionate with their desirability within this analysis.

6.52. (Continued)

The method initially involves identifying the natural frequencies of the structure from a frequency sweep performed by hand. The response signal from the accelerometer under consideration is displayed on the y axis of an oscilloscope in conjunction with the signal representing the force input on the x axis. The resulting trace is a lissajoux figure. This method of examining the response shows the change in phase as well as magnitude when passing through a natural frequency, and hence is a more satisfactory method of identification than the peak amplitude method. Also noted at this stage is the degree of freedom with the largest amplitude of vibration at each natural frequency.

These initial estimates are now used as the basis for an accurate frequency sweep in the neighbourhood of the natural frequencies. This time, the PCTFA is programmed to vary the frequency, select the input channel and take the response readings. The resulting vector response loci are then analysed to produce a revised calculation of the natural frequencies; this being based on the point at which maximum spacing occurs between successive response points taken at equal intervals of frequency. Figure 6.14. shows a typical vector response plot.

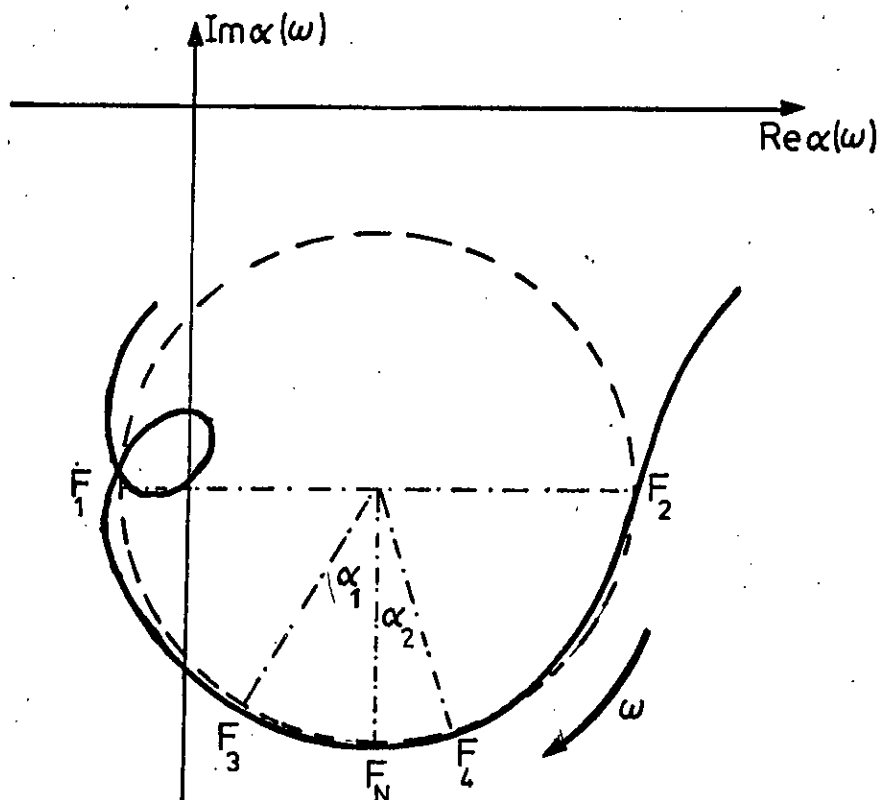


Figure 6.14.

Typical Response Locus

A circle is fitted to the experimental data in the region of the natural frequency. If F_n is the natural frequency and F_1 and F_2 are frequencies at points 90° displaced to each side of this, then from a graphical analysis of the vector plot the damping constant ζ for that particular mode can be calculated using the equation [12]

$$\zeta = \frac{F_1 - F_2}{F_n}$$

If the circle does not coincide with the experimental data for as much as 180° , then the damping may be calculated using the alternative expression

6.52. (Continued)

$$\xi = 2(F_3 - F_4) \left(\frac{\tan \alpha_1}{2} - \frac{\tan \alpha_2}{2} \right) F_n$$

where F_3 , F_4 , α_1 and α_2 are as defined in Figure 6.14.

To measure the normal modes of the structure, the system is excited at each of the natural frequencies in turn. An initial estimate is obtained from the magnitude of the response signals from each accelerometer. An attempt is made to identify nodes in the normal mode using a stroboscope to highlight the movement of the structure. Besides this visual approach, the structure is examined physically by touch to sense the vibration. This additional information proves useful when analysing the experimentally calculated normal mode vectors. After this preliminary examination, the PCTFA is programmed to excite the structure at the required frequencies and to obtain the response readings for each of the eight degrees of freedom making up the normal mode. The accelerometers attached to the structure have individual variable gain amplifiers and prior to taking normal mode readings the amplifiers are adjusted such that they all give the same magnitude of signal when their respective accelerometers are being subjected to 1g acceleration. This matching of the accelerometers is necessary for the normal mode data to be meaningful. Having obtained a set of response readings for each normal mode, the data is analysed to give the magnitude of each vector and also its real and imaginary components in the complex plane. The magnitudes of the vectors in each mode are sorted and normalised such that the highest value is unity.

The method outlined in this section may be relied upon to give reasonably accurate estimates of the natural frequencies of the structure.

6.52. (Continued)

However, those frequency response plots obtained in the frequency range above 159 Hz do not possess a sufficient degree of resolution to allow any meaningful graphical analysis. The natural frequencies in this range are obtained using the peak amplitude method, whilst the corresponding damping coefficients are estimated by interpolating data from the sparsely populated vector response plots.

The experimental techniques used to produce the normal mode vectors of the system includes certain approximations which may provide grounds for casting doubt upon the accuracy of the results. The first approximation involves the instrumentation used in the measurement of rotational response. Figure 6.15. shows the position in which the accelerometer is mounted in order to pick up the rotational response of the block.

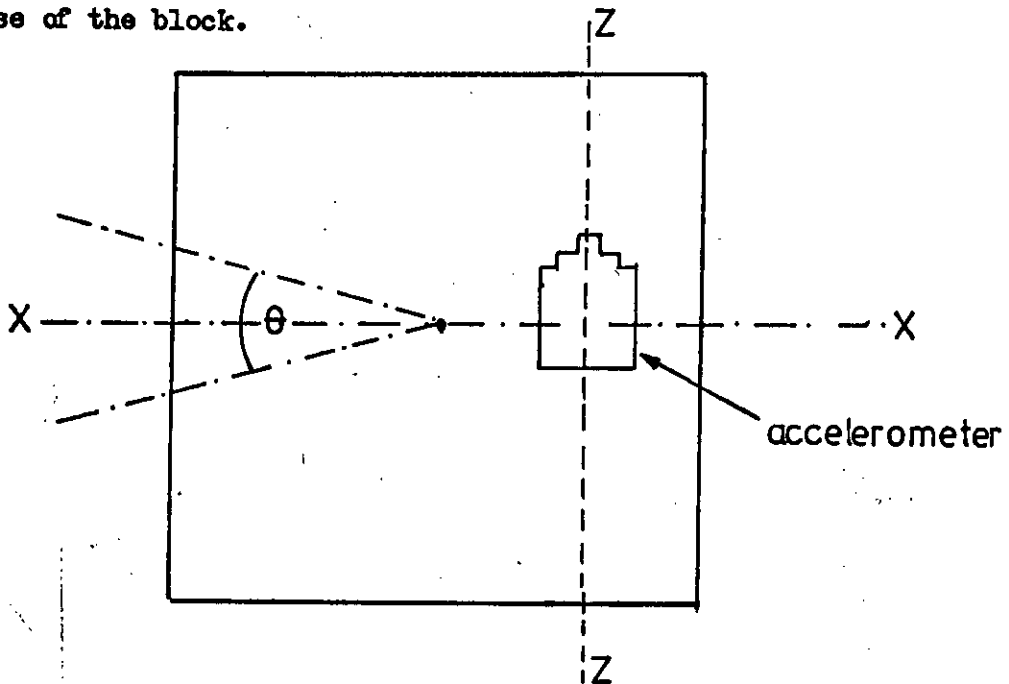


Figure 6.15.

The Measurement of Rotational Response

6.52. (Continued)

Any given rotation Θ of the block results in a displacement in the zz direction which coincides with the most sensitive axis of the accelerometer. However, any coincident motion in the xx direction will also be picked up by the accelerometer and will tend to distort the originally desired signal. It is fortunate that the accelerometer is only 10% as sensitive in the xx direction as it is in the ZZ plane, which helps minimise the effect of this unwanted signal. The second, and probably the most important factor influencing the normal modes concerns the degree to which it is possible to excite a pure normal mode. In theory, the structure should be excited at at least as many points as there are degrees of freedom in order to produce a pure normal mode (undamped). In practice it is usually possible to excite a reasonably pure mode using only one vibrator; however, the exciter must be positioned favourably within the structure to achieve the maximum effect. In the investigation under consideration the exciters were positioned on the basis of the theoretically produced modes and remained in the chosen position throughout the analysis.

Thus, the experimental normal mode data may firstly be distorted by unwanted signals and, secondly, it may not be representative of the pure normal modes of the structure.

6.6. The Mathematical Model of the Test Structure.

The importance of a mathematical model as a link between experiment and theory should not be understated. Moreover, just as the accuracy with which experimental results can be obtained sheds light on their validity, so does the relevance and accuracy of the mathematical model. However, before experimental or theoretical data can be used in confidence for the purpose of comparison, there must be reasonable justification for thinking that the mathematical model is a good representation of the real physical system. This essentially involves laying down a set of criteria for comparison, in this instance the natural frequencies of the two systems have been chosen. Since the experimental results are considered to be fixed then the mathematical model must be manipulated to achieve the best possible fit with reality. This in itself is a difficult undertaking.

The mathematical model shown schematically in Figure 6.16. consists of 12 nodes, five of which are considered to be rigidly constrained. The nodes are interconnected by 14 plane bending elements which are considered to be inextensible. With the maximum number of degrees of freedom being two, there are 16 redundants leaving 8 active degrees of freedom. The numbering of the elements, nodes and degrees of freedom is also shown in Figure 6.16. The mass and inertia of the system are considered concentrated at the nodes, whilst the stiffness matrix is assembled using finite element techniques. In the first instance, the mass, inertia and stiffness data are taken as the measured values from the test structure. Damping is included in the model as a percentage of critical damping in each normal mode.

6.6. (Continued)

One major difference between the mathematical model and the test structure concerns the modelling of the structural nodes. In practice, these have finite dimensions and the stiffness elements are not connected at a point. The element stiffness matrices used in the mathematical model provide a relationship between the forces and displacements at the ends of each element. But on the test structure the equivalent parameters are measured at the centre of each block which is rigidly connected to but displaced from the end of the beam. In accordance with this, the element stiffness matrices may be transformed into a new coordinate system which coincides with the centres of adjacent blocks. Details of this transformation are given in Appendix H. The presence of the variable stiffness element was accounted for in the mathematical model by adding the appropriate stiffness value directly into the stiffness matrix (see Appendix J).

The natural frequencies and normal mode shapes of the structure were calculated and compared with those found experimentally. The aim of the exercise was to match the two sets of natural frequencies as closely as possible; no attempt was made to match the normal modes. The manipulation of the mathematical model was achieved by varying any of the following parameters.

Affecting the mass matrix

- i) The mass and/or inertia at each end of the nodes.

Affecting the stiffness matrix

- ii) Young's Modulus.
- iii) The second moment of area of individual elements.

6.6. (Continued)

- iv) The elements of the stiffness matrix (directly).

The effects these parameter changes had on the natural frequencies of the system may be summarised as follows:

- I) Varying the mass and inertia terms was used to change individual natural frequencies. The degree of freedom with the maximum amplitude in the relevant normal mode indicated the most sensitive point at which to effect the change. Problems arose when the chosen point was also effective in another normal mode. In that situation a compromise was reached.
- II) Increasing or decreasing Young's Modulus was used to effect changes on all the natural frequencies.
- III) It was never found necessary to alter second moments of area or the elements of the stiffness matrix, and consequently the effects of these changes are not known.

The process of matching the mathematical model to the test structure was an iterative one. In each new cycle the alterations were based on the experience of past changes and, to some extent, on insight and intuition. There came a time in the iterative process when the time spent trying to improve on the previous guess became disproportionate with the magnitude of the improvement itself; it was at this point that the final version of the mathematical model was decided upon. In practice it was only found necessary to alter the

6.6. (Continued)

mass and inertia data of the model in order to match up the natural frequencies satisfactorily.

Full details of the data used in the calculation of the mathematical model are given in Appendix J, these include the experimental evaluation of Young's Modulus and also the experimentally determined stiffness at a point in the structure which was used to provide a check with the theoretically determined value.

6.7. Results.

The experimental results are divided into two sections. The first presents a comparison between the experimental and theoretical frequencies and normal mode shapes and is intended to indicate the degree of accuracy with which the test structure has been modelled mathematically. The second deals with the experimental evaluation of response as a function of variable stiffness. The results are compared with those predicted theoretically.

6.7.1. Natural Frequencies, Normal Mode Shapes and Associated Damping.

The results in this section are presented both graphically and in tabular form, and are primarily intended for the purpose of comparison. The natural frequencies of the experimental and theoretical models have been chosen as the basis for comparison between the two systems. No attempt has been made to match up the normal mode shapes in the same manner. Three sets of experimental data are presented, frequency response plots, tabulated natural frequencies and a tabulated and schematic representation of the normal mode shapes.

Figures 6.17. - 6.20. contain the frequency response plots used for the evaluation of the natural frequencies and associated

6.71. (Continued)

damping constants. Table 6.1. presents a comparison between the natural frequencies of the two systems and consists of four columns.

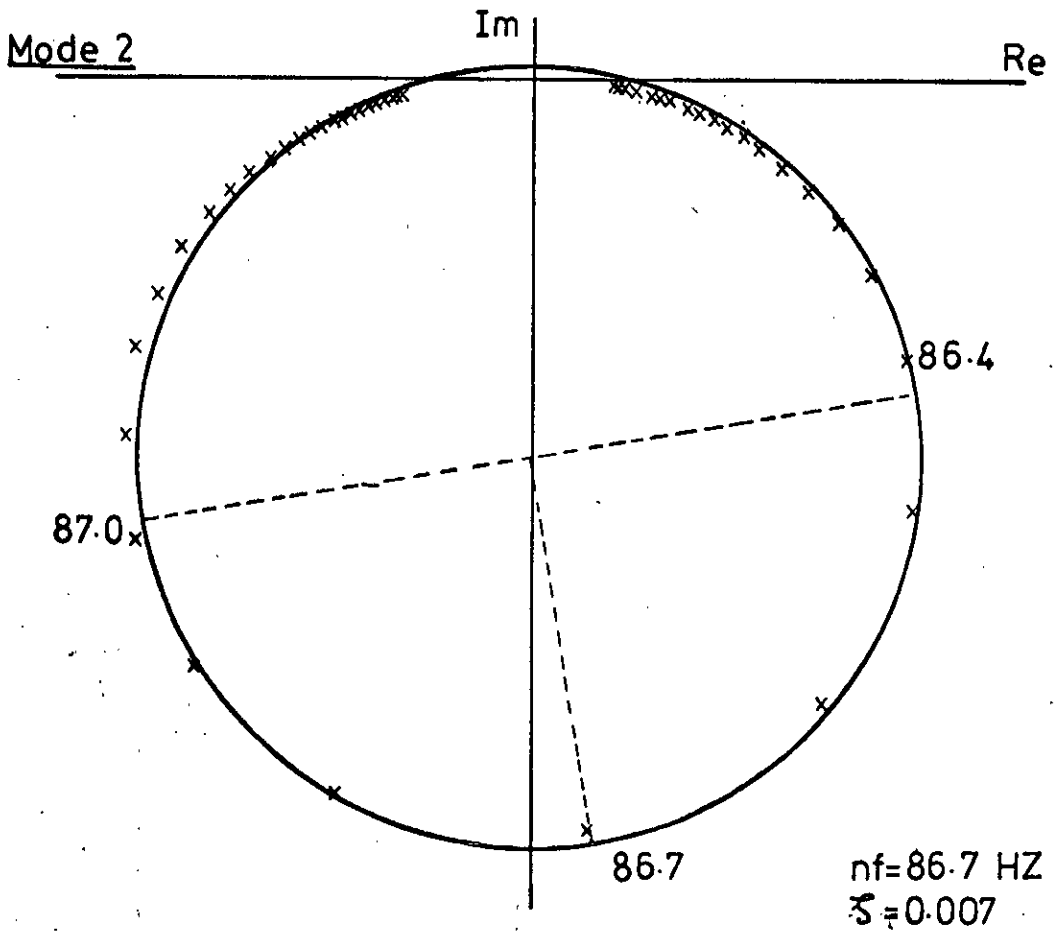
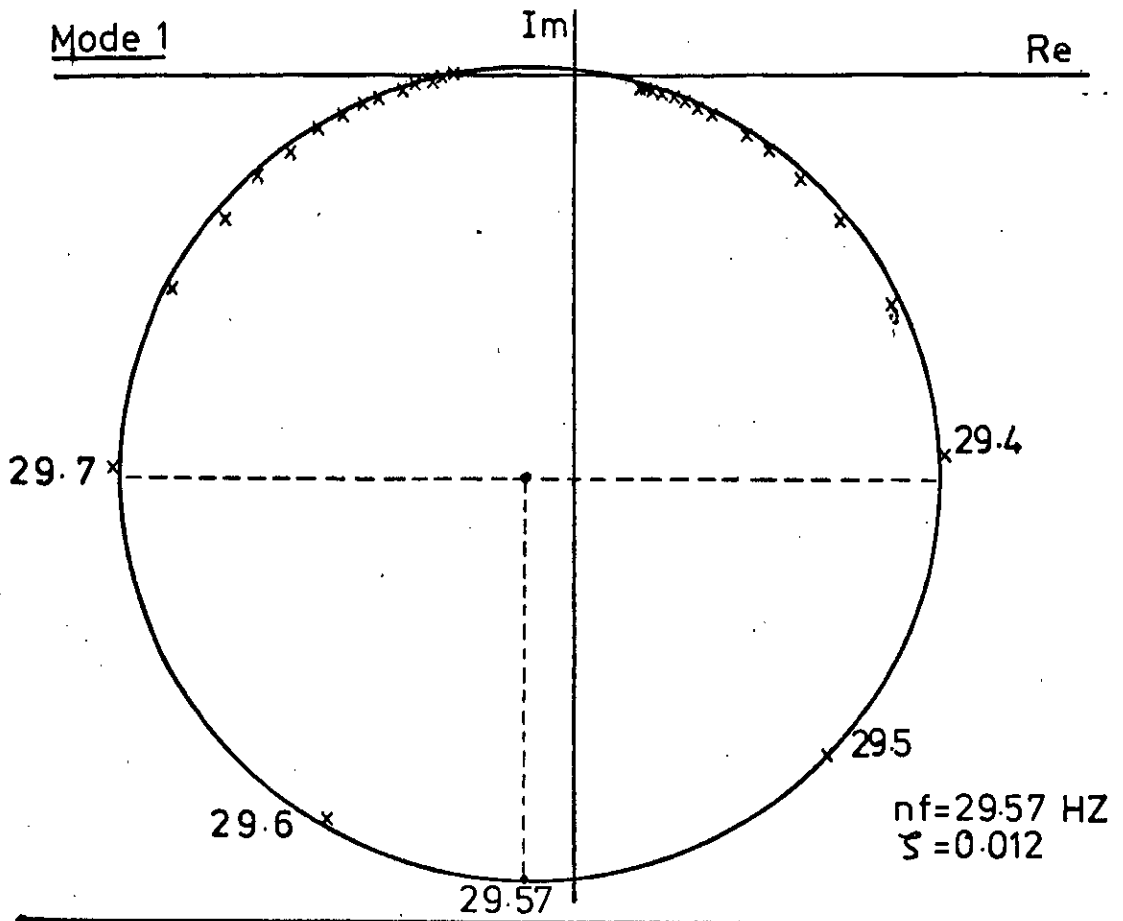
The data listed in each column is as follows:

<u>Column (i)</u>	The theoretical natural frequencies obtained using the experimentally measured data. This is prior to any manipulation of the mathematical model.
<u>Column (ii)</u>	The matched natural frequencies achieved by manipulating the mathematical model.
<u>Column (iii)</u>	The experimentally determined natural frequencies.
<u>Column (iv)</u>	The damping coefficients in each normal mode.

The changes in the mathematical model as a result of the manipulation process are listed in Table 6.2., these consist solely of changes to the initial mass and inertia data. Table 6.3. lists the normal mode shapes corresponding to the three sets of natural frequencies given in Table 6.1. Included with each mode shape is a plot of the experimentally determined mode vectors. The phase relationships for the experimental modes were obtained using these plots. It will be noted that there is no experimental data for the response corresponding to degree of freedom 1 in all but the first normal mode (signified by **** in column 3). The reason for this was that when exciting the rotational modes of the structure the response signal from the accelerometer corresponding to degree of freedom 1 was so small that it was identified as zero by the PCTFA. This zero reading caused programming faults in the PDP8 and it was consequently decided that

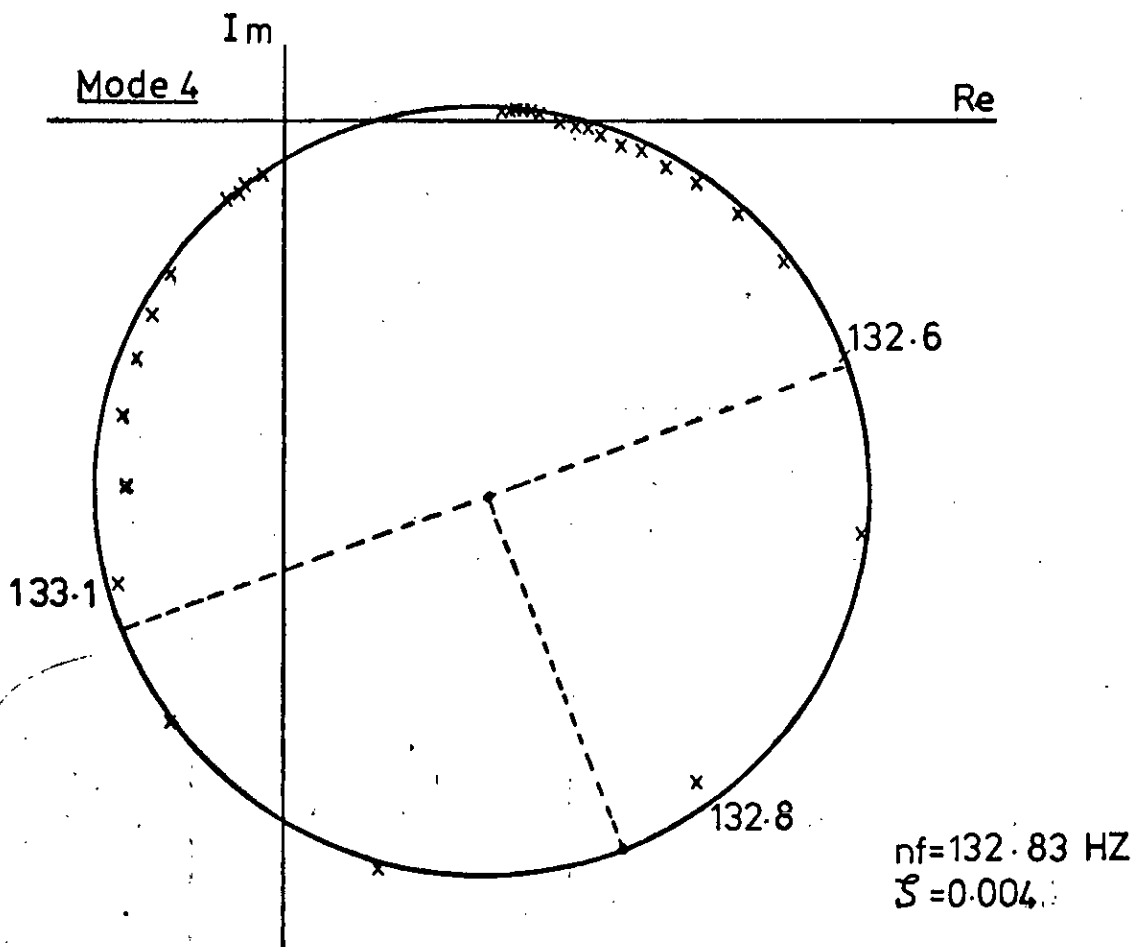
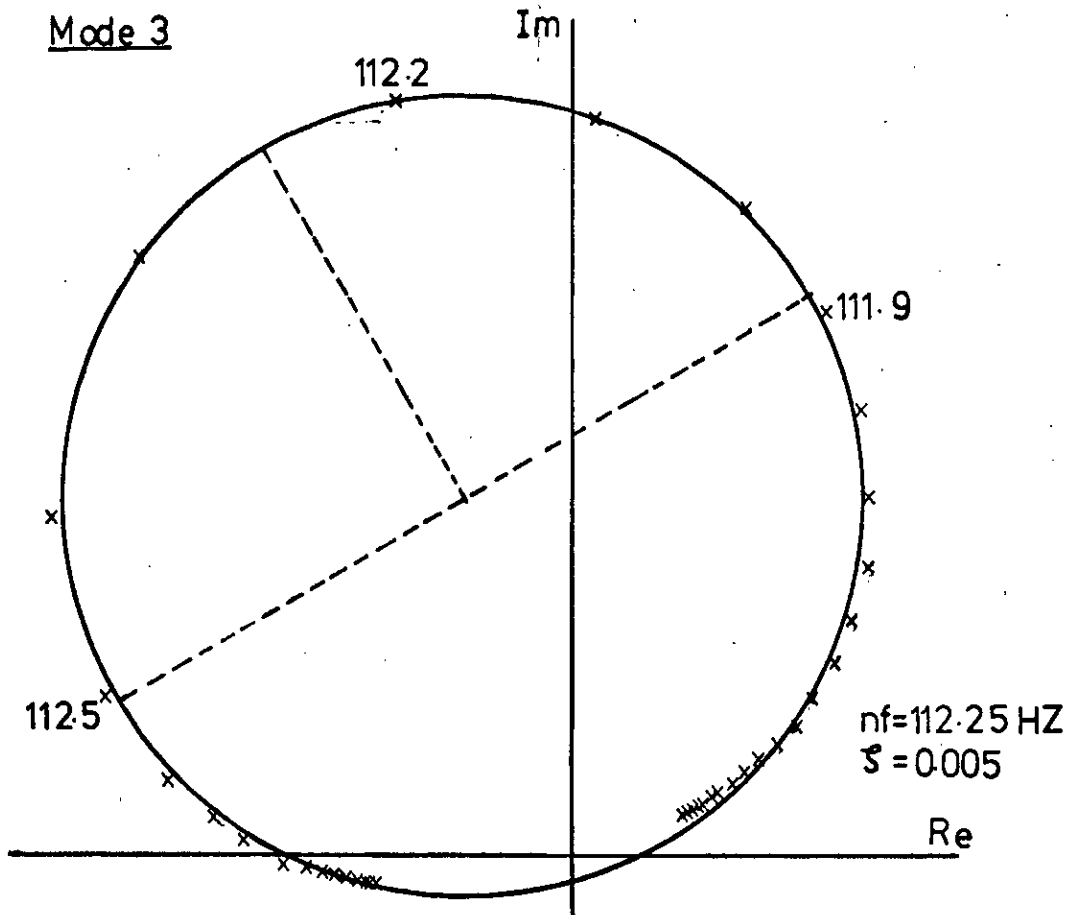
6.71. (Continued)

the reading should be omitted. Finally, Figures 6.21. - 6.23. show schematically the normal mode shapes for experiment and theory.



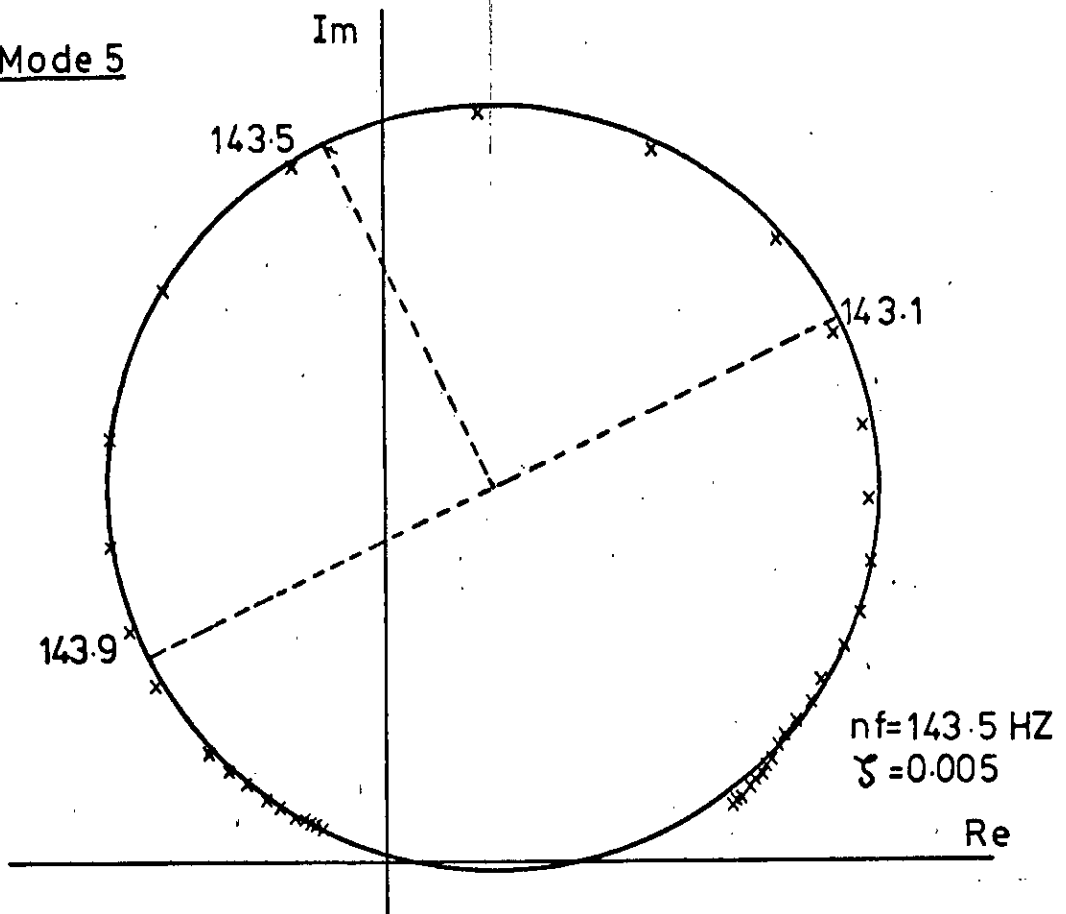
Frequency Response Plots for Modes 1 and 2.

Figure 6.17.

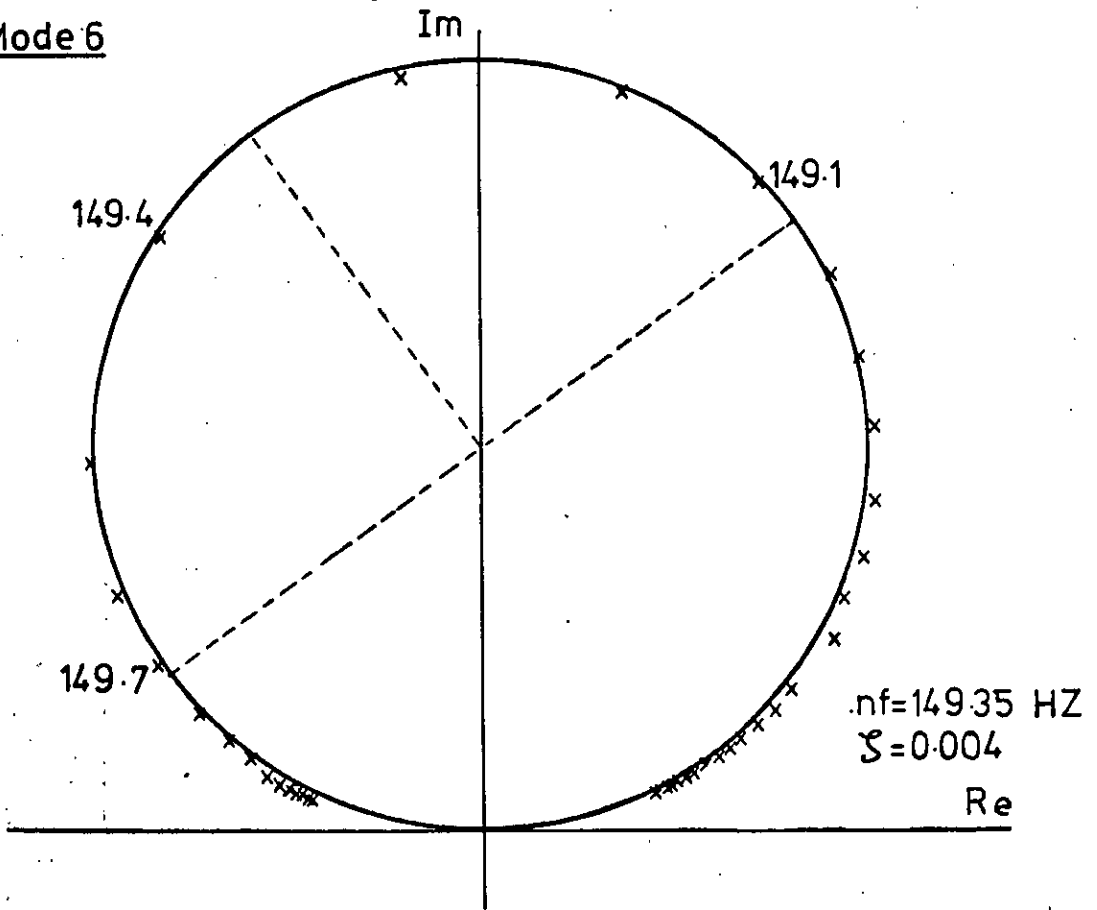


Frequency Response Plots for Modes 3 and 4.

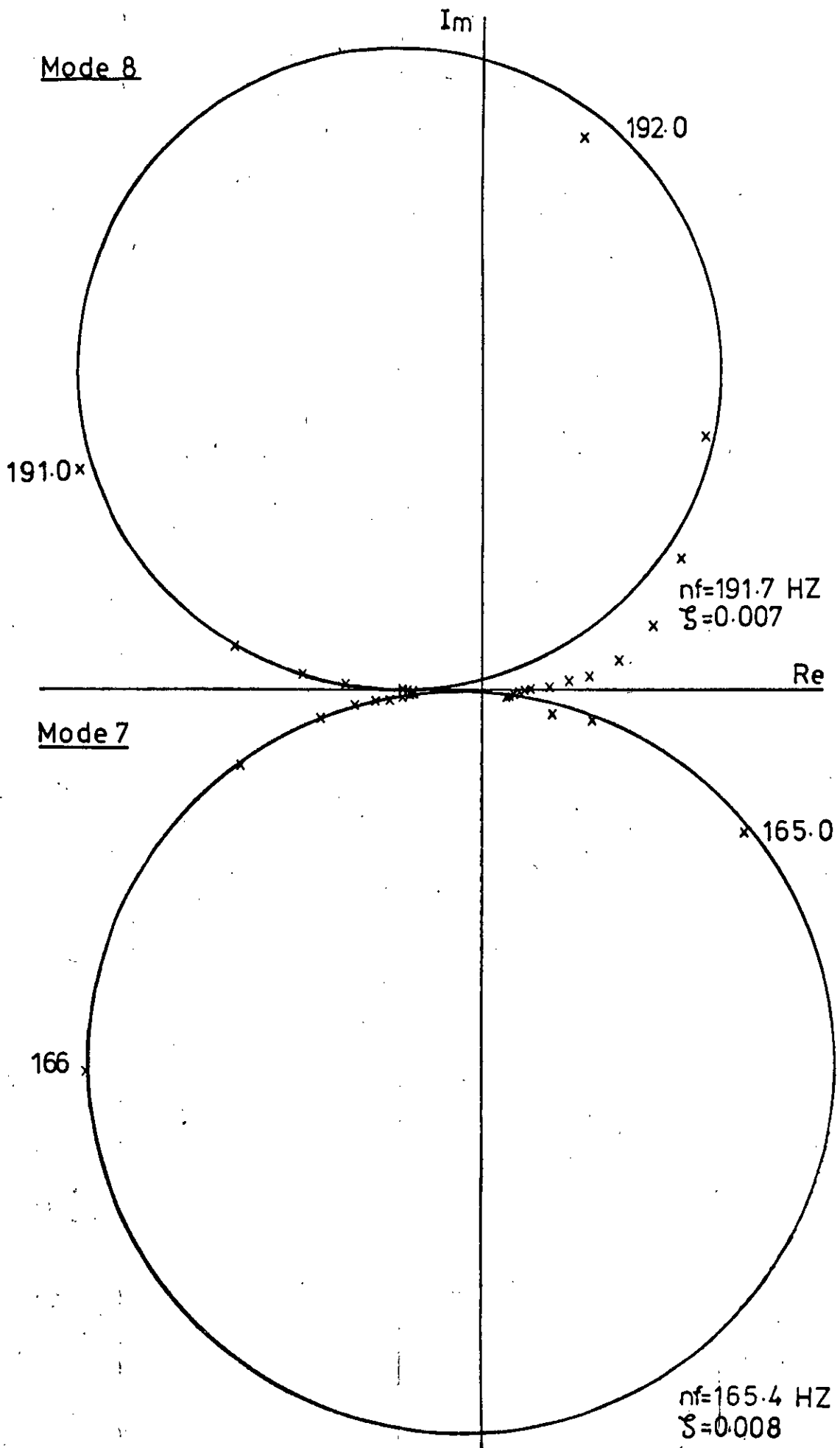
Mode 5



Mode 6



Frequency Response Plots for Modes 5 and 6



Frequency Response Plots for Modes 7 and 8

Table 6.1. Experimental and Theoretical Natural Frequencies

Initial Estimate Nat. Frequencies Hz	"Best Fit" Nat. Frequencies Hz	Experimental Nat. Frequencies Hz	Damping Coefficients
31.6	29.58	29.57	.012
98.4	86.86	86.7	.007
124.3	112.0	112.25	.005
149.5	132.4	132.83	.004
160.5	143.6	143.5	.005
166.4	149.3	149.35	.004
185.6	165.4	165.4	.007
202.6	191.3	191.7	.008

Table 6.2. Changes to Mass and Inertia Data for "Best Fit" Model

Degree of Freedom	Nodes	Mass/Inertia Units	Initial Value	"Best Fit" Value
1	2,3,4, 5	lbm	1.8×10^{-2}	2.06×10^{-2}
2	2	lbm.in. ²	2.5×10^{-3}	3.15×10^{-3}
3	3	lbm.in. ²	2.45×10^{-3}	2.43×10^{-3}
4	4	lbm.in. ²	2.42×10^{-3}	3.40×10^{-3}
5	5	lbm.in. ²	2.42×10^{-3}	3.15×10^{-3}
6	6	lbm.in. ²	2.50×10^{-3}	3.29×10^{-3}
7	7	lbm.in. ²	2.42×10^{-3}	3.17×10^{-3}
8	8	lbm.in. ²	2.42×10^{-3}	2.71×10^{-3}

Table 6.3. Mode Shapes for Modes 1, 2, 3 and 4.

Initial Estimate	"Best Fit"	Experimental	Normal Mode Vector Plot
1.00 0.06 0.008 0.03 -0.005 -0.21 -0.08 -0.14	1.00 0.06 0.008 0.03 -0.005 -0.21 -0.08 -0.14	1.00 0.19 0.16 0.17 -0.10 -0.12 -0.10 -0.09	nf = 29.57 Hz No vector plot - data unsatisfactory.
0.03 -0.53 0.32 -0.15 0.03 1.00 -0.60 0.27	0.03 -0.51 0.27 -0.13 0.03 1.00 -0.57 0.23	**** 0.08 -0.36 0.63 -0.74 1.00 -0.98 0.45	nf = 86.7 Hz
-0.006 0.32 0.32 -0.56 0.19 -0.62 -0.59 1.00	-0.01 0.31 0.35 -0.66 0.25 -0.61 -0.74 1.00	**** 0.34 -0.64 0.05 0.47 -0.52 -0.45 1.00	nf = 112.25 Hz

Continued/....

Table 6.3. (Continued)

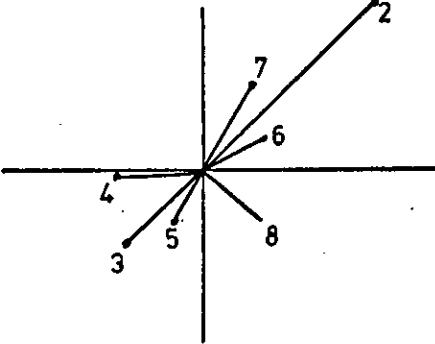
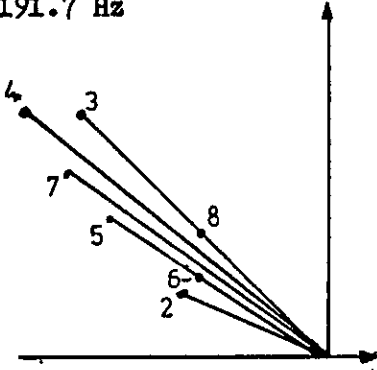
Initial Estimate	"Best Fit"	Experimental	Normal Mode Vector Plot
0.04	0.003	****	<p data-bbox="851 563 1095 594">nf = 132.83 Hz.</p> 
-0.21	-0.26	1.00	
-0.49	-0.26	-0.46	
-0.49	-0.68	-0.40	
0.45	0.69	-0.31	
0.35	0.26	0.25	
1.00	1.00	0.53	
0.68	0.47	0.36	

Table 6.4. Normal Mode Vectors for Modes 5,6,7 and 8.

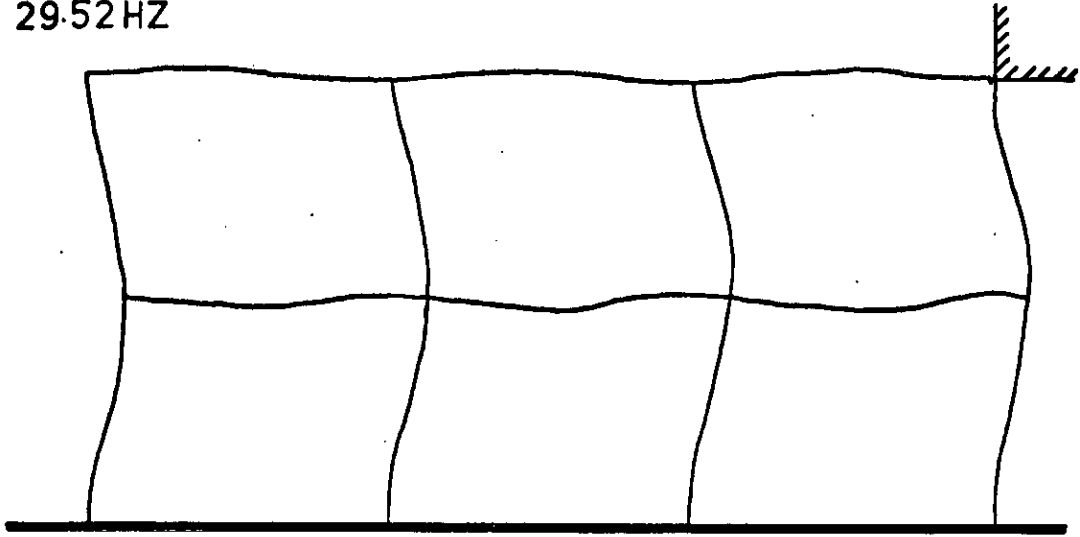
Initial Estimate	"Best Fit"	Experimental	Normal Mode Vector Plot
-0.01 -0.19 0.31 -0.21 1.00 -0.16 -0.05 -0.48	-0.01 0.03 0.16 0.07 1.00 -0.08 -0.31 -0.63	**** -0.91 -0.41 0.42 -0.77 0.26 1.00 0.67	nf = 143.5 Hz
0.002 1.00 -0.47 0.12 0.42 0.52 -0.30 -0.04	0.01 1.00 -0.38 0.07 0.11 0.52 -0.04 0.12	**** -0.49 -0.18 1.00 -0.91 -0.90 -0.015 -0.37	nf = 149.35 Hz.
-0.004 -0.64 -0.83 1.00 0.49 -0.34 -0.46 0.45	0.009 -0.29 -0.47 1.00 0.42 -0.11 -0.05 0.84	**** -0.75 -0.98 0.15 1.00 0.75 0.51 -0.32	nf = 165.4 Hz.

Continued/.....

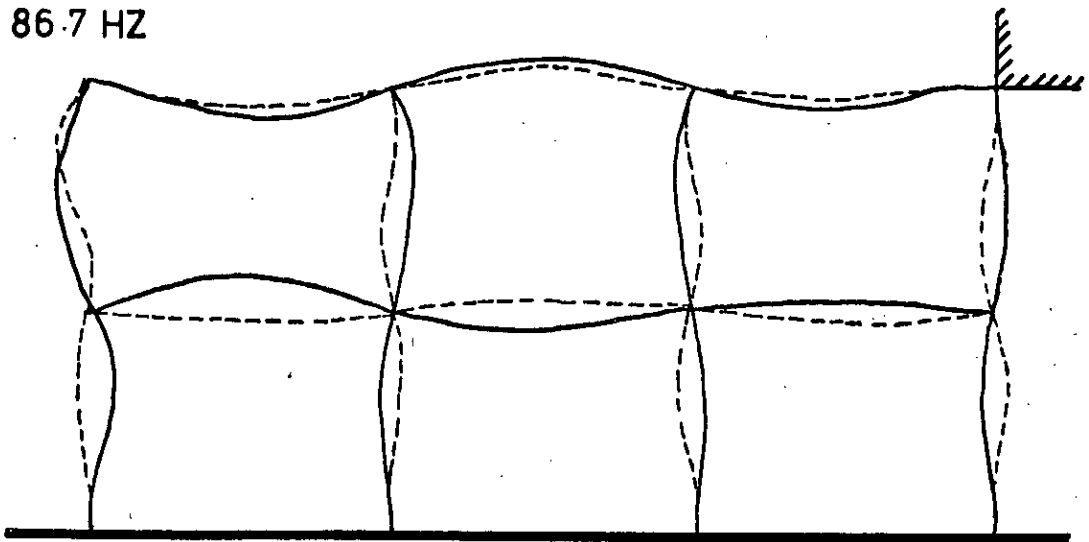
Table 6.4. (Continued)

Initial Estimate	"Best Fit"	Experimental	Normal Mode Vector Plot
0.01	0.006	****	<p data-bbox="839 497 1055 530">nf = 191.7 Hz</p> 
0.32	0.21	0.24	
0.99	1.00	0.66	
1.00	0.28	1.00	
0.26	0.05	0.63	
0.17	0.08	0.39	
0.53	0.32	0.71	
0.50	0.18	0.40	

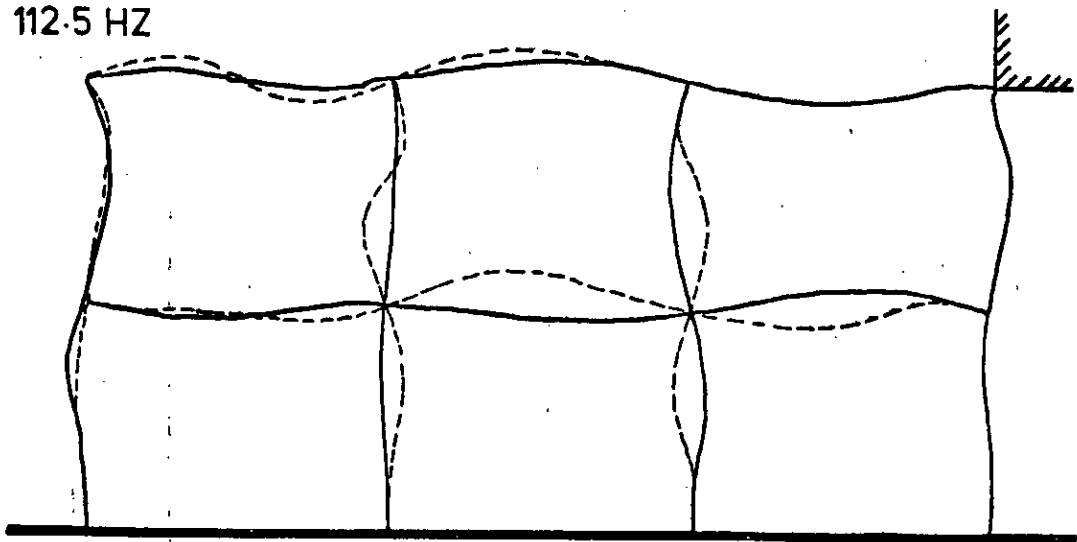
29.52 HZ



86.7 HZ



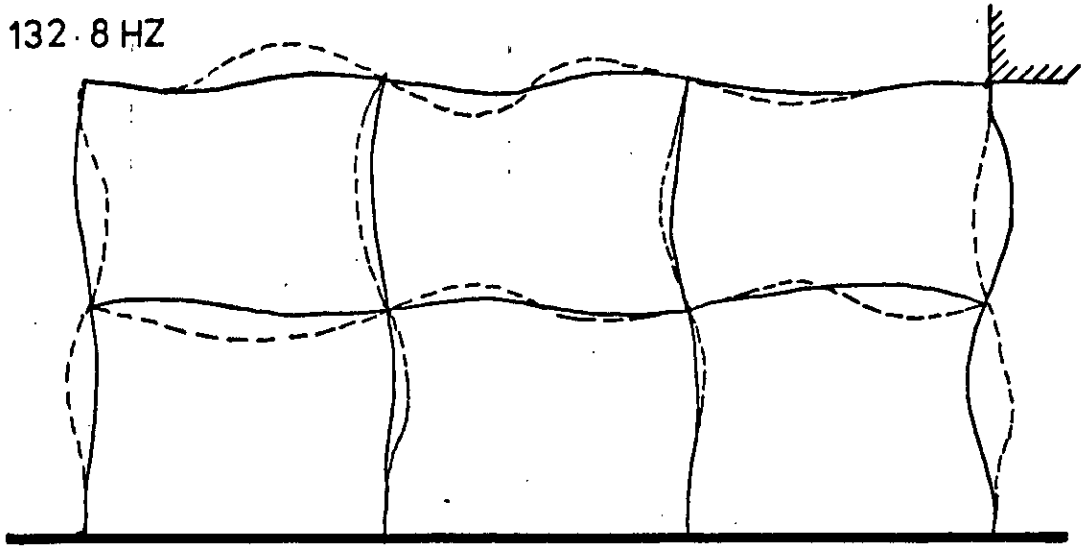
112.5 HZ



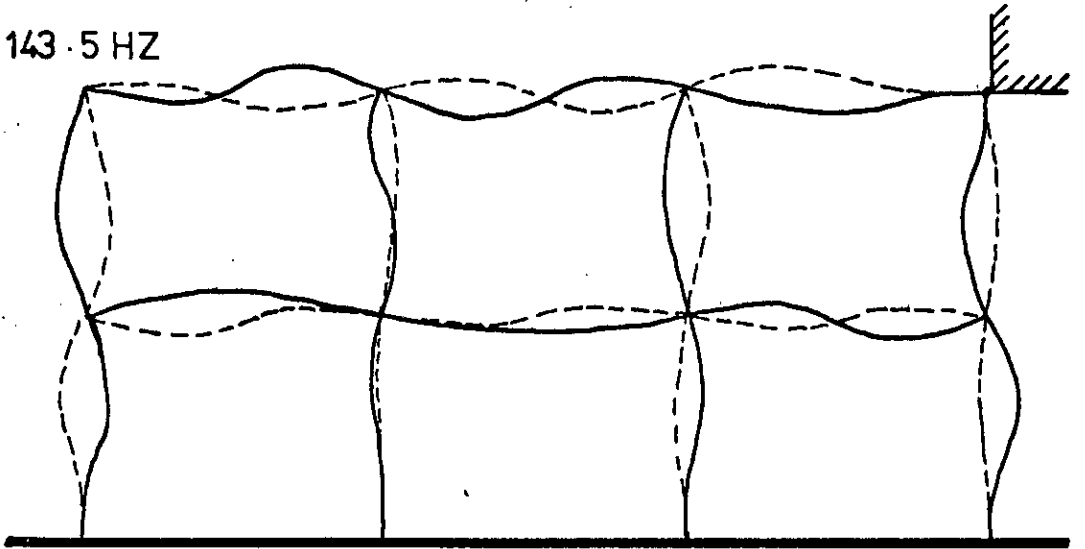
— Experimental
- - - Theoretical

Schematic Representation of Normal Modes

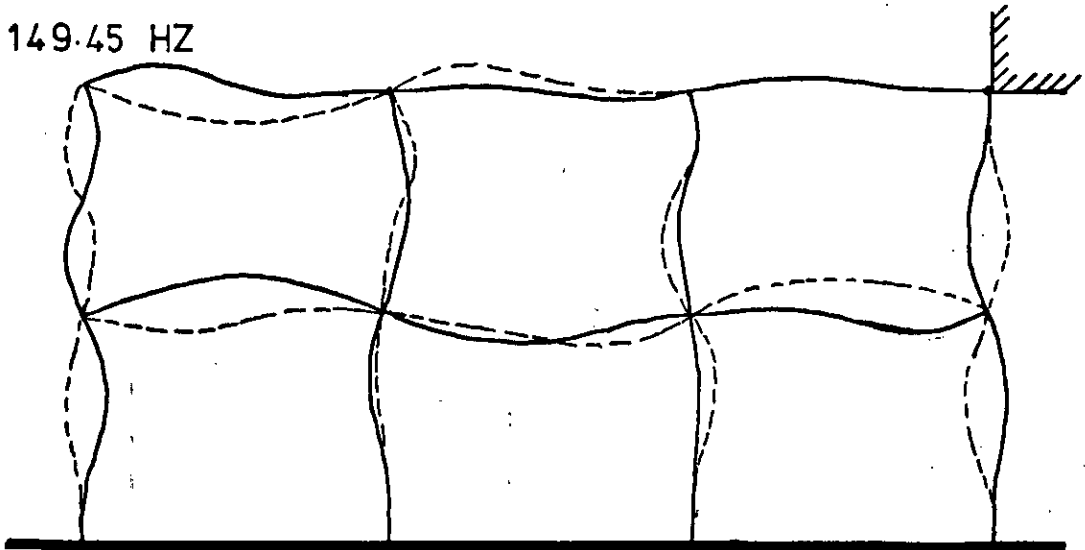
132.8 HZ



143.5 HZ



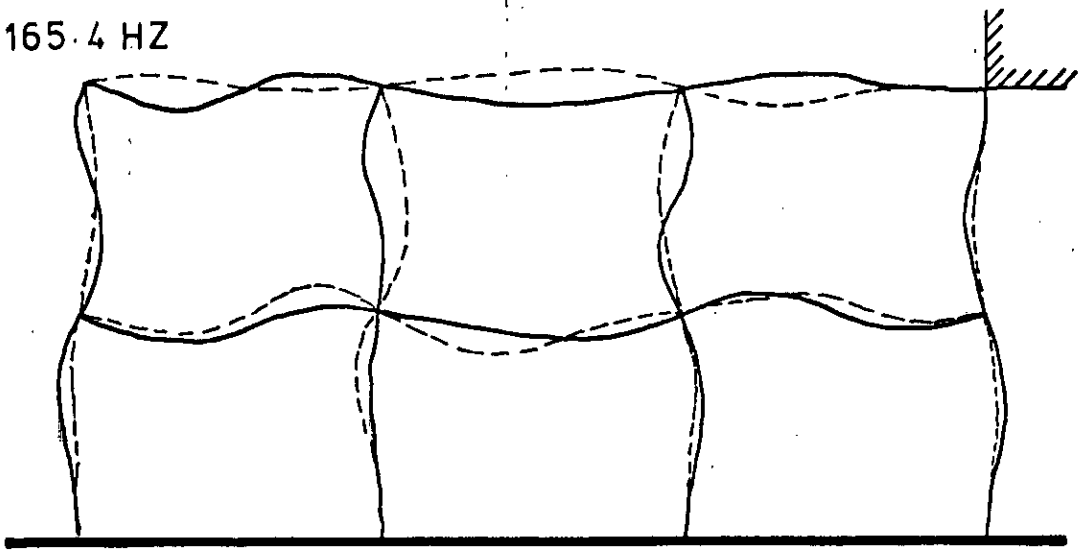
149.45 HZ



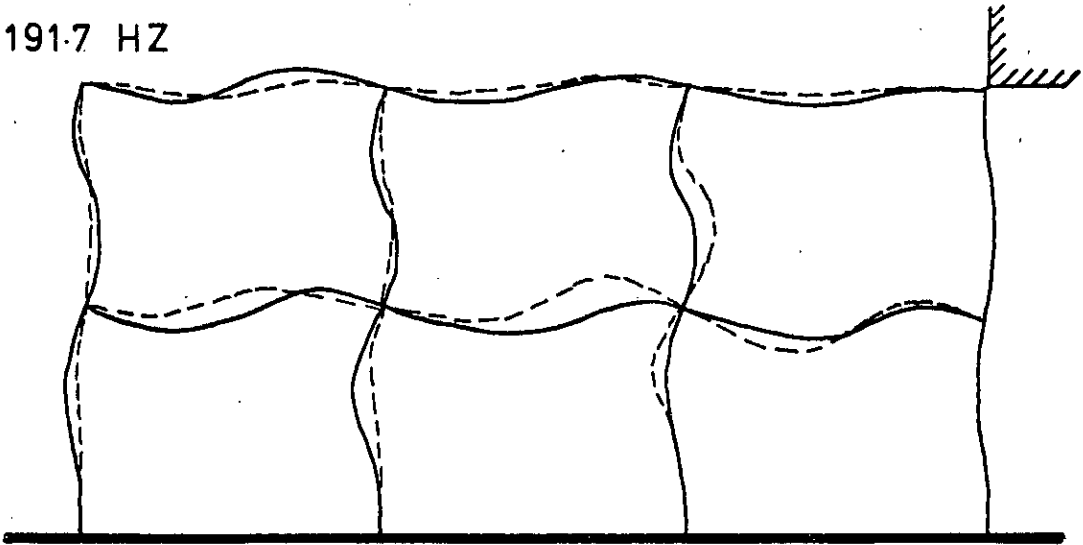
— Experimental
- - - Theoretical

Schematic Representation of Normal Modes

165.4 HZ



191.7 HZ



— Experimental
- - - Theoretical

Schematic Representation of Normal Modes

Figure 6.23.

6.72. Response as a Function of Variable Stiffness.

The response vector corresponding to degree of freedom 1 was examined for the variation of stiffness in the same direction at frequencies of 35 Hz and 40 Hz. The vector response plots at each of these frequencies are shown in Figure 6.24. Circles have been fitted to the data and the calculation of the diameters of these in terms of receptance is given below.

Experimental Data at 35 Hz.

In the experimental analysis, the structure was excited at block 1 in the horizontal direction, and the response was examined in the same direction at block 3.

Frequency:	35 Hz.
Magnitude of force input:	0.5 lb.f peak
Accelerometer calibration:	0.357 V/g peak
Maximum response signal:	0.85 V r.m.s.
Stiffness varied in the range:	17-6624 lb/ins.
Maximum acceleration =	$\frac{0.85 \times 1.414 \times 32.2 \times 12}{0.357}$
-	1300.88 in/sec ²
Maximum displacement =	$\frac{\text{Max. Accn.} = 1300.88}{\omega^2 (35 \times 2\pi)^2}$
-	2.689 x 10 ⁻² in.
Maximum receptance vector =	$\frac{2.689 \times 10^{-2}}{0.5} = 5.379 \times 10^{-2}$ in/lb f
Radius of Response Circle =	2.689 x 10 ⁻² in/lb f

6.72. (Continued)

Theoretically Determined Circle Data.

In the theoretical analysis, the examination point, forcing point and position of the variable stiffness parameter were the same as for the experimental analysis.

Frequency:	35 Hz.
Radius of Response Circle:	2.44×10^{-2} in/lb f
Centre of Circle:	$(2.21 \times 10^{-19}, -2.44 \times 10^{-2})$
Coordinates at $k = 0$:	$(-3.45 \times 10^{-3}, -2.45 \times 10^{-4})$
Coordinates at $k =$:	$(-5.45 \times 10^{-20}, -5.42 \times 10^{-20})$
Minimum receptance:	2.42×10^{-17} in/lb f
Value of k for minimum receptance:	10^{35} lb/in

Correlation between experimental and theoretical circle radii is 90.7%

Experimental data at 40 Hz.

Frequency:	40 Hz.
Magnitude of force input:	0.43 lb f peak.
Accelerometer calibration:	0.357 V/g peak
Maximum response signal:	0.732 V r.m.s.
Stiffness varied in the range:	17 - 6624 lb/in.
Maximum acceleration:	$\frac{0.732 \times 1.414 \times 32.2 \times 12}{0.357}$ $= 1120.28$ in/sec ²
Maximum displacement:	$\frac{1120.28}{(40 \times 2\pi)^2} = 1.773 \times 10^{-2}$ in

6.72. (Continued)

Maximum receptance vector: $\frac{1.773 \times 10^{-2}}{0.43} = 4.124 \text{ in/lb f}$

Radius of Response Circle: $2.062 \times 10^{-2} \text{ in/lb f}$

Theoretically determined Circle Data.

Frequency: 40 Hz.

Radius of response circle: $2.13 \times 10^{-2} \text{ in/lb f}$

Centre of circle: $(5.4 \times 10^{-20}, -2.13 \times 10^{-2})$

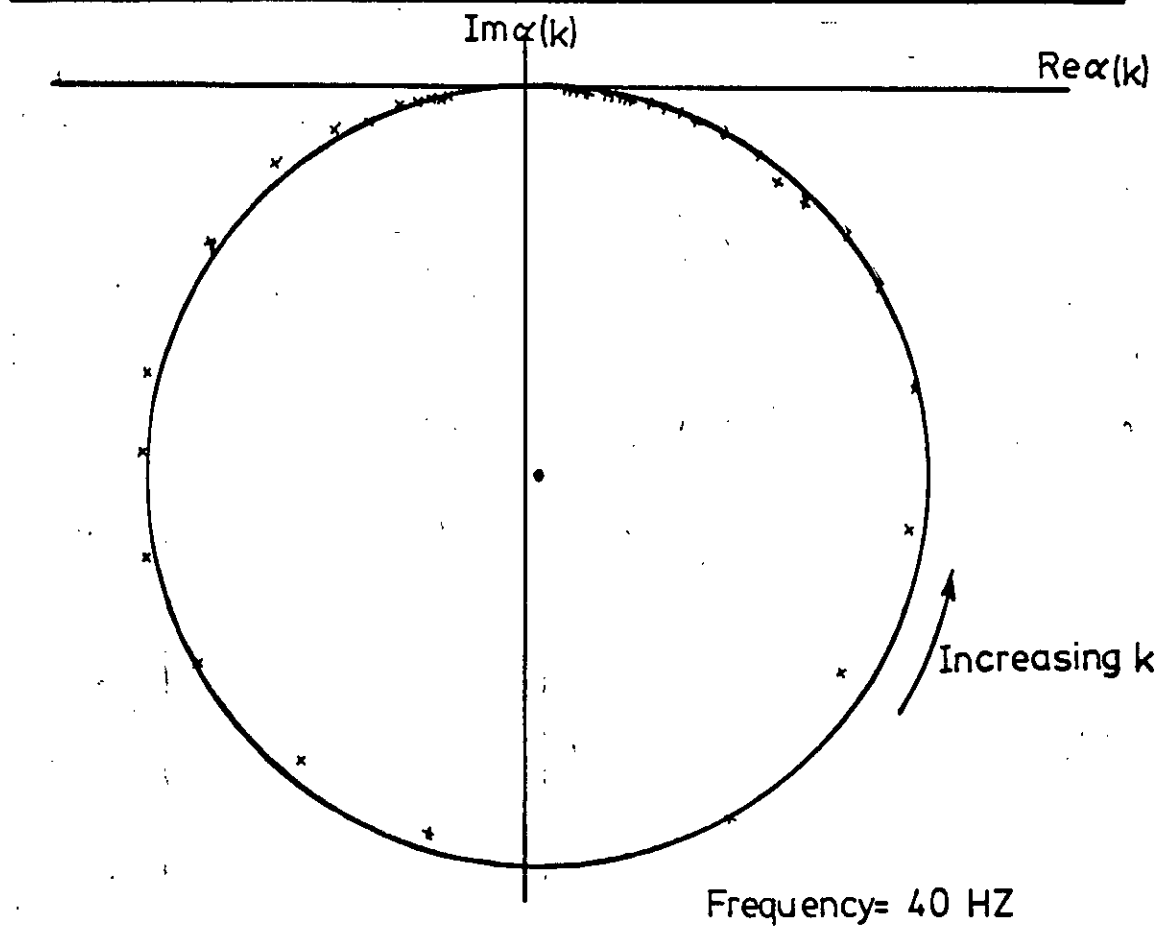
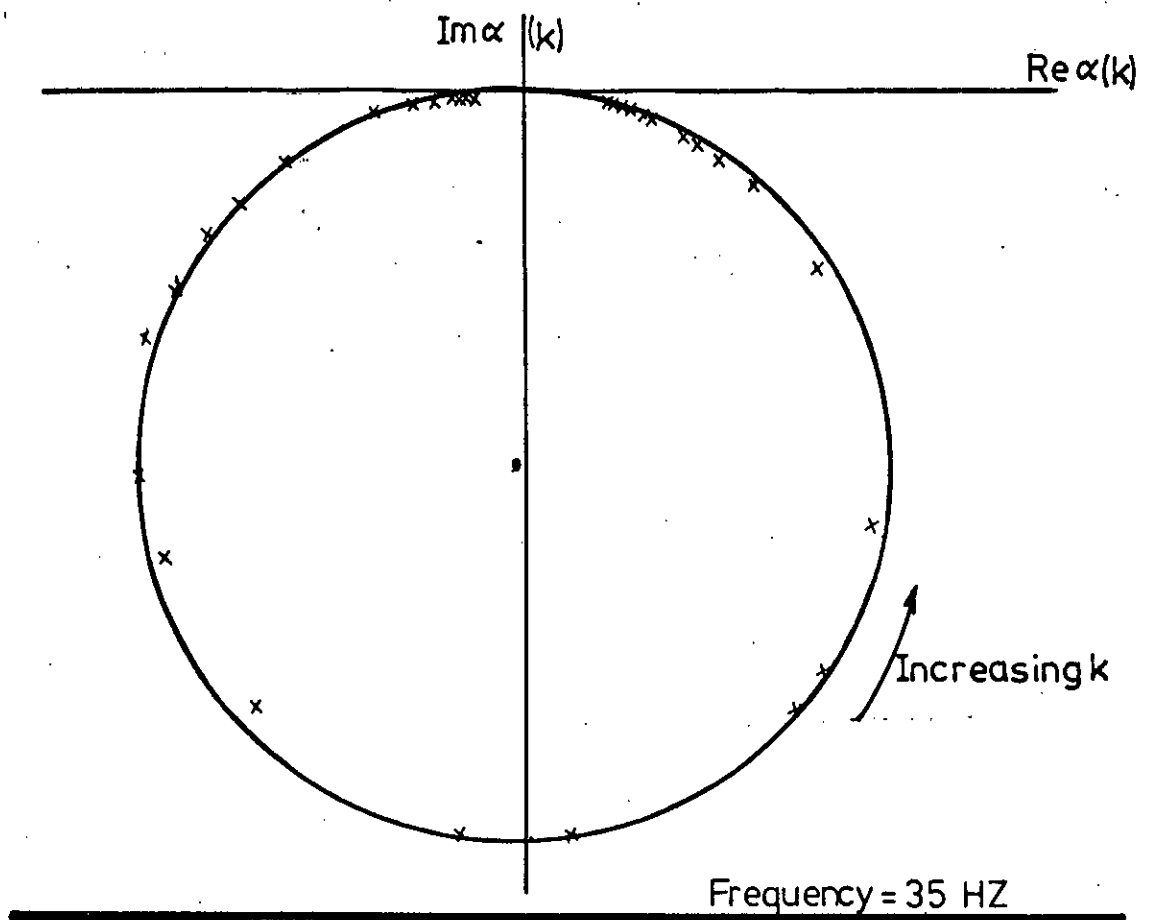
Coordinates at $k = 0$ $(-1.67 \times 10^{-3}, -6.55 \times 10^{-5})$

Coordinates at $k =$ $(-2.17 \times 10^{-19}, -3.38 \times 10^{-21})$

Minimum receptance: 0.0

Value of k for minimum
receptance: 10^{35} lb/in

Correlation between experimental and theoretical circle radii is
96.8%



Vector Response as a Function of a Single Variable
Stiffness Parameter

6.8. Conclusions.

6.8.1. The Mathematical Model of the Test Structure.

The accuracy of the mathematical model may be assessed by considering the following structural characteristics: stiffness, mass and inertia data, and the natural frequencies of the system. Appendix J lists the stiffness matrix for the manipulated mathematical model and also gives the experimentally determined stiffness of the structure in the horizontal direction at block 1. The theoretically calculated stiffness at this point was 721 lb/in., which compared very favourably with the experimental value of 728 lb/in. The stiffness data, which included Young's Modulus and the second moment of area of the spring steel strips, was thus considered to be a good representation of the real structure.

The initial estimates for the mass and inertia data were calculated from the dimensions of the blocks in the test structure. It was not possible, however, to determine these values experimentally as was the case with stiffness. Wherever possible, the added mass and inertia of couplings, fastenings and accelerometers was accounted for. The amount by which the initial data had to be changed in the process of matching the mathematical model varied from 1% to 30%, but on average this worked out to be 20% for inertia and 13% for mass. In almost all cases, the final data were higher than the predicted values.

The natural frequencies calculated using the initial estimate model were all larger than the experimental values by approximately 10%. However, it was found that the natural frequencies of the manipulated model could be made to match almost exactly the required values. The manipulated model was thus considered to be a good representation of the test structure.

6.82. Response as a Function of Variable Stiffness.

The main aim of this analysis was to determine experimentally the way in which the response at a point in a structure varied with changes in a simple stiffness element. It can be seen from Figure 6.24. that the form of the response circle predicted theoretically can be reproduced experimentally to a high degree of accuracy. The response vector traces out a circle in the complex plane and the position and radius of the circle correlate extremely well with the predicted values.

The aims of the experimental analysis have been fulfilled in as much as the theoretically predicted phenomena pertaining to structural manipulation can be reproduced in practical situations.

CHAPTER 7

CONCLUSIONS

A new approach to the problem of vibration reduction in dynamical structures has been developed. The dynamic response of a structure has been considered directly as a function of structural parameters. It has been shown that the response of a single degree of freedom system for variations in mass, stiffness or damping traces out a circle in the complex plane. For multi-degree of freedom systems the variation of a single mass or stiffness parameter has also been shown to produce a circular locus, the variation of damping not being considered in such systems. Where two or more parameters, either two mass, two stiffness or a mass and a stiffness parameter, were varied simultaneously, then a feasible response region was formed in the complex plane. Within this region it was found that either of two pairs of parameter values could be used to give a desired response, whilst only one pair of values was defined on the boundaries. A general equation for any response of the system as a function of m parameters has been developed in terms of the receptance matrices, however, where more than two parameters were considered then the reduction of the matrix equation was found to be complex. The term "Structural Manipulation" has been used to describe this type of analysis where structural response is considered as a function of structural modifications. The method does not involve either optimisation or iterative techniques and relies purely on the properties of linear dynamic systems.

In the aforementioned analyses, the properties of response circles and feasible response regions have been used to develop criteria

for the purpose of assessing the effect or sensitivity of parameters in changing structural response. These criteria are used in two main areas, namely,

- (a) To assess the ability of a parameter in achieving any given response.
- (b) To assess the ability of a parameter in achieving zero response.

In (a) the criterion used is the diameter of the response circle produced by a single variable parameter; those parameters with the largest diameter circles are considered to be the most effective. Where zero response is required, then two criteria are used, namely, the minimum response obtainable using a single parameter (derived from the response circle) and the feasibility of achieving zero response using two parameters. In the practical application of the theory to a helicopter fuselage, the criteria have been shown to give mutually consistent results; this applies for both mass and stiffness parameters. The criteria have been shown to be successful in highlighting sensitive areas of the structure, these being interpreted as the most suitable areas for structural modifications for the purpose of reducing vibration in another part of the structure. The bias diameter criterion described in Chapter 4, Section 4.3. was the only criterion that gave results that were not consistent with the others. In general, this criterion failed to show up any sensitive area within the structure. Surprisingly, according to this criterion, all the parameters in some cases had approximately the same effectiveness value. No logical explanation can be given for this, other than the fact that the bias diameter criterion was not suitable for this particular application.

The Structural Manipulation Program described in Chapter 5 has

been shown to be an indispensable tool for the purpose of testing theoretical results, and also in the practical application of the techniques to realistic problems. As a research tool the program has also proved invaluable.

An experimental analysis was performed in order to verify the form of the circular response locus predicted theoretically as a result of the variation of a simple stiffness parameter. A continuously variable linear stiffness element was designed for this purpose. Some difficulties were encountered in the mathematical modelling of the test structure, but even so it was found that the circular locus could be reproduced to a high degree of accuracy. These experimental results provide an extra element of confidence in the choice of any structural modifications that are indicated by a theoretical analysis.

Although the idealised stiffness parameters used throughout the analysis are unlikely to be encountered in practical situations, it has been shown that it is possible to model real structural elements by means of an equivalent linear spring system. It has also been shown that a variation in a real structural parameter, such as beam inertia, web depth or skin thickness, results in the variation of two linear stiffness parameters which are constrained to vary in a related manner. It has been shown that two parameters varying in this way no longer produce a feasible response region in the complex plane, but that the response is restricted to following a closed curve known as a Cassinian Oval.

Proposals for Future Development.

The techniques described here have been used to analyse simplified models of complex structures. The purpose of the analysis was to highlight sensitive areas within the structure suitable for the

purpose of structural modification. The results produced were of a qualitative nature and were not intended to be of any practical use in determining quantitatively the size of the real structural parameter changes that would be necessary to produce a desired response. It is hoped that once the sensitive areas of a structure have been identified on a coarse model of the system, then further analyses would be performed on more representative models of the sensitive substructures. This time it should be possible to identify effective elements within the substructure. It is envisaged that at this stage a formal optimisation of the whole structure would take place, using as variables the effective parameters indicated by the previous analyses.

The process by which a substructure could be examined is best illustrated by an example. Consider the case of a large detailed model of a structure too large for the Structural Manipulation Program to handle. It is assumed that the sensitive substructures have been identified using a simplified model which possesses fewer degrees of freedom than in the original system. The model could be in a form such as the Lynx helicopter stick model described in Chapter 4, or it could be produced by reducing the number of degrees of freedom of the full scale model by a process such as a Guyan reduction [28] which involves redistributing the mass of the system at a reduced number of node points in the structure. It is now required to perform a sensitivity analysis on a given substructure, the degrees of freedom that are of interest are the examination and forcing points x_q and x_p and the degrees of freedom of the substructure X_s . The analysis requires only the direct and cross receptances for these points. The latter may be obtained from the receptances of the full scale system by partitioning the appropriate matrices. If X_{-sub} and F_{-sub} are the

displacements and forces of interest, then the corresponding receptances are given in the relationship

$$\underline{X}_{\text{sub}} = \underline{G}_{\text{sub}} \underline{F}_{\text{sub}}$$

Providing that the order of $\underline{G}_{\text{sub}}$ is small enough then the receptance matrix could be fed directly into the Structural Manipulation Program where the relevant analyses would be performed. The one disadvantage in this method is that the receptances could not be altered within the Structural Manipulation Program, thus limiting the analysis to those techniques requiring constant frequency data; this is, however, not an unrealistic limitation. It is envisaged that further developments in the analysis would be needed in the area of modelling of real structural parameters; there is also the need for procedures to take into account any constraints that might be imposed on the values that any given parameter could take.

The techniques involved in Structural Manipulation have been shown to be useful in the dynamic analysis of complex structures and in particular in the connection with vibration reduction. The procedures described in the preceding chapters have been developed successfully and are in a reasonably advanced state of refinement. There is, of course, considerable scope for future improvements to be made in the analysis which would be best concentrated on its practical application.

APPENDIX A

The Constants in the Equation giving Receptance as a Function of a Single Parameter.

The equation for the complex receptance of a system at a point q due to a force at point p as a function of a single variable stiffness parameter is as follows:

$$\frac{x_q}{F_p} = G_{qp} + \frac{k(G_{sp} - G_{rp})(G_{qr} - G_{qs})}{1 + k(G_{rr} + G_{ss} - G_{rs} - G_{sr})} \quad (A1)$$

where r and s are the spring coordinates and G_{ij} are the complex receptances of the system. Equation A1 may be written in the more general form:

$$\frac{x_q}{F_p} = \frac{(e + if) + k(a + ib)}{1 + k(c + id)} \quad (A2)$$

where the constants a, b, c, d, e and f are all real. The complex receptances G_{ij} may be split into real and imaginary components where:

$$G_{ij} = C_{ij} + iD_{ij}$$

The constants a, b, c, d, e and f may be expressed as functions of these and are as follows:

$$a = (C_{qr} - C_{qs})(C_{sp} - C_{rp}) - (D_{qr} - D_{qs})(D_{sp} - D_{rp})$$

$$b = (C_{qr} - C_{qs})(D_{sp} - D_{rp}) + (D_{qr} - D_{qs})(C_{sp} - C_{rp})$$

$$c = C_{rr} + C_{ss} - C_{sr} - C_{rs}$$

$$d = D_{rr} + D_{ss} - D_{rs} - D_{sr}$$

$$e = C_{qp}$$

$$f = D_{qp}$$

APPENDIX B

The Constants Involved in the Equation for the Complex Receptance as a Function of Two Variable Stiffness Parameters.

The equation for the complex receptance $\alpha = \frac{x}{F_p}$ as a function of two variable stiffness parameters k_1 and k_2 is given generally by:

$$\alpha = \frac{G_{qp} + k_1 \phi_1(k_2) + \phi_2(k_2)}{k_1 \phi_3(k_2) + \phi_4(k_2)} \quad (B1)$$

where q and p refer to the examination and forcing points respectively, and parameter k_1 is connected between points r and s and parameter k_2 between points t and v . The functions $\phi_i(k_2)$ are given by:

$$\phi_1(k_2) = a_1 b_1 (1 + k_2 c_{22}) + a_2 b_2 c_{11} k_2 + k_2 (a_2 b_1 c_{21} + a_1 b_2 c_{12})$$

$$\phi_2(k_2) = a_2 b_2 k_2$$

$$\phi_3(k_2) = c_{11} (1 + k_2 c_{22}) - c_{21} c_{12} k_2$$

$$\phi_4(k_2) = 1 + k_2 c_{22}$$

where a_i , b_i and c_{ij} are the complex elements of matrices A, B and C respectively and are defined in Chapter 3, Section 3.4. The elements are functions of the complex receptances G_{ij} and are given by:

$$a_1 = G_{qr} - G_{qs}$$

$$a_2 = G_{qt} - G_{qv}$$

$$b_1 = G_{sp} - G_{rp}$$

$$b_2 = G_{vp} - G_{tp}$$

$$c_{11} = G_{rr} + G_{ss} - G_{rs} - G_{sr}$$

APPENDIX B(Continued)

$$c_{12} = G_{sv} - G_{st} - G_{rv} + G_{rt}$$

$$c_{21} = G_{vs} - G_{vr} - G_{ts} + G_{tr}$$

$$c_{22} = G_{tt} + G_{vv} - G_{vt} - G_{tv}$$

APPENDIX C

The Relationship between Parameters k_1 and k_2 on the Boundaries of a Feasible Response Region.

The equation for the complex receptance $\alpha = \frac{x_q}{F_p}$ as a function of two stiffness parameters k_1 and k_2 may be written:

$$\alpha = G_{qp} + \frac{k_1 \phi_1(k_2) + \phi_2(k_2)}{k_1 \phi_3(k_2) + \phi_4(k_2)} \quad (C1)$$

where $\phi_j(k_2)$ are defined in Appendix B. Equation C1 may be split into its real and imaginary components to give:

$$\alpha = G_{qp} + \frac{[z(1)k_1 + z(2)k_2 + z(3)k_1k_2] + i[z(4)k_1 + z(5)k_2 + z(6)k_1k_2]}{[1 + z(7)k_1 + z(8)k_2 + z(9)k_1k_2] + i[z(10)k_1 + z(11)k_2 + z(12)k_1k_2]} \quad (C2)$$

where the constants $z(I)$ are real functions of the real and imaginary components of the receptances G_{ij} , and are given at the end of the Appendix.

The relationship between k_1 and k_2 on the boundaries of the feasible response region is given by:

$$\text{Im} \left[\frac{\partial \alpha}{\partial k_1} \cdot \frac{\partial \bar{\alpha}}{\partial k_2} \right] = 0 \quad (C3)$$

where $\frac{\partial \bar{\alpha}}{\partial k_2}$ is the complex conjugate of $\frac{\partial \alpha}{\partial k_2}$

Differentiating equation C1 partially with respect to k_1 gives:

$$\frac{\partial \alpha}{\partial k_1} = (Ak_2^2 + Bk_2 + C) + i(Dk_2 + Ek_2 + F) \quad (C4)$$

APPENDIX C (CONTINUED)

where

$$A = z(3) z(8) - z(6) z(11) - z(2) z(9) + z(5) z(12)$$

$$B = z(1) z(8) + z(3) z(4) z(11) - z(2) z(7) + z(10) z(5)$$

$$C = z(1)$$

$$D = z(6) z(8) + z(3) z(11) - z(5) z(9) - z(12) z(2)$$

$$E = z(4) z(8) + z(6) z(1) z(4) - z(5) z(7) - z(10) z(2)$$

$$F = z(2)$$

The product of two terms, say, $z(3)$ and $z(8)$, is written as $z(3) z(8)$ for convenience. The complex conjugate of the partial differential of equation C2 with respect to k_2 is given by:

$$\frac{\partial \bar{\alpha}}{\partial k_2} = (Gk_1^2 + Hk_1 + J) + i(Lk_1^2 + Mk_1 + N) \quad (C5)$$

where

$$G = z(3) z(7) - z(6) z(10) - z(1) z(9) + z(12) z(4)$$

$$H = z(2) z(7) + z(3) z(4) z(11) - z(5) z(10) - z(1) z(8) + z(4) z(11)$$

$$J = z(4)$$

$$L = -z(3) z(10) - z(6) z(7) + z(9) z(4) + z(12) z(1)$$

$$M = -z(10) z(2) - z(5) z(7) - z(6) z(4) z(8) + z(11) z(1)$$

$$N = -z(5).$$

It will be noted that the denominators in equation C4 and C5 have been omitted. This has been done for the sake of simplicity. The denominators are in fact the complex conjugates of each other, and consequently when equations C4 and C5 are substituted into C3 then the product of the denominators is a real non-zero number and may be cancelled.

Given a value of k_1 and letting equation C5 be of the form:

APPENDIX C (Continued)

$$\frac{\delta \bar{\alpha}}{\delta k_2} = X + iY \quad (C6)$$

then the values of X and Y may be calculated, and when these are substituted for $\frac{\delta \bar{\alpha}}{\delta k_2}$ in equation C3, then the resulting equation is a quadratic in k_2 and is of the form:

$$k_2^2 (AY + DX) + k_2 (BY + EX) + (CY + FX) = 0 \quad (C7)$$

The roots of this equation yield two values of k_2 , one for each boundary of the feasible region. The two pairs of values $(k_1, k_2)_1$ and $(k_1, k_2)_2$ may now be substituted into equation C2 to give the coordinates of the corresponding points on the boundaries. If a sufficient number of values of k_1 are chosen in the range $-\infty$ to $+\infty$, then a good representation of the boundaries may be plotted in the complex plane.

The real constants $z(I)$ can be given as functions of the real and imaginary components of the receptances C_{ij} and D_{ij} respectively as follows:

let

$$AA = (C_{qr} - C_{qs})(C_{vp} - C_{tp}) - (D_{qr} - D_{qs})(D_{vp} - D_{tp})$$

$$AB = (C_{qr} - C_{qs})(D_{vp} - D_{tp}) + (D_{qr} - D_{qs})(C_{vp} - C_{tp})$$

$$AC = (C_{sp} - C_{rp})(C_{qt} - C_{qv}) - (D_{qt} - D_{qv})(D_{sp} - D_{rp})$$

$$AD = (C_{sp} - C_{rp})(D_{qt} - D_{qv}) + (D_{sp} - D_{rp})(C_{qt} - C_{qv})$$

$$AE = C_{sv} - C_{st} - C_{rv} + C_{rt}$$

$$AF = D_{sv} - D_{st} - D_{rv} + D_{rt}$$

APPENDIX C (CONTINUED)

and $K(1) = (C_{qr} - C_{qs})(C_{sp} - C_{rp}) - (D_{qr} - D_{qs})(D_{sp} - D_{rp})$

$$K(2) = (C_{qt} - C_{qv})(C_{vp} - C_{tp}) - (D_{qt} - D_{qv})(D_{vp} - D_{tp})$$

$$K(3) = AE \times (AA + AC) - AF \times (AB + AD)$$

$$K(4) = C_{ss} + C_{rr} - C_{rs} - C_{sr}$$

$$K(5) = AE^2 - AF^2$$

$$K(6) = C_{vv} + C_{tt} - C_{vt} - C_{tv}$$

$$L(1) = (C_{qr} - C_{qs})(D_{sp} - D_{rp}) + (D_{qr} - D_{qs})(C_{sp} - C_{rp})$$

$$L(2) = (C_{qt} - C_{qv})(D_{vp} - D_{tp}) + (D_{qt} - D_{qv})(C_{vp} - C_{tp})$$

$$L(3) = AE \times (AB + AD) + AF \times (AA + AC)$$

$$L(4) = D_{ss} + D_{rr} - D_{rs} - D_{sr}$$

$$L(5) = 2 \times AE \times AF$$

$$L(6) = D_{vv} + D_{tt} - D_{tv} - D_{vt}$$

Then

$$Z(1) = K(1)$$

$$Z(2) = K(2)$$

$$Z(3) = K(1)K(6) - L(1)L(6) + K(2)K(4) - L(2)L(4) - K(3)$$

$$Z(4) = L(1)$$

$$Z(5) = L(2)$$

$$Z(6) = K(1)L(6) + L(1)K(6) + K(2)L(4) + L(2)K(4) - L(3)$$

$$Z(7) = K(4)$$

$$Z(8) = K(6)$$

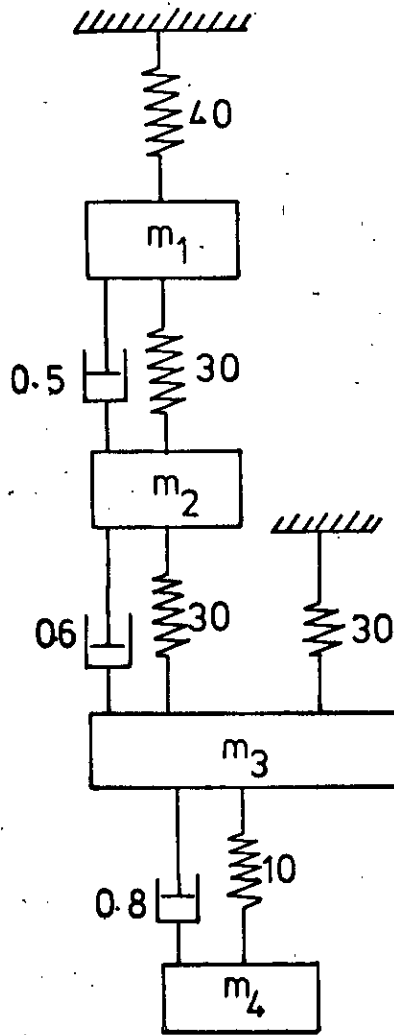
$$Z(9) = K(4)K(6) - L(4)L(6) - K(5)$$

$$Z(10) = L(4)$$

$$Z(11) = L(6)$$

$$Z(12) = K(4)L(6) + L(4)K(6) - L(5)$$

APPENDIX D.



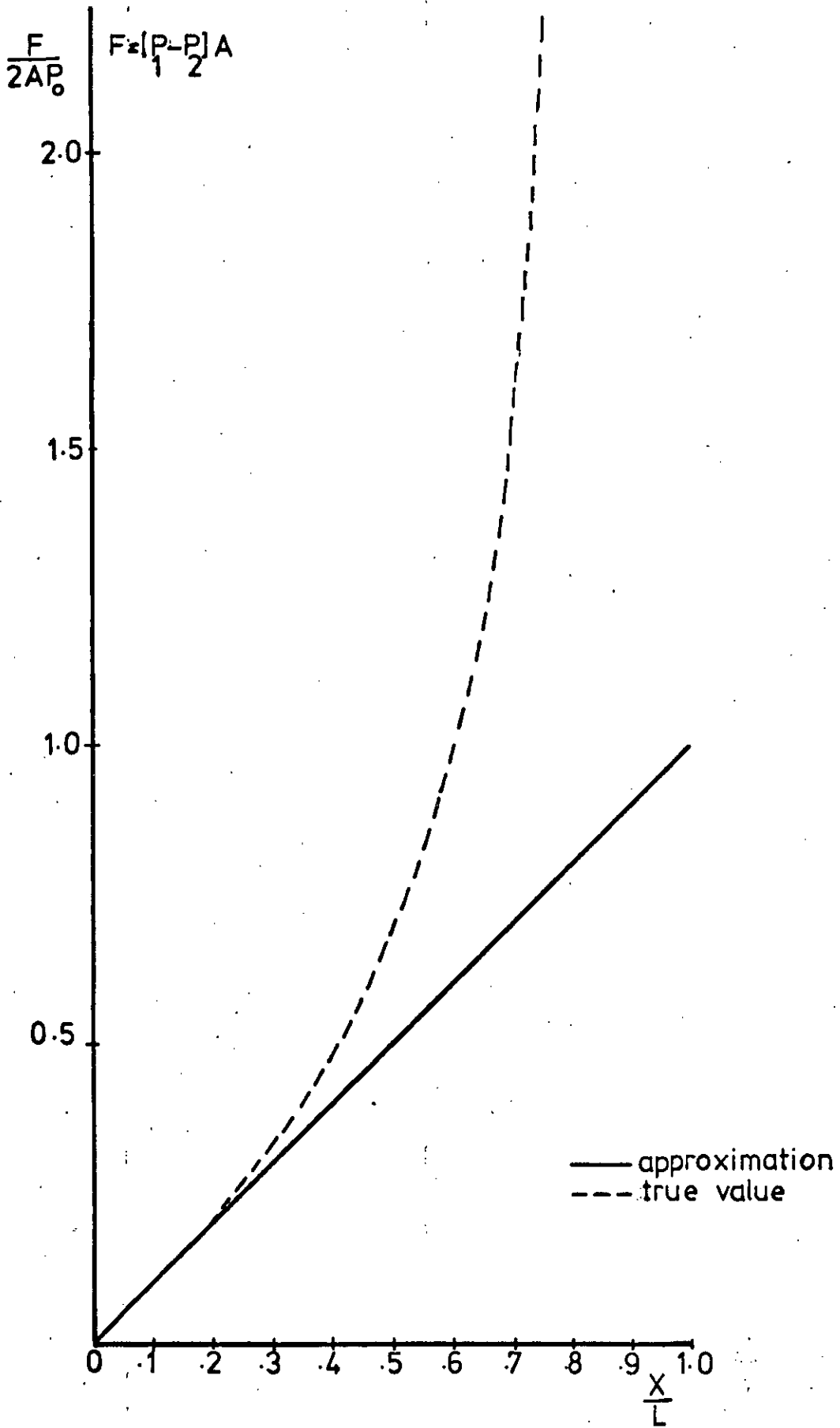
Mass values

m_1	3
m_2	10
m_3	20
m_4	5

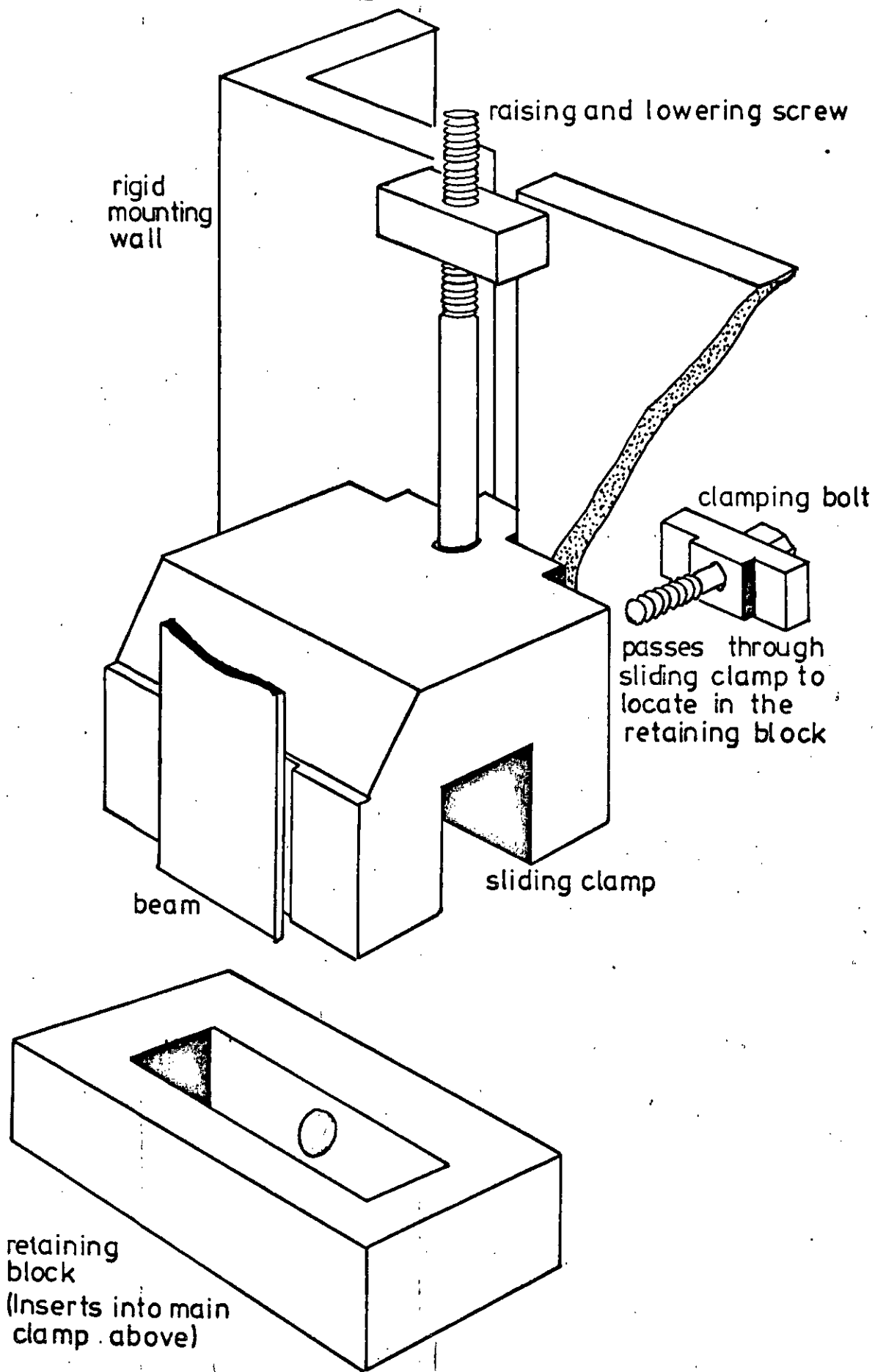
All units are compatible

The Mass, Spring, Dashpot System Used in the Calculation
Of feasible Response Region Boundaries.

APPENDIX E



The Graph of $\frac{F}{AP_0}$ Against $\frac{X}{L}$ for an Air Spring



Details of the Clamped Cantilever Spring.

APPENDIX G

Output from the Structural Manipulation Program.

SYSTEM (400)

****MODEL OF EXPERIMENTAL SYSTEM USING BLOCK 30/5/75****

DATA FROM LAST RUN

FREQUENCY : 2.000@ 2 HZ

EXAM, FORCING: 2 6

CHOICE: CIRCLE

DR: 2

DS: 3

RESPONSE CIRCLE FOR VARIABLE STIFFNESS

EXAM/FORCING : 2 6

SPRING COORDS : 2 3

FORCING FREQU : 2.00000@ 2 HZ

RADIUS : 9.58097@ -6

MIN RECEPT MOD : 1.02635@ -4

CENTRE OF CIRC :-1.12215@ -4 , 3.88173@ -7

COORDS AT K=0 :-1.10444@ -4 , -9.02773@ -6

COORDS AT K=INF:-1.12774@ -4 , -9.17646@ -6

K AT MIN RECEPT: 4.23910@ 2

COORDINATES :-1.02634@ -4 , 3.55031@ -7

CHOICE:

Data Concerning the Response Circle for a Single Variable
Parameter.

APPENDIX G (Continued)

CHOICE:ASSESS

22 SELECTED PARAMETERS

FREQUENCY : 2.0000 2 HZ
EXAM, FORCING: 2 6

STIFFNESS PARAMETERS

ELEMENT ANALYSIS BASED ON ASSOCIATED PARAMETERS

		LOG SCALE			CIRCLE			BIAS	
	ELEM	MINIMUM	RESPONSE	ELEM	DIAMETER	ELEM	CIRC	ARC	
1)	1	1.00	0	8	1.00	0	1	1.00	0
2)	8	3.00	-1	1	3.60	-1	8	1.00	0
3)	2	2.50	-1	2	3.00	-2	2	8.70	-1
4)	9	2.50	-1	9	2.40	-2	9	7.90	-1
5)	3	2.40	-1	13	2.30	-2	3	6.10	-1
6)	10	2.30	-1	6	2.10	-2	6	5.40	-1
7)	4	2.30	-1	12	2.00	-2	13	5.30	-1
8)	11	2.30	-1	3	1.70	-2	10	4.30	-1
9)	6	2.80	-2	10	1.20	-2	11	3.10	-1
10)	13	2.50	-2	4	9.20	-3	4	3.10	-1
11)	7	9.40	-3	11	9.20	-3	7	2.60	-1
12)	14	7.20	-3	7	5.90	-3	14	2.00	-1
13)	5	1.00	-3	14	4.30	-3	12	3.60	-2
14)	12	0.00	-99	5	0.00	-99	5	0.00	-99

PRINTOUT?:N

CHOICE:

Effectiveness Criteria for a Single Variable Stiffness Parameter.

APPENDIX G (Continued)

CHOICE:ASSESSALL

PARAMETER SELECTIONS ALREADY MADE

ZERO RESPONSE USING TWO STIFFNESS PARAMETERS

22 SELECTED PARAMETERS
253 POSSIBLE PAIRED COMBINATIONS
43 PAIRS GIVE ZERO RESPONSE

ELEM LIST?:Y

FREQUENCY : 2.0000 2 HZ
EXAM/FORCING: 2 6

OCCURRENCE OF ELEMENTS BASED ON SUCCESSFUL PARAMETERS:-

			PARAMETER BREAKDOWN						
ELEM	NORM	TOT	X	Y	Z	T1	T2	T3	
1)	1	1.00	24	3	0	0	0	21	0
2)	2	0.52	13	3	0	0	0	10	0
3)	6	0.35	9	0	0	0	0	9	0
4)	8	0.26	7	3	0	0	0	4	0
5)	9	0.22	6	3	0	0	0	3	0
6)	3	0.13	4	3	0	0	0	1	0
7)	4	0.13	4	3	0	0	0	1	0
8)	5	0.13	4	0	0	0	0	4	0
9)	10	0.13	4	3	0	0	0	1	0
10)	11	0.13	4	3	0	0	0	1	0
11)	12	0.13	4	0	0	0	0	4	0
12)	7	0.00	1	0	0	0	0	1	0
13)	13	0.00	1	0	0	0	0	1	0
14)	14	0.00	1	0	0	0	0	1	0

PRINTOUT?:Y
HOW MANY:2

DR DS	DT DV	COORDINATES	
2 G	2 6		
1.000000000000@ 35	1.12213745730-14	-2.7110-20	-8.4700-22
9.54320302760 18	5.06365646340 2	3.3880-21	0.0000-99
2 G	3 4		
4.99161181470 18	5.71546325760 2	-1.7620-19	1.0860-19
-1.33518919320 19	1.91440894630-13	1ST NG	

ANY MORE?:N

Assessing for Zero Response Using Two Parameters.

APPENDIX H

The Transformation Matrix used in the Mathematical Model
to Account for the Finite Size of Structural Nodes.

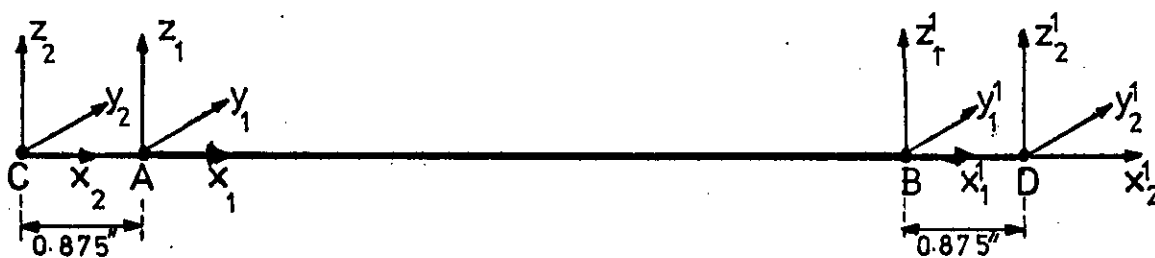


Figure H1

Finite Element AB and Rigid Extensions CA and BD

Figure H1 represents a simple finite element beam AB with rigid extensions CA and BD of length 0.875". Considering the left hand end of the beam, the transformation between the coordinate systems at points A and C is:

$$\begin{bmatrix} x_1 \\ y_1 \\ z_1 \\ \alpha_1 \\ \theta_1 \\ \phi_1 \end{bmatrix} = \begin{bmatrix} 1 & 0 & 0 & 0 & 0 & 0 \\ 0 & 1 & 0 & 0 & 0 & 0.875 \\ 0 & 0 & 1 & 0 & -0.875 & 0 \\ 0 & 0 & 0 & 1 & 0 & 0 \\ 0 & 0 & 0 & 0 & 1 & 0 \\ 0 & 0 & 0 & 0 & 0 & 1 \end{bmatrix} \begin{bmatrix} x_2 \\ y_2 \\ z_2 \\ \alpha_2 \\ \theta_2 \\ \phi_2 \end{bmatrix}$$

APPENDIX H (Continued)

or in matrix notation:

$$\underline{X}_e = \underline{\lambda}_e \underline{X}_e^* \quad (H1)$$

The relationship between the forces in the two coordinate system is given by:

$$\underline{F}_e^* = \underline{\lambda}_e^T \underline{F}_e \quad (H2)$$

where $\underline{\lambda}_e^T$ is the transpose of $\underline{\lambda}_e$.

For the right hand end of the beam:

$$\begin{bmatrix} x_1^1 \\ y_1^1 \\ z_1^1 \\ \alpha_1^1 \\ \theta_1^1 \\ \phi_1^1 \end{bmatrix} = \begin{bmatrix} 1 & 0 & 0 & 0 & 0 & 0 \\ 0 & 1 & 0 & 0 & 0 & -0.875 \\ 0 & 0 & 1 & 0 & 0.875 & 0 \\ 0 & 0 & 0 & 1 & 0 & 0 \\ 0 & 0 & 0 & 0 & 1 & 0 \\ 0 & 0 & 0 & 0 & 0 & 1 \end{bmatrix} \begin{bmatrix} x_2^1 \\ y_2^1 \\ z_2^1 \\ \alpha_2^1 \\ \theta_2^1 \\ \phi_2^1 \end{bmatrix}$$

or, in matrix notation

$$\underline{X}_r = \underline{\lambda}_r \underline{X}_r^* \quad (H3)$$

The relationship between the forces in the two coordinate system is

$$\underline{F}_r^* = \underline{\lambda}_r^T \underline{F}_r \quad (H4)$$

The relationship between the forces and displacements for the element is:

$$\underline{F} = \underline{K} \underline{X}$$

where

$$\underline{F} = \begin{bmatrix} F_e \\ F_r \end{bmatrix} \quad \underline{K} = \begin{bmatrix} K1 & K2 \\ K2^T & K3 \end{bmatrix} \quad \underline{X} = \begin{bmatrix} X_e \\ X_r \end{bmatrix}$$

Substituting for F_e , F_r , X_e and X_r from equations H1, H2, H3 and H4 gives

$$\underline{F}^* = \underline{K}^* \underline{X}^*$$

APPENDIX H (CONTINUED)

where

$$\underline{F}^* = \begin{bmatrix} F_L^* \\ F_r^* \end{bmatrix} \quad \underline{X}^* = \begin{bmatrix} X_L^* \\ X_r^* \end{bmatrix}$$

and

$$\underline{K}^* = \begin{bmatrix} \lambda_L^T K1 \lambda_L & \lambda_L^T K2 \lambda_r \\ \lambda_r^T K2^T \lambda_L & \lambda_r^T K3 \lambda_r \end{bmatrix}$$

which provides a relationship between the forces and displacements at points C and D on the beam.

APPENDIX I

The Constants Involved in Calculating the Feasibility of a Desired Response.

For a single stiffness parameter k the response at a point in the structure is given by:

$$\alpha = e + if + \frac{k(a + ib)}{1 + k(c + id)} \quad (I 1)$$

where, a, b, c, d, e and f are real constants and are defined in Appendix A. The real and imaginary components of α are:

$$u = e + \frac{k(a + k(ac + bd))}{1 + 2ck + k^2(c^2 + d^2)} \quad (I2)$$

and

$$v = f + \frac{k(b + k(bc - ad))}{1 + 2ck + k^2(c^2 + d^2)} \quad (I3)$$

respectively. Now $|\alpha|^2$ may be written:

$$|\alpha|^2 = \frac{Ak^2 + Bk + C}{Pk^2 + Qk + R} \quad (I4)$$

where

$$\begin{aligned} A &= (a^2 + b^2) + (e^2 + f^2)(c^2 + d^2) + 2e(ac + bd) + 2f(bc - ad) \\ B &= 2c(e^2 + f^2) + 2(fb + ea) \\ C &= e^2 + f^2 \\ P &= c^2 + d^2 \\ Q &= 2c \\ R &= 1 \end{aligned}$$

APPENDIX I (Continued)

The first derivative of $|\alpha|^2$ with respect to k is

$$\frac{d}{dk} |\alpha|^2 = \frac{k^2(QA - PB) + 2k(RA - PC) + (RB - QC)}{(Pk^2 + Qk + R)^2} \quad (I5)$$

and the second derivative of $|\alpha|^2$ with respect to k is

$$\frac{d^2}{dk^2} |\alpha|^2 = \frac{\sigma_1(k) - \sigma_2(k)}{\sigma_3(k)}$$

where

$$\sigma_1(k) = 2(Pk^2 + Qk + R)^2(k(QA - PB) + (RA - BC))$$

$$\sigma_2(k) = 2(k^2(QA - PB) + 2k(RA - PC) + (RB - QC))(Pk^2 + Qk + R)(2Pk + Q)$$

$$\sigma_3(k) = (Pk^2 + Qk + R)^4$$

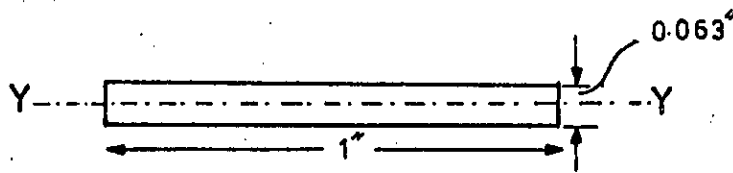
APPENDIX J

Data Used in the Preparation of the Mathematical Model.

Refer to Figure 6.16.

Stiffness Elements.

Second Moment of Area.



$$I_{yy} = \frac{bd^3}{12} = \frac{1 \times (0.063)^3}{12} = 2.083 \times 10^{-5} \text{ in.}^4$$

Element lengths

Elements 5,6,7,12,13 and 14 = 6"

Elements 1,2,3,4,8,9 and 10 = 4"

Young's Modulus.

Young's Modulus was determined experimentally by measuring the tip deflection of one of the spring steel beams comprising the test structure.

For a beam, length 5", the tip deflection under a load of 1.2 lbs. was .0905".

From simple beam theory

$$E = \frac{Pl^3}{3Ix} = \frac{125 \times 1.2 \times 10^5}{3 \times 2.083 \times 0.0905} = 2.6524 \times 10^7 \text{ lb/in.}^2$$

APPENDIX J (CONTINUED)

The added stiffness of the variable stiffness element.

The variable stiffness element is a simple cantilever of maximum length 4.6". (This remained constant during the measurement of natural frequencies and mode shapes). The stiffness at the tip of this element is given by:

$$k = \frac{3EI}{l^3}$$

Thus $k = \frac{3 \times 2.65 \times 10^7 \times 2.083 \times 10^{-5}}{(4.6^3)} = 17.0 \text{ lb/in}$

This value was added to element k(1,1) in the structure stiffness matrix.

The stiffness matrix of the mathematical model of the test structure is as follows: (units lb/in.)

844.9	0	0	0	0	297.5	297.5	297.5
	2539.4	368.5	0	0	717.5	0	0
		3091.9	368.5	0	0	717.5	0
			3091.9	368.5	0	0	717.5
	SYM			2539.4	0	0	0
					1545.9	368.5	0
						2098.4	368.5
							2098.4

In order to determine the accuracy of this data, the stiffness of the test structure in the horizontal direction at node 5 was determined experimentally. A horizontal load of 10.2 lb. was applied at this point, and the corresponding deflection was found to be 0.014".

Thus, the stiffness at that point was:

$$\frac{10.2}{0.014} = 728 \text{ lb/in.}$$

APPENDIX J (CONTINUED)

To obtain the equivalent term from the theoretical stiffness matrix, consider the matrix in the partitioned form

$$\begin{bmatrix} F_1 \\ F_2 \end{bmatrix} = \begin{bmatrix} k_1 & k_2 \\ k_3 & k_4 \end{bmatrix} \begin{bmatrix} \delta_1 \\ \delta_2 \end{bmatrix} \quad (J1)$$

where F_1 is the force in the x direction of node 5 and δ_1 the corresponding deflection.

F_2 , k_3 and δ_2 are of the order (7 x 1)

k_2 is (1 x 7)

k_4 is (7 x 7)

We require to know the deflection δ_1 for $F_1 = 1$ lb. and $F_2 = 0$

Now, if equation J1 is expanded, then

$$F_1 = k_1 \delta_1 + k_2 \delta_2 \quad (J2)$$

and

$$F_2 = 0 = k_3 \delta_1 + k_4 \delta_2$$

Therefore,

$$\delta_2 = -k_4^{-1} k_3 \delta_1$$

which may be substituted into equation (J2) to give

$$F_1 = (k_1 - k_2 k_4^{-1} k_3) \delta_1$$

Thus, the required stiffness term is

$$(k_1 - k_2 k_4^{-1} k_3)$$

When these terms are calculated from the stiffness matrix given above, then the following value is obtained:

$$[844.9 - 123] = 721.9 \text{ lb/in.}$$

This corresponds favourably with the value of 728 lb/in. obtained experimentally.

APPENDIX J (CONTINUED)

Mass and Inertia Data.

The mass of the structure in the direction corresponding to degree of freedom 1 comprises the total mass of four blocks, three beams and associated accelerometers and couplings. This value was measured experimentally and found to be

$$1.8 \times 10^{-2} \text{ lbf in}^{-1} \text{sec}^2$$

Figure J.1. shows one of the structural node blocks

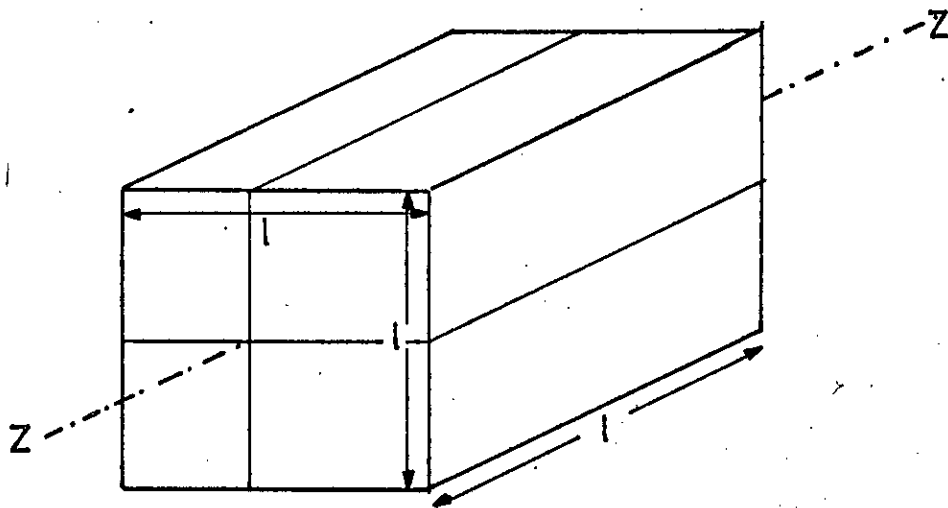


Figure J.1.

Structural Node Block

The moment of inertia of the block in the zz direction is given by the equation

$$\frac{MI_{zz}}{12} = \frac{2Ml^2}{12}$$

Now, the weight of each block was found to be 1.8 lbf and $l = 1.75$ in, therefore

APPENDIX J (CONTINUED)

$$MI_{ZZ} = \frac{2 \times 1.8 \times (1.75)^2}{12 \times 32.2 \times 12} = 2.377 \times 10^{-3} \text{ lbf in. sec}^2$$

The moment of inertia of an accelerometer mounted as shown in Figure 6.15. about the ZZ axis is

$$0.056 \times 10^{-3} \text{ lbf in. sec}^2$$

Thus, the total inertia of the block plus accelerometer is

$$2.426 \times 10^{-3} \text{ lbf in. sec}^2$$

This value was adjusted according to the amount of additional instrumentation on any given block. The following were the initial estimates for the inertia data.

Block	Inertia lbf in. sec ²
1	2.5 x 10 ⁻³
2	2.45 x 10 ⁻³
3	2.42 x 10 ⁻³
4	2.42 x 10 ⁻³
5	2.5 x 10 ⁻³
6	2.42 x 10 ⁻³
7	2.42 x 10 ⁻³

The inertias of individual blocks were not determined experimentally.

APPENDIX K

The Stiffness Matrix for a Linearly Tapering I Beam.

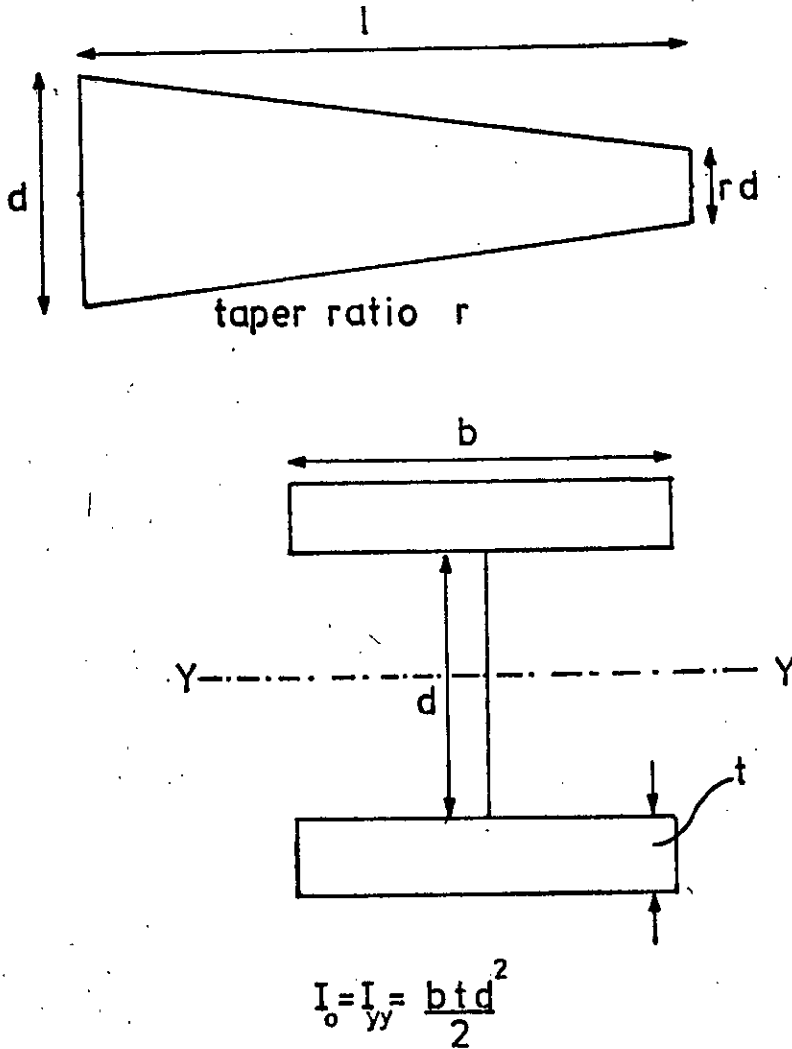


Figure K.1.

The stiffness matrix for the beam shown in Figure K.1. may be obtained using standard techniques [15], and is given overleaf.

APPENDIX K (CONTINUED)

$$\underline{K} = EI_0 \quad \text{SYM} \quad \begin{bmatrix} k_1 + k_2 (l^2 - x^2) & k_2 (l - x) & k_2 (lx - x^2) - k_1 & -k_2 (l - x) \\ & k_2 & k_2 x & -k_2 \\ & & k_1 + k_2 x^2 & -k_2 x \\ & & & k_2 \end{bmatrix}$$

when

$$k_1 = \frac{1}{4l} \frac{(r^4 + 4r^3 + 10r^2 + 4r + 1)}{(2r^2 + r + 2)}$$

$$k_2 = \frac{12}{5l^2} (2r^2 + r + 2)$$

and

$$x = \frac{l}{12} \frac{(17r + 6r + 7)}{(2r^2 + r + 2)}$$

REFERENCES

- (1) Newman, K.W. Predicting the Effects of Parameter Changes in Dynamical Systems. RAE T.R. 69142 (A.R.C 32597) July 1969
- (2) Simpson, A. Eigenvalue and Vector Sensitivities in Kron's Method. Journal of Sound and Vibration (1973)31 (1),73-87.
- (3) Vincent, A.H. A Note on the Properties of the Variation of Structural Response with Respect to a Single Structural Parameter When plotted in the Complex Plane. GEN/DYN/RES/OLOR Sept. 1973. (Unpublished Westland Helicopters Report)
- (4) Bishop, R.E.D. and Gladwell, G.M.L. An Investigation into the Theory of Resonance Testing. Phil. Trans. Roy. Soc. Series A, No 1055, 255 January, 1963.
- (5) Spiegel, M.R. Theory and Problems of Complex Variables. Schaums Outline Series. McGraw-Hill, 1964.
- (6) Sneddon, I.N. Elements of Partial Differential Equations. McGraw-Hill, 1957.
- (7) Kyrala, A. Applied Functions of a Complex Variable. Wiley-Interscience, 1972.
- (8) Susholz, B. Forced and Free Motion on an Airspring. Journal of Applied Mechanics, June 1944, 101-107.
- (9) Thompson, W.T. Vibration Theory and Application. London 1966.
- (10) Gaukroger, D.R. Numerical Analysis of Vector Response Loci. Skingle, C.W. and Heron, K.H. Journal of Sound and Vibration (1973)29(3), 341-353.

- (11) Milne, R.D. and Simpson, A. Reconciliation of Calculated and Measured Natural Frequencies and Normal Modes. Journal of Sound and Vibration (1973)30(1), 45-63.
- (12) Marples, V. The Derivation of Modal Damping Ratios from Complex Plane Response Plots. Journal of Sound and Vibration (1973)31(1), 105-117.
- (13) Nottingham Algorithms NAG mini Manual for the NAG IEM 360-370 Group. Library, 1973.
- (14) Pestle, E.C.E. and Leckie, F.A. Matrix Methods in Elastomechanics. McGraw-Hill, 1963.
- (15) Jenkins, W.M. Matrix and Digital Methods in Structural Analysis. McGraw-Hill, 1969.
- (16) Sciarra, J.J. Application of Impedance Methods to Helicopter Vibration Reduction. Paper Presented at Imperial College London, July 1973.
- (17) Sciarra, J.J. Application of Combined Direct Stiffness and Mobility Methods to Vibration Absorber Studies. American Society of Mechanical Engineers. 67-VIBR-65, 1967.
- (18) Sciarra, J.J. Helicopter Fuselage Vibration Prediction by stiffness Mobility Methods. The Shock and Vibration Bulletin. (1968)37 (6),19-28.
- (19) Woodcock, D.L. The Rate of Change of Eigenvalues of a Lambda Matrix and Their use in Flutter Investigations. Journal of Roy. Aero. Soc. (1966)70,364-365.

(30) Rubin, C.P.

Dynamic Optimisation Of Complex Structures.
AIAA Dynamics and Aerolasticity Specialists
Conference, New Orleans, La(April, 1969).

PUBLISHED WORK

Done, G.T.S. and
Hughes, A.D.

The Response of a Vibrating Structure
as a Function of Structural Parameters.
Journal of Sound and Vibration (1975) 38(2),
255-266.

THE RESPONSE OF A VIBRATING STRUCTURE AS A FUNCTION OF STRUCTURAL PARAMETERS

G. T. S. DONE AND A. D. HUGHES

*Department of Mechanical Engineering,
University of Edinburgh, Edinburgh EH9 3JL, Scotland*

(Received 14 May 1974, and in revised form 13 August 1974)

The response of a structure excited by an external oscillatory force is examined for variations in certain structural parameters of the system. This is done with a view to manipulating the structure in order to achieve a desired response. The variation of the response with one structural parameter is seen to be simple, and the effect of changing in addition the forcing frequency is illustrated. When two structural parameters are considered, it is seen that a desired response may or may not be attainable, as defined by a "feasible response region". The application to practical cases is discussed briefly.

1. INTRODUCTION

Linear structural analysis is now a relatively straightforward task, and has been greatly aided in the recent past by the advent of digital computers. However, the results of an analysis can be so large in quantity and extent that in the case of a vibration problem producing unacceptable results the answer to the question "How does one alter the structure to produce the originally desired dynamic characteristics?" is very far from evident. Small perturbation analysis exists [1, 2] which goes some way towards providing an answer and, of course, it is possible to make use of one of the many computer based formal optimization routines. Neither of these is entirely satisfactory; in the former case it may be that gross rather than small changes in the structure are needed to achieve the desired results, whilst in the latter, although it is possible to effect a gross change by a succession of many small ones, the disadvantage of the process being heavily computer orientated remains.

The reason why a heavy reliance on the computer is not altogether satisfactory in the present problem is because of the lack of freedom of action to change parameters following the assessment of some subsidiary analysis: that is, to change the parameters in a non-predetermined manner. In a formalized optimization the parameters *are* changed in a predetermined way dependent on the mathematical method, the constraints and the objective function chosen. The knowledge that is a necessary prerequisite in allowing the above-mentioned freedom of action is really the same thing as "feel" or "insight".

It is not only in dealing with the mathematical model of a structure that insight is valuable. When the vibration performance of a newly assembled structure is not up to expectation or specification then the integrity of the mathematical model used for the design is rendered uncertain, and the model itself may not be used as a means of finding suitable modifications. In such a situation in practical engineering any modification suggested by a dynamicist (who at this stage would be under considerable pressure to produce a satisfactory solution) is likely to be the result of fairly simple calculations, which provide some insight, and past experience. More insight at an earlier stage would have placed the dynamicist in a better position to be able to suggest modifications; he might, for instance, have known in advance which parts of the structure are most effective in controlling unwanted vibration.

The above preamble provides the justification for the present work which arises from the desire to know what are the effects on the dynamic properties of a structure resulting from a gross change or changes in one or more structural parameters. The particular aspect examined was stimulated by the necessity in helicopters to keep the rotor induced vibration levels in the passenger and pilot area of the fuselage down to a minimum. The helicopter problem has been used as a basis for the simplified model employed in this work. In this model, a linear structure is subjected to a single oscillatory force and the effect of changing one or more structural parameters on the response at some point on the structure is examined. The structural parameter itself is idealized by using a simple spring, and the examples used in calculations are simple mass, dash pot and spring systems. The theory for this model follows on the lines of that established by Vincent [3].

2. RESPONSE AS A FUNCTION OF ONE STRUCTURAL PARAMETER

2.1. SINGLE DEGREE OF FREEDOM SYSTEM

Although it is of little importance practically, an initial appreciation of the behaviour of a simple one degree of freedom case is helpful in examining more complicated systems.

The equation of motion of a single degree of freedom system subject to harmonic excitation at circular frequency ω may be written as

$$m\ddot{x} + \frac{h}{\omega}\dot{x} + kx = Fe^{i\omega t}, \quad (1)$$

where m is the mass, k the stiffness and F the magnitude of the excitation. The damping, represented by the coefficient h , is considered to be hysteretic for reasons of simplicity in the following analysis. The steady-state solution for the response is

$$x = G(\omega) Fe^{i\omega t},$$

where

$$G(\omega) = \frac{1F}{(k - m\omega^2) + ih} \quad (2)$$

and is the complex receptance of the system. It is well known that the locus of the end of the vector $G(\omega)$ on the complex plane as ω varies is a circle of diameter $1/h$ passing through the origin and with its centre on the negative imaginary axis [4]. Figure 1 shows the response circle appearing as a projection from the three-dimensional locus of $G(\omega)$ produced by including ω as one of the co-ordinates. Part of the circle is not physically realizable as it corresponds to $\omega^2 < 0$ (shown dashed in the figure).

The circular locus arises by virtue of the variation of the real part of the denominator ($k - m\omega^2$) in the right-hand side of equation (2). Thus, a variation of k or m , or indeed k , m and ω^2 in proportional amounts, leads to the same locus. By considering the signs of k , m and ω^2 in the term ($k - m\omega^2$) it is seen that the end of the receptance vector $G(k)$ as k increases, m and ω^2 being held constant, traces out a circle in the opposite direction (i.e., anti-clockwise) as that for increasing ω^2 and m . The effect of varying the damping coefficient h is illustrated in reference [4], in which $G(h)$ is seen to produce a circle whose centre lies on the line of the real axis.

If the circles representing $G(k)$ are plotted in three dimensions as in Figure 2 for all values of ω , then a circular cylindrical envelope is developed. Those parts of the loci corresponding to negative k are shown by dashed curves. On the envelope, curves of constant k can be plotted as indicated, these being of the same type as that in Figure 1.

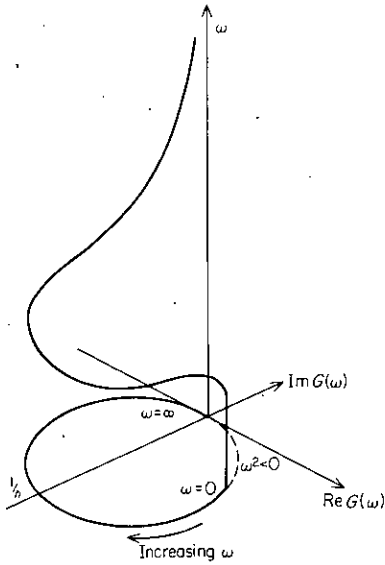


Figure 1. Response as a function of frequency.

Thus it may be seen in the simple case of a one degree of freedom hysteretic system there is a straightforward relationship between the complex response as mass or stiffness varies and the more familiar response as frequency varies.

2.2. MULTI-DEGREE OF FREEDOM SYSTEM

As in the single degree of freedom case it is convenient to express the responses of the system by means of receptances. These follow from consideration of the equations of motion which

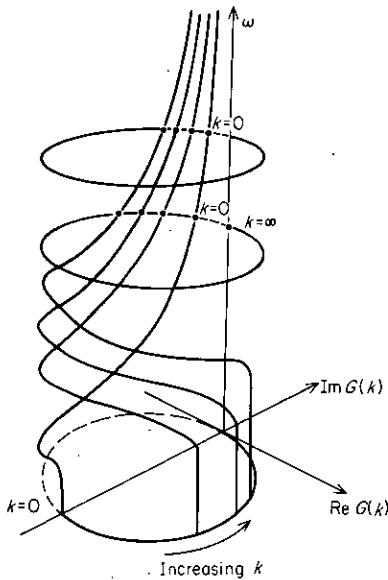


Figure 2. Response as a function of stiffness and frequency (one degree of freedom).

may be written as

$$\mathbf{M}\ddot{\bar{\mathbf{x}}} + \mathbf{C}\dot{\bar{\mathbf{x}}} + \mathbf{K}\bar{\mathbf{x}} = \mathbf{F}e^{i\omega t}, \quad (3)$$

where \mathbf{M} , \mathbf{C} and \mathbf{K} are the mass, damping and stiffness matrices, respectively. \mathbf{F} is a vector of force amplitudes and $\bar{\mathbf{x}}$ is a vector of time-varying structural displacements. The system is considered subject to harmonic excitation at circular frequency ω and since no particular advantage is now to be gained by using hysteretic damping, the damping is assumed to be viscous. The steady-state solution for the response is $\bar{\mathbf{x}} = \mathbf{x}e^{i\omega t}$ where

$$\mathbf{x} = \mathbf{G}\mathbf{F} \quad (4)$$

and

$$\mathbf{G} = [\mathbf{K} - \mathbf{M}\omega^2 + i\omega\mathbf{C}]^{-1}. \quad (5)$$

The system to which these equations apply is shown schematically in Figure 3. It represents a structure having many degrees of freedom for which it is required to examine the response at the material point q due to a single forced excitation at point p .

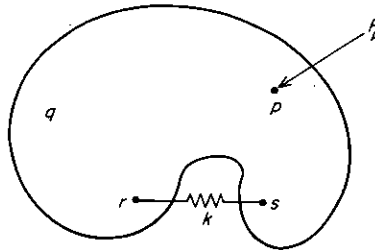


Figure 3. Structure and variable stiffness spring.

A simple structural modification is made by inserting a linear spring of stiffness k between two points r and s that have mutually compatible degrees of freedom. The spring is adjusted so as to exert zero force when the system is in equilibrium. When the original structure is considered as a free body, the forces exerted on it at points r and s by the spring are F_r and F_s , respectively, which have the relationship

$$F_r = k(x_s - x_r) = -F_s. \quad (6)$$

The forcing vector \mathbf{F} in equation (4) contains three non-zero elements, F_r , F_s and F_p , whereas the elements of immediate interest in the response vector \mathbf{x} are x_q , x_r and x_s . Partitioning and expanding equation (4) yields

$$x_q = G_{qp}F_p + G_{qr}F_r + G_{qs}F_s, \quad (7)$$

$$x_r = G_{rp}F_p + G_{rr}F_r + G_{rs}F_s, \quad (8)$$

$$x_s = G_{sp}F_p + G_{sr}F_r + G_{ss}F_s, \quad (9)$$

in which G_{ij} is the complex receptance providing the displacement at point i due to a force at point j .

The forces F_r and F_s may be expressed in terms of x_r and x_s by using equation (6) and subsequent elimination of x_r and x_s gives

$$\frac{x_q}{F_p} = G_{qp} + \frac{k(G_{sp} - G_{rp})(G_{qr} - G_{qs})}{1 + k(G_{rr} + G_{ss} - G_{rs} - G_{sr})} \tag{10}$$

This is now the modified complex receptance between points q and p in terms of k and the original complex receptances G_{ij} . In turn, it may be rewritten in more general terms: i.e.,

$$\begin{aligned} \zeta &= \xi + i\eta \\ &= (e + if) + \frac{k(a + ib)}{1 + k(c + id)} \end{aligned} \tag{11}$$

where $\zeta \equiv x_q/F_p$ and a, b, c, d, e and f are all real.

It can be shown that as k varies from $-\infty$ to $+\infty$ the locus of the tip of the complex receptance vector, ζ , traces out a circle in the complex plane (see Appendix A), the equation of the circle being

$$\left[\xi - \left(e + \frac{b}{2d} \right) \right]^2 + \left[\eta - \left(f - \frac{a}{2d} \right) \right]^2 = \frac{a^2 + b^2}{4d^2} \tag{12}$$

It is worth noting here that the co-ordinates of two important points on the circle, namely $k = 0$ and $k = \infty$, are

$$\begin{aligned} k = 0 &: [e, f], \\ k = \infty &: \left[e + \frac{(ac + bd)}{c^2 + d^2}, f + \frac{(bc - ad)}{c^2 + d^2} \right]. \end{aligned}$$

These points bound the arc of the circle containing negative values of k . Strictly, if k is associated with a real spring then this part of the circle is not physically realizable. However,

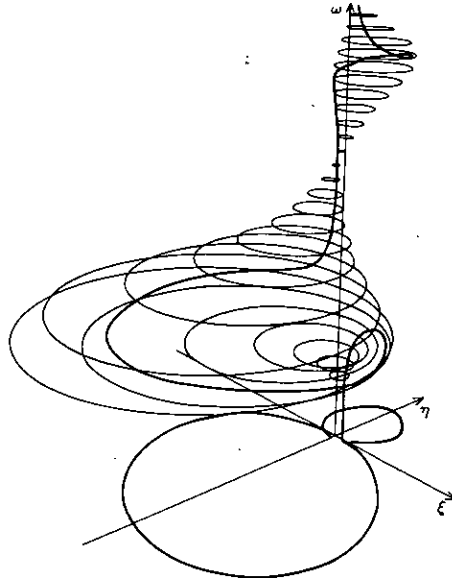


Figure 4. Response as a function of stiffness and frequency (several degrees of freedom).

it is possible to consider negative k as subtracting from existing structural stiffness and in this case the situation is physically attainable whilst the overall stiffness matrix remains positive definite: i.e., whilst static stability is maintained. Of the two possible arcs, that which is associated with negative k may be determined from the direction of the locus with increasing k . This can be shown to be anti-clockwise for the negative values of the constant d in equation (11) which invariably have been found to occur in practical cases. As with the single degree of freedom case it is possible, by introducing forcing frequency as a co-ordinate, to construct a surface corresponding to a given stiffness parameter upon which the three-dimensional response curve can be drawn for various values of that parameter. Figure 4 shows the pictorial representation of a typical surface, the response for the curve corresponding to $k = 0$ being projected below on to the complex plane (the latter is often referred to as a Kennedy-Pancu plot). Information concerning the system from which this surface was generated is given in Appendix B.

3. RESPONSE AS A FUNCTION OF TWO STRUCTURAL PARAMETERS

3.1. FEASIBLE RESPONSE REGIONS

As in section 2.2 the response at a point q on the structure due to a force at point p is sought. Two-variable spring elements of stiffnesses k_1 and k_2 are connected between points r, s and t, v , respectively, where

$$F_r = k_1(x_s - x_r) = -F_s, \quad F_t = k_2(x_v - x_t) = -F_v. \quad (13)$$

Equation (4) again can be utilized to give the relevant equations:

$$x_i = \sum_j G_{ij} F_j, \quad \left\{ \begin{array}{l} i = q, r, s, t, v \\ j = p, q, r, s, t, v \end{array} \right\}. \quad (14)$$

Substituting for $F_r, F_s, F_t,$ and F_v in equations (14) and eliminating x_r, x_s, x_t and x_v gives the following equation:

$$\frac{x_q}{F_p} = G_{qp} + \frac{k_1 \phi_1(k_2) + \phi_2(k_2)}{k_1 \phi_3(k_2) + \phi_4(k_2)}, \quad (15)$$

where the $\phi_i(k_2)$ are complex linear functions of k_2 and are given in Appendix C. It may be seen that the form of this equation when k_2 , say, is held constant whilst k_1 is allowed to vary

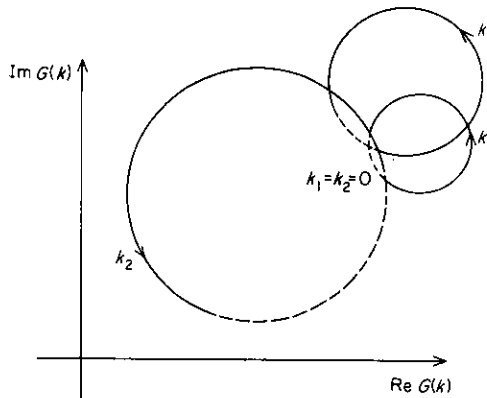


Figure 5. Response circles for two structural parameters.

is similar to that of equation (11). Thus, in this case a circular response locus is produced. When k_2 assumes another value, another circular response locus is obtained as k_1 varies. If the k_1 circle is "started" at the same value of k_1 each time, then these starting points lie on the response locus of the system when k_2 alone is varied (see Figure 5). By covering all possible combinations of k_1 and k_2 a region in the complex plane is formed inside which the response at point q due to an oscillatory force at p must lie. This is referred to as a "feasible response region". Figure 6 shows an example. As in the single varying parameter case, some parts of

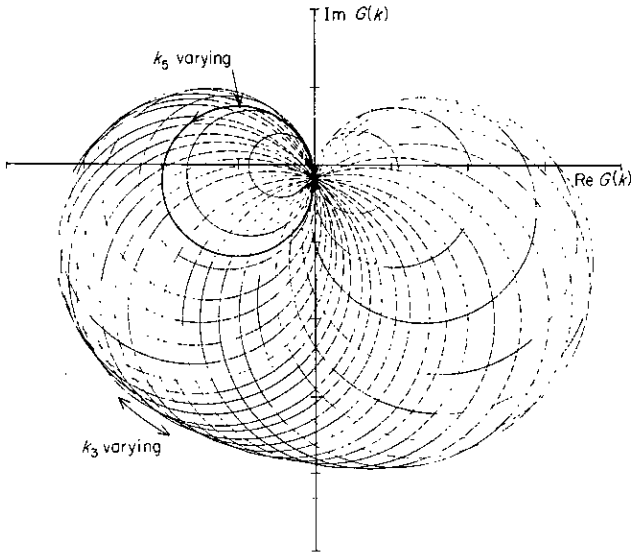


Figure 6. Feasible response region from response circles. Details of system given in Appendix B. Dashed line indicates negative stiffness.

the region violate the physical requirement that the overall stiffness matrix must remain positive definite. Details of the system used in the examples are given in Appendix B.

An alternative formulation of the problem, which relies on the use of matrices, is given in Appendix D. Any number of structural parameters can be considered, but so far no attempt has been made to apply the theory to a practical example.

3.2. THE BOUNDARIES OF THE FEASIBLE RESPONSE REGIONS

The boundaries of the feasible response region are given when the Jacobian, $\partial(\xi, \eta)/\partial(k_1, k_2)$ is zero [5]: i.e.,

$$\begin{vmatrix} \partial\xi/\partial k_1 & \partial\xi/\partial k_2 \\ \partial\eta/\partial k_1 & \partial\eta/\partial k_2 \end{vmatrix} = 0, \tag{16}$$

or, alternatively,

$$\text{Im} \left(\frac{\partial\xi}{\partial k_1} \frac{\partial\bar{\zeta}}{\partial k_2} \right) = 0 \tag{17}$$

where $\partial\bar{\zeta}/\partial k_2$ is the complex conjugate of $\partial\zeta/\partial k_2$ and $\zeta = \xi + i\eta \equiv x_q/F_p$.

Equation (17) is found to be of the second order in k_1 and k_2 and the possibility of two boundaries exists. At any point on these boundaries the values of k_1 and k_2 are uniquely

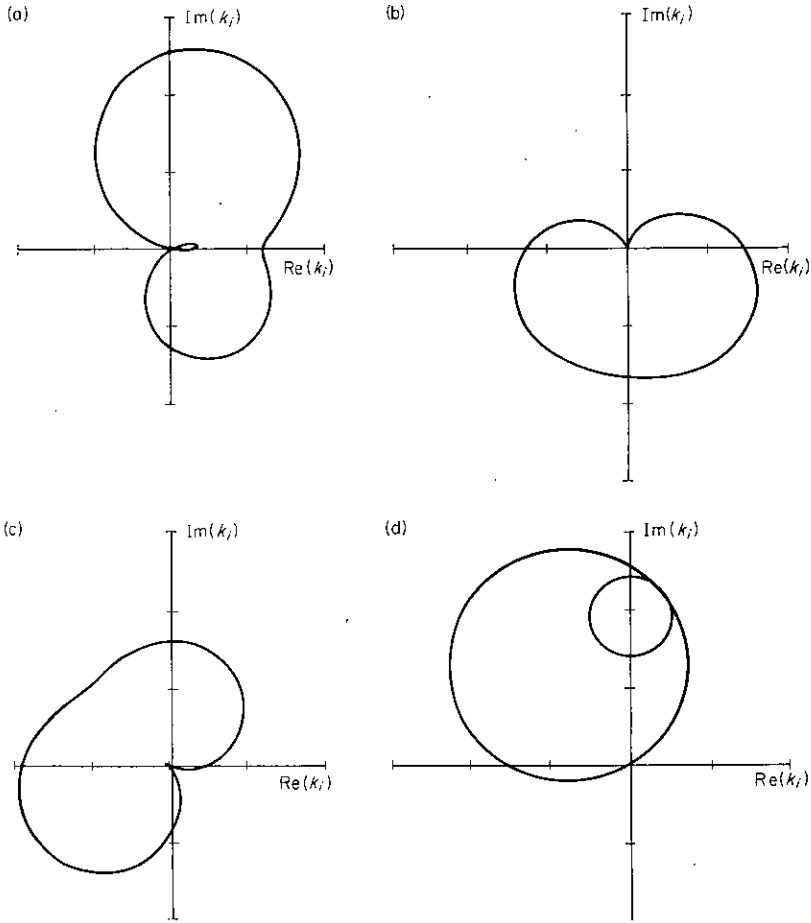


Figure 7. Typical feasible response regions.

defined, whereas within the region it may be observed from Figure 6 that there are two sets of values (k_1, k_2) corresponding to each response point. Figure 7 gives some examples of typical feasible regions obtained by direct solution of equation (17) following the appropriate differentiations in equation (15). The systems concerned again are defined in Appendix B.

4. DISCUSSION

The mathematical models considered in the present work are idealized and, although there is presumably a certain intrinsic academic interest in the results, it remains to be seen how useful the theory would be in a practical case. In most practical cases of manipulating a structure to produce a desired vibratory response the aim would be to *minimize* the response over all or part of the structure. (An exception to this would be changing a normal mode shape on an aircraft wing, say, for the purpose of changing the aerodynamic generalized forces and thence the flutter characteristics.) In the present formulation, with not more than two spring variables, the minimum response (if zero is not a feasible response) could be obtained uniquely by using the equation of the outward normal to the boundary with no recourse to search techniques. When zero response is feasible, i.e., when the feasible region surrounds the origin, there is a choice between two uniquely defined sets of variables.

In practical applications one of the problems is to choose the regions of the structure in

which a change of structural parameter or parameters is most effective. In such applications of the present formulation it is proposed, initially anyway, to use the relative magnitude of the response circle for a single parameter as a measure of effectiveness. In this connection, it should be noted that the systems discussed in this paper are not meaningful in any numerical sense, but have been used only to illustrate in the most general way the variation of the response. As the main purpose of this paper is to draw attention to some of the more interesting phenomena, the discussion here is confined to outlining some of the difficulties expected in practical applications.

Another problem is to obtain a transformation between the ideal springs considered as structural parameters and the geometric parameters, (which would affect mass as well as stiffness), such as skin thickness, tube wall thickness, beam web depth, etc., that would be used in practice. This also is a difficult area when one is using the more conventional optimization methods because the mathematical equations of motion of vibration systems are usually expressed in terms of variables other than the geometric parameters: e.g., generalized coordinates.

The direct application of the present work to simple and more practical examples of structures is in progress, and will be reported on in due course.

ACKNOWLEDGMENTS

Thanks are due to several people at Westland Helicopters Limited for providing the stimulus for this work and for their continued encouragement and assistance.

REFERENCES

1. K. W. NEWMAN 1969 (July) *RAE T.R.* 69142 (A.R.C. 32597). Predicting the effects of parameter changes in a dynamical system.
2. A. SIMPSON 1973 *Journal of Sound and Vibration* **31**, 73-87. Eigenvalue and vector sensitivities in Kron's method.
3. A. H. VINCENT 1973 (September) *Westland Helicopters Ltd. Report GEN/DYN/RES/01OR*. A note on the properties of the variation of structural response with respect to a single structural parameter when plotted in the complex plane.
4. R. E. D. BISHOP and G. M. L. GLADWELL 1963 *Philosophical Transactions of the Royal Society London, Series A*, **255**, 241-280. An investigation into the theory of resonance testing.
5. I. N. SNEDDON 1957 *Elements of Partial Differential Equations*. New York: McGraw-Hill Book Company, Inc.
6. A. KYRALA 1972 *Applied Functions of a Complex Variable*. New York: Wiley-Interscience.

APPENDIX A

It is required to find the nature of the complex equation

$$\zeta = (e + if) + \frac{k(a + ib)}{1 + k(c + id)} \quad (\text{A1})$$

as k is varied between $-\infty$ and ∞ .

Let $\zeta = \xi + i\eta$. Then

$$(\xi - e) + i(\eta - f) = \frac{a + ib}{(1/k) + c + id} \quad (\text{A2})$$

giving

$$(1/k) + c + id = \frac{(a + ib)((\xi - e) - i(\eta - f))}{(\xi - e)^2 + (\eta - f)^2} \quad (\text{A3})$$

The imaginary part of equation (A3) gives

$$(\xi - e)^2 + (\eta - f)^2 = (\xi - e)b/d - (\eta - f)a/d, \quad (\text{A4})$$

which can be rearranged to give the equation

$$[\xi - (e + b/2d)]^2 + [\eta - (f - a/2d)]^2 = \frac{a^2 + b^2}{4d^2}, \quad (\text{A5})^\dagger$$

which is that of a circle.

Equation (A1), in fact, can be regarded as providing a mapping from the k -plane (in which k is assumed in general to be complex) into the ζ -plane. It may be seen to be an example of the *bilinear* class of mappings for which it is known [6] that circles and straight lines map into circles and straight lines. In the present case, k is real and thus provides a straight line in the k -plane and maps into a circle or a straight line in the ζ -plane. It may be useful to note that if damping is incorporated into the stiffness by introducing an imaginary component on the real stiffness, the response on the ζ -plane is still a circle or straight line.

APPENDIX B

All the systems used in the computations corresponding to Figures 4, 6 and 7 consist of simple combinations of masses, springs and dashpots. The number of degrees of freedom in each case was four, and the maximum number of interconnections between adjacent masses was two for Figures 4 and 7(a), the number being three in all the other cases. As an example, the system used to generate the region illustrated in Figure 6 is shown in Figure B1. The

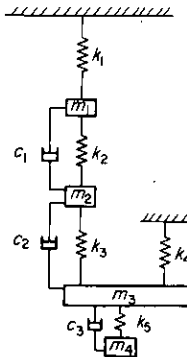


Figure B1. Sketch of system used for feasible response region illustrated in Figure 6. Stiffness: $k_1 = 40$, $k_2 = 30$, $k_3 = 30$, $k_4 = 30$, $k_5 = 10$; mass: $m_1 = 3$, $m_2 = 10$, $m_3 = 20$, $m_4 = 5$; damping: $c_1 = 0.5$, $c_2 = 0.6$, $c_3 = 0.8$. All units are compatible.

maximum number of interconnections on this system is three on mass m_3 . The point at which excitation is applied is on mass m_4 and that at which the response is examined is on mass m_1 . The variable parameters are k_3 and k_5 . The numbers used in this and other examples have no particular significance.

† This version of the proof is due to Professor A. R. Collar.

APPENDIX C

The equation for the complex responses $\zeta \equiv x_q/F_p$ as a function of two variable spring parameters k_1 and k_2 is given generally by

$$\zeta = G_{qp} + \frac{k_1 \phi_1(k_2) + \phi_2(k_2)}{k_1 \phi_3(k_2) + \phi_4(k_2)}, \tag{C1}$$

where q and p refer to examination and forcing co-ordinates, respectively. The functions $\phi_i(k_2)$ are

$$\begin{aligned} \phi_1(k_2) &= a_1 b_1(1 + k_2 c_{22}) + a_2 b_2 c_{21} k_2 - k_2(a_2 b_1 c_{21} + a_1 b_2 c_{12}), \\ \phi_2(k_2) &= a_2 b_2 k_2, \\ \phi_3(k_2) &= c_{11}(1 + k_2 c_{22}) - c_{21} k_2, \\ \phi_4(k_2) &= 1 + k_2 c_{22}, \end{aligned}$$

where a_i, b_i and c_{ij} are the complex elements of matrices **A**, **B** and **C** in Appendix D. These elements are functions of the complex receptances G_{ij} and are given by

$$\begin{aligned} a_1 &= G_{qr} - G_{qs}, & a_2 &= G_{qt} - G_{qv}, \\ b_1 &= G_{sp} - G_{rp}, & b_2 &= G_{vp} - G_{ip}, \\ c_{11} &= G_{rr} + G_{ss} - G_{rs} - G_{sr}, & c_{12} &= G_{sv} - G_{st} - G_{rv} + G_{rt}, \\ c_{21} &= G_{vs} - G_{vr} - G_{ts} + G_{tr}, & c_{22} &= G_{tt} + G_{vv} - G_{vt} - G_{tv}, \end{aligned}$$

where k_1 is connected between co-ordinates r and s and k_2 between co-ordinates t and v .

APPENDIX D

The setting up and reduction of equations (14) to give the single expression for the complex receptance as shown in equation (15) rapidly becomes more complex as the number of variable parameters considered increases. As a consequence of this it is convenient to have a general matrix expression for the complex receptance x_q/F_p in terms of m variable stiffness parameters.

The response at the examination point, q , may be written in terms of the external force, internal spring forces and the corresponding receptances:

$$x_q = G_{qp} F_p + k_1 \delta_1 (G_{q1} - G_{q2}) + k_2 \delta_2 (G_{q3} - G_{q4}) \dots k_m \delta_m (G_{q, 2m-1} - G_{q, 2m}), \tag{D1}$$

where k_i is the i th variable stiffness parameter and $\delta_i = x_{2i} - x_{2i-1}$ is the extension of the i th spring (x_{2i} and x_{2i-1} being the actual axial displacements at each end). Equation (D1) alternatively may be expressed as

$$x_q = G_{qp} F_p + \mathbf{AK}\delta \tag{D2}$$

where **A** is a $(1 \times m)$ row vector of the terms

$$\{(G_{q1} - G_{q2}), (G_{q3} - G_{q4}), \dots (G_{q, 2m-1} - G_{q, 2m})\},$$

K is an $(m \times m)$ diagonal matrix of the stiffness parameters k_i and δ is an $(m \times 1)$ column vector of extensions.

The values δ_i themselves may be expressed in the same way as x_q in equation (D1): i.e.,

$$\begin{aligned} \delta_1 &= F_p(G_{2p} - G_{1p}) - k_1 \delta_1[(G_{22} - G_{21}) - (G_{12} - G_{11})] - k_2 \delta_2[(G_{24} - G_{23}) - (G_{14} - G_{13})] \dots, \\ \delta_2 &= F_p(G_{4p} - G_{3p}) - k_1 \delta_1[(G_{42} - G_{41}) - (G_{32} - G_{31})] \dots, \\ &\vdots \\ \delta_m &= F_p(G_{2m,p} - G_{2m-1,p}) \dots \dots - k_m \delta_m[(G_{2m,2m} - G_{2m,2m-1}) - (G_{2m-1,2m} - G_{2m-1,2m-1})], \end{aligned} \quad (D3)$$

which can be written in matrix notation as

$$\delta = F_p \mathbf{B} - \mathbf{CK} \delta \quad (D4)$$

where \mathbf{B} is an $(m \times 1)$ column vector of terms

$$\{(G_{2p} - G_{1p}), (G_{4p} - G_{3p}), \dots, (G_{2m,p} - G_{2m-1,p})\}$$

and \mathbf{C} is an $(m \times m)$ matrix of complex constants in which $C_{ij} = (G_{2i,2j} - G_{2i,2j-1}) - (G_{2i-1,2j} - G_{2i-1,2j-1})$. An expression for δ can be found from equation (D4) and substituted into equation (D2) to give

$$\frac{x_q}{F_p} = G_{qp} + \mathbf{A}[\mathbf{K}^{-1} + \mathbf{C}]^{-1} \mathbf{B}, \quad (D5)$$

which provides the complex receptance, x_q/F_p , as a general function of m stiffness parameters.